

TROTICENE LITHIATION AND PLATINUM-CATALYZED HYDROSILYLATION
USING DIMETHYLSILYL- TROTICENE AND FERROCENE DERIVATIVES

By

RHYAN JOSEPH SORIANO TERRADO

A dissertation submitted to the
Graduate School-Newark
Rutgers, The State University of New Jersey
in partial fulfillment of the requirements

for the degree of

Doctor of Philosophy

Graduate Program in Chemistry

Written under the direction of

Professor John B. Sheridan

and approved by

Newark, New Jersey

May, 2009

ABSTRACT OF THE DISSERTATION

Troticene Lithiation and Platinum-Catalyzed Hydrosilylation Using Dimethylsilyl- Troticene and Ferrocene Derivatives

By RHYAN JOSEPH SORIANO TERRADO

Dissertation Director:

Professor John B. Sheridan

The lithiation of troticene was studied. Monolithiation of troticene at 0 °C preferentially occurred at the cycloheptatrienyl (Cht) ligand,^{1,2} while monolithiation at room temperature preferentially occurred at the cyclopentadienyl (Cp) ligand. Dimethylsilyl-, trimethylstannyl-, diphenylphosphino-, and trimethylsilyl-derivatives were prepared in this manner. The monolithio-cycloheptatrienyl-troticene was found to be less stable at higher temperatures than the monolithio-cyclopentadienyl-troticene. Dilithiation of troticene was readily achieved using 2.5 equiv. *n*-butyllithium/TMEDA,³ and using an even greater excess of lithiating agent led to greater degrees of lithiation of up to 4 lithiums. Disubstituted Cp ligands are predominantly 1,3-disubstituted, while disubstituted Cht ligands are predominantly 1,4-disubstituted. Substituted troticene derivatives were also lithiated. Just like the 1-pot polyolithiation, disubstituted Cp ligands are predominantly 1,3-disubstituted. However, disubstituted Cht ligands are either 1,4- or 1,3-disubstituted.

Dimethylsilyl-troticene derivatives were used in the preparation of troticene-based polymers/oligomers containing silylenevinylene-phenylene-/thienylene-bridged metallocene units along with the appropriate model compounds. The regiochemical distributions obtained were consistent with those obtained by Jain and coworkers using dimethylsilyl ferrocene derivatives, with low molecular weights and no metal-metal interaction between the metallocene units.^{4,5}

Hydrosilylation reactions of *bis*(dimethylsilyl)- ferrocene or troticene gave lower β (E)- to α - olefinic proton ratios compared to dimethylsilyl- ferrocene or troticene, the latter two giving regiochemical distributions consistent with those of 1,4-*bis*(dimethylsilyl)benzene or dimethylsilylbenzene. These results were consistent regardless of whether phenylacetylene, ethynyltoluene, or ethynylthiophene was used as the alkyne.

A comparison between the hydrosilylation mono- β (E)- and mono- α - adducts of 1,4-*bis*(dimethylsilyl)benzene and 1,1'-*bis*(dimethylsilyl)ferrocene with phenylacetylene was done. The hydrosilylation reactions of the mono- β (E)- adducts of both compounds as well as the mono- α - adduct of 1,4-*bis*(dimethylsilyl)benzene were all consistent with each other, preferring a β (E)- configuration in the hydrosilylation of the second dimethylsilyl-moiety. In contrast, the mono- α - adduct of 1,1'-*bis*(dimethylsilyl)ferrocene preferred an α - configuration in the hydrosilylation of the second dimethylsilyl-moiety. In addition, the mono- α - adduct of 1,1'-*bis*(dimethylsilyl)ferrocene was more readily converted into the *bis*-adducts than the mono- β (E)- adduct. These factors led to an increased amount of α -olefinic protons in hydrosilylation reactions of 1,1'-*bis*(dimethylsilyl)ferrocene.

Acknowledgements

I would like to extend my deepest gratitude to my advisor, Dr. John B. Sheridan, for his patience and invaluable guidance and help towards the completion of this work.

To my committee members, Dr. Frieder Jäkle, Dr. Roger A. Lalancette, and Dr. Wayne Schnatter, for taking the time to review and critique this dissertation.

To my former group mates, for their companionship and being there to teach me the basics of working in the lab.

To Dr. Lazaros Kakalis, for his much appreciated help with the collection of NMR data, and to Dr. Roger A. Lalancette and Dr. Alan J. Lough, for all the X-ray crystallographic studies.

To Dr. Frieder Jäkle and his group, for all their help and suggestions, specially Chengzhong Cui for his suggestions on the lithiation work, and Dr. Anand Sundararaman for his help with the collection of MALDI-TOF/TOF data.

To the chemistry department at Rutgers Newark, for giving me the opportunity to study a discipline that I truly love.

To the Benzon family, for helping and supporting me in starting out in a new country, and to my sister Russel Terrado, for being there when I was at one of the lowest points in my life.

To my parents, for nurturing me into the person I am today.

To my brother Fulgencio Terrado Jr., for urging me to study chemistry.

To my cousin Father Jim Cerezo, for giving me back a part of my life.

And to Cheryl Cang, who is a constant reminder of what I am striving for.

Table of Contents

| | |
|--|------|
| Abstract of the Dissertation. | ii |
| Acknowledgements. | iv |
| Table of Contents. | v |
| List of Schemes. | ix |
| List of Figures. | xiii |
| List of Tables. | xvi |
| | |
| Chapter 1. Introduction | 1 |
| 1.1. Lithiation Reactions | 1 |
| 1.1.1. Factors Affecting Lithiation | 4 |
| 1.1.1.1. Effect of Lewis Basic Solvents and Additives | 4 |
| 1.1.1.2. Effect of Temperature | 8 |
| 1.1.1.3. Effect of the Organolithium Reagent Used | 11 |
| 1.1.1.4. Effect of Ring Substituents | 13 |
| 1.1.2. Metallation of Sandwich Complexes | 14 |
| 1.1.2.1. Metallation of Ferrocene | 15 |
| 1.1.2.2. Lithiation of Alkyl Ferrocene Derivatives | 22 |
| 1.1.2.3. Directed Lithiation of Ferrocene | 24 |
| 1.1.2.4. Lithiation of Tropicene | 26 |
| 1.1.2.5. Lithiation of other (η^7-C₇H₇) M (η^5-C₅H₅) Mixed Sandwich Complexes | 29 |
| 1.2. Hydrosilylation Chemistry | 30 |

| | |
|---|--------|
| 1.2.1. Transition-Metal Catalyzed Hydrosilylation Mechanism | 31 |
| 1.2.2. Hydrosilylation of Alkenes and Alkynes | 34 |
| 1.2.3. Hydrosilylation of Alkynes using Pt Catalysts | 35 |
| 1.2.4. Pt-Catalyzed Hydrosilylation to Produce Macromolecules | 37 |
| 1.2.5. Hydrosilylation of Fe/ferrocenyl-based Systems | 40 |
| 1.2.6. Poly{ferrocene- <i>bis</i> (silylenevinylene)(phenylene)}s | 44 |
| Chapter 2. Preferential Monosubstitution of (η^7 -Cycloheptatrienyl) (η^5 -cyclopentadienyl)titanium(II) via Lithiation | 49 |
| 2.1. Monosubstitution of Tropicene | 49 |
| 2.1.1. Monosubstitution on the Cycloheptatrienyl Ligand | 49 |
| 2.1.2. Monosubstitution on the Cyclopentadienyl Ligand | 53 |
| 2.1.3. Effect of Temperature on the Lithiation of Tropicene | 59 |
| 2.2. Disubstitution of Tropicene | 61 |
| 2.3. Polyolithiation of Tropicene in a 1-Pot reaction | 65 |
| 2.3.1. Trimethylsilyl Derivatives | 66 |
| 2.3.2. Dimethylsilyl Derivatives | 76 |
| 2.4. Summary | 79 |
| Chapter 3. Lithiation of Substituted (η^7 -Cycloheptatrienyl) (η^5 -cyclopentadienyl)titanium(II) Derivatives | 80 |
| 3.1. Monolithiation of Substituted Tropicene Derivatives | 80 |
| 3.1.1. Monolithiation of the Cycloheptatrienyl ligand of Monosubstituted Tropicenes | 80 |
| 3.1.2. Monolithiation of <i>Bis</i> (trimethylsilyl)tropicene 203d | 89 |

| | |
|--|-----|
| 3.2. Dilithiation of Substituted Troiticene Derivatives | 90 |
| 3.2.1. Dilithiation of Monosubstituted Troiticene Derivatives 201d and 202d | 90 |
| 3.2.2. Dilithiation of <i>Bis</i>(trimethylsilyl)troiticene 203d | 97 |
| 3.3. Summary | 104 |
| Chapter 4. Poly{troiticene-<i>bis</i>(silylenevinylene)(phenylene)}s | 105 |
| 4.1. Type 1 Model Compounds | 107 |
| 4.2. Type 2 Model Compounds | 118 |
| 4.3. Type 3 Model Compounds | 133 |
| 4.4. Synthesis and Characterization of poly{troiticene-<i>bis</i>(silylenevinylene)(phenylene)}s using Karstedt's catalyst. | 146 |
| 4.5. Cyclic Voltammetry | 165 |
| 4.6. Summary | 165 |
| Chapter 5. Comparison of the Hydrosilylation of Alkynes with Various Silanes | 166 |
| 5.1. Effect of Alkyne Substituent on Hydrosilylation | 166 |
| 5.2. Comparison of 1,4-<i>bis</i>(dimethylsilyl)benzene and 1,1'-<i>bis</i>(dimethylsilyl)ferrocene | 175 |
| 5.2.1. Preparation of Mono-Hydrosilylated <i>Bis</i>-Silanes | 175 |
| 5.2.2. Hydrosilylation of Phenylacetylene with Mono-Hydrosilylated <i>Bis</i>-Silanes | 179 |
| 5.2.3. ¹H NMR Monitored Hydrosilylation of Phenylacetylene | 181 |
| 5.3. Summary | 199 |
| Experimental Section. | 200 |

| | |
|--|-----|
| References. | 236 |
| Appendix. Data for X-ray Crystallography. | 255 |
| Vita. | 289 |

List of Schemes

| | |
|---|----|
| Scheme 1.1.1. Lithiation of Fluorene with Ethyllithium. | 2 |
| Scheme 1.1.2. Reaction of 2-Bromo-dibenzofuran with <i>n</i> -Butyllithium. | 3 |
| Scheme 1.1.1.1.1. Lithiation of Benzene. | 5 |
| Scheme 1.1.1.1.2. Lithiation of 4-methoxy-N,N-dimethylaminomethylbenzene. | 7 |
| Scheme 1.1.1.1.3. Lithiation of 1-Methoxynaphthalene. | 8 |
| Scheme 1.1.1.2.1. Lithiation of 4-Fluoroanisole with <i>sec</i> -Butyllithium. | 9 |
| Scheme 1.1.1.2.2. Lithiation of 1-Aryl-1-butyne. | 10 |
| Scheme 1.1.1.3.1. Lithiation of 1,2,3,4-Tetrachlorobenzene. | 12 |
| Scheme 1.1.1.3.2. <i>Ortho</i> - and <i>Peri</i> -Lithiation of 1-Methoxynaphthalene. | 13 |
| Scheme 1.1.2.1.1. Initial Reports on the Lithiation of Ferrocene. | 15 |
| Scheme 1.1.2.1.2. Monolithioferrocene via Halogen-Metal Exchange. | 16 |
| Scheme 1.1.2.1.3. Monolithioferrocene via Transmetallation. | 16 |
| Scheme 1.1.2.1.4. Monolithiation of Ferrocene with <i>t</i> -Butyllithium/ <i>t</i> -BuOK. | 17 |
| Scheme 1.1.2.1.5. Dilithiation of Ferrocene with <i>n</i> -Butyllithium/TMEDA. | 18 |
| Scheme 1.1.2.1.6. Permetallation of Ferrocene with Excess <i>n</i> -Butyllithium /TMEDA. | 19 |
| Scheme 1.1.2.1.7. Decamercuration of Ferrocene with Excess Mercuric Acetate. | 20 |
| Scheme 1.1.2.1.8. Octamercuration of 1,1'-Dimethylferrocene with Excess Mercuric Acetate. | 20 |
| Scheme 1.1.2.1.9. Decamercuration of Ferrocene with Excess Mercuric Butyrate. | 21 |
| Scheme 1.1.2.2.1. Metallation of Monoalkyl Ferrocenes with <i>n</i> -Pentylsodium. | 23 |
| Scheme 1.1.2.3.1. Lithiation of N,N-Dimethylaminomethylferrocene. | 25 |

| | |
|--|----|
| Scheme 1.1.2.3.2. Diastereoselective Lithiation of Ferrocenes. | 25 |
| Scheme 1.1.2.3.3. Enantioselective Lithiation of Ferrocenes. | 26 |
| Scheme 1.1.2.3.4. Borylation of 1,1'- <i>Bis</i> (trimethylstannyl)ferrocene. | 26 |
| Scheme 1.1.2.4.1. Monolithiation of the Cycloheptatrienyl Ligand of Tropicene. | 27 |
| Scheme 1.1.2.4.2. Dilithiation of Tropicene. | 28 |
| Scheme 1.1.2.4.3. <i>Ansa</i> -Bridged Tropicene Derivative. | 28 |
| Scheme 1.2.1.1. Chalk and Harrod Mechanism (A) with Modified Chalk and Harrod Mechanism (B). | 32 |
| Scheme 1.2.1.2. Lewis Mechanism. | 33 |
| Scheme 1.2.2.1. Hydrosilylation of Terminal Alkenes. | 34 |
| Scheme 1.2.2.2. Hydrosilylation of Terminal Alkynes. | 35 |
| Scheme 1.2.2.3. Hydrosilylation of Internal Alkynes. | 35 |
| Scheme 1.2.4.1. General Hydrosilylation Polymerization Scheme 1 . | 37 |
| Scheme 1.2.4.2. General Hydrosilylation Polymerization Scheme 2 . | 37 |
| Scheme 1.2.4.3. Hydrosilylation Polymerization of Ethynylsilanes. | 38 |
| Scheme 1.2.4.4. Hydrosilylation Polymerization of <i>o</i> -, <i>m</i> -, <i>p</i> -(Dimethylsilyl)phenylacetylene. | 39 |
| Scheme 1.2.4.5. Hydrosilylation Polymerization of <i>Bis</i> (dimethylsilyl)acetylene with Diethynylbenzene. | 39 |
| Scheme 1.2.5.1. Hydrosilylation of Ferrocene-based Disilanes and Alkynes. | 41 |
| Scheme 1.2.5.2. Hydrosilylation Polymerization of 18b with 17a . | 42 |
| Scheme 1.2.5.3. Hydrosilylation of Dendron 22 . | 43 |
| Scheme 1.2.5.4. Modification of Poly(ferrocenylmethylhydrosilane) via Hydrosilylation. | 44 |
| Scheme 1.2.6.1. Hydrosilylation Polymerization of 1,1'- <i>Bis</i> (dimethylsilyl)ferrocene with Dialkynes. | 45 |

| | |
|--|-----|
| Scheme 1.2.6.2. Type 1 Model Compounds. | 46 |
| Scheme 1.2.6.3. Type 2 Model Compounds. | 48 |
| Scheme 2.1.1.1. Preferential Monolithiation of the Cht Ligand of Tropicene. | 51 |
| Scheme 2.1.2.1. Preferential Monolithiation of the Cp Ligand of Tropicene. | 53 |
| Scheme 2.1.3.1. Monolithiation of Tropicene at 0 °C and Room Temperature. | 60 |
| Scheme 2.1.3.2. Monolithiation of Tropicene at Room Temperature. | 61 |
| Scheme 2.2.1. Dilithiation of Tropicene. | 62 |
| Scheme 2.3.1. Polyolithiation of Tropicene. | 65 |
| Scheme 3.1. Monolithiation of Methyltropicene. | 80 |
| Scheme 3.1.1.1. Monolithiation of 201 . | 81 |
| Scheme 3.1.2.1. Monolithiation on either the Cht or Cp Ligand of 203d . | 89 |
| Scheme 3.2.1.1. Major Product Distribution and Isolated Yield for the Dilithiation of 201d . | 91 |
| Scheme 3.2.1.2. Major Product Distribution and Isolated Yield for the Dilithiation of 202d . | 92 |
| Scheme 3.2.1.3. Synthesis of Silatroticenophane. | 94 |
| Scheme 3.2.1.4. Proposed Synthesis of Silatroticenophane via Dilithiation of 202d . | 94 |
| Scheme 3.2.2.1. Major Products for the Dilithiation of 203d . | 97 |
| Scheme 4.1. General Scheme for Type 1 Model Compounds. | 106 |
| Scheme 4.2. General Scheme for Type 2 Model Compounds. | 106 |
| Scheme 4.3. General Scheme for Type 3 Model Compounds. | 106 |
| Scheme 4.1.1. Type 1 Model Compounds from 201a and Monoalkynes. | 107 |
| Scheme 4.1.2. Type 1 Model Compounds from 202a and Monoalkynes. | 108 |

| | |
|--|-----|
| Scheme 4.1.3. Type 1 Model Compounds from 41a and Monoalkynes. | 109 |
| Scheme 4.2.1. Type 2 Model Compounds from 203a and Monoalkynes. | 118 |
| Scheme 4.2.2. Type 2 Model Compounds from 28 and Monoalkynes. | 120 |
| Scheme 4.3.1. Type 3 Model Compounds from 201a and Dialkynes. | 133 |
| Scheme 4.3.2. Type 3 Model Compounds from 202a and Dialkynes. | 134 |
| Scheme 4.3.3. Type 3 Model Compounds from 41 and Dialkynes. | 135 |
| Scheme 4.4.1. Polymers/Oligomers from 203a and Dialkynes. | 147 |
| Scheme 4.4.2. Polymers/Oligomers from 28 and Dialkynes. | 148 |
| Scheme 5.2.1.1. Synthesis of 233B . | 176 |
| Scheme 5.2.2.1. Hydrosilylation of Phenylacetylene with 233B . | 179 |
| Scheme 5.2.2.2. Hydrosilylation of Phenylacetylene with 234B . | 180 |
| Scheme 5.2.3.1. Products from Pt-Catalyzed Hydrosilylation of a <i>Bis</i> -Hydrosilane and a Mono-Alkyne. | 184 |
| Scheme 5.2.3.2. β (E)- and α - Regioisomers from Insertion of Alkyne into Pt-H and Pt-Si. | 192 |

List of Figures

| | |
|---|-----|
| Figure 1.1.2.1.1. Structure of $[\{\text{Fe}(\text{C}_5\text{H}_3)_2\}\text{Na}_4\text{Mg}_4\{i\text{-Pr}_2\text{N}\}_8]$. | 22 |
| Figure 1.2.5.1. Phenylene-bridged Ferrocenes. | 40 |
| Figure 1.2.5.2. Poly(ferrocenylsilane) | 40 |
| Figure 1.2.5.3. Dendrimers 24 and 25 via Hydrosilylation. | 43 |
| Figure 2.1.2.1. ORTEP drawing of 202c . | 55 |
| Figure 2.1.2.2. C-H and C-P Bond Distortion Angles of 202c . | 56 |
| Figure 2.1.2.3. Deviation of Hydrogen Atoms from the Plane of Cyclic C_nH_n Ligands in Metal π -Complexes. | 57 |
| Figure 2.3.1.1. ORTEP drawing of 206d . | 68 |
| Figure 2.3.1.2. C-H and C-Si Bond Distortion Angles of 206d . | 68 |
| Figure 2.3.1.3. ORTEP drawing of 204d . | 70 |
| Figure 2.3.1.4. ORTEP drawing of 204d molecule A . | 70 |
| Figure 2.3.1.5. C-H and C-Si Bond Distortion Angles of 204d . | 71 |
| Figure 2.3.1.6. ORTEP drawing of 207d . | 73 |
| Figure 2.3.1.7. C-H and C-Si Bond Distortion Angles of 207d . | 73 |
| Figure 3.1.1.1. Cp and Cht $^{13}\text{C}\{^1\text{H}\}$ NMR Carbon Signals of 210c . | 84 |
| Figure 3.1.1.2. ORTEP drawing of 210c . | 85 |
| Figure 3.1.1.3. C-H and C-P Bond Distortion Angles of 210c . | 85 |
| Figure 3.2.2.1. Isomers of 207da and 208da . | 98 |
| Figure 3.2.2.2. Cht $^{13}\text{C}\{^1\text{H}\}$ NMR Carbon Signals of 207da and 208da . | 101 |
| Figure 4.2.1. ^1H NMR of 214a Methyl Protons. | 121 |
| Figure 4.2.2. ^1H NMR of 214b Methyl Protons. | 122 |

| | |
|---|-----|
| Figure 4.2.3. ^1H NMR Spectrum of 215 Methyl Protons. | 123 |
| Figure 4.2.4. ^1H NMR Spectrum of 211a (top), 212a (mid), and 214a (bot) Olefinic Protons. | 125 |
| Figure 4.2.5. ^1H NMR Spectrum of 211b (top), 212b (mid), and 214b (bot) Olefinic Protons. | 126 |
| Figure 4.2.6. ^1H NMR Spectrum of 213 (top) and 215 (bot) Olefinic Protons. | 127 |
| Figure 4.4.1. ^1H NMR Spectrum of 216a (top), 217a (mid), and 219a (bot) Olefinic Protons. | 153 |
| Figure 4.4.2. MALDI-TOF/TOF Spectrum of 219a . | 154 |
| Figure 4.4.3. ^1H NMR Spectrum of 216b (top), 217b (mid), and 219b (bot) Olefinic Protons. | 155 |
| Figure 4.4.4. MALDI-TOF/TOF Spectrum of 219b . | 156 |
| Figure 4.4.5. ^1H NMR Spectrum of 216c (top), 217c (mid), and 219c (bot) Olefinic Protons. | 157 |
| Figure 4.4.6. MALDI-TOF/TOF Spectrum of 219c . | 158 |
| Figure 4.4.7. ^1H NMR Spectrum of 218 (top) and 220 (bot) Olefinic Protons. | 159 |
| Figure 4.4.8. MALDI-TOF/TOF Spectrum of 220 . | 160 |
| Figure 5.2.3.1. Mono- β (E)- vs. Mono- α - Hydrosilylation. | 190 |
| Figure 5.2.3.2. 234A -Chelated Pt-catalyst. | 191 |
| Figure 5.2.3.3. ^1H NMR Spectra of Reaction 223 Methyl Protons after 5 Hours. | 193 |
| Figure 5.2.3.4. ^1H NMR Spectra of Reaction 223 Methyl Protons after 20 Hours. | 194 |
| Figure 5.2.3.5. ^1H NMR Spectra of Reaction 223 Methyl Protons after Completion. | 195 |
| Figure 5.2.3.6. ^1H NMR Spectra of Reaction 224 Cp Protons after 1 Hour. | 196 |
| Figure 5.2.3.7. ^1H NMR Spectra of Reaction 224 Cp Protons after 5 Hours. | 197 |

Figure 5.2.3.8. ^1H NMR Spectra of Reaction **224** Cp Protons after Completion. 198

List of Tables

| | |
|---|-----|
| Table 2.1.1.1. NMR Data for Products with a Single Substituent on the Cycloheptatrienyl Ring. | 52 |
| Table 2.1.2.1. NMR Data for Products with a Single Substituent on the Cyclopentadienyl Ring. | 58 |
| Table 2.2.1. NMR Data for 1,1'-Disubstituted Tropicene Derivatives. | 64 |
| Table 2.3.1.1. NMR Data for Isolated Products from Chlorotrimethylsilane-Quenched Polyolithiation of Tropicene. | 75 |
| Table 2.3.2.1. NMR Data for Isolated Products from Chlorodimethylsilane-Quenched Polyolithiation of Tropicene. | 78 |
| Table 3.1.1.1. NMR Data for Major Products from Chlorotrimethylsilane-Quenched Monolithiation of 201d . | 87 |
| Table 3.1.1.2. NMR Data for Major Products from Chlorodiphenylphosphine-Quenched Monolithiation of 201d . | 88 |
| Table 3.2.1.1. NMR Data for Major Products from Dilithiation of 201d . | 95 |
| Table 3.2.1.2. NMR Data for Major Products from Dilithiation of 202d . | 96 |
| Table 3.2.2.1. <i>Ipso</i> -Carbon Chemical Shifts of 207 and 208 Tropicene Derivatives. | 100 |
| Table 3.2.2.2. NMR Data for Major Products from Chlorotrimethylsilane-Quenched Dilithiation of 203d . | 102 |
| Table 3.2.2.3. NMR Data for Major Products from Chlorodimethylsilane-Quenched Dilithiation of 203d . | 103 |
| Table 4.1.1. NMR Data for 211a . | 112 |
| Table 4.1.2. NMR Data for 211b . | 113 |
| Table 4.1.3. NMR Data for 212a . | 114 |
| Table 4.1.4. NMR Data for 212b . | 115 |
| Table 4.1.5. NMR Data for 213a . | 116 |

| | |
|---|-----|
| Table 4.1.6. NMR Data for 213b . | 117 |
| Table 4.2.1. NMR Data for 214a . | 128 |
| Table 4.2.2. NMR Data for 214b . | 130 |
| Table 4.2.3. NMR Data for 215 . | 123 |
| Table 4.3.1. NMR Data for 216a . | 139 |
| Table 4.3.2. NMR Data for 216b . | 140 |
| Table 4.3.3. NMR Data for 216c . | 141 |
| Table 4.3.4. NMR Data for 217a . | 142 |
| Table 4.3.5. NMR Data for 217b . | 143 |
| Table 4.3.6. NMR Data for 217c . | 144 |
| Table 4.3.7. NMR Data for 218 . | 145 |
| Table 4.4.1. NMR Data for Polymer/Oligomer 219a . | 161 |
| Table 4.4.2. NMR Data for Polymer/Oligomer 219b . | 162 |
| Table 4.4.3. NMR Data for Polymer/Oligomer 219c . | 163 |
| Table 4.4.4. NMR Data for Polymer/Oligomer 220 . | 164 |
| Table 5.1.1. Hydrosilylation of Phenylacetylene Using Various Silanes. | 169 |
| Table 5.1.2. Hydrosilylation of 4-Ethynyltoluene Using Various Silanes. | 170 |
| Table 5.1.3. Hydrosilylation of 2-Ethynylthiophene Using Various Silanes. | 171 |
| Table 5.1.4. ¹ H NMR data for products from reactions in Table 5.1.1 . | 172 |
| Table 5.1.5. ¹ H NMR data for products from reactions in Table 5.1.2 . | 173 |
| Table 5.1.6. ¹ H NMR data for products from reactions in Table 5.1.3 . | 174 |
| Table 5.2.1.1. NMR data for 233B . | 178 |
| Table 5.2.1.2. NMR data for 234B . | 178 |

| | |
|---|-----|
| Table 5.2.3.1. Reaction 223 Monitored by ^1H NMR. | 182 |
| Table 5.2.3.2. Reaction 224 Monitored by ^1H NMR. | 183 |
| Table 5.2.3.3. Product Distribution of Reaction 223 <i>Bis</i> -Adducts via Path $\beta(\text{E})$ - or α -. | 187 |
| Table 5.2.3.4. Product Distribution of Reaction 224 <i>Bis</i> -Adducts via Path $\beta(\text{E})$ - or α -. | 187 |
| Table 5.2.3.5. Distribution of 223 <i>Bis</i> -Adducts via Path $\beta(\text{E})$ - or α - from Table 5.2.3.1 . | 188 |
| Table 5.2.3.6. Distribution of 224 <i>Bis</i> -Adducts via Path $\beta(\text{E})$ - or α - from Table 5.2.3.2 . | 188 |

Chapter 1. Introduction

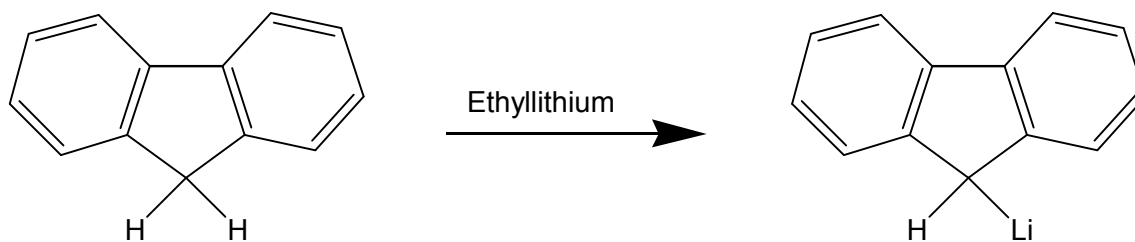
This thesis describes the lithiation of (η^7 -cycloheptatrienyl)(η^5 -cyclopentadienyl)titanium(II),⁶ or troticene,⁷ and the Pt-catalyzed hydrosilylation of alkynes with dimethylsilyl-derivatives of troticene and ferrocene. The introduction is divided into two parts. The first part (**Section 1.1**) deals with lithiation, particularly that of aromatic and other unsaturated ring systems as well as metallocenes such as ferrocene and troticene. The second part (**Section 1.2**) deals with Pt-catalyzed hydrosilylation of alkynes which includes a study by Jain and coworkers involving the hydrosilylation polymerization of ferrocene dimethylsilyl-derivatives.^{4,5}

1.1. Lithiation Reactions

Metallation can be described as a process by which a hydrogen atom is replaced by a metal (such as -Na, -K, and -Li) or groups containing metals (such as -MgBr and -HgOAc) to form an organometallic compound.⁸⁻¹⁰ While there are a variety of reagents that can be used for metallation, organolithium reagents and Grignard reagents are the most widely used for organic and organometallic synthesis, generally being much more soluble in organic solvents, less reactive with ethers (a commonly used solvent in metallations) than organosodium and organopotassium compounds, and less toxic than organomercury compounds.¹¹ Compared with Grignard reagents, organolithiums are generally more reactive, as illustrated by phenyllithium and phenylmagnesium bromide, allowing for ease in further derivatization. While the former was able to react with both *p*-bromoanisole and 1,3-dimethoxy-4,6-dibromobenzene via metallation and metal-

halogen exchange, respectively, the latter was unable to do so.^{11,12} Organolithium reagents such as *n*-, *sec*-, and *tert*-butyllithium are also commercially available due to the fact that they are effective catalysts for the industrial process of synthetic rubber production via the organolithium initiation route.^{11,13-18} The available literature on the preparation of organolithiums is much too extensive for the purpose of this introduction, and detailed information on this subject can be found in published reviews.^{10,19-21} For the most part, the metallation reactions covered in this introduction involve the use of organolithium reagents in lithiation reactions of aromatic and other unsaturated ring systems to be specific.

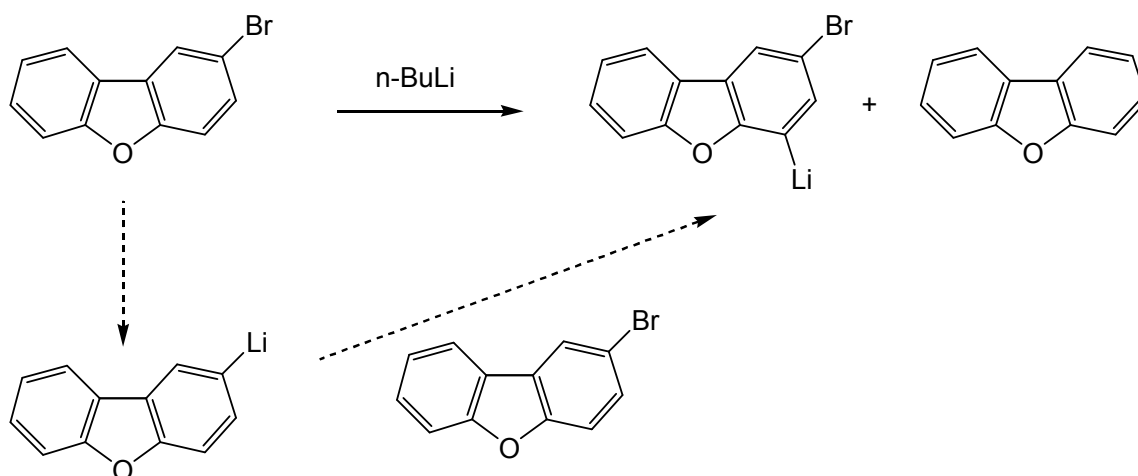
The first lithiation reaction was reported by Schlenk and Bergmann in 1928, in which fluorene was reacted with ethyllithium resulting in lithium replacing an acidic hydrogen (**Scheme 1.1.1**).^{19,22} Over the years, metallations using organolithium reagents has been applied to a wide variety of compounds, with butyl- and phenyllithium being the most commonly used due to their availability.¹⁹ The synthetic utility of lithiations have long been recognized by virtue of the reactivity of the lithiated product, capable of reacting with electrophiles, allowing for further derivatization into a wide array of products.²³⁻²⁶



Scheme 1.1.1. Lithiation of Fluorene with Ethyllithium.

The presence of potentially acidic hydrogen is an important prerequisite for lithiations.^{10,19,20,23,27} In aromatic rings and various heterocycles, the relative acidity of the protons is influenced by inductive effects of ring substituents.^{9,12,28} Factors which increase the acidity of the hydrogens, such as electron-withdrawing groups, facilitate lithiation,¹⁹ while methyl and other alkyl groups deactivate the ring towards metallation.²⁹⁻³¹

While the identity of the products obtained from quenched metallation reactions usually reflect the site where lithiation initially occurred during the course of the reaction, this is not always the case. One example is the two-stage lithiation of 2-bromodibenzofuran with *n*-butyllithium. 2-Bromodibenzofuran initially underwent halogen-metal exchange to give 2-lithiodibenzofuran, which then lithiated unreacted 2-bromodibenzofuran to give 2-bromo-4-dibenzofuryllithium (based on the carbonation derivative) along with dibenzofuran (**Scheme 1.1.2**).^{32,33} Literature on rearrangement of organolithiums is extensive and more information can be found in published reviews.^{10,20,34}



Scheme 1.1.2. Reaction of 2-Bromo-dibenzofuran with *n*-Butyllithium.

1.1.1. Factors Affecting Lithiation

Many factors can affect the outcome of a reaction between an organolithium reagent and a substrate. These include solvents and additives used, reaction temperature, the kind of organolithium reagent used, and of course, the nature of the substrate itself. In the following sections, a few examples are used to illustrate the effects these factors can have on lithiations.

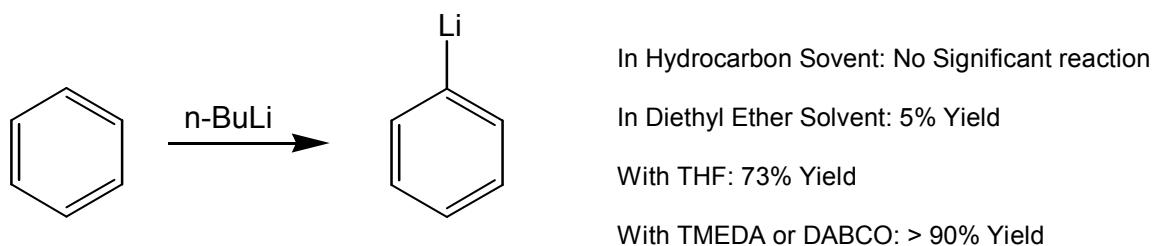
1.1.1.1. Effect of Lewis Basic Solvents and Additives

Organolithiums usually exist as aggregates,^{20,35,36} and in some cases, are relatively inert unless activated by complexation with an electron donor (Lewis bases such as ethers and amines), with the effect, in general, becoming more pronounced with increasing Lewis basicity.^{20,36}

Lewis basic solvents (such as diethyl ether and THF) and additives (such as TMEDA, DABCO, and *t*-BuOK) facilitate lithiations by being able to coordinate with the electron deficient organolithium compounds.^{14,20,21,23,36-42} This, in effect, partially breaks up the organolithium aggregates,^{20,43-46} making lithiation more kinetically favorable.^{14,20,38,41,47-49}

An example is *n*-butyllithium, which exists as a hexamer in benzene and cyclohexane,^{35,50-52} a tetramer in diethyl ether and THF,^{35,52-54} and either a dimer or monomer in the presence of TMEDA,^{14,40,42,55} depending on the R-Li / TMEDA ratio and concentration. Comparable observations have been made for methyllithium, ethyllithium, and *t*-butyllithium in various solvents.^{35,44-46,51,52,56}

The kinetic enhancement in reactivity gained by the break-up of the organolithium aggregates is illustrated by the lithiation of benzene, which is relatively inert towards hexameric *n*-butyllithium in hydrocarbon solvents.^{23,57-59} Reaction with tetrameric *n*-butyllithium in diethyl ether did not fare much better, reacting slowly and gave poor yield (about 5 % yield).^{10,57} Much better results (73 % yield) were obtained when THF was used.^{20,60} Lithiation with the aid of additives such as TMEDA or DABCO gave the best results, with shorter reaction times and high yields (at least 90 %) (Scheme 1.1.1.1.1).^{20,23,38-41,55,61} Using *n*-butyllithium with *t*-BuOK was similarly successful in metallating (and even dimetallating) benzene.^{21,62,63}



Scheme 1.1.1.1.1. Lithiation of Benzene.

In addition to breaking up the organolithium aggregates, coordination of Lewis bases also enhances the reactivity of organolithium compounds by increasing the ionic character of the Li-C bond (increased negative charge on the carbanion).^{14,40,41,55,64} An example is *n*-butyllithium, whose proton NMR showed an upfield shift in the α -methylene protons of *n*-butyllithium when complexed with TMEDA, attributed to an increase in the negative charge of the carbanion. This was accompanied by a significantly increased reactivity of the *n*-butyllithium/TMEDA complex relative to the uncomplexed

organolithium reagent.^{55,64} Similar observations were also found in the use of other amines as well as ethers.^{10,14,19-21,23,36-41,65}

More examples on the effect of Lewis basic solvents and additives on organolithium reactivity can be found in the literature.^{20,23,43-45,59,66-79}

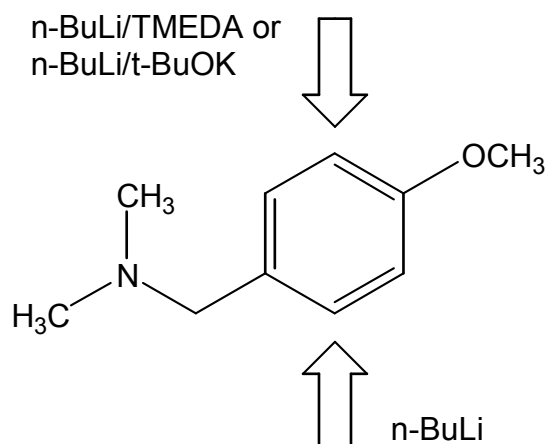
Solvents can affect the stability of the organolithium reagent. Organolithiums are known to be relatively unstable in ethereal solvents compared to hydrocarbon solvents.^{19,20,41,80-84} While ethereal solvents give the benefit of enhanced reactivity,^{10,20} they can be detrimental under certain conditions, reacting with the organolithium reagent itself which can compete with the desired metallation reaction.^{19,80-86}

The typical pathway for a reaction of organolithiums with ethereal solvents is via ether cleavage leading to alkenes and lithium alkoxides.^{19,20,81,86-90} Among alkyllithiums, secondary and tertiary alkyllithiums generally react more rapidly with ethers than primary alkyllithiums, with methyllithium being the most stable.^{20,81,85,86,91} Aryllithiums in general react slower with ethers than alkyllithiums (except methyllithium).^{20,81,86}

Certain ethers are more easily cleaved than others. As an example, *n*-butyllithium has a half-life of 18 days in diisopropyl ether at 25 °C, 6 days in diethyl ether, and only 10 minutes in DME (1,2-dimethoxyethane).⁹² Another example is *t*-butyllithium, with a half-life of 483 ± 25 minutes in diethyl ether at -20 °C, and only 42 ± 3 minutes in THF.⁹³ Methyl- and phenyllithium are similarly more stable in diethyl ether than in THF.^{20,90,94} More information on the relative stabilities of organolithium reagents in ethereal solvents can be found in the literature.^{19,20,71,81,83,86-89,93-102}

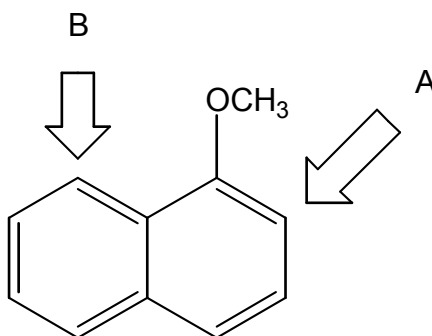
The use of additives can affect the regioselectivity of a given lithiation reaction. Organolithium reagents activated by electron donors attack the most acidic site,

usually adjacent to the most electron withdrawing group.³⁶ This was apparent in the metallation of 4-methoxy-N,N-dimethylaminomethylbenzene, which has two different functional groups on the benzene ring. Using *n*-butyllithium alone, the position *ortho*- to the dimethylaminomethyl- group was metallated.^{103,104} In contrast, when *n*-butyllithium/TMEDA was used, the position *ortho*- to the methoxy- group was metallated predominantly (**Scheme 1.1.1.1.2**).^{38,103} Alternatively, that same position was also selectively metallated using *n*-butyllithium/*t*-BuOK.¹⁰⁵



Scheme 1.1.1.1.2. Lithiation of 4-methoxy-N,N-dimethylaminomethylbenzene.

Another example is the lithiation of 1-methoxynaphthalene with either *n*-butyllithium or *n*-butyllithium/TMEDA . Using *n*-butyllithium gave a mixture of products derived from the 2-lithio- and 8-lithio-derivatives, the former comprising about 72 % of the total amount of products. The selectivity (as well as yield) was improved with the use of *n*-butyllithium/TMEDA instead, increasing the percentage of the 2-lithio-derivative to > 99.3 % of the total amount of products (**Scheme 1.1.1.1.3**).^{41,106}



Major sites for Lithiation

Using *n*-BuLi: A = 72% of total products

Using *n*-BuLi/TMEDA: A > 99.3 %

Scheme 1.1.1.1.3. Lithiation of 1-Methoxynaphthalene.

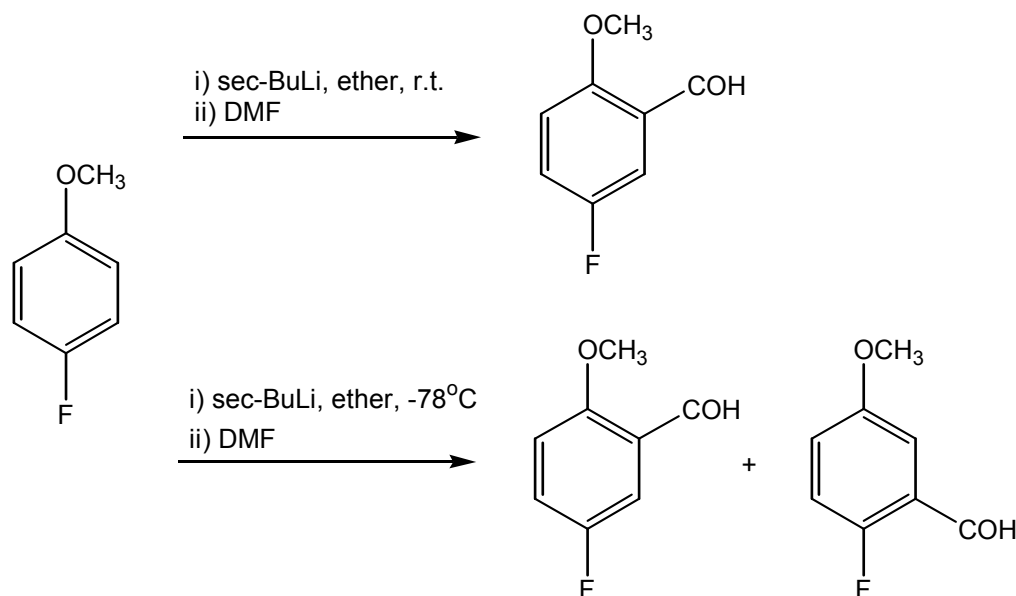
1.1.1.2. Effect of Temperature

Reaction temperature is a significant factor in lithiation reactions, potentially affecting the reaction rate, regioselectivity of the reaction, stability of the organolithium reagent, isomerization/rearrangement of the lithiated product, and promoting or minimizing side reactions, among others.

Temperature can affect the rate of lithiation. An example is the lithiation of ferrocene with *n*-butyllithium. At -8 °C, the reaction was only 16 % complete after 5 hours. In contrast, the reaction carried out at 25 °C was virtually complete after the same length of time.⁷⁰ Another example is the lithiation of 1,4-di(*tert*-butyl)benzene with *n*-butyllithium/*t*-BuOK, whose yield was increased from 10 % to 24 % when the temperature was increased from 25 °C to 75 °C.¹⁰⁷

Temperature can affect the regioselectivity of lithiation. This was observed in the lithiation of 4-fluoroanisole with *sec*-butyllithium. Lithiation at room temperature

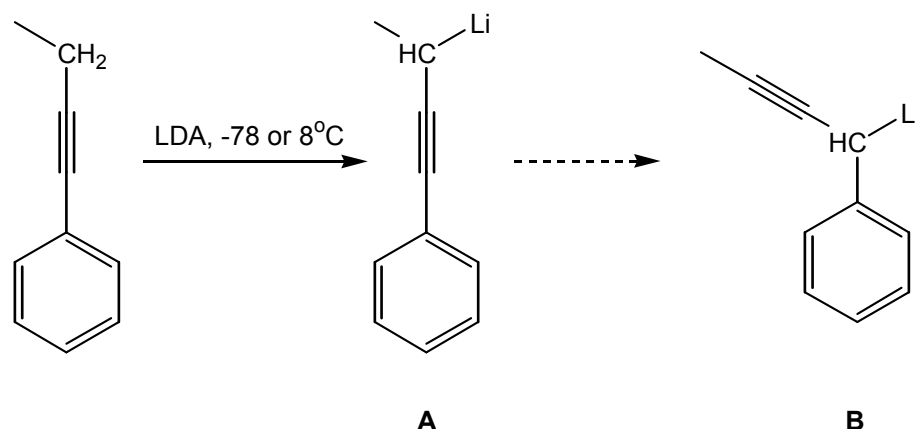
followed by DMF quench gave 5-fluoro-2-methoxybenzaldehyde as the only detectable product, a result of lithiation *ortho*- to the methoxy- group. In contrast, the reaction carried out at $-78\text{ }^{\circ}\text{C}$ gave an additional detectable product, 2-fluoro-5-methoxybenzaldehyde, a result of lithiation *ortho*- to the fluoro- group (**Scheme 1.1.1.2.1**).^{103,108}



Scheme 1.1.1.2.1. Lithiation of 4-Fluoroanisole with *sec*-Butyllithium.

Temperature can promote or minimize side reactions. The lithiation of 3-fluoroanisole led to preferential lithiation at the 2-position, *ortho*- to both substituents. At $-35\text{ }^{\circ}\text{C}$ or higher, this reaction was accompanied by extensive benzyne formation. This unwanted side-reaction was minimized by doing the reaction at $-75\text{ }^{\circ}\text{C}$.¹⁰⁹⁻¹¹¹ A similar observation was made in the lithiation of fluorobenzene with *n*-butyllithium, where the formation of benzyne from the *ortho*-lithiated product was minimized by keeping the reaction temperature between $-50\text{ }^{\circ}\text{C}$ and $-60\text{ }^{\circ}\text{C}$.¹¹²⁻¹¹⁶

Temperature can promote isomerization of the lithiated product. The lithiation of 1-aryl-1-butyne with LDA can result in the preferential formation of one of two possible lithiated products, their ratio being affected by the temperature (**Scheme 1.1.1.2.2**). At $-78\text{ }^{\circ}\text{C}$, lithiation preferentially occurred at the 3-position of the butyne to give lithiated product **A** (**A** / **B** = 91 / 9). However, at $8\text{ }^{\circ}\text{C}$, product **A** undergoes a 1,3-lithium shift to preferentially give lithiated product **B** (**A** / **B** = 0 / 100).^{117,118} Other studies on 1,3-lithium shifts can be found in the literature.¹¹⁹⁻¹²¹



Scheme 1.1.1.2.2. Lithiation of 1-Aryl-1-butyne.

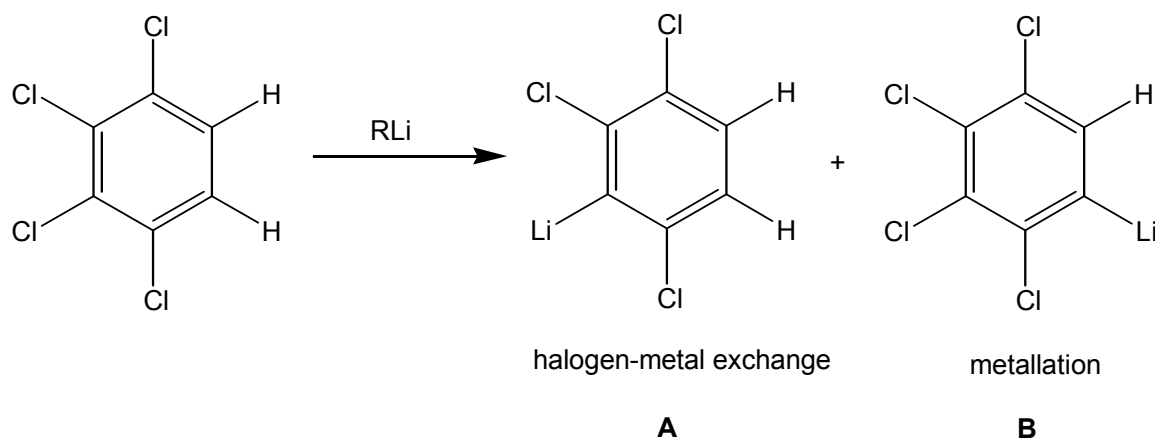
Temperature can affect the stability of the organolithium reagent. Common ethereal solvents, such as diethylether and THF, are more readily cleaved by organolithium compounds at higher temperatures, consuming the organolithium reagent in the process.^{20,86,89,93,94,102} As an example, the half-life of *n*-butyllithium in diethyl ether at $25\text{ }^{\circ}\text{C}$ is 153 hours, compared to only 31 hours at $35\text{ }^{\circ}\text{C}$.⁸⁶ In THF, the half-life of *n*-butyllithium at $-30\text{ }^{\circ}\text{C}$ is 5 days, while it is only 23.5 hours at $0\text{ }^{\circ}\text{C}$.⁹² In another example,

the half-life of *t*-butyllithium in diethyl ether at -20 °C is 483 ± 25 minutes, while at 0 °C, the half-life is 61 ± 8 minutes.⁹³

Aside from being conducive to ether cleavage by organolithiums, elevated temperatures also lead to thermal decomposition of the organolithiums,^{20,86} with primary alkylolithiums (such as *n*-butyllithium) being more stable than tertiary alkylolithiums (such as *t*-butyllithium). The typical products from such decompositions are formed via elimination of lithium hydride to give an alkene.^{20,83,86,122-128} Elimination of lithium hydride can occur readily if the process results in aromatization or an increase in conjugation.^{10,20,129}

1.1.1.3. Effect of the Organolithium Reagent Used

The kind of organolithium reagent used can affect what kind of reaction it will have with a given substrate. As an example, 1,2,3,4-tetrachlorobenzene can preferentially undergo either halogen-metal exchange or metallation, depending on the organolithium reagent employed. Using *n*-butyllithium led to both halogen-metal exchange and metallation, with the reaction showing preference for the former. A similar outcome was achieved with *t*-butyllithium, selectively leading to halogen-metal exchange. In contrast, the use of phenyllithium or methyllithium resulted preferentially in metallation (**Scheme 1.1.1.3.1**). Similar results were obtained from reactions involving 1,2,3-trichlorobenzene.^{130,131}



n-BuLi: Predominantly gives product **A**; **A** / **B** = 72 / 28.

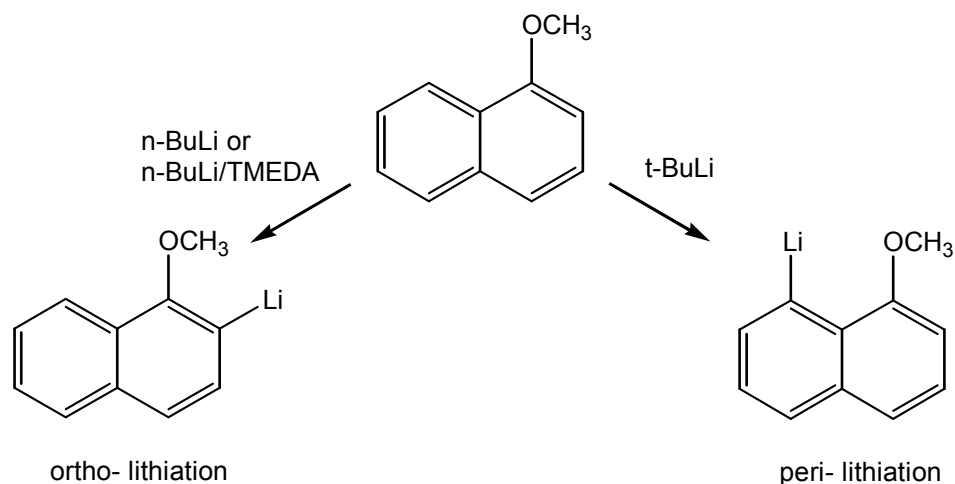
t-BuLi: Exclusively gives product **A**.

PhLi: Predominantly gives product **B**; **A** / **B** = 11 / 89.

MeLi: Predominantly gives product **B**; **A** / **B** = 7 / 93.

Scheme 1.1.1.3.1. Lithiation of 1,2,3,4-Tetrachlorobenzene.

The choice of organolithium reagent can affect regioselectivity. The lithiation of 1-methoxynaphthalene using *n*-butyllithium led to *ortho*-lithiation, while the use of *t*-butyllithium led to *peri*-lithiation (**Scheme 1.1.1.3.2**).^{38,106,132} This was confirmed by experiments conducted by other researchers, although the observed selectivity for the lithiation with *n*-butyllithium/TMEDA, while still favoring lithiation at the *ortho*-position, has a lower selectivity than previously reported by Shirley and coworkers.^{105,132,133} Studies by Betz and coworkers led them to the conclusion that *n*-butyllithium affords the kinetically preferred products, while *t*-butyllithium affords the thermodynamically preferred products.^{105,132}



Scheme 1.1.1.3.2. *Ortho*- and *Peri*-Lithiation of 1-Methoxynaphthalene.

Another example is the metallation of 3,5-dimethoxyphenyl oxazoline. The use of either *n*-butyllithium or *t*-butyllithium in THF at -78 °C led to preferential metallation at the 4-position (*ortho*- to both methoxy groups), while the use of *s*-butyllithium led to preferential metallation at the 2-position (*ortho*- to the oxazoline group).¹³⁴

1.1.1.4. Effect of Ring Substituents

Substituents can activate or deactivate an aromatic ring towards lithiation.

The inductive effect of ring substituents can influence the relative acidity of aromatic ring protons.¹³⁵ While electron withdrawing groups on an aromatic ring facilitate metallation by increasing the overall acidity of the protons,¹⁹ methyl and other alkyl groups deactivate the ring towards metallation.²⁹⁻³¹ As an example, while *n*-butyllithium was unable to metallate benzene to a significant degree,^{10,23,57,58,136,137} it was able to metallate benzene with fluorine or fluorine bearing substituents (such as -CF₃).^{112,135,138,139} Similarly, pentachlorobenzene was metallated by *n*-butyllithium.¹⁴⁰

Substituents can affect lithiation regioselectivity. Depending on their inductive effects or ability to coordinate with organolithium reagents, certain ring substituents are able to direct lithiation to the *ortho*-position. An example is the *ortho*-lithiation of anisole, where lithiation occurs predominantly at the *ortho*-position.^{135,141-143} Another example is the lithiation of m-cresol which was predominantly metallated at the 6-position (59 - 61 %), followed by the 2-position (39 - 41 %), and the methyl group (0.5 %). In both products, lithiation occurred at the positions *ortho*- to the hydroxy- group.¹³⁵ The literature on directed lithiation is much too extensive for the purpose of this introduction, and only a few examples will be mentioned briefly in **Section 1.1.2.3** regarding the directed lithiation of ferrocene derivatives. More information on directed lithiations can be found in the literature.^{8,10,38,144}

The following section of this introduction will deal mainly with the lithiation of sandwich complexes, mainly ferrocene due to the large quantity of literature available on its lithiation and its relevance to the experimental work discussed in **Chapter 2** on the lithiation of (η^7 -cycloheptatrienyl)(η^5 -cyclopentadienyl)titanium(II).

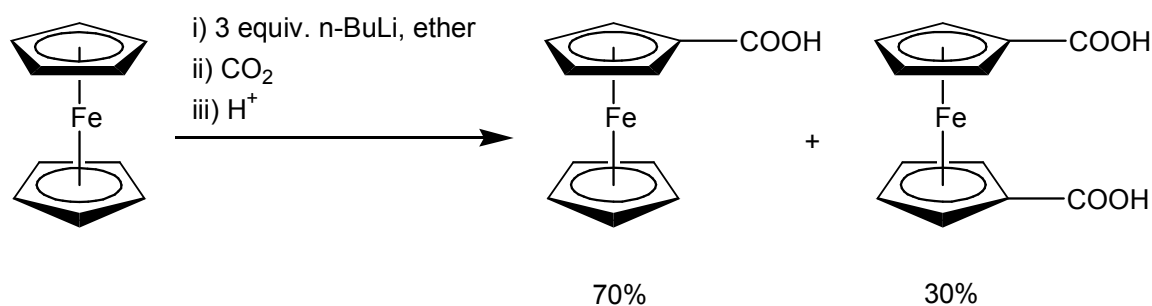
1.1.2. Metallation of Sandwich Complexes

While metallocenes have a well-known ability to undergo electrophilic substitution, many such common reactions such as the introduction of -Cl, -Br, -NO₂, -OH, and -NH₂ have failed due to the tendency of the metal atoms to be oxidized. A tried and true method for the synthesis of substituted metallocenes is the use of alkali metal reagents to form a metallated product, followed by reaction with a variety of electrophiles or other reagents to produce the desired substituted metallocene.^{24,145}

The lithiation of metallocene sandwich complexes, particularly ferrocene, has been extensively studied.^{24,38,146} This is the basis for the work presented in **Chapter 2** on the lithiation of troticene. The next section contains a brief introduction on ferrocene lithiation, as well as the reported lithiations of troticene and other mixed-sandwich complexes.

1.1.2.1. Metallation of Ferrocene

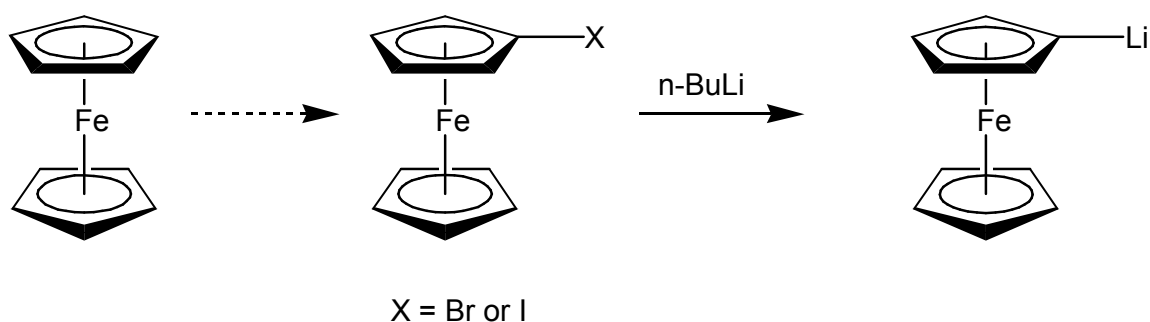
The ease of lithiation of arenes coordinated to transition metals has been noted in the literature, attributed to the decrease in electron density of the ring thus acidifying the ring protons.³⁸ This has been illustrated by the reported lithiation of ferrocene with *n*-butyllithium (first reported independently by Benkeser and Nesmeyanov in 1954), which always led to a mixture of mono- and disubstituted products (**Scheme 1.1.2.1.1**).^{23,41,147-153} In contrast, benzene does not react with *n*-butyllithium to a significant degree in hydrocarbon solvents (**Scheme 1.1.1.1.1**).^{136,137}



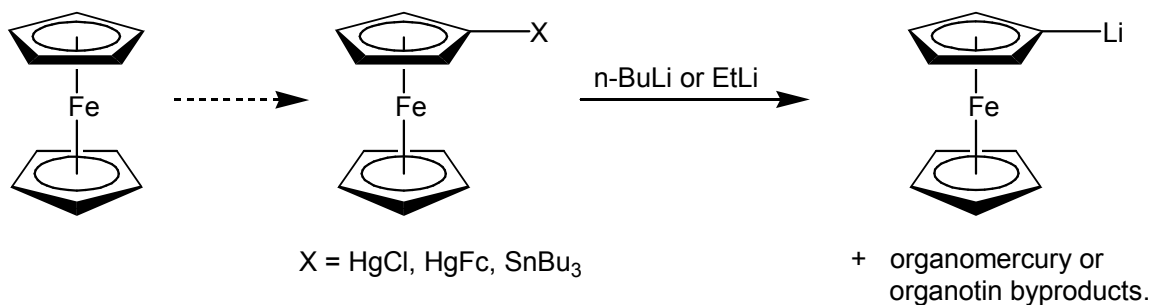
Scheme 1.1.2.1.1. Initial Reports on the Lithiation of Ferrocene.

Monolithiation. Early reports on the preparation of monolithioferrocene from direct lithiation of ferrocene gave poor conversions,^{24,151} or contamination with

dilithioferrocene.¹⁴⁷ Other reported methods are quite inconvenient, such as using a halogen-metal exchange reaction between monohaloferrocenes (bromo- or iodoferrocene) and *n*-butyllithium (**Scheme 1.1.2.1.2**),^{153,154} requiring the tedious preparation of monohaloferrocene as starting material.¹⁵⁵⁻¹⁵⁹ Another method involves using transmetallation of chloromercuriferrocene, diferrocenylmercury, or tributylstannylferrocene with *n*-butyllithium or ethyllithium, giving relatively toxic organomercury or organotin byproducts (**Scheme 1.1.2.1.3**).¹⁶⁰⁻¹⁶⁴ It is preferable if monolithioferrocene can be prepared directly from ferrocene.



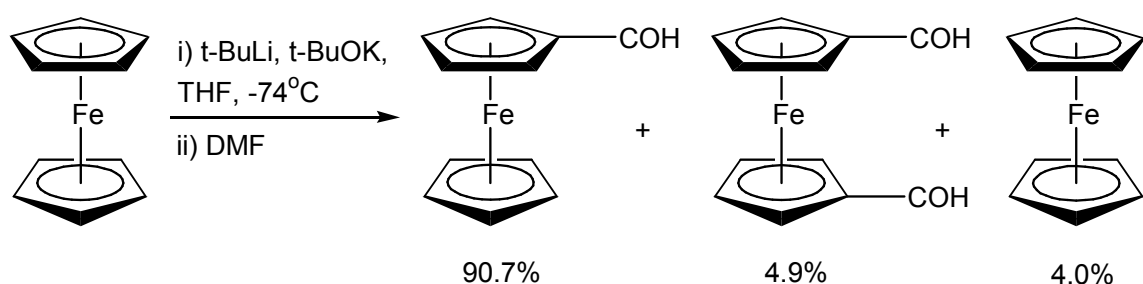
Scheme 1.1.2.1.2. Monolithioferrocene via Halogen-Metal Exchange.



Scheme 1.1.2.1.3. Monolithioferrocene via Transmetallation.

A more convenient procedure was later reported by Rebiere and coworkers, wherein monolithioferrocene was prepared from the reaction of ferrocene with less than 1 equivalent of *t*-butyllithium in THF at 0 °C, although the amounts of dilithioferrocene and recovered ferrocene were not reported.¹⁶⁵ This was later improved upon by Mueller-Westerhoff and coworkers, using excess *t*-butyllithium in THF at -20 °C to give a 91 % yield of ferrocene mono-aldehyde, along with trace amounts of ferrocene dialdehyde and 5 % of recovered ferrocene.¹⁶⁶ These procedures, however, proved to be non-reproducible or unreliable, containing significant quantities of the dilithiated product.^{164,167}

An improved procedure for the monolithiation of ferrocene reported by Sanders and coworkers involved the use of *t*-butyllithium in the presence of *t*-BuOK in THF at -74 °C, achieving good conversions with only small quantities of the dilithiated product (Scheme 1.1.2.1.4).¹⁶⁷ Other reported procedures involved isolation of the monolithioferrocene prior to further derivatization, either via precipitation from THF/Hexane at -80 °C,¹⁶⁸ or crystallization from THF at -30 °C.¹⁶⁹

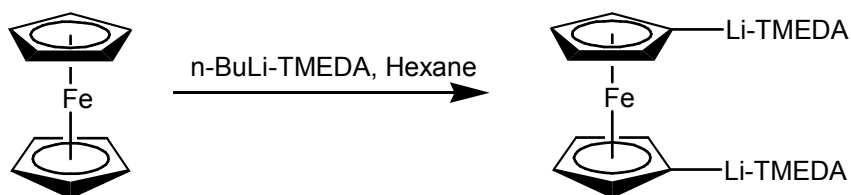


Scheme 1.1.2.1.4. Monolithiation of Ferrocene with *t*-Butyllithium/*t*-BuOK.

Dilithiation. Initial lithiation procedures for ferrocene produced 1,1'-dilithioferrocene, along with large quantities of monolithioferrocene even with the use of

excess of *n*-butyllithium (**Scheme 1.1.2.1.1**).^{70,147-149,160,170} Other procedures for the dimetallation of ferrocene have been reported using phenylsodium or *n*-pentylsodium,^{23,150,160,170-172} although significant quantities of the monosubstituted product were still produced, attributed to an incomplete reaction between the metallated products and the electrophiles.^{160,170} Dimetallation of ferrocene using *n*-pentylsodium produced a mixture of mono- (20 %), di- (60 %), and polymetallated (20 %) products in a relatively low yield (~20-25 %). Doing the reaction in the presence of TMEDA improved the yield and selectivity, producing mono (10-15 %) and dimetallated (85-90 %) products in nearly quantitative yield (90-100 %).¹⁷³

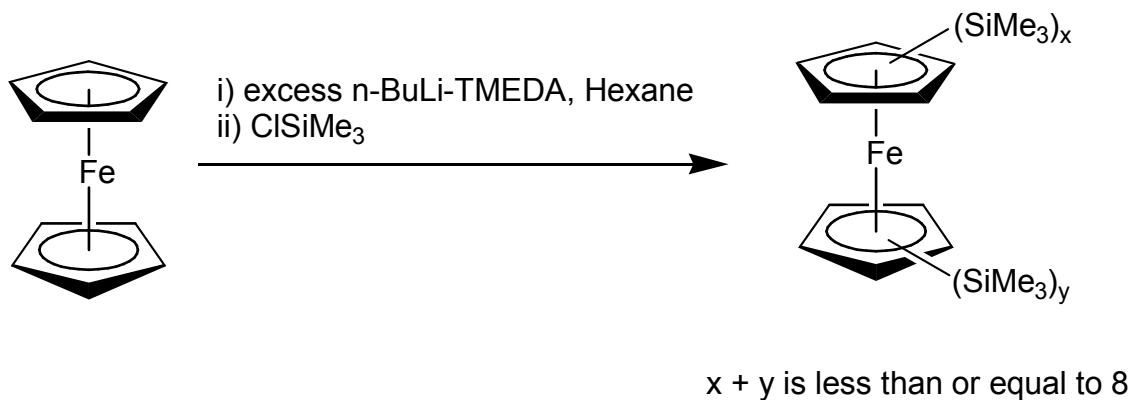
A reported procedure for the successful 1,1'-dilithiation of ferrocene involved the use of *n*-butyllithium in the presence of a chelating tertiary amine such as TMEDA or PMDETA (**Scheme 1.1.2.1.5**).^{23,174,175} The N-chelated dilithioferrocene was isolated with two TMEDA molecules per dilithioferrocene.^{25,174} The improved degree of lithiation with the use of the chelating tertiary amine is reminiscent of the fact that while *n*-butyllithium alone failed to lithiate benzene to a significant degree,^{10,23,57,58,136,137} using *n*-butyllithium with TMEDA or DABCO proved successful (**Scheme 1.1.1.1.1**).^{23,39,40,55,61}



Scheme 1.1.2.1.5. Dilithiation of Ferrocene with *n*-Butyllithium/TMEDA.

Polymetallation. Polymetallation is important due to the potential of the metallated derivatives to be used for the synthesis of polyfunctionalized products in a single step.^{176,177} The susceptibility of metallocenes such as ferrocene to metallation is evidenced by polymetallated products reported from the reaction of ferrocene with sodium,^{173,178} potassium,¹⁷⁹ and lithium¹⁸⁰ reagents.

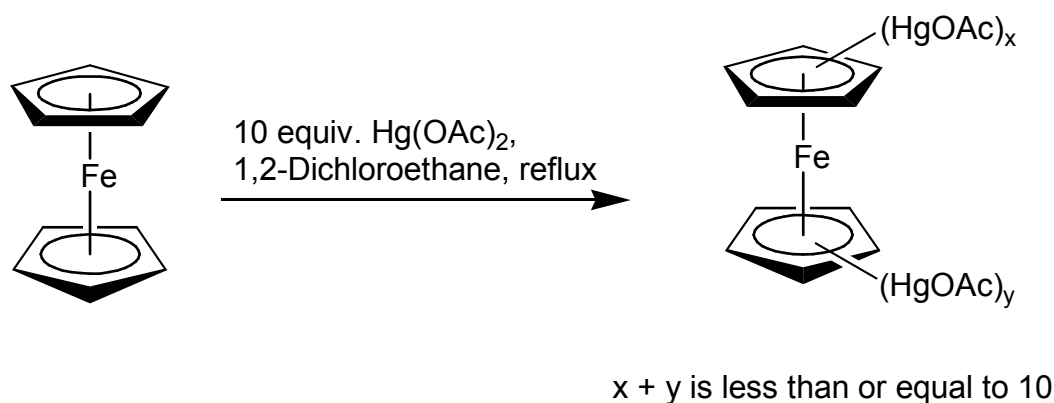
As mentioned earlier, the metallation of ferrocene with excess alkyllithium reagents (2.5 equivalents) in the presence of a chelating diamine such as TMEDA led predominantly to a dilithiated product (**Scheme 1.1.2.1.5**).^{23,174,175} Using an even larger excess (4 to 8 equivalents) along with elevated temperatures produced a mixture products with varying degrees of metallation, ranging from 1 to 8 lithiums on each ferrocene molecule (**Scheme 1.1.2.1.6**).¹⁸⁰



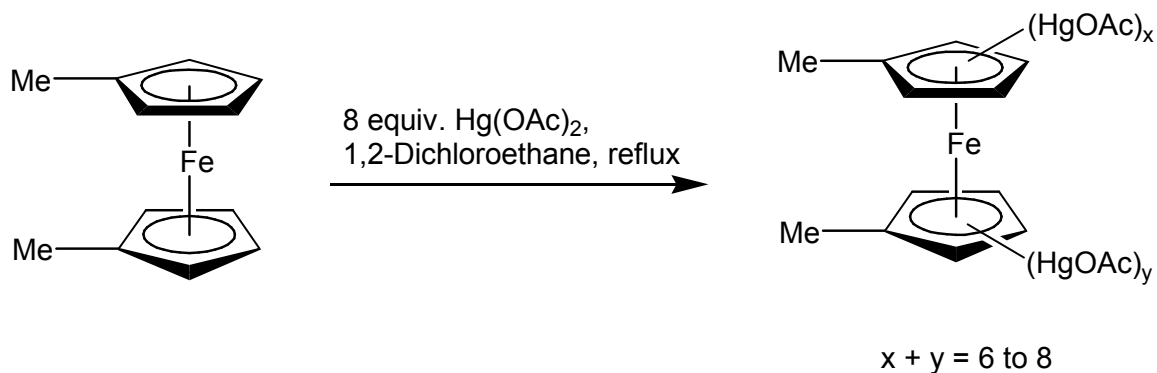
Scheme 1.1.2.1.6. Permetalation of Ferrocene with Excess n -Butyllithium/TMEDA.

While the possibility of polymetallation of ferrocene has been demonstrated by the examples mentioned, these reactions produce a complex mixture of products, diminishing their synthetic utility. Other metallation reagents or methods have been used to obtain more useful results.¹⁸¹ Coworkers Boev and Dombrovskii reported the

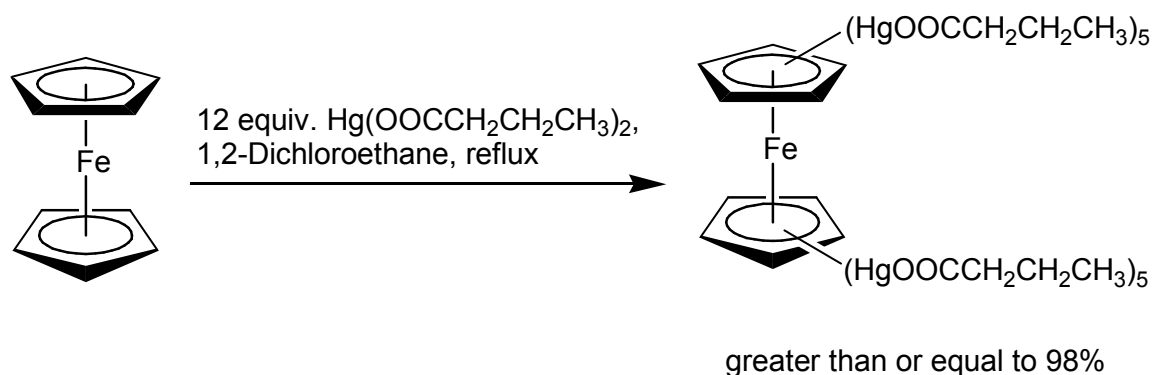
decamercuration of ferrocene, as well the octamercuration of 1,1'-dimethylferrocene using large excesses of mercuric trifluoroacetate.^{182,183} Later studies by Winter and coworkers revealed that these reactions did not effect exhaustive mercuration of the substrates, attributed to insolubility of the higher mercured species (**Scheme 1.1.2.1.7** and **Scheme 1.1.2.1.8**).^{184,185} Exhaustive decamercuration of ferrocene was achieved using a different organomercury compound, mercuric butyrate (12 equivalents), achieving $\geq 98\%$ decamercuration which was attributed to the more lipophilic butyrate groups (**Scheme 1.1.2.1.9**).²⁶



Scheme 1.1.2.1.7. Decamercuration of Ferrocene with Excess Mercuric Acetate.



Scheme 1.1.2.1.8. Octamercuration of 1,1'-Dimethylferrocene with Excess Mercuric Acetate.



Scheme 1.1.2.1.9. Decamercuration of Ferrocene with Excess Mercuric Butyrate.

Ferrocene was tetrametallated using “ $\{\text{NaMg}(i\text{-Pr}_2\text{N})_3\}$ ”, produced from the reaction of 3 equivalents of diisopropylamine ($i\text{Pr}_2\text{NH}$) with an equimolar mixture of *n*-butylsodium and Bu_2Mg , to produce $[\{\text{Fe}(\text{C}_5\text{H}_3)_2\}\text{Na}_4\text{Mg}_4\{i\text{-Pr}_2\text{N}\}_8]$, in which ferrocene is encapsulated by a 16-membered tetrasodium-tetramagnesium amide cationic ring.¹⁸¹ The same method has been employed with success on other sandwich complexes such as ruthenocene and osmocene to produce $[\{\text{M}(\text{C}_5\text{H}_3)_2\}\text{Na}_4\text{Mg}_4\{i\text{-Pr}_2\text{N}\}_8]$, where $\text{M} = \text{Fe}$, Ru , or Os .¹⁷⁷ As seen in **Figure 1.1.2.1.1**, the 1,1',3,3'-positions are deprotonated. These metallated products are of potential synthetic utility, undergoing reactions with various electrophiles to produce various products.^{181,186}

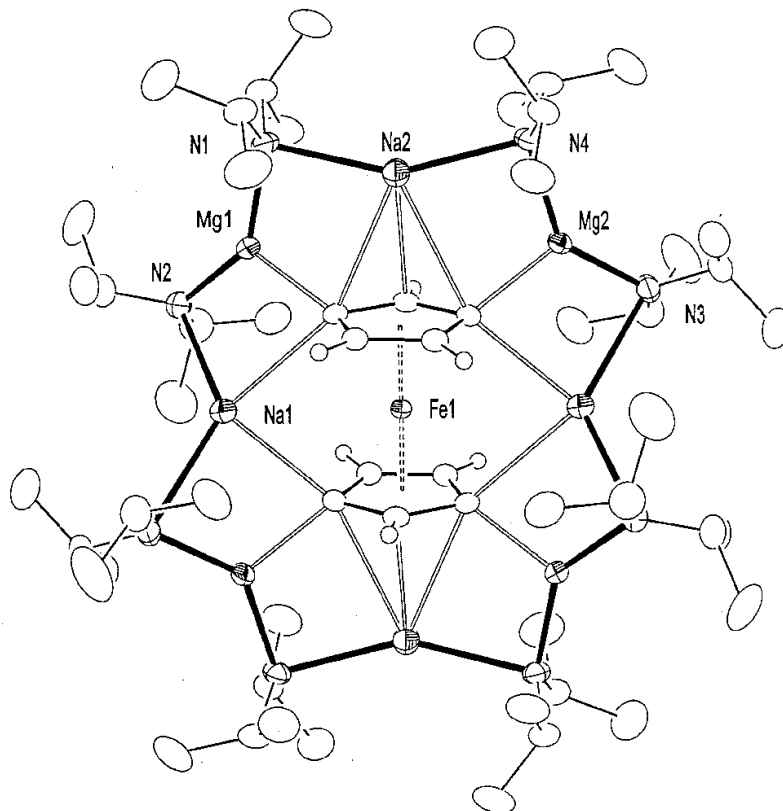


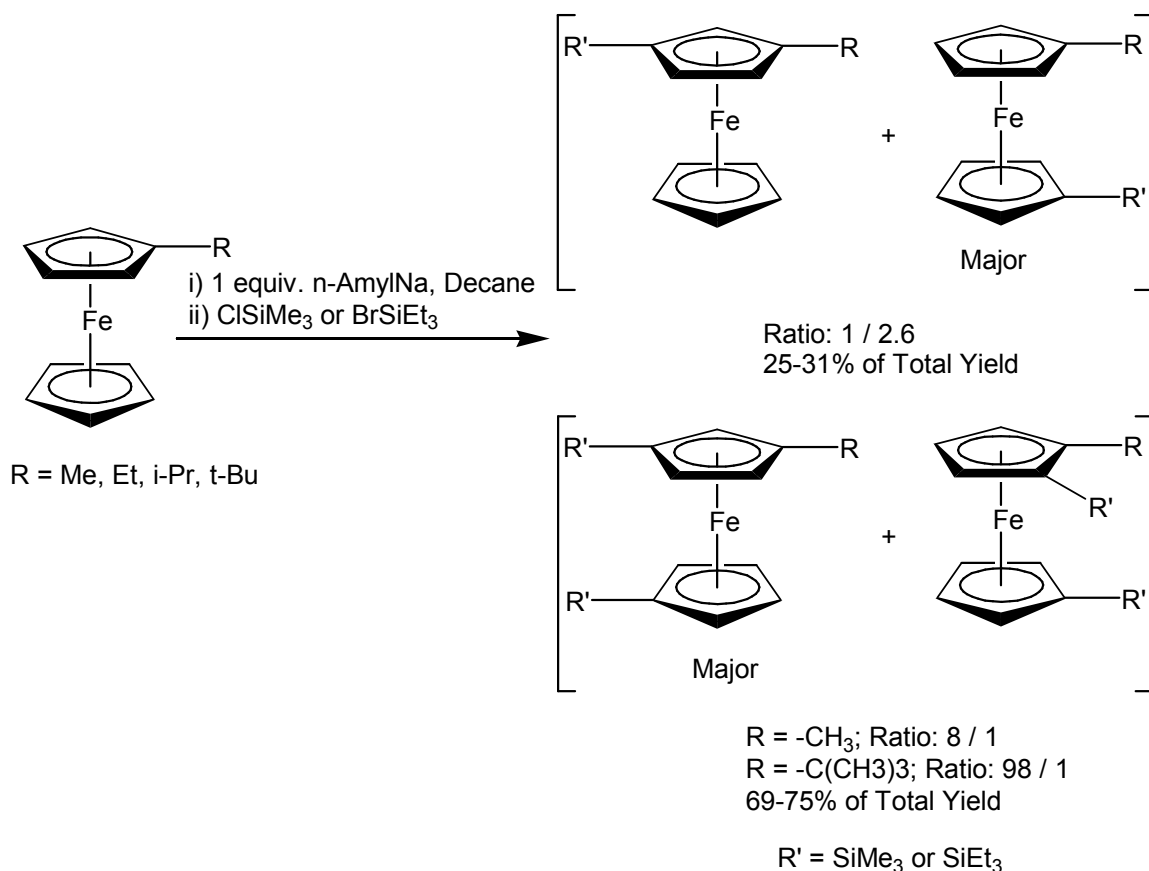
Figure 1.1.2.1.1. Structure of $[\{\text{Fe}(\text{C}_5\text{H}_3)_2\}\text{Na}_4\text{Mg}_4\{i\text{-Pr}_2\text{N}\}_8]$.¹⁷⁷

1.1.2.2. Lithiation of Alkyl Ferrocene Derivatives

The metallation of alkyl ferrocene derivatives has been reported by Nesmeyanov and coworkers.^{152,171,187} Using *n*-butyllithium alone failed to metallate 1,1'-dimethylferrocene, unlike its parent compound, ferrocene (**Scheme 1.1.2.1.1**).^{171,187} This observation is consistent with reports that methyl and other alkyl groups deactivate the ring towards metallation.²⁹⁻³¹ Metallation of 1,1'-dimethylferrocene was accomplished by using a more reactive metallating reagent, *n*-pentylsodium.¹⁸⁷

Benkeser and coworkers studied the metallation of methyl-, ethyl-, isopropyl, and *t*-butylferrocene using *n*-pentylsodium and *n*-pentylpotassium. It was apparent from the metallation of methylferrocene and *t*-butylferrocene that steric effects play a role in

determining the site of lithiation on a substituted Cp ligand. The former gave an 8:1 ratio of the 1,3,1'-trisubstituted to 1,2,1'-trisubstituted products, while the latter gave a ratio of 98:1 (Scheme 1.1.2.2.1).¹⁵²



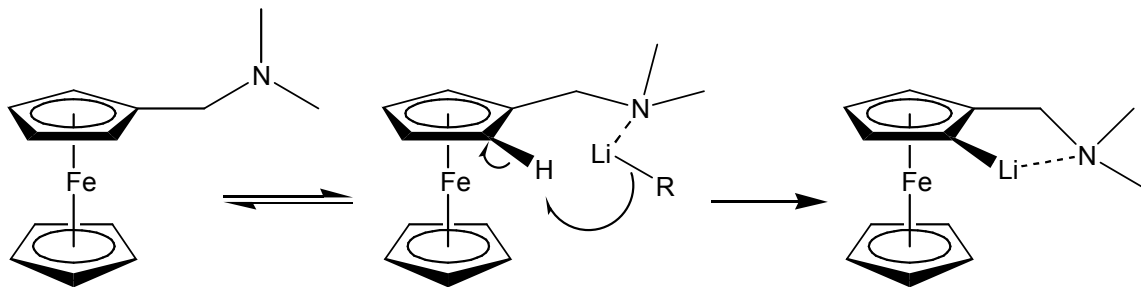
Scheme 1.1.2.2.1. Metallation of Monoalkyl Ferrocenes with *n*-Pentylsodium.

It is apparent that while metallation of alkyl substituent-bearing ferrocenes is possible, they seem to be randomly metallated,^{24,172} hampering their use in synthesis. Other substituents, generally referred to as *ortho*-lithiation directors, lead to more predictable (and thus useful) metallation products.

1.1.2.3. Directed Lithiation of Ferrocene

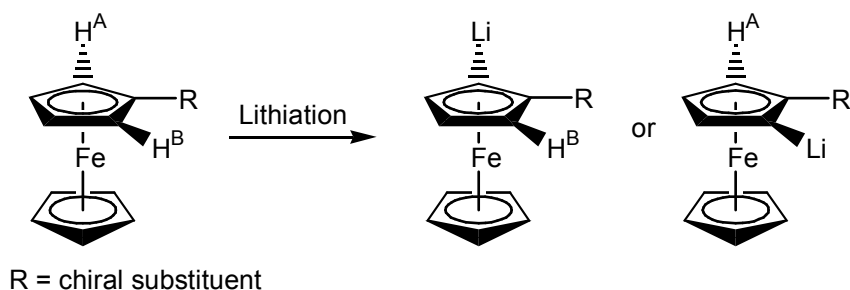
Directed metallations were first reported in the late 1930s, when certain ring substituents were found to direct metallation to an adjacent position.^{8,12,38,132,141,142,188-192} One of the earliest examples is the reaction of anisole with pentylsodium,¹⁸⁸ phenyllithium,¹² and butyllithium,¹⁴¹ all three resulting in metallation at the *ortho*-position. Since then, a wide variety of functional groups have been shown to have a directing effect on metallation reactions, with a large amount of literature and myriads of examples, much too extensive to be covered in this introduction. In general, the same *ortho*-lithiation directing groups used on aromatic rings also work on ferrocene. In contrast to the lithiation of alkyl ferrocene derivatives which occur predominantly at the 1' or 3'- positions,¹⁵² the lithiation of ferrocene derivatives bearing *ortho*-lithiation directing groups lead to lithiation at the 2-position, and have been used to prepare ferrocenes with one or two 1,2-disubstituted Cp ligands.^{24,38}

The directing group must either be able to provide a point of coordination for the lithiating agent in order to increase the reactivity near the coordination site due to favorable geometry, or be electronegative enough to increase the acidity of nearby protons via inductive electron withdrawal.³⁸ In the directed lithiation of N,N-dimethylaminomethylferrocene, coordination of the lithiating agent (with the free electron pair of the amine nitrogen) allowed for lithiation at the 2-position leading to a favorable 5-membered chelate ring (**Scheme 1.1.2.3.1**).^{24,38,191,193,194} The lithiation of methoxy and ethoxymethylferrocene similarly resulted in lithiation at the 2-position.¹⁹⁵⁻¹⁹⁷ More information on directed metallation reactions can be found in the literature.^{8,10,20,24,38,132,144,191,198-202}

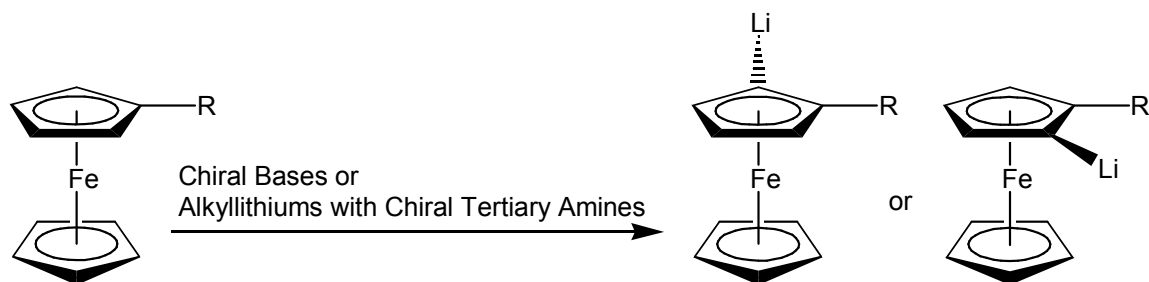


Scheme 1.1.2.3.1. Lithiation of N,N-Dimethylaminomethylferrocene.

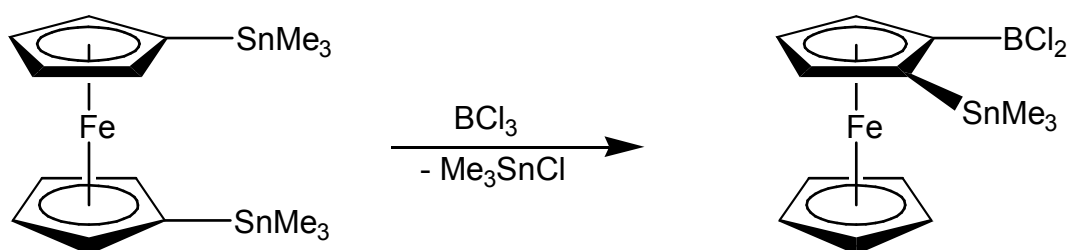
Certain *ortho*-lithiation directing groups on ferrocene facilitate enantioselective directed lithiation leading to planar chiral ferrocene derivatives, some of which are useful ligands. Enantioselective directed lithiation can be achieved in two ways: **Method A)** Using a ferrocene derivative with a chiral substituent which can direct lithiation to one of the two diastereotopic protons (H^a or H^b from **Scheme 1.1.2.3.2**), or **Method B)** Using a chiral base to selectively remove one of two enantiotopic protons (**Scheme 1.1.2.3.3**). Both methods have been pioneered by Aratani and coworkers.^{38,203,204} Alternatively, planar chiral ferrocene derivatives have been prepared by Jäkle and coworkers via borylation of 1,1'-bis(trimethylstannyl)ferrocene (**Scheme 1.1.2.3.4**).^{205,206} More information on the synthesis of planar chiral ferrocene derivatives can be found in the literature.³⁸



Scheme 1.1.2.3.2. Diastereoselective Lithiation of Ferrocenes.



Scheme 1.1.2.3.3. Enantioselective Lithiation of Ferrocenes.



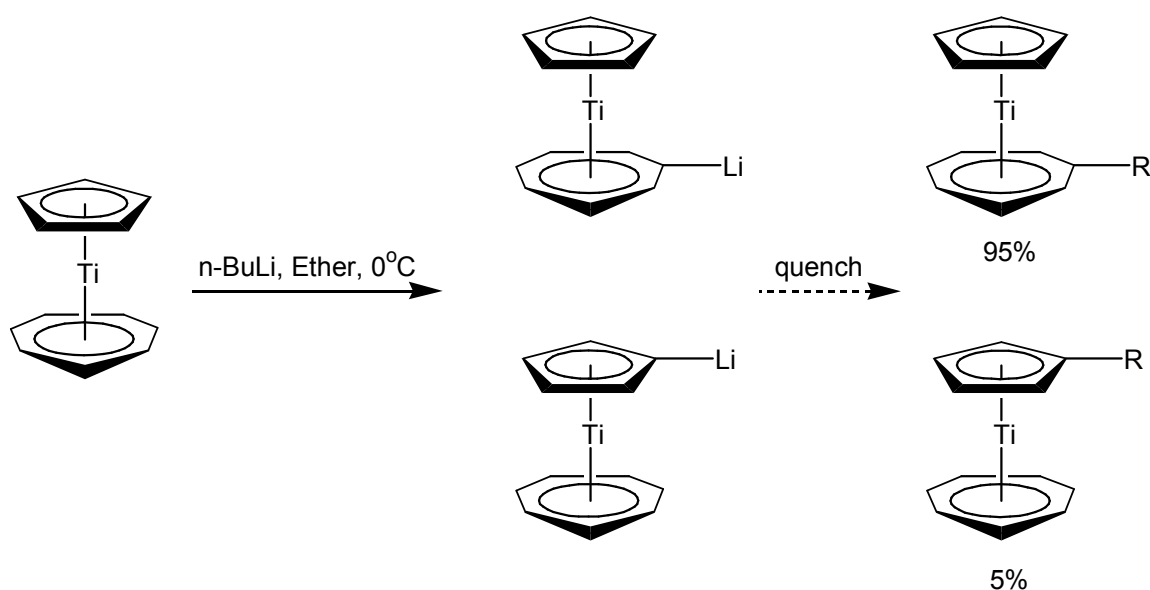
Scheme 1.1.2.3.4. Borylation of 1,1'-Bis(trimethylstannyl)ferrocene.

1.1.2.4. Lithiation of Tropicene

As in the case of ferrocene, the mixed sandwich complex (η^7 -cycloheptatrienyl)(η^5 -cyclopentadienyl)titanium(II),⁶ or tropicene,⁷ can be lithiated using organolithium reagents, allowing for further derivatization by reacting the metallated product with various reagents.^{1,2,207}

Monolithiation. Being a mixed sandwich complex, it is to be expected that the two ring ligands of tropicene (a cycloheptatrienyl ring and a cyclopentadienyl ring) would behave differently in a given lithiation reaction condition. The monolithiation of tropicene was first reported by Groenenboom and coworkers, wherein the reaction carried out using

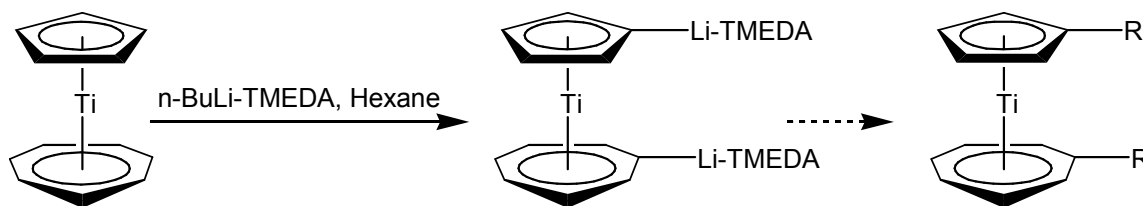
one equivalent of *n*-butyllithium at 0 °C in diethyl ether resulted in preferential monolithiation at the cycloheptatrienyl ligand. Based on the total monosubstituted product yield of the reported iodomethane-quenched reaction, 95 % of the monolithiation occurred at the cycloheptatrienyl ligand, while only 5 % occurred at the cyclopentadienyl ligand (Scheme 1.1.2.4.1).^{1,2} Other derivatives prepared in a similar fashion include mono- trimethylsilyl-,²⁰⁷ diphenylphosphino-,^{208,209} and carboxy-²¹⁰ derivatives. The observed preferential lithiation of the cycloheptatrienyl ligand has been attributed to its stronger negative charge compared with the cyclopentadienyl ligand.^{1,2,211,212}



Scheme 1.1.2.4.1. Monolithiation of the Cycloheptatrienyl Ligand of Tropicene.

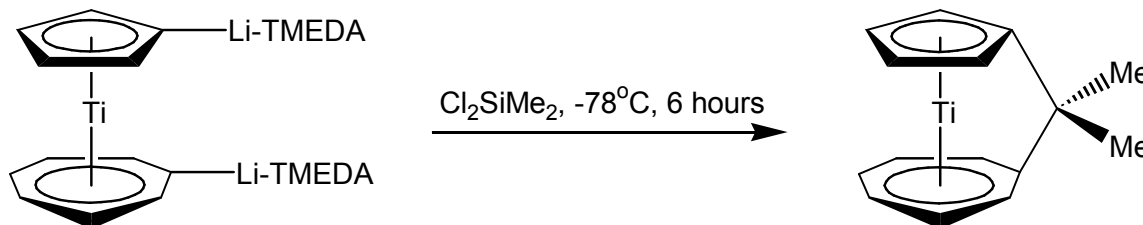
Dilithiation. Just like ferrocene, dilithiation of tropicene has been achieved with *n*-butyllithium/TMEDA (Scheme 1.1.2.4.2), yielding tropicene derivatives with one substituent on both the cycloheptatrienyl and cyclopentadienyl ligands.³ These include

1,1'-dimethyl-,¹ *bis*(trimethylsilyl)-,²¹⁰ *bis*(diphenylphosphino)-,^{3,213} *bis*(dimethylphosphino)-,²¹⁴ and dicarboxy-²¹⁰ derivatives.



Scheme 1.1.2.4.2. Dilithiation of Tropicene.

Aside from the unstrained 1,1'-disubstituted derivatives, strained *ansa*-bridged silatroticenophane derivatives have been prepared from 1,1'-dilithiotropicene (**Scheme 1.1.2.4.3**).^{7,215,216} The main difference was that the lithiation reaction was quenched with dichlorodimethylsilane at a very low temperature (-78 °C) over a relatively long period of time (6 hours). A similar protocol was employed for the synthesis of germatroticenophane from dilithio-tropicene.²¹⁶



Scheme 1.1.2.4.3. *Ansa*-Bridged Tropicene Derivative.

Lithiation of Substituted Tropicene Derivatives. Groenenboom and coworkers were able to add a second methyl group onto $\{\eta^7\text{-methylcycloheptatrienyl}\}\{\eta^5\text{-}$

cyclopentadienyl)titanium(II) and $\{\eta^7\text{-cycloheptatrienyl}\}(\eta^5\text{-methylcyclopentadienyl})\text{titanium(II)}$ via lithiation. In both cases, substitution occurred on the cycloheptatrienyl ligand.¹

1.1.2.5. Lithiation of other $(\eta^7\text{-C}_7\text{H}_7)$ M $(\eta^5\text{-C}_5\text{H}_5)$ Mixed Sandwich Complexes

The metallation of other $(\eta^7\text{-C}_7\text{H}_7)$ M $(\eta^5\text{-C}_5\text{H}_5)$ mixed sandwich complexes has also been reported in the literature. While trocticene was easily metallated with *n*-butyllithium with or without TMEDA,^{1-3,207} analogous lithiations of trozircene (M = Zr) and trohafcene (M = Hf) were unsuccessful.²¹⁷

The lithiation of trovacene (M = V) at either -10 °C or room temperature with *n*-butyllithium resulted in lithiation at the Cp ring.^{1,2,218,219} As in the case of trocticene, trovacene was similarly dilithiated using *n*-butyllithium/TMEDA, leading to *ansa*-bridged silatrovacenophanes,^{7,215,220,221} and boratrovacenophanes.²²²

While *n*-butyllithium alone was successfully used to lithiate trocticene and trovacene, lithiation of trochrocene (M = Cr) was unsuccessful, although amylsodium was reported to metallate trochrocene at the Cp ring.^{1,2,212,223} Dilithiation of trochrocene was successful with *n*-butyllithium/TMEDA, leading to unstrained 1,1'-disubstituted derivatives, as well as *ansa*-bridged boratrochrocenophanes and silatrochrocenophanes.²²⁴⁻²²⁶

The relative ease of lithiation of the three mixed sandwich complexes (trocticene > trovacene > trochrocene) was attributed to the negative charge on the Cp and Cht ligands as well as the metal contribution into the metal-ligand bonds. It was inferred from qualitative molecular orbital arguments that the Cht ligand becomes more negative in the

sequence $M = Cr < V < Ti$ with increasing metal contribution into the metal-ligand bond in the same trend,^{1,2,212} accounting for the preferential metallation at the Cp ligand of trochrocene and trovacene, and at the Cht ligand of troticene.

1.2. Hydrosilylation Chemistry

Hydrosilylation can be described as the addition of a Si-H bond across an unsaturated bond, and is a very effective method for the synthesis of organosilicon compounds. There are three types of hydrosilylation reactions, depending on the catalyst used: **1) Ionic**; **2) Radical**; and **3) Transition-metal catalyzed**,²²⁷ the latter being the focus of this introduction.

Transition-metal hydrosilylation catalysts are mainly complexes of late transition metals (Groups 8, 9 and 10),²²⁷ and lanthanides.²²⁸ Although first documented in 1949, no specific examples were mentioned until 1953, when platinum deposited on charcoal (Wagner's Catalyst) was used for the hydrosilylation of olefins and alkynes by trichlorosilane.^{229,230} The same catalyst was also used by James Curry in 1956 for the self-hydrosilylation of vinylaryl(alkyl)silanes to form organosilicon polymers and possibly cyclic products, with the regioselective addition of the Si-H bond occurring in either a β - or α - mode.²³¹ In 1957, Speier and co-workers reported the use of chloroplatinic acid (CPA; Speier's Catalyst), which is still in use today, a testament to its effectivity in the synthesis of organosilicon compounds.²³⁰

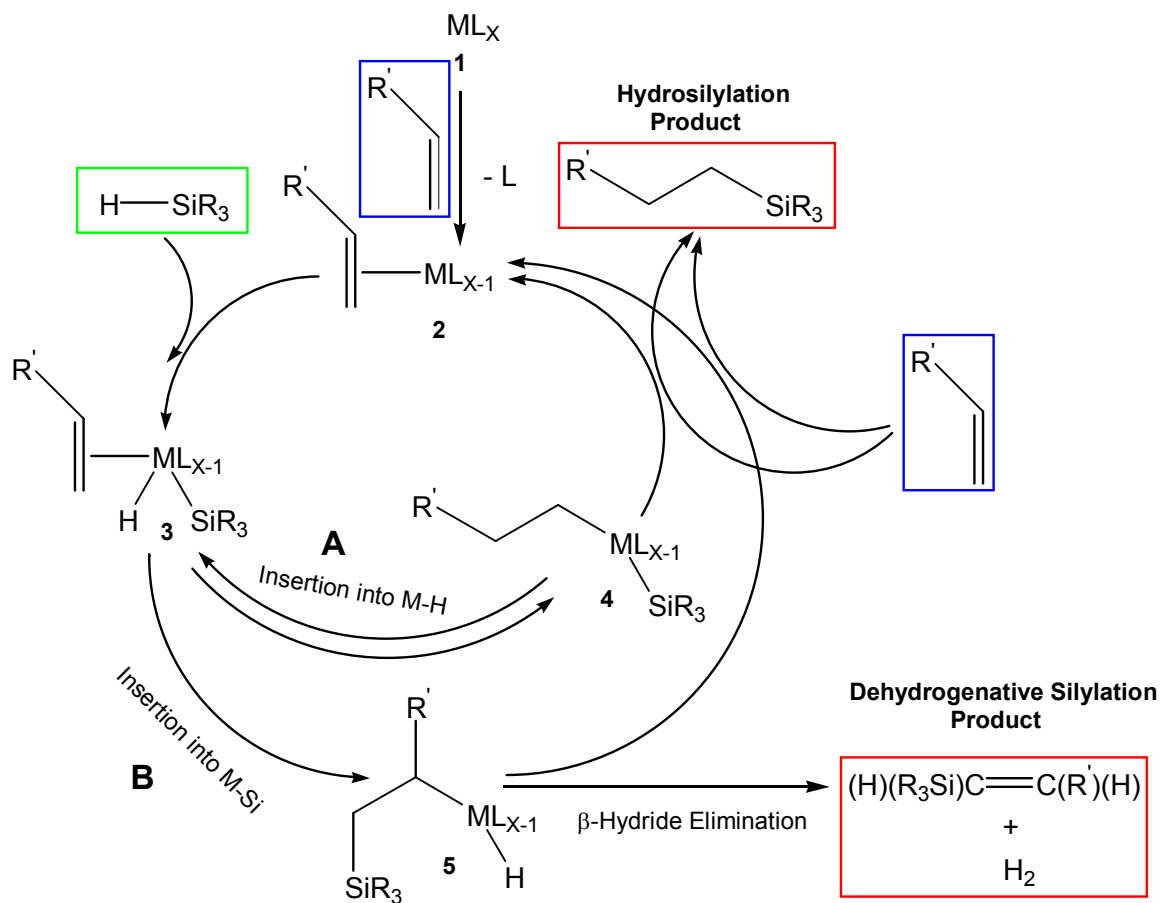
A wide array of transition-metal complexes has since been utilized as hydrosilylation catalysts,^{227,230} and various reaction mechanisms have been proposed to account for the regiochemistry of the products, as well as the fate of the catalysts

themselves. The proposed mechanisms attempt to take into account various factors such as the type of catalysts used, the need for certain co-catalysts, the nature of the substrates (the silane and the unsaturated bond), solvent, and other reaction conditions, all of which can potentially affect the outcome of a particular hydrosilylation reaction.²²⁷

1.2.1. Transition-Metal Catalyzed Hydrosilylation Mechanism

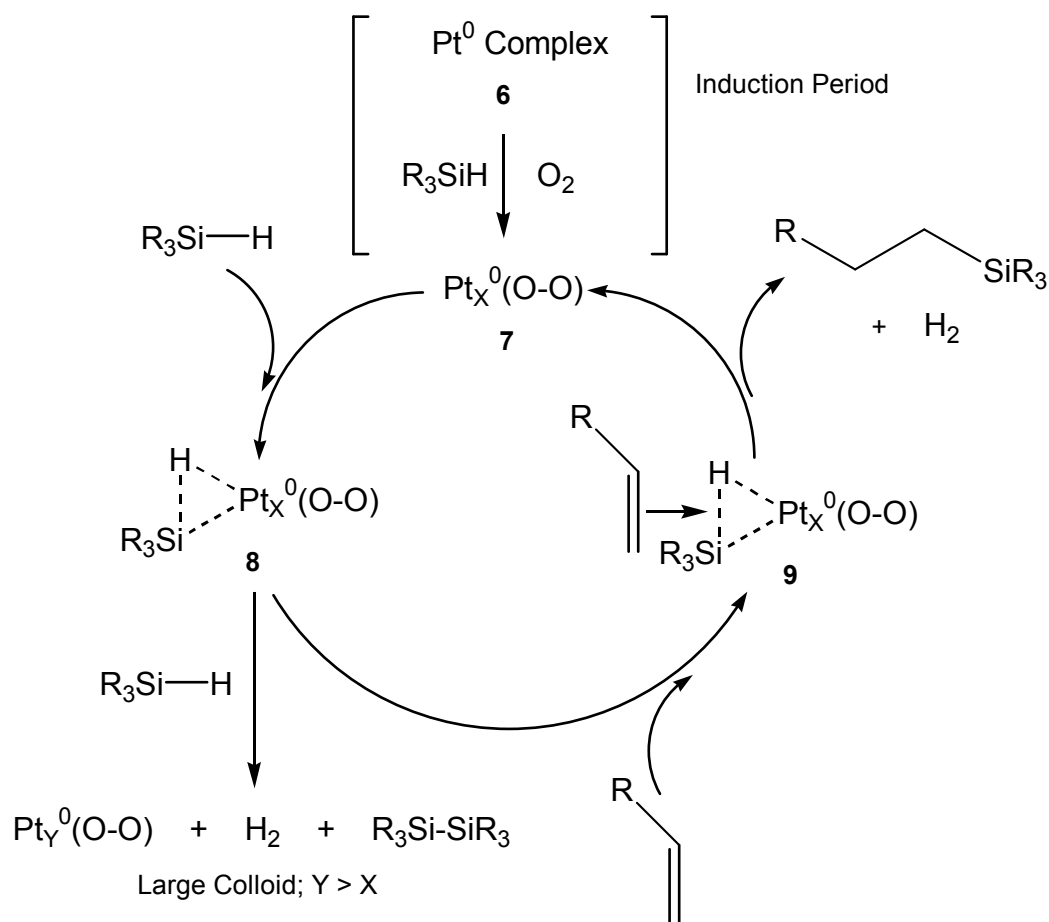
While many schemes have been proposed in the past 50 years or so, a precise understanding of the hydrosilylation reaction mechanism allowing for reaction predictability has been elusive. The Chalk and Harrod mechanism, proposed in 1965, is a general mechanism for metal-complex catalyzed hydrosilylation reactions (**Scheme 1.2.1.1, Route A**),²³²⁻²³⁵ and involves substitution of a labile ligand in an activated d^8 complex **1** with an unsaturated compound to give **2**, with subsequent oxidative addition of a silane to form the d^{10} intermediate **3**. The usual rate-determining step is the insertion of the olefin into the M-H bond to yield **4**, with either a β - or α - regioselectivity. Reductive elimination yields the product and restarts the catalytic cycle.²³³

This mechanism (**Route A**), however, doesn't account for the observed dehydrogenative silylation and disilane byproducts,^{236,237} and so a modified Chalk and Harrod mechanism was proposed in which the unsaturated compound inserts into the M-Si bond to yield intermediate **5** (**Scheme 1.2.1.1, Route B**). Reductive elimination would yield a hydrosilylation product, but intermediate **5** can also undergo β -hydride elimination to yield the observed dehydrogenative silylation byproducts.²³⁸⁻²⁴⁰



Scheme 1.2.1.1. Chalk and Harrod Mechanism (A) with Modified Chalk and Harrod Mechanism (B).

An alternative mechanism (**Scheme 1.2.1.2**) was proposed in the mid 1980's by Lewis and coworkers which takes into account the observed role of O_2 as well as the appearance of colored bodies during the reaction.²⁴¹⁻²⁴³



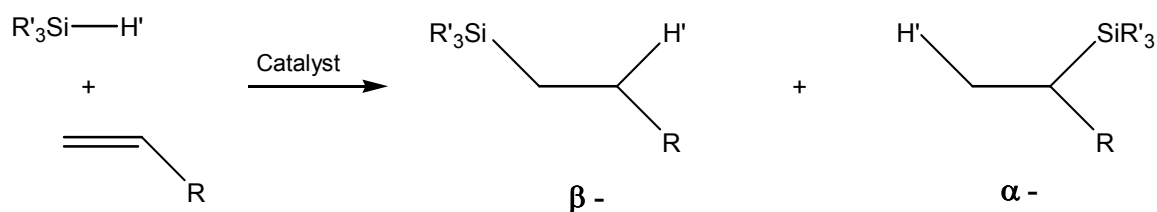
Scheme 1.2.1.2. Lewis Mechanism.

During an induction period, the $\text{Pt}(0)$ complex **6** (e.g. Karstedt's precatalyst *tris*(tetramethyl-1,3-divinyldisiloxane)diplatinum(0) (PDVTMDS)) decomposes into colloidal platinum **7** through reaction with the silane (HSiR_3). In contrast to the Chalk and Harrod mechanism, the silane adds onto the catalyst before the olefin. Oxygen prevents the irreversible agglomeration of the colloids (leading to lower reactivity), responsible for the colored bodies observed during Pt-catalyzed hydrosilylation reactions. Intermediate **8** is considered to be the electrophile, with the insertion of the olefin into the Si-H bond in a β - or α - fashion leading to the hydrosilylation product. In addition, another

equivalent of the silane (HSiR_3) can react with intermediate **8** to yield the coupled disilane byproduct.²⁴² More recently Stein, Lewis and coworkers have proposed a mononuclear homogenous Pt complex as active catalyst as opposed to previous reports suggesting colloidal catalysts, with oxygen serving to disrupt the formation of inactive multinuclear Pt species.²⁴³

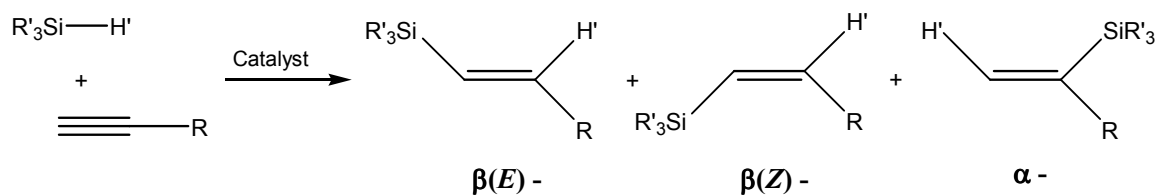
1.2.2. Hydrosilylation of Alkenes and Alkynes

Two regioisomers can be expected from the hydrosilylation of alkenes, depending on how the Si-H bond of a silane adds across the double bond of a terminal alkene (**Scheme 1.2.2.1**): **1**) the silicon attacks the sterically more accessible terminal carbon to give the β -regioisomer, or **2**) the silicon attacks the internal carbon to give the α -regioisomer.²²⁷



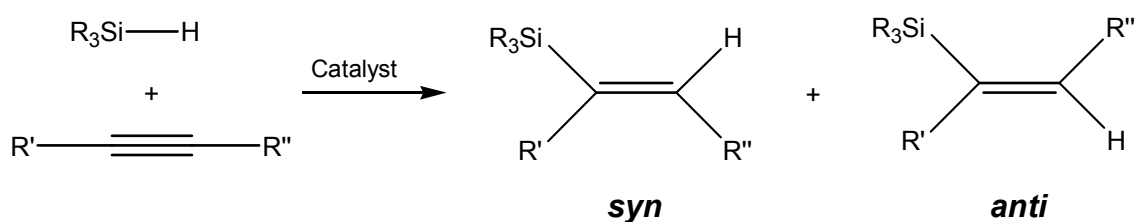
Scheme 1.2.2.1. Hydrosilylation of Terminal Alkenes.

In the case of alkynes, three regioisomers can be expected (**Scheme 1.2.2.2**): **1**) *anti* or *trans*- addition of the Si-H to give the *cis*-product ($\beta(\text{Z})$ - regioisomer), **2**) *syn* or *cis*-addition of the Si-H to give *trans*-product ($\beta(\text{E})$ - regioisomer), or **3**) addition of Si to the internal carbon to give the α - regioisomer.²²⁷



Scheme 1.2.2.2. Hydrosilylation of Terminal Alkynes.

The regioselectivity of a given hydrosilylation reaction depends on a variety of factors, including the catalyst used and steric effects. For alkene hydrosilylation, platinum and rhodium complexes favor β - regioisomers, while palladium complexes favor α - regioisomers.²²⁷ Consistent regioselectivity has been achieved with complexes of platinum, rhodium, ruthenium, and nickel with alkynes.^{227,244-246} Steric crowding, in addition to making internal alkenes and alkynes less susceptible to hydrosilylation also influences the regioselectivity, with the silicon adding to the less sterically hindered carbon ($\text{R}' < \text{R}''$) (**Scheme 1.2.2.3**).^{227,247}



Scheme 1.2.2.3. Hydrosilylation of Internal Alkynes.

1.2.3. Hydrosilylation of Alkynes using Pt Catalysts

Examples of common Pt catalysts are hexachloroplatinic acid (CPA; Speier's catalyst), Pt on carbon (Pt/C; Wagner's catalyst), and platinum 1,3-

divinyltetramethyldisiloxane (PDVTMDS; Karstedt's catalyst).²²⁷ Compared with other transition-metal complexes, Pt-complex catalyzed hydrosilylations are largely unaffected by the nature of the substituents on the silane, and have the advantage of having fewer side reactions.^{227,248} Pt-catalyzed hydrosilylation of alkynes mainly produces $\beta(E)$ - and α - regioisomers, with the proportion of α -regioisomers increasing with an increase in temperature.²²⁷ Compared to alkenes, alkynes have been shown to be more reactive, the latter being preferentially hydrosilylated in alkyne/alkene mixtures as well as in enynes.^{227,249}

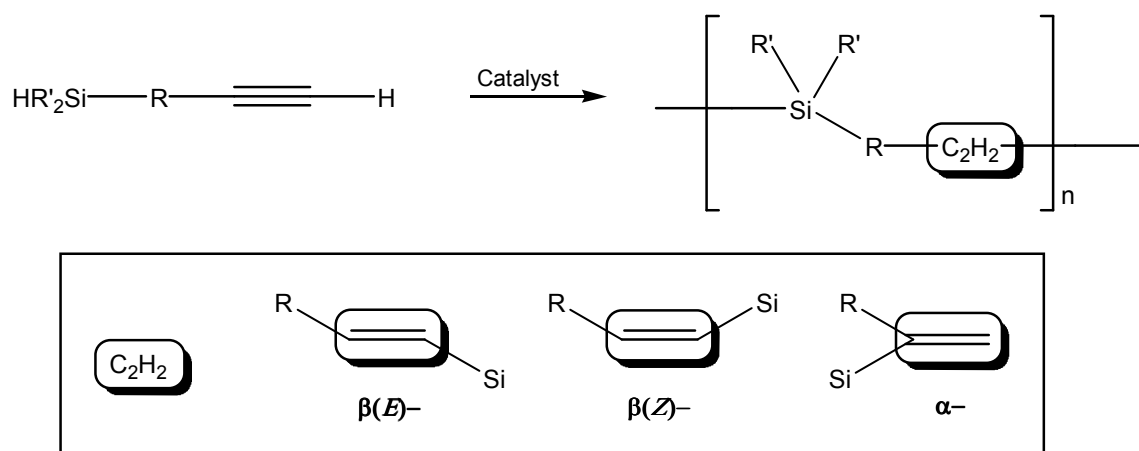
In 1980, Tsipis documented factors that account for the regioselectivity observed for terminal and internal alkynes using (*trans*-di- μ -hydrido *bis*(tricyclohexylphosphine)-*bis*-(silyl)diplatinum as catalyst.^{247,248} The major product obtained was from the anti-Markovnikov *cis*-addition of the Si-H bond to the C \equiv C triple bond to give $\beta(E)$ - adducts, while the minor product was from the Markovnikov *cis*-addition to give the α - adduct. In addition, minor amounts of a disilane species was obtained from a side reaction as accounted for in the Lewis mechanism. The resulting alkene products were found to be inert towards further hydrosilylation even though the catalyst retained its activity.

While the nature of the silane, silane to alkyne ratio, and catalyst concentration had little or no effect on regioselectivity of the reaction, an increase in silane to alkyne ratio or catalyst concentration led to increased reaction rates. It was inferred that the regioselectivity was influenced mainly by the nature of the alkyne.²⁴⁷ Electron-withdrawing substituents on the acetylenic carbons made the alkyne more active towards hydrosilylation, due to the alkyne being a better π -acceptor. However, very strong π -

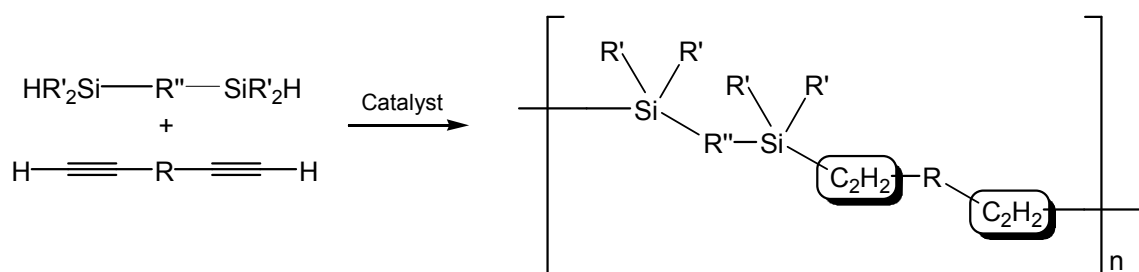
acceptor alkynes (e.g. hexafluoro-but-2-yne) do not react at all, presumably due to the formation of very stable alkyne-metal complexes that prevent an attack of the silane.²⁴⁷

1.2.4. Pt-Catalyzed Hydrosilylation to Produce Macromolecules

There are two basic methods in utilizing transition metal-complex catalyzed hydrosilylations for polymerization: **1)** using a molecule with both the Si-H and unsaturated moiety (**Scheme 1.2.4.1**), and **2)** using equimolar amounts of a disilane and a dialkyne or dialkyne (**Scheme 1.2.4.2**).²⁵⁰⁻²⁵⁴

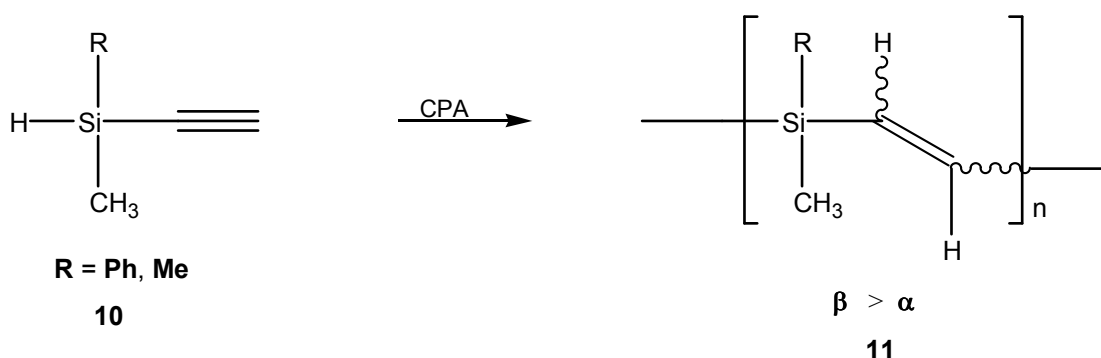


Scheme 1.2.4.1. General Hydrosilylation Polymerization Scheme 1.



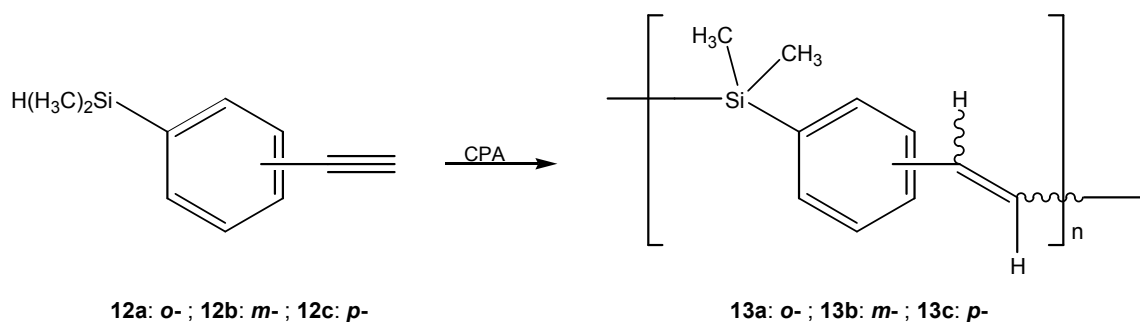
Scheme 1.2.4.2. General Hydrosilylation Polymerization Scheme 2.

The first method has the advantage of incorporating both the silane and alkyne as part of the monomer, thus avoiding the need for equimolar amounts of a disilane and a dialkyne in order to obtain high molecular weights in the polymeric products.²⁵⁰ An early example of this method involved the use of chloroplatinic acid (CPA) to catalyze the hydrosilylation polymerization of ethynylsilanes (**10**) into high molecular weight silylene-vinylene polymers (**11**) (Scheme 1.2.4.3).²⁵⁰ The regioselectivity of the hydrosilylation reaction was $\beta(E)$ - > α -, consistent with Pt catalyzed systems.²⁵⁰ Only alkynyl end-groups were observed.



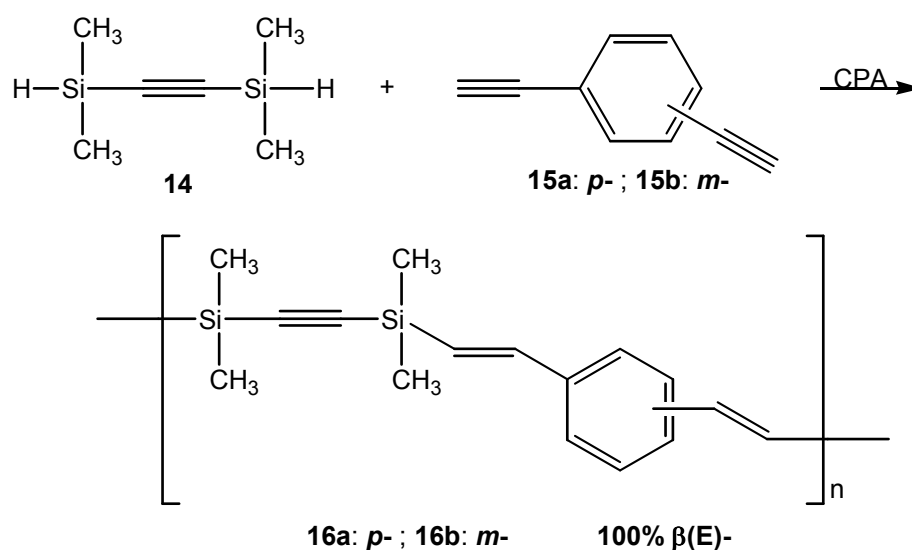
Scheme 1.2.4.3. Hydrosilylation Polymerization of Ethynylsilanes.

Organosilicon polymers having σ - π conjugation were similarly prepared from *o*-, *m*-, *p*- (dimethylsilyl) phenylacetylene (**12a-c**) to produce poly(silylenephenylenevinylene)s (**13a-c**) with alternating polydimethylsilane and poly(phenylenevinylene) units (Scheme 1.2.4.4).²⁵⁴ While products **13b** and **13c** have a $\beta(E)$ - to α - ratio of 1:2, **13a** has only $\beta(E)$ - olefins due to the sterically unfavorable α -configuration.



Scheme 1.2.4.4. Hydrosilylation Polymerization of *o*-, *m*-, *p*- (Dimethylsilyl)phenylacetylene.

An example of the second method involved the hydrosilylation of *bis*(dimethylsilyl)acetylene (**14**) with 1,4- (**15a**) and 1,3- diethynylbenzene (**15b**) to produce copolymers **16a** and **16b** with 100% β (E)- regioselectivity (**Scheme 1.2.4.5**).²⁵² This combines the conductive phenylene-vinylene units with silylene-acetylene units which have remarkable σ - π conjugation.²⁵¹



Scheme 1.2.4.5. Hydrosilylation Polymerization of *Bis*(dimethylsilyl)acetylene with Diethynylbenzene.

The next sections describe some examples of hydrosilylation involving ferrocene-based systems, including the work done by Jain from this group (**Chapter 1.2.6**).^{4,5}

1.2.5. Hydrosilylation of Fe/ferrocenyl-based Systems

Conjugated structures containing bridged ferrocene units have been studied extensively due to their potential for interesting electronic properties.²⁵⁵⁻²⁵⁷ Examples include ferrocenes with phenylene bridges (**Figure 1.2.5.1**) and ferrocene-based polymers with $\text{-SiR}_2\text{-}$ bridges (poly(ferrocenylsilane)s; **Figure 1.2.5.2**).^{255,256}

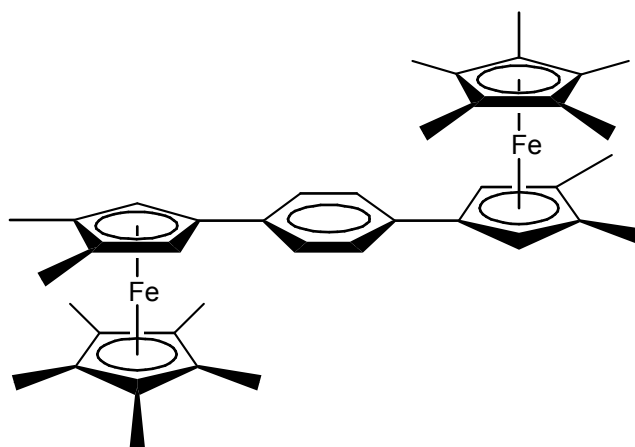


Figure 1.2.5.1. Phenylene-bridged Ferrocenes.

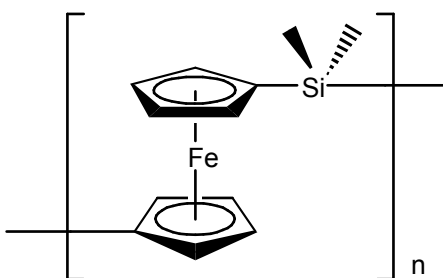
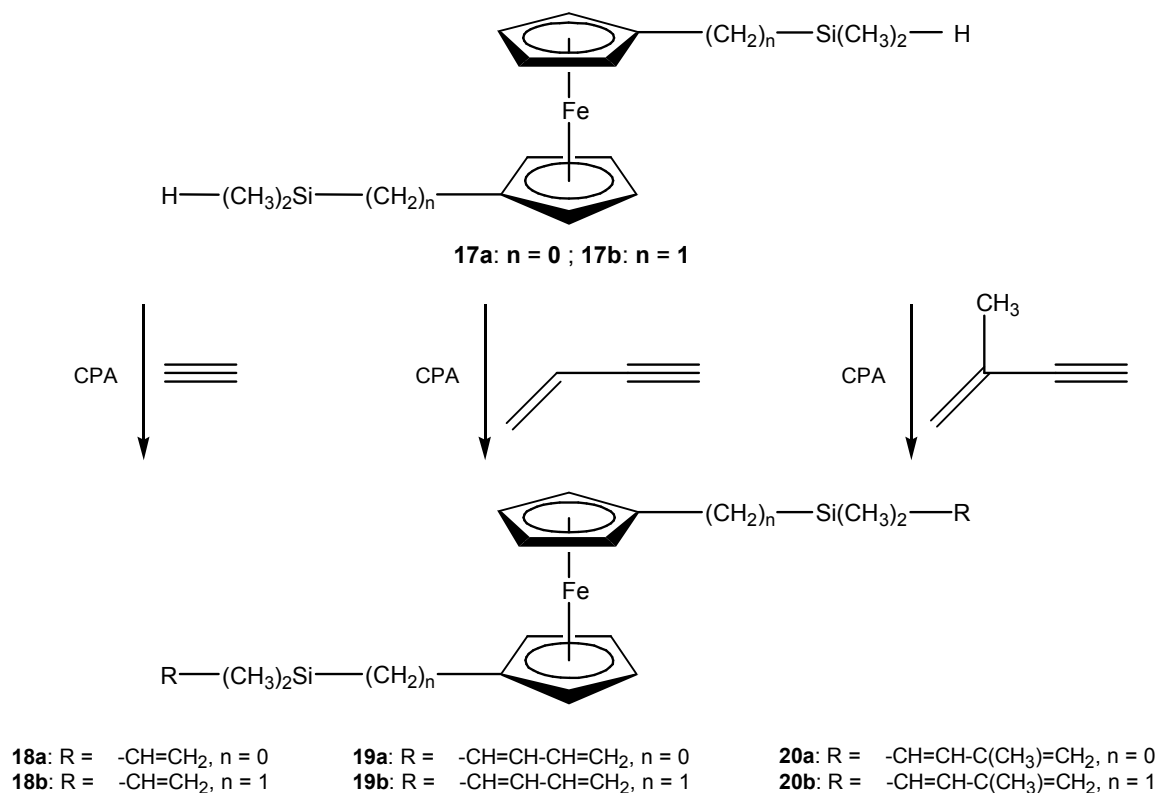


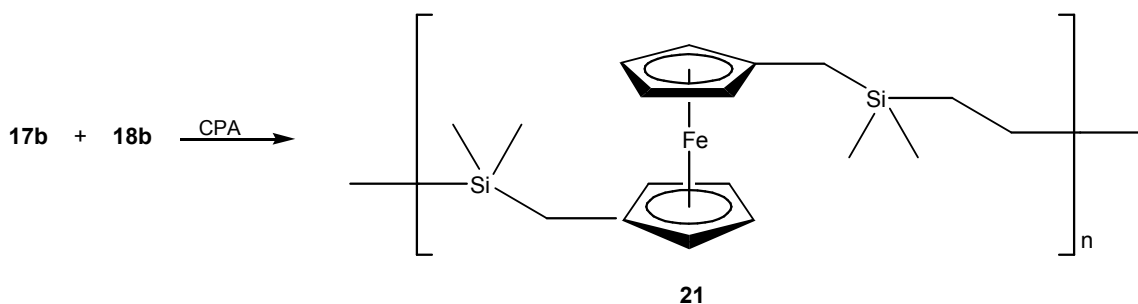
Figure 1.2.5.2. Poly(ferrocenylsilane)

Incorporation of ferrocene units into a polymeric backbone via hydrosilylation was first reported in 1965.²⁵⁸ Chloroplatinic acid - catalyzed hydrosilylation of 1,1'-*bis*-(dimethylsilyl)ferrocene (**17a**) and 1,1'-*bis*-(dimethylhydrosilylmethyl)ferrocene (**17b**) with either acetylene, vinylacetylene, or isopropenylacetylene gave products **18a/b**, **19a/b**, and **20a/b**, respectively (Scheme 1.2.5.1). The resulting divinyl derivative **18a** could conceivably be reduced in the presence of Na in anhydrous THF to form a double radical anion which can then be used as an initiator and terminating agent for the polymerizations of styrene, methylmethacrylate and acrylonitrile. Unfortunately, little data on the polymers or precursors was reported.



Scheme 1.2.5.1. Hydrosilylation of Ferrocene-based Disilanes and Alkynes.

The authors also reported hydrosilylation of **18b** with **17a** to give polymer **21** (Scheme 1.2.5.2),²²⁷ but again, no definitive proof or data and/or regioselective behavior was provided.

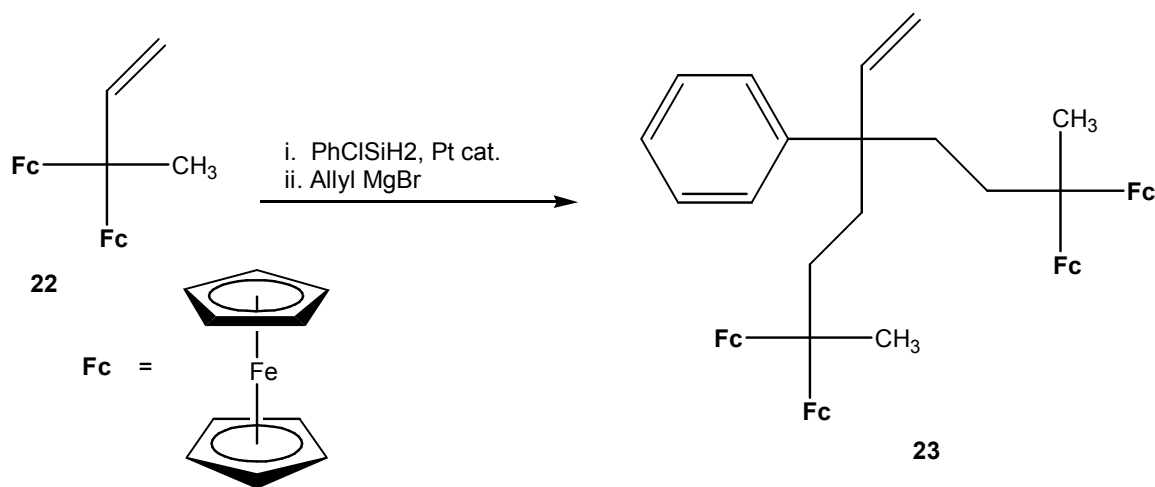


Scheme 1.2.5.2. Hydrosilylation Polymerization of **18b** with **17a**.

A similar approach was used by Asatiani and coworkers, wherein chloroplatinic acid was used to catalyze the hydrosilylation of diphenyldiacetylenyl and diethyldiacetylenyl silane with 1,1'-bis(methylphenylsilyl)ferrocene. The reported oligomeric products were inadequately characterized, using only elemental analyses as well as IR spectroscopy which revealed a band at 980 cm^{-1} to indicate the presence of stereospecific *trans*-products.²⁵⁹

Hydrosilylation reactions have been successfully used in preparing ferrocene-containing macromolecular structures such as dendrimers that exhibit electronic interactions between the ferrocene units. Hydrosilylation of dendron **22** followed by treatment with allylmagnesium bromide led to the formation of **23** (Scheme 1.2.5.3). Dendrons **22** and **23** were further added to $\text{Si}((\text{CH}_2)_3\text{Si}(\text{CH}_3)_2\text{H})_4$ to form a dendrimer with either eight (**24**) or sixteen (**25**) ferrocenyl units, respectively (Figure 1.2.5.3).²⁶⁰

As in the case of poly(ferrocenylsilane)s,^{255,256,261-263} the reported dendrimers showed significant electronic interactions between the ferrocenyl units bridged by a Si atom.²⁶⁰



Scheme 1.2.5.3. Hydrosilylation of Dendron 22.

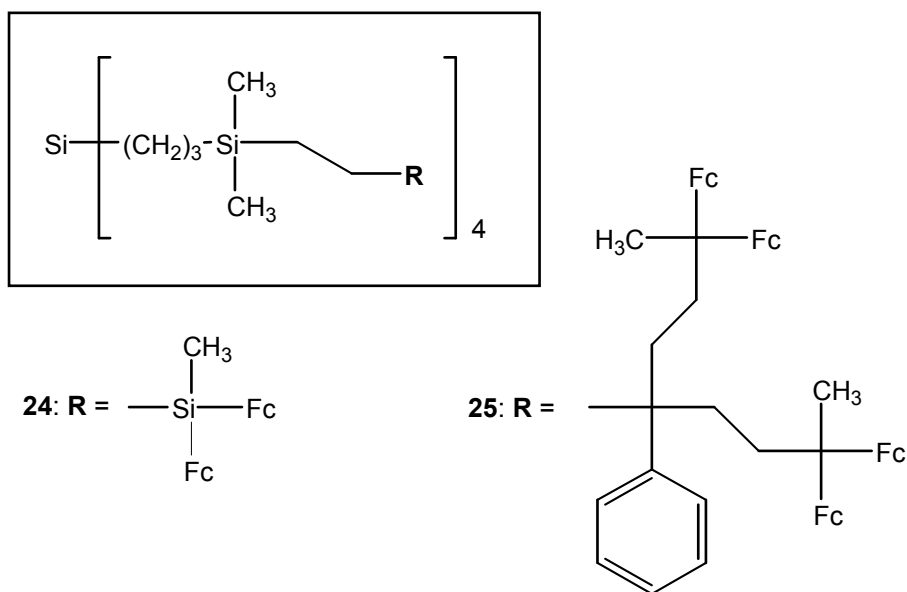
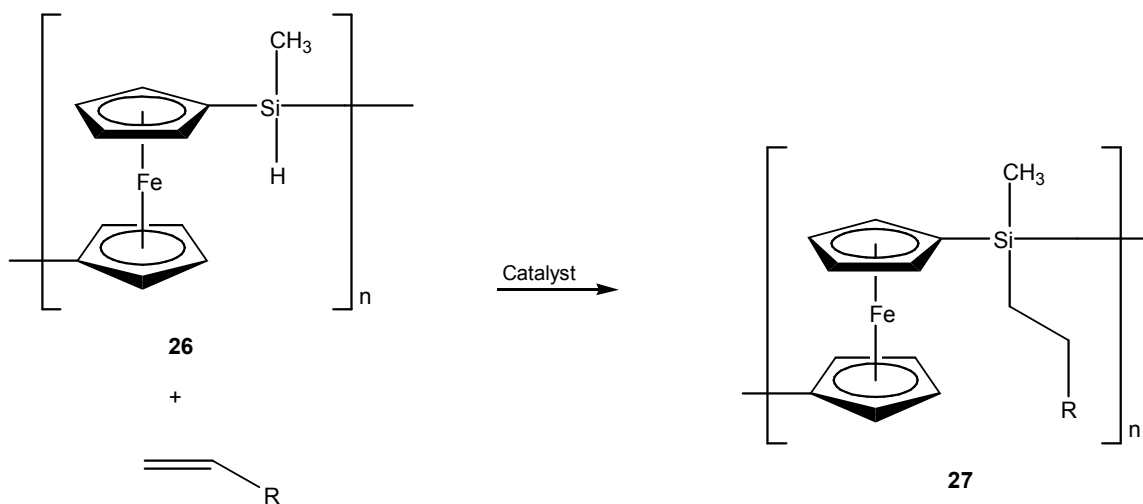


Figure 1.2.5.3. Dendrimers 24 and 25 via Hydrosilylation.

In addition to incorporating ferrocenyl units into polymers and dendrimers, hydrosilylation has also been used in modifying polymers with Si-H side groups. Thus, vinylferrocene was grafted onto a methylhydrosiloxane-dimethylsiloxane copolymer,²⁶⁴ and poly(ferrocenylmethylhydrosilane) (**26**) was modified using terminal olefins (Scheme 1.2.5.4).^{265,266}

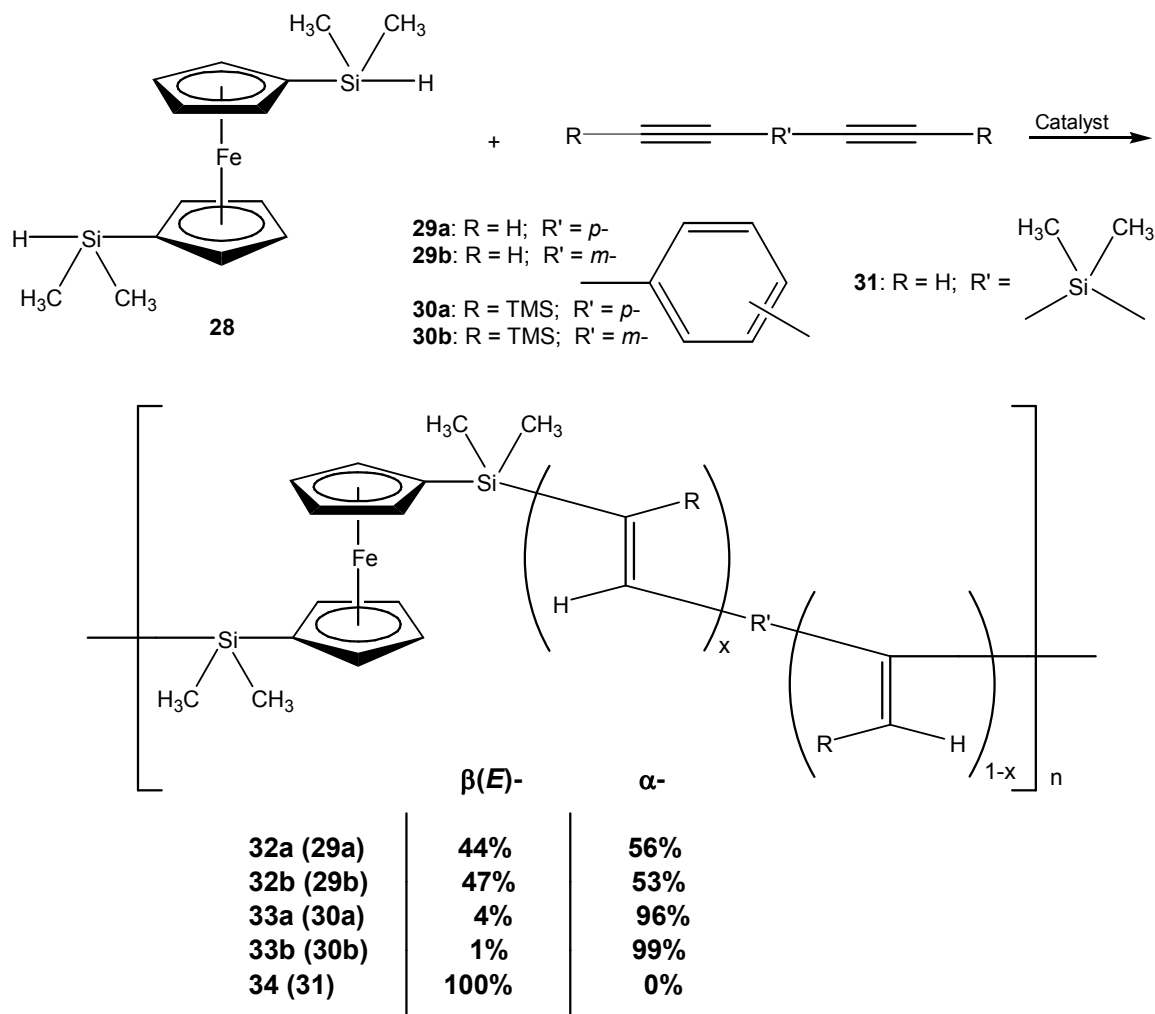


Scheme 1.2.5.4. Modification of Poly(ferrocenylmethylhydrosilane) via Hydrosilylation.

1.2.6. Poly{ferrocene-*bis*(silylenevinylene)(phenylene)}s

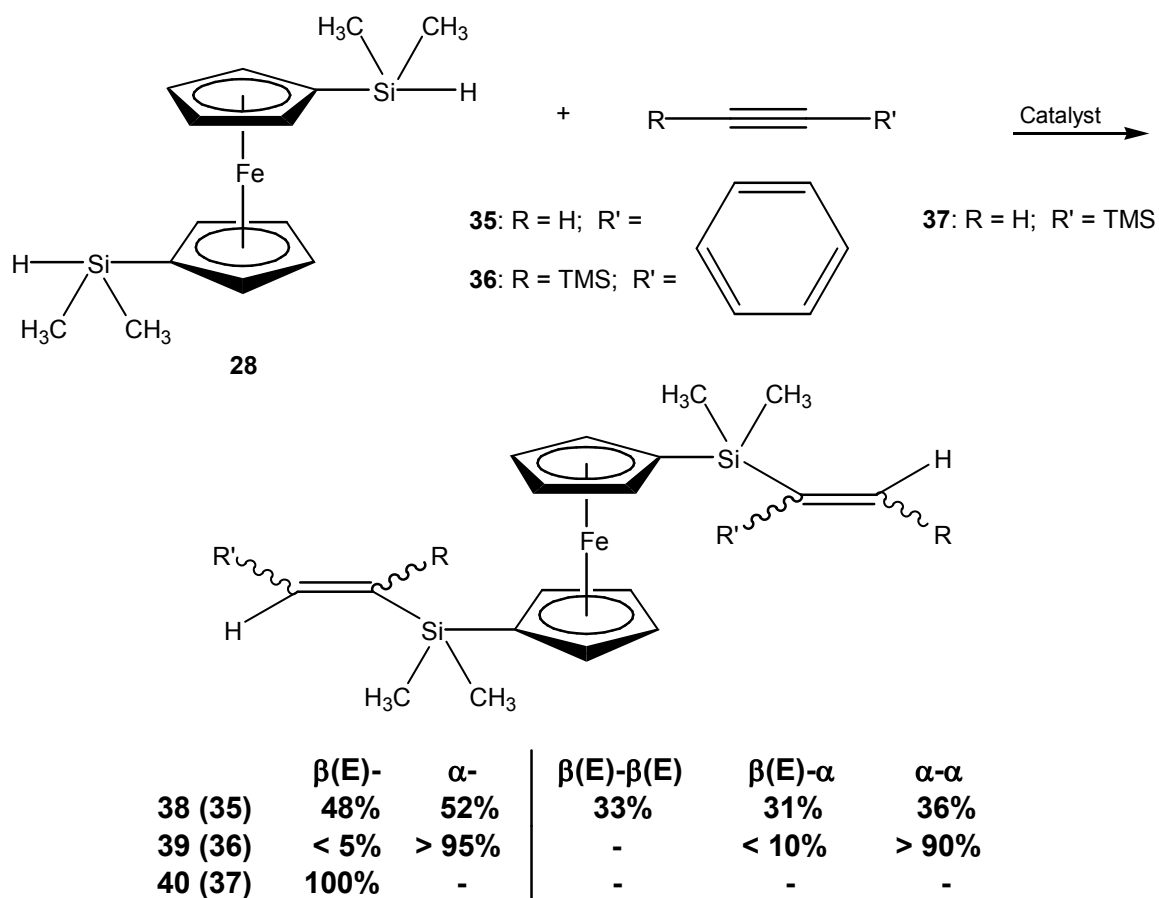
The polymers/oligomers (poly{ferrocene-*bis*(silylenevinylene)(phenylene)}s) were prepared via transition-metal catalyzed (Karstedt's catalysts, to be specific) hydrosilylation of 1,1'-*bis*(dimethylsilyl)ferrocene (**28**) with dialkynes by Jain of this group (Scheme 1.2.6.1).⁴ Bulky TMS groups in **30a**, **30b**, and **31** (in the case of **31**, the dimethylsilyl moiety on the dialkyne) played a big part in influencing the regioselectivity of the reactions, with the silane silicon preferentially attacking the alkyne carbon not bonded to a TMS group, giving predominantly α - adducts for **33a** and **33b**, and only

$\beta(E)$ - adducts for **34**. In the case of **29a** and **29b**, the absence of TMS groups on the alkyne resulted in higher α - to $\beta(E)$ - ratio in both **32a** and **32b** relative to **33a** and **33b**. These observations are consistent with other reports in the literature, where steric effects play a big role in the regioselectivity of hydrosilylation reactions.^{227,247}



Scheme 1.2.6.1. Hydrosilylation Polymerization of 1,1'-Bis(dimethylsilyl)ferrocene with Dialkynes.

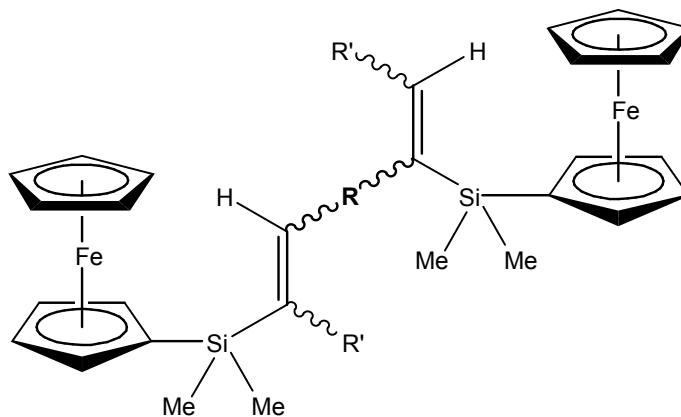
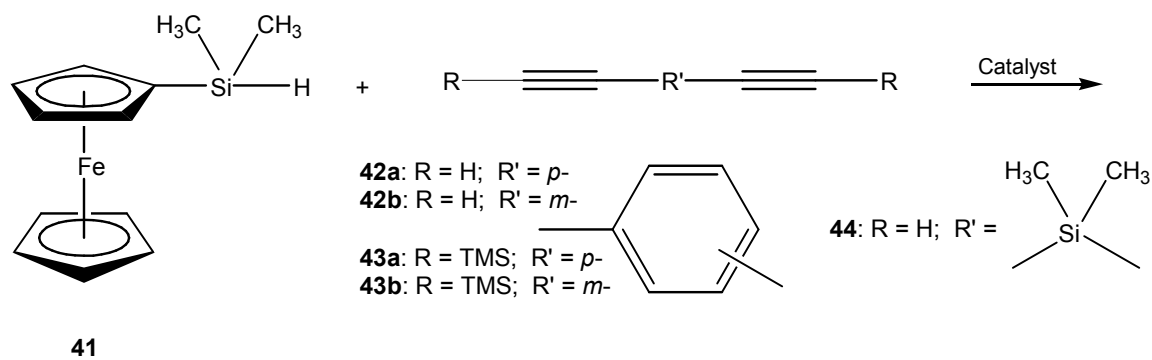
In addition to the polymers, two types of model compounds were prepared via hydrosilylation, depending on the silane and alkyne used.⁵ The first type of model compound was made from one equivalent of the disilane 1,1'-bis(dimethylsilyl)ferrocene (**28**) with two equivalents of several alkynes (**Scheme 1.2.6.2**). The regiochemical distributions observed in the model compounds are quite consistent with that of the corresponding polymer: model **38** has approximately one to one $\beta(E)$ - to α - ratio just like polymers **32a** and **32b**; predominance of α - adducts in both model **39** and polymers **33a** and **33b**; and $\beta(E)$ - selectivity in both model **40** and polymer **34**.



Scheme 1.2.6.2. Type 1 Model Compounds.

The second type of model compound was made from two equivalents of the monosilane dimethylsilylferrocene (**41**) with one equivalent of several dialkynes (**Scheme 1.2.6.3**). While model **47** was exclusively $\beta(E)$ - just like model **40** and polymer **34**, the other model compounds differed from the regiochemical distribution of the corresponding polymers. Both **46a** and **46b** showed an increased $\beta(E)$ - to α - ratio (relative to model **39** and polymers **33a** and **33b**) with increased presence of the $\beta(E)$ - α regioisomer. This was attributed to steric effects: the increased bulk of the partially hydrosilylated dialkyne with a ferrocenyl moiety makes a $\beta(E)$ - addition of the second silane more favorable. In the case of model **45a** and **45b**, there was also an observed increase in $\beta(E)$ - to α - ratio relative to model **38** and polymers **32a** and **32b**. This was attributed by Jain to the different silanes employed and their effect on migration patterns.^{4,5}

It is the intention of this dissertation to use Jain's hydrosilylation protocol to prepare polymers/oligomers containing bridged troiticene and ferrocene units along with relevant model compounds, and explore the potential for electronic communication between the metal centers. In addition, the observed discrepancy in regiochemical distributions obtained from the hydrosilylation reactions of dimethylsilylferrocene and 1,1'-bis(dimethylsilyl)ferrocene is further explored.



| | $\beta(\text{E})$ - | α - | $\beta(\text{E})$ - $\beta(\text{E})$ | $\beta(\text{E})$ - α | α - α |
|------------------|---------------------|------------|---------------------------------------|------------------------------|---------------------|
| 45a (42a) | 81% | 19% | 66% | 29% | 5% |
| 45b (42b) | 78% | 22% | 64% | 27% | 9% |
| 46a (43a) | 12% | 88% | - | 24% | 76% |
| 46b (43b) | 12% | 88% | - | 25% | 75% |
| 47 (44) | 100% | - | - | - | - |

Scheme 1.2.6.3. Type 2 Model Compounds.

Chapter 2. Preferential Monosubstitution of (η^7 -Cycloheptatrienyl)(η^5 -cyclopentadienyl)titanium(II) via Lithiation

Polymers/oligomers based on sandwich complexes have been extensively studied,²⁵⁵⁻²⁵⁷ and Jain of our group was able to incorporate 1,1'-*bis*(dimethylsilyl)ferrocene into a polymeric backbone via hydrosilylation polymerization. The polymers were then characterized with the aid of model compounds.^{4,5} Using a similar system, polymers/oligomers with (η^7 -cycloheptatrienyl)(η^5 -cyclopentadienyl)titanium(II) (troticene) in the backbone along with appropriate model compounds were prepared and characterized, and the results presented in **Chapter 4** and **5**. Preparation of the polymers/oligomers and model compounds required the synthesis of disubstituted as well as both isomers of the monosubstituted dimethylsilyl derivatives of troticene via metallation with *n*-butyllithium and quenching with chlorodimethylsilane.

This chapter presents the synthesis of various derivatives of troticene via the above mentioned protocol, with single substituents being preferentially added to either the cycloheptatrienyl or the cyclopentadienyl ligand, as well as the preparation of derivatives with two, three, or four substituents. While the monolithiation of troticene has been shown to occur predominantly on the cycloheptatrienyl ring,^{1,2} there is no published procedure for the preferential monolithiation and substitution of the cyclopentadienyl ring, nor for the polyolithiation of troticene.

2.1. Monosubstitution of Tropicene

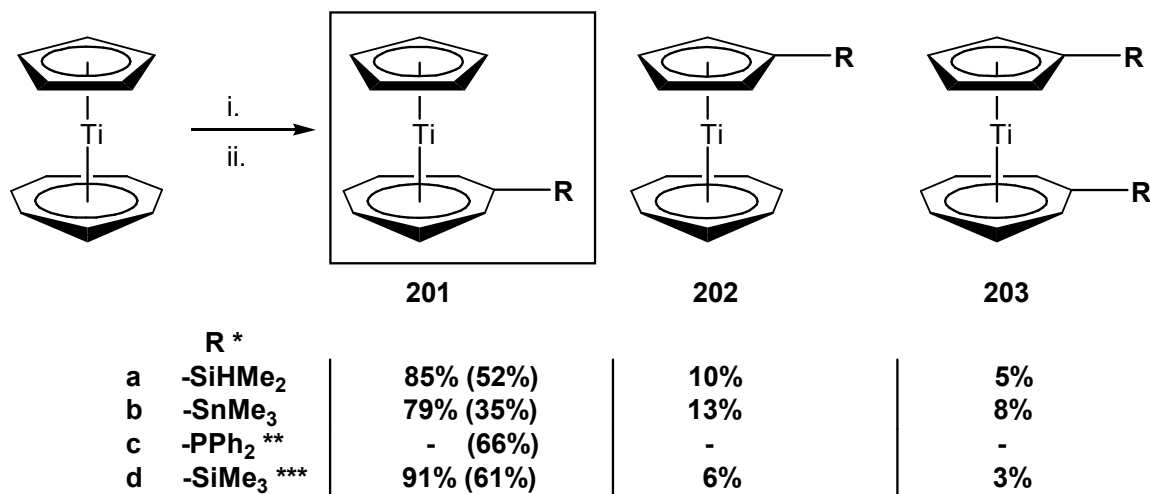
2.1.1. Monosubstitution on the Cycloheptatrienyl Ligand

Monolithiation of the cycloheptatrienyl ligand of tropicene was achieved using the literature procedure by adding one equiv. of *n*-BuLi to a stirred slurry of tropicene in diethyl ether at 0°C.^{1,2,207,210} Quenching with chlorodimethylsilane gave the blue oil { η^7 -(dimethylsilyl)cycloheptatrienyl}{ η^5 -cyclopentadienyl}titanium(II) (**201a**) as the major product (52 % yield) (Scheme 2.1.1.1). The ¹H NMR spectra of the crude product mixture revealed the presence of two other products, **202a** with a single substituent on the Cp ligand and **203a** with one substituent on both rings. The overall ratio was 85 % **201a** / 10 % **202a** / 5 % **203a**. Similar reactions quenched with chlorotrimethyltin, chlorodiphenylphosphine, and chlorotrimethylsilane produced **201b** (35 % yield; blue solid), **201c**^{208,209} (66 % yield; blue solid), and **201d**²⁰⁷ (61 % yield; blue solid), respectively, as major products, with crude product distributions comparable with that of the chlorodimethylsilane-quenched reaction. These results were similar to the results obtained by Groenenboom and coworkers for the monolithiation of tropicene,^{1,2} although **201b** has a lower isolated yield due to decomposition during chromatography.

Complex **201a** was characterized by GC/MS, ¹H, ¹³C{¹H}, and ²⁹Si DEPT NMR Spectroscopy (Table 2.1.1.1). The ¹H NMR spectrum confirmed the substituent is on the cycloheptatrienyl ligand with a singlet at δ 4.93 for the **Cp** protons. The ¹³C{¹H} NMR spectrum concurs and shows the **Cp** carbons at δ 97.8 and the *ipso* carbon of **Ch**-SiH(CH₃)₂ at δ 93.2.

Complex **201b** was also characterized by GC/MS, ¹H, and ¹³C{¹H}, as well as ¹¹⁹Sn{¹H} NMR Spectroscopy (Table 2.1.1.1). The ¹H and ¹³C{¹H} NMR spectra of

201b have common features with those of **201a**, indicative of a single trimethylstannyl substituent on the cycloheptatrienyl ring which was confirmed by a single peak observed at δ 13.3 in the $^{119}\text{Sn}\{^1\text{H}\}$ NMR spectrum.



i. 1 equiv. *n*-BuLi, ether, 0°C; ii. Cl-R (R = -SiHMe₂, -SnMe₃, -PPh₂, -SiMe₃), -78°C – room temp.

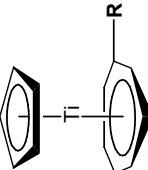
* Product distribution determined from integration of ^1H NMR of crude product. Isolated yield of desired product shown in parenthesis.

** Demerseman, B.; Dixneuf, P. H. *Journal of Organometallic Chemistry* **1981**, 210, C20-C22. Demerseman, B.; Dixneuf, P. H.; Douglade, J.; Mercier, R. *Inorganic Chemistry* **1982**, 21, 3942-3947.

*** Mikami, K.; Matsumoto, Y.; Shiono, T. In *Science of Synthesis (Houben-Weyl Methods of Molecular Transformations)*; Georg Thieme Verlag: New York, **2003**; Vol. 2, pp 457-679.

Scheme 2.1.1.1. Preferential Monolithiation of the Cht Ligand of Troiticene.

Table 2.1.1.1. NMR Data^a for Products with a Single Substituent on the Cycloheptatrienyl Ring.

|  | δ (¹ H) ^b | δ (¹³ C { ¹ H}) ^b | δ (²⁹ Si DEPT) ^c δ (¹¹⁹ Sn { ¹ H}) ^d δ (³¹ P { ¹ H}) ^e |
|---|---|---|--|
| 201a R = SiH(CH ₃) ₂ | 0.38 (d, 6H, -SiH(CH ₃) ₂), 4.82 (septet, 1H, -SiH(CH ₃) ₂), 4.93 (s, 5H, Cp), 5.43-5.65 (m, 6H, Cht -SiH(CH ₃) ₂) | -1.4 (-SiH(CH ₃) ₂), 93.2 (<i>ipso</i> C, Cht -SiH(CH ₃) ₂), 87.5, 89.6, 91.6 (Cht -SiH(CH ₃) ₂), 97.8 (Cp) | -7.0 (Cht- Si H(CH ₃) ₂) |
| 201b R = Sn(CH ₃) ₃ | 0.30 (s, 9H, -Sn(CH ₃) ₃), 4.95 (s, 5H, Cp), 5.45-5.60 (m, 6H, Cht -Sn(CH ₃) ₃) | -7.8 (-Sn(CH ₃) ₃), 96.1 (<i>ipso</i> C, Cht -Sn(CH ₃) ₃), 87.2, 89.5, 92.4 (Cht -Sn(CH ₃) ₃), 97.0 (Cp) | 13.3 (Cht- Sn (CH ₃) ₃) |
| 201c ^f R = PPh ₂ | 4.89 (s, 5H, Cp), 5.36-5.46, 5.78-5.88 (m, 6H, Cht -PPh ₂), 6.98-7.12, 7.46-7.56 (m, 10H, -PPh ₂) | 94.0 (d, <i>ipso</i> C, Cht -PPh ₂ , ¹ J _{C-P} = 10Hz), 87.6 (Cht -PPh ₂), 88.5, 93.3 (d, Cht -PPh ₂), 98.89 (Cp), 141.3 (d, <i>ipso</i> C, -PPh ₂ , ¹ J _{C-P} = 14Hz), 129.0 (-PPh ₂), 128.9, 134.5 (d, -PPh ₂) | 17.8 (Cht- P Ph ₂) |
| 201d ^g R = Si(CH ₃) ₃ | 0.34 (s, 9H, -Si(CH ₃) ₃), 4.93 (s, 5H, Cp), 5.45-5.65 (m, 6H, Cht -Si(CH ₃) ₃) | 0.8 (-Si(CH ₃) ₃), 96.9 (<i>ipso</i> C, Cht -Si(CH ₃) ₃), 87.3, 89.2, 91.3 (Cht -Si(CH ₃) ₃), 97.5 (Cp) | 2.4 (Cht- Si (CH ₃) ₃) |

^a Solvent used: C₆D₆. ^b Internal reference: C₆D₆ (¹H NMR: δ 7.16 ppm; ¹³C NMR: δ 128.38 ppm).

^c External reference: Tetramethylsilane (δ 0.0 ppm). ^d External reference: Tetraethyltin (δ 1.0 ppm). ^e External reference: 85 % Phosphoric Acid (δ 0.0 ppm).

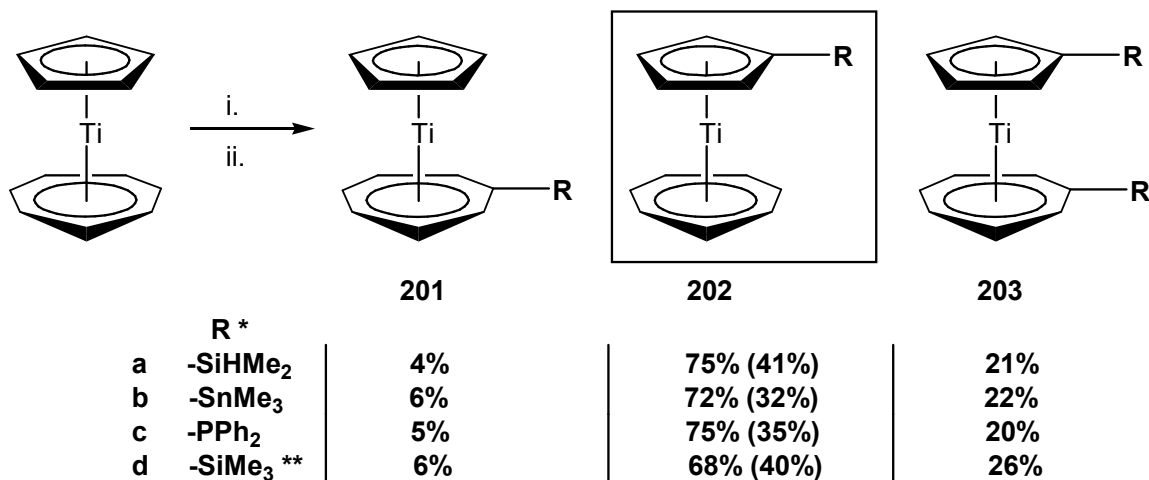
^f Demerseman, B.; Dixneuf, P. H. *Journal of Organometallic Chemistry* **1981**, 210, C20-C22. Demerseman, B.; Dixneuf, P. H.; Douglade, J.; Mercier, R.

Inorganic Chemistry **1982**, 21, 3942-3947.

^g Mikami, K.; Matsumoto, Y.; Shiono, T. In *Science of Synthesis (Houben-Weyl Methods of Molecular Transformations)*; Georg Thieme Verlag: New York, **2003**; Vol. 2, pp 457-679.

2.1.2. Monosubstitution on the Cyclopentadienyl Ligand

In contrast to the reactions discussed above, addition of 1 equiv. of *n*-butyllithium to troiticene at room temperature followed by quenching with chlorodimethylsilane produced the blue solid (η^7 -cycloheptatrienyl){ η^5 -(dimethylsilyl)cyclopentadienyl}titanium(II) (**202a**) as the major product (41 % yield) (Scheme 2.1.2.1). Complexes **201a** and **203a** were also observed in the crude product mixture (4 % **201a** / 75 % **202a** / 21 % **203a**). Similar reactions quenched with chlorotrimethyltin, chlorodiphenylphosphine, and chlorotrimethylsilane produced **202b** (32 % yield; blue solid), **202c** (35 % yield; blue solid), and **202d**²⁶⁷ (40 % yield; blue solid), respectively, as major products, again with crude product distributions like that of the chlorodimethylsilane-quenched reaction.



i. 1 equiv. *n*-BuLi, ether, r.t.; ii. Cl-R (R = -SiHMe₂, -SnMe₃, -PPh₂, -SiMe₃), -78°C - r.t.

* Product distribution determined from integration of ¹H NMR of crude product. Isolated yield of desired product shown in parenthesis.

** Verkouw, H. T.; Van Oven, H. O. *Journal of Organometallic Chemistry* **1973**, 59, 259-266.

Scheme 2.1.2.1. Preferential Monolithiation of the Cp Ligand of Troiticene.

Complex **202a** was characterized by GC/MS, ^1H , $^{13}\text{C}\{^1\text{H}\}$, and ^{29}Si DEPT NMR Spectroscopy (Table 2.1.2.1), confirming monosubstitution at the cyclopentadienyl ligand. The ^1H NMR spectrum of **202a** clearly shows two pseudo triplets at δ 5.08 and δ 5.12 assigned to the cyclopentadienyl ring protons, and a singlet at δ 5.44 assigned to the cycloheptatrienyl ring. The $^{13}\text{C}\{^1\text{H}\}$ NMR spectrum **202a** shows a signal at δ 87.0 for the *Cht* carbons, and δ 106.2 for the *Cp*-SiH(CH₃)₂ *ipso* carbon. The ^{29}Si DEPT NMR spectrum showed one signal at δ -23.3, more upfield compared to that of **201a** at δ -7.03.

Complexes **202b** and **202c** were also characterized by GC/MS, ^1H , $^{13}\text{C}\{^1\text{H}\}$, and either $^{119}\text{Sn}\{^1\text{H}\}$ or $^{31}\text{P}\{^1\text{H}\}$ NMR (Table 2.1.2.1). Their ^1H and $^{13}\text{C}\{^1\text{H}\}$ NMR spectra have common features with those of **202a**, indicative of a single substituent on the cyclopentadienyl ring. For **202b**, the $^{119}\text{Sn}\{^1\text{H}\}$ NMR spectrum showed one signal at δ -32.0, more upfield than that of its Cht- monosubstituted counterpart **201b** at δ 13.3. In the case of **202c**, the lone $^{31}\text{P}\{^1\text{H}\}$ NMR signal was at δ -18.5 (c.f. **201c**, δ 17.8).

Complex **202c** was also characterized by X-ray crystallography (Table A.1.1 to A.1.4). Blue crystals of **202c** were grown from toluene at -30 °C, and an ORTEP drawing is shown in Figure 2.1.2.1. The C-C bond lengths for the cycloheptatrienyl and cyclopentadienyl rings average 1.405 Å and 1.413 Å, respectively, whereas the average Ti-C(Cht) bond length of 2.196 Å and the Ti-Centroid(Cht) distance of 1.485 Å are shorter than their cyclopentadienyl counterparts (average Ti-C(Cp) 2.328 Å; Ti-Centroid(Cp) 1.994 Å). The Centroid(Cht)-Ti-Centroid(Cp) angle is approximately linear (174.70°) and is comparable with that of troticene,²⁶⁸ ($\eta^5\text{-C}_5\text{H}_5$)Ti($\eta^7\text{-C}_7\text{H}_6[\text{PPh}_2\{\text{Mo}(\text{CO}_5)\text{C}_6\text{H}_5\text{CH}_3\}]\text{}$),²⁰⁹ and $\{\eta^7\text{-(diphenylphosphino)cycloheptatrienyl}\}\{\eta^5\text{-(diphenylphosphino)cyclopentadienyl}\}$ titanium(II) (**203c**).³ In general, the Ti-C(Cht)

bonds are much shorter than the Ti-C(Cp) bonds, revealing a stronger interaction between the metal center and the cycloheptatrienyl ring.^{7,221} This is consistent with the conclusion by Kaltsoyannis regarding the difference in interaction between the two rings and the metal. While the valence π orbitals of the cyclopentadienyl ring undergo little mixing with the metal d orbitals, the metal-cycloheptatrienyl ring interaction is much more covalent in nature compared to the largely ionic metal-cyclopentadienyl ring interaction.²⁶⁹

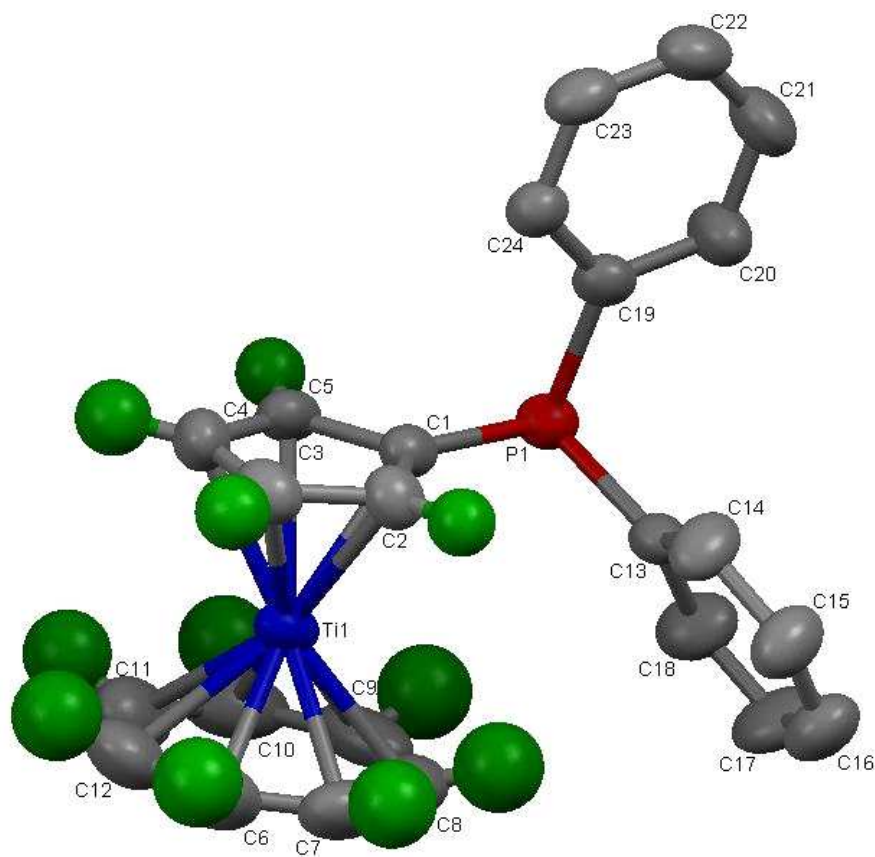


Figure 2.1.2.1. ORTEP drawing of **202c**.

Other notable features are the positions of the ring protons and the diphenylphosphino group relative to the ring planes. The cycloheptatrienyl ring protons are bent from the ring plane towards the metal center with an average angle of 24.17° , while the cyclopentadienyl ring protons are bent from the ring plane away from the metal center with an average angle of 4.65° . The phosphorous atom is also bent from the ring plane away from the metal center at an angle of 6.58° (**Figure 2.1.2.2**). Comparable structural distortions were observed for various other sandwich and half-sandwich complexes of Ti and other transition metals.²⁷⁰⁻²⁷⁵

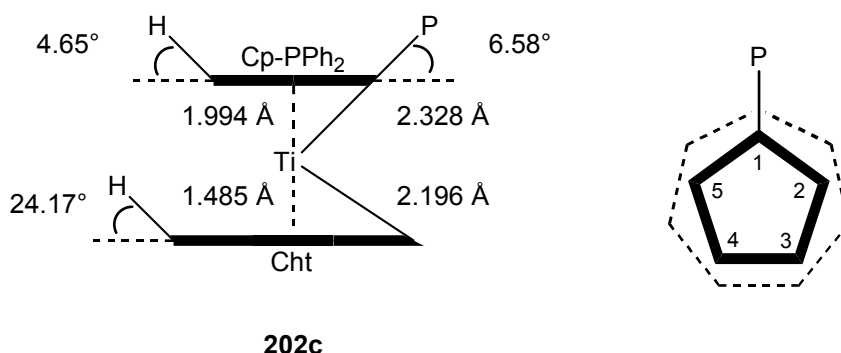


Figure 2.1.2.2. C-H and C-P Bond Distortion Angles of **202c**.

Similar distortions were also observed in the X-ray structures of **206d**, **204d**, and **207d**, which are discussed in **Section 2.3**. Such distortions are mainly attributed to the reorientation of the unhybridized ring p orbitals to maximize overlap with the metal d orbitals. Several other factors are also in play: steric effects, ring size, and metal d orbital (particularly the d_{xz} and d_{yz}) size.^{270,271,275} Steric effects become more important with smaller ring sizes, while more diffuse metal d_{xz} and d_{yz} orbitals require less ring distortion to achieve maximum overlap (**Figure 2.1.2.3**). Henceforth, for the purpose of discussion

on observed bond distortions from the ring planes, distortions which are more bent towards the metal center will be referred to as more positive distortions (**B**), while those which are more bent away from the metal center will be referred to as more negative distortions (**A**).

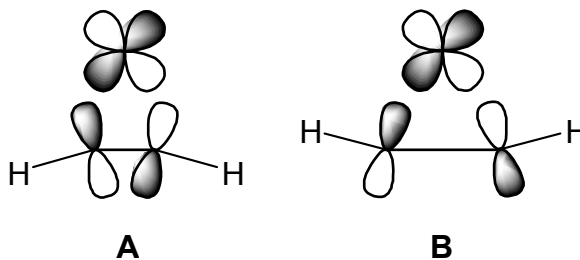
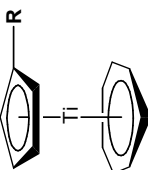


Figure 2.1.2.3. Deviation of Hydrogen Atoms from the Plane of Cyclic C_nH_n Ligands in Metal π -Complexes.^{271,275}

Table 2.1.2.1. NMR Data^a for Products with a Single Substituent on the Cyclopentadienyl Ring.

|  | δ (¹ H) ^b | δ (¹³ C { ¹ H}) ^b | δ (²⁹ Si DEPT) ^c δ (¹¹⁹ Sn { ¹ H}) ^d δ (³¹ P { ¹ H}) ^e |
|---|--|--|--|
| 202a R = SiH(CH ₃) ₂ | 0.17 (d, 6H, -SiH(CH ₃) ₂), 4.52 (septet, 1H, -SiH(CH ₃) ₂), 5.08, 5.12 (t, 4H, <i>Cp</i> -SiH(CH ₃) ₂), 5.44 (s, 7H, <i>Ch</i> t) | -2.6 (-SiH(CH ₃) ₂), 87.0 (<i>Ch</i> t), 106.2 (<i>ipso</i> C, <i>Cp</i> -SiH(CH ₃) ₂), 100.7, 103.6 (<i>Cp</i> -SiH(CH ₃) ₂) | -23.3 (<i>Cp</i> - <i>Si</i> H(CH ₃) ₂) |
| 202b R = Sn(CH ₃) ₃ | 0.18 (s, 9H, -Sn(CH ₃) ₃), 5.04, 5.24 (t, 4H, <i>Cp</i> -Sn(CH ₃) ₃), 5.44 (s, 7H, <i>Ch</i> t) | -8.4 (-Sn(CH ₃) ₃), 86.4 (<i>Ch</i> t), 106.1 (<i>ipso</i> C, <i>Cp</i> -Sn(CH ₃) ₃), 100.7, 104.1 (<i>Cp</i> -Sn(CH ₃) ₃) | -32.0 (<i>Cp</i> - <i>Sn</i> (CH ₃) ₃) |
| 202c R = PPh ₂ | 5.03-5.06, 5.06-5.10 (m, 4H, <i>Cp</i> -PPh ₂), 5.42 (s, 7H, <i>Ch</i> t), 6.98-7.10, 7.34-7.44 (m, 10H, -PPh ₂) | 87.8 (<i>Ch</i> t), 109.0 (d, <i>ipso</i> C, <i>Cp</i> -PPh ₂), ¹ J _{C-P} = 10Hz), 100.2, 103.0 (d, <i>Cp</i> -PPh ₂), 140.4 (d, <i>ipso</i> C, -PPh ₂ , ¹ J _{C-P} = 12Hz), 129.2 (-PPh ₂), 128.9, 134.3 (d, -PPh ₂) | -18.5 (<i>Cp</i> - <i>P</i> Ph ₂) |
| 202d ^f R = Si(CH ₃) ₃ | 0.14 (s, 9H, -Si(CH ₃) ₃), 5.05, 5.15 (triplet, 4H, <i>Cp</i> -Si(CH ₃) ₃), 5.43 (s, 7H, <i>Ch</i> t) | 0.2 (-Si(CH ₃) ₃), 86.7 (<i>Ch</i> t), 110.6 (<i>ipso</i> C, <i>Cp</i> -Si(CH ₃) ₃), 100.5, 103.1 (<i>Cp</i> -Si(CH ₃) ₃) | -8.3 (<i>Cp</i> - <i>Si</i> (CH ₃) ₃) |

^a Solvent used: C₆D₆. ^b Internal reference: C₆D₆ (¹H NMR: δ 7.16 ppm; ¹³C NMR: δ 128.38 ppm).

^c External reference: Tetramethylsilane (δ 0.0 ppm). ^d External reference: Tetraethyltin (δ 1.0 ppm). ^e External reference: 85 % Phosphoric Acid (δ 0.0 ppm).

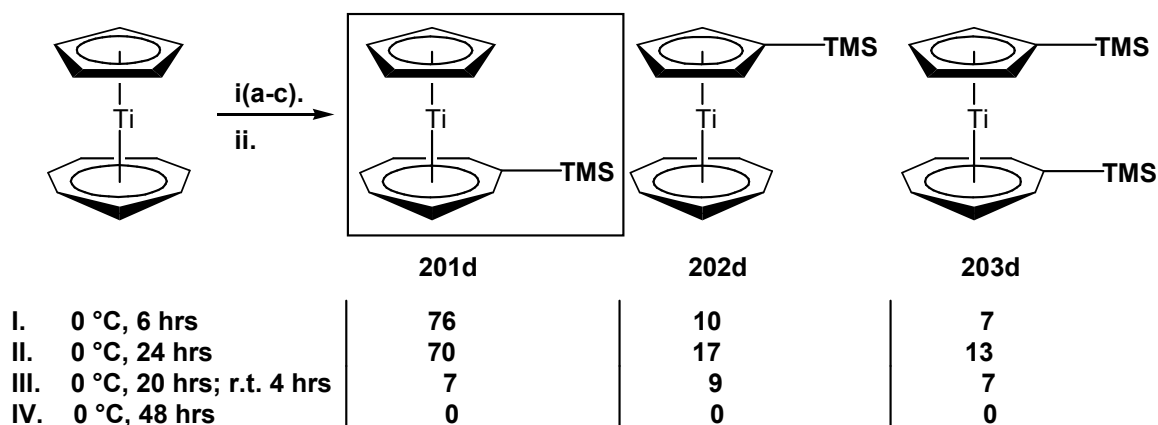
^f Verkouw, H. T.; Van Oven, H. O. *Journal of Organometallic Chemistry* **1973**, 59, 259-266.

2.1.3. Effect of Temperature on the Lithiation of Tropicene

The monolithiation of tropicene at 0 °C occurs preferentially at the cycloheptatrienyl ring, and was attributed to its stronger negative charge compared with the cyclopentadienyl ring.^{1,2,211,212} However, this does not explain the product distribution obtained at room temperature, prompting further study on the lithiation at 0 °C and at room temperature.

In this study, a long reaction time as well as less than one equivalent of *n*-butyllithium was used in an attempt to minimize the amount of unreacted *n*-butyllithium before quenching at the 24 hour mark. Thus, 0.8 equiv. of *n*-BuLi was added to tropicene at 0 °C along with hexamethylbenzene as an internal standard. One aliquot was drawn after 6 hours then quenched at -78°C with chlorotrimethylsilane. Two more aliquots were drawn after 20 hours, one of which was kept at 0°C and the other was warmed up to room temperature for another four hours, then quenched at -78°C with chlorotrimethylsilane. The remaining reaction mixture was allowed to react for 48 hours before quenching with chlorotrimethylsilane (**Scheme 2.1.3.1**).

It is apparent that the amount of Cht-monolithio-tropicene (**201**) product drops dramatically when the temperature was warmed up from 0 °C to room temperature (**II** vs. **III**). The observed decrease in either **202** (50 % decrease) and **203** (44 % decrease) were significantly less than that of **201** (90 % decrease). When the reaction time increased from 6 to 24 hours (**I** vs. **II**), the amount of **201** decreased, while both **202** and **203** increased. This result could be taken to mean that while **201** was formed faster (kinetic product), **202** and **203** are more stable (thermodynamic products) under the same conditions.

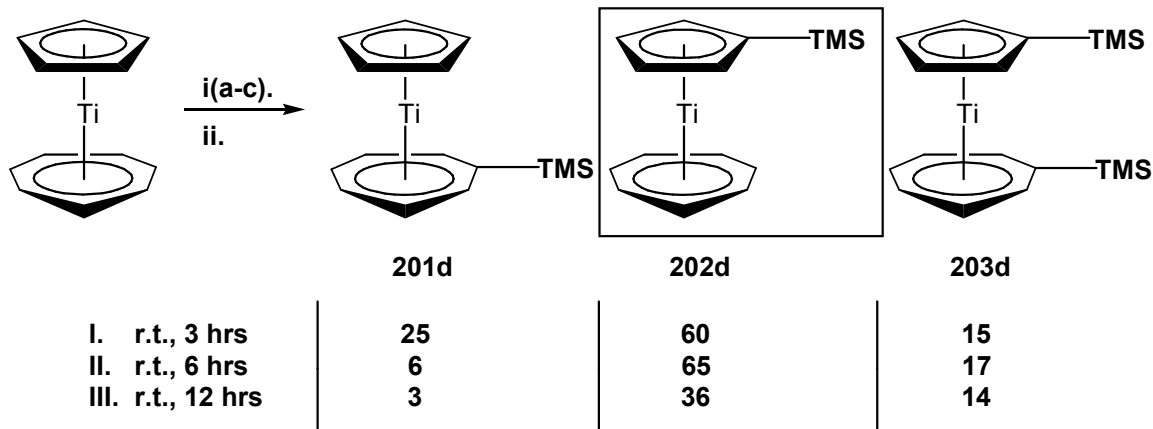


i. 0.8 equiv. *n*-BuLi, ether, C₆Me₆; ii. Cl-SiMe₃, -78°C - r.t.

* Product distribution determined from integration of ¹H NMR of crude product.

Scheme 2.1.3.1. Monolithiation of Tropicene at 0 °C and Room Temperature.

To confirm this, a reaction was done at room temperature in which 0.8 equiv. of *n*-butyllithium was added to tropicene along with hexamethylbenzene as an internal standard. Aliquots were drawn after 3 and 6 hours then quenched at -78°C with chlorotrimethylsilane. The remaining reaction mixture was allowed to react for 12 hours before quenching with chlorotrimethylsilane. The product distributions were then determined from integration of the ¹H NMR spectra relative to the internal standard C₆Me₆ (Scheme 2.1.3.2). Again, **201** appeared to be less stable than **202** and **203**, with a significant decrease in **201** observed in the 6 hour aliquot while **202** and **203** increased (**I** vs. **II**). Both **202** and **203** decreased after 12 hours (**III**) and are less stable at room temperature than at 0 °C (c.f. Scheme 2.1.3.1: both **202** and **203** increased between **I** and **II** at 0 °C). This is consistent with the fact that, in general, organolithiums are more prone to thermal decomposition and ether cleavage at elevated temperatures.^{20,86,89,93,94,102}



i. 0.8 equiv. *n*-BuLi, ether, C₆Me₆; ii. Cl-SiMe₃, -78°C - r.t.

* Product distribution determined from integration of ¹H NMR of crude product.

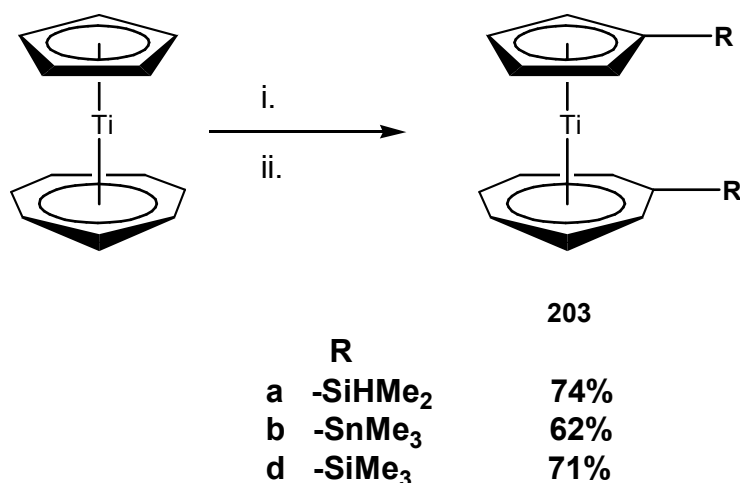
Scheme 2.1.3.2. Monolithiation of Trocticene at Room Temperature.

We propose that the observed preference for **202** in the room temperature lithiation of trocticene is due to two factors. Firstly, the monolithio-product **201**, while it is formed faster than **202**, is thermally less stable. Any **201** formed at room temperature either undergoes thermal decomposition, or reacts with the ether solvent (ether cleavage). This leads to the observed lower amounts of **201** in the reaction. Secondly, the monolithio-product **201** could possibly lithiate the Cp ligand of trocticene or another **201** to form more **202** and **203**, respectively.

2.2. Disubstitution of Trocticene

Dilithiation of trocticene was achieved using the literature procedure.^{3,210,214} Addition of a slurry of trocticene in hexane to 2.5 equiv. *n*-BuLi-TMEDA at room temperature followed by quenching with chlorodimethylsilane gave the blue oil {η⁷-(dimethylsilyl)cycloheptatrienyl}{η⁵-(dimethylsilyl)cyclopentadienyl}titanium(II) (**203a**)

as the major product (74 % yield) (**Scheme 2.2.1**). Similar reactions quenched with chlorotrimethyltin and chlorotrimethylsilane produced **203b** (62 % yield; blue solid), and **203d**²¹⁰ (71 %; blue solid), respectively.



i. 2.5 equiv. *n*-BuLi/TMEDA, hexane, r.t.; ii. Cl-**R** (**R** = -SiHMe₂, -SnMe₃, -SiMe₃), -78°C – r.t.

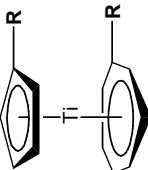
Scheme 2.2.1. Dilithiation of Trocticene.^{3,210,214}

Complex **203a** was characterized by GC/MS, ¹H, ¹³C{¹H}, and ²⁹Si DEPT NMR Spectroscopy (**Table 2.2.1**), and shows a molecular ion (M⁺) with *m/e* = 320, consistent with two dimethylsilyl groups. The ¹H NMR spectrum of shows two doublets at δ 0.17 and δ 0.40 for the Cp-SiH(CH₃)₂ and Cht-SiH(CH₃)₂ methyl groups, respectively, and a multiplet at δ 5.43-5.65 for the **Cht**-SiH(CH₃)₂ ring protons among other signals, and are comparable to those of **201a** and **202a**. The ¹³C{¹H} NMR spectrum of **203a** shows two signals at δ 93.1 and δ 106.8 for the *ipso* carbons on **Cht**-SiH(CH₃)₂ and **Cp**-SiH(CH₃)₂, respectively. The ²⁹Si DEPT NMR also shows two signals at δ -23.2 and δ -7.0.

Complex **203b** was similarly characterized (**Table 2.2.1**). The ¹H and ¹³C{¹H} NMR spectra of **203b** have common features with those **203a**, indicative of a single

trimethylstannyl substituent on each ring, and was confirmed by signals at δ -31.4 and δ 13.9 in the $^{119}\text{Sn}\{^1\text{H}\}$ NMR spectrum.

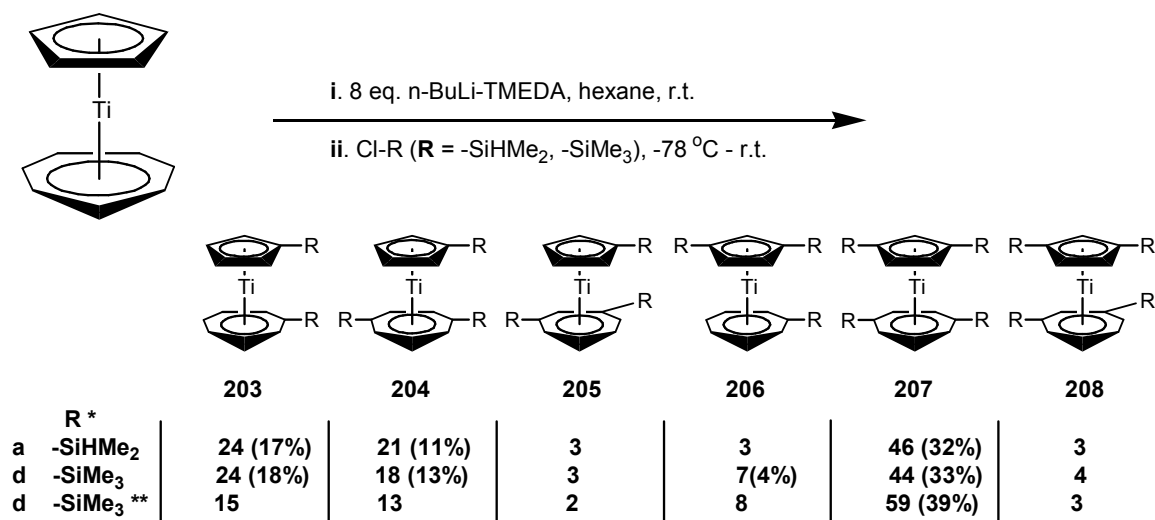
Table 2.2.1. NMR Data^a for 1,1'-Disubstituted Troiticene Derivatives.

|  | δ (¹ H) ^b | δ (¹³ C { ¹ H}) ^b | δ (²⁹ Si DEPT) ^c δ (¹¹⁹ Sn { ¹ H}) ^d |
|---|--|---|---|
| 203a R = SiH(CH ₃) ₂ | 0.17 (d, 6H, Cp-SiH(CH ₃) ₂), 0.40 (d, 6H, Cht-SiH(CH ₃) ₂), 4.52 (septet, 1H, Cp-Si H (CH ₃) ₂), 4.84 (septet, 1H, Cht-Si H (CH ₃) ₂), 5.12, 5.16 (t, 4H, Cp -SiH(CH ₃) ₂), 5.43-5.65 (m, 6H, Cht -SiH(CH ₃) ₂) | -2.6 (Cp-SiH(CH ₃) ₂), -1.4 (Cht-SiH(CH ₃) ₂), 93.2 (<i>ipso</i> C, Cht -SiH(CH ₃) ₂), 87.9, 90.0, 91.8 (Cht -SiH(CH ₃) ₂), 106.8 (<i>ipso</i> C, Cp -SiH(CH ₃) ₂), 101.14, 104.0 (Cp -SiH(CH ₃) ₂) | -23.2 (Cp- Si H(CH ₃) ₂), -7.0 (Cht- Si H(CH ₃) ₂) |
| 203b R = Sn(CH ₃) ₃ | 0.20 (s, 9H, Cp-Sn(CH ₃) ₃), 0.33 (s, 9H, Cht-Sn(CH ₃) ₃), 5.09, 5.28 (t, 4H, Cp -Sn(CH ₃) ₃), 5.47-5.57 (m, 6H, Cht -Sn(CH ₃) ₃) | -8.3 (Cp-Sn(CH ₃) ₃), -7.7 (Cht-Sn(CH ₃) ₃), 95.5 (<i>ipso</i> C, Cht -Sn(CH ₃) ₃), 87.0, 89.2, 91.9 (Cht -Sn(CH ₃) ₃), 106.0 (<i>ipso</i> C, Cp -Sn(CH ₃) ₃), 100.3, 103.8 (Cp -Sn(CH ₃) ₃) | -31.4 (Cp- Sn (CH ₃) ₃), 13.9 (Cp- Sn (CH ₃) ₃) |
| 203d ^e R = Si(CH ₃) ₃ | 0.15 (s, 9H, Cp-Si(CH ₃) ₃), 0.359 (s, 9H, Cht-Si(CH ₃) ₃), 5.09, 5.18 (t, 4H, Cp -Si(CH ₃) ₃), 5.48-5.64 (m, 6H, Cht -Si(CH ₃) ₃) | 0.3 (Cp-Si(CH ₃) ₃), 0.77 (Cht-Si(CH ₃) ₃), 96.5 (<i>ipso</i> C, Cht -Si(CH ₃) ₃), 87.4, 89.3, 91.1 (Cht -Si(CH ₃) ₃), 111.0 (<i>ipso</i> C, Cp -Si(CH ₃) ₃), 100.5, 103.2 (Cp -Si(CH ₃) ₃) | -8.2 (Cp- Si (CH ₃) ₃), 2.45 (Cht- Si (CH ₃) ₃) |

^a Solvent used: C₆D₆. ^b Internal reference: C₆D₆ (¹H NMR: δ 7.16 ppm; ¹³C NMR: δ 128.38 ppm).
^c External reference: Tetramethylsilane (δ 0.0 ppm). ^d External reference: Tetraethyltin (δ 1.0 ppm).
^e Rausch, M. D.; Ogasa, M.; Rogers, R. D.; Rollins, A. N. *Organometallics* **1991**, *10*, 2084-2086.

2.3. Polyolithiation of Tropicene in a 1-Pot reaction

Using a large excess of *n*-BuLi-TMEDA was attempted to improve the yield of tropicene dilithiation, but gave surprising results. Thus, addition of a slurry of tropicene in hexane to a stirred hexane solution of 8 equiv. *n*-BuLi-TMEDA at room temperature followed by quenching with chlorodimethylsilane gave a mixture of six products (**Scheme 2.3.1**). GC/MS of the crude product showed that the four major species were a disubstituted product ($m/e = 320$), two trisubstituted products ($m/e = 378$), and one tetrasubstituted product ($m/e = 436$) which is the largest peak. Three complexes were isolated as blue oils, **203a** (17 %), $[\eta^7\text{-}\{1,4\text{-bis(dimethylsilyl)}\}\text{cycloheptatrienyl}][\eta^5\text{-(dimethylsilyl) cyclopentadienyl}]\text{titanium(II)}$ (**204a**) (11 %), and $[\eta^7\text{-}\{1,4\text{-bis(dimethylsilyl)}\}\text{cycloheptatrienyl}][\eta^5\text{-}\{1,3\text{-bis(dimethylsilyl)}\}\text{cyclopentadienyl}]\text{titanium(II)}$ (**207a**) (32 %).



* Product distribution determined from integration of ¹H NMR of crude product. Isolated yield of desired product shown in parenthesis.

** Lithiation with 24 eq. of *n*-Buli-TMEDA; No attempts were made to isolate any product other than **207d**.

Scheme 2.3.1. Polyolithiation of Tropicene.

The substitution patterns were inferred from their trimethylsilyl-substituted counterparts prepared via quenching with chlorotrimethylsilane. GC/MS also showed four major species, and in this case, four products were isolated, **203d** (18 %), $\{\eta^7\text{-(trimethylsilyl)cycloheptatrienyl}\}[\eta^5\text{-}\{1,3\text{-bis(trimethylsilyl)}\}\text{cyclopentadienyl}]$ titanium(II) (**206d**) (4 %), $[\eta^7\text{-}\{1,4\text{-bis(trimethylsilyl)}\}\text{cycloheptatrienyl}]\{\eta^5\text{-(trimethylsilyl)cyclopentadienyl}\}$ titanium(II) (**204d**) (13 %), and $[\eta^7\text{-}\{1,4\text{-bis(trimethylsilyl)}\}\text{cycloheptatrienyl}][\eta^5\text{-}\{1,3\text{-bis(trimethylsilyl)}\}\text{cyclopentadienyl}]$ titanium(II) (**207d**) (33 %). Using a larger excess of *n*-BuLi, (24 equiv.) did not lead to products with higher degrees of substitution, but rather increased the isolated yield of **207d** to 39 % (59 % of the product distribution).

2.3.1. Trimethylsilyl Derivatives

The trisubstituted derivative **206d** was characterized by GC/MS, ^1H , $^{13}\text{C}\{^1\text{H}\}$, and ^{29}Si DEPT NMR spectroscopy (Table 2.3.1.1), and has a molecular ion ($m/e = 420$) consistent with three trimethylsilyl groups. Complex **206d** has one trimethylsilyl group on the cycloheptatrienyl ring, and two on the cyclopentadienyl ring, with the ^1H NMR spectrum showing two singlets at δ 0.17 and δ 0.38 for the methyl protons on Cp-(Si(CH₃)₃)₂ and Cht-Si(CH₃)₃ in a 2:1 ratio, respectively. The $^{13}\text{C}\{^1\text{H}\}$ NMR spectrum shows two signals at δ 0.41 and δ 0.83 for the methyl carbons, and two signals at δ 96.82 and δ 114.81 for the *ipso* carbons on Cht-Si(CH₃)₃ and Cp-(Si(CH₃)₃)₂, respectively. The ^{29}Si DEPT NMR spectrum of **206d** shows signals at δ -8.34 and δ 2.42 for Cp-(Si(CH₃)₃)₂ and Cht-Si(CH₃)₃.

Blue crystals of **206d** grown from hexanes at -30 °C were characterized by X-ray crystallography (**Table A.2.1 to A.2.4**), and an ORTEP drawing is shown in **Figure 2.3.1.1**. There is a plane of symmetry bisecting H1, C1, Ti1, C7, Si2, C12, and H12A. Both rings are approximately planar and coplanar with each other, with an approximately linear Centroid(Cht)-M-Centroid(Cp) angle of 179.19°.

The bond distortions on the Cht ligand are more positive than those on the Cp ligand (**Figure 2.3.1.2**), consistent with the explanation discussed in **Section 2.1.2**: a larger ring size leads to a more positive distortion while a smaller ring size leads to a more negative distortion.^{270,271,275} All the cycloheptatrienyl ring protons have a more positive distortion (24.72° average towards metal) compared to their silicon counterpart (0.33° towards metal), which can be attributed to steric effects playing a large role in the bulky trimethylsilyl substituent.^{270,271,275} In contrast, the cyclopentadienyl protons have a less positive distortion (H1: 3.56° and H3: 4.20° away from metal) compared to their silicon counterparts (3.29° away from metal). It is not clear why the bulkier Cp-trimethylsilyl groups are bent closer to the metal relative to the Cp protons.

The average Ti-C(Cht) bond length of 2.214 Å as well as the Ti-Centroid(Cht) distance of 1.490 Å are shorter than their cyclopentadienyl counterparts, with an average Ti-C(Cp) bond length of 2.328 Å and a Ti-Centroid(Cp) distance of 1.986 Å. These differences in bond lengths and distances are consistent with those of other troticene derivatives and have been discussed previously (**Section 2.1.2**).^{7,221,269}

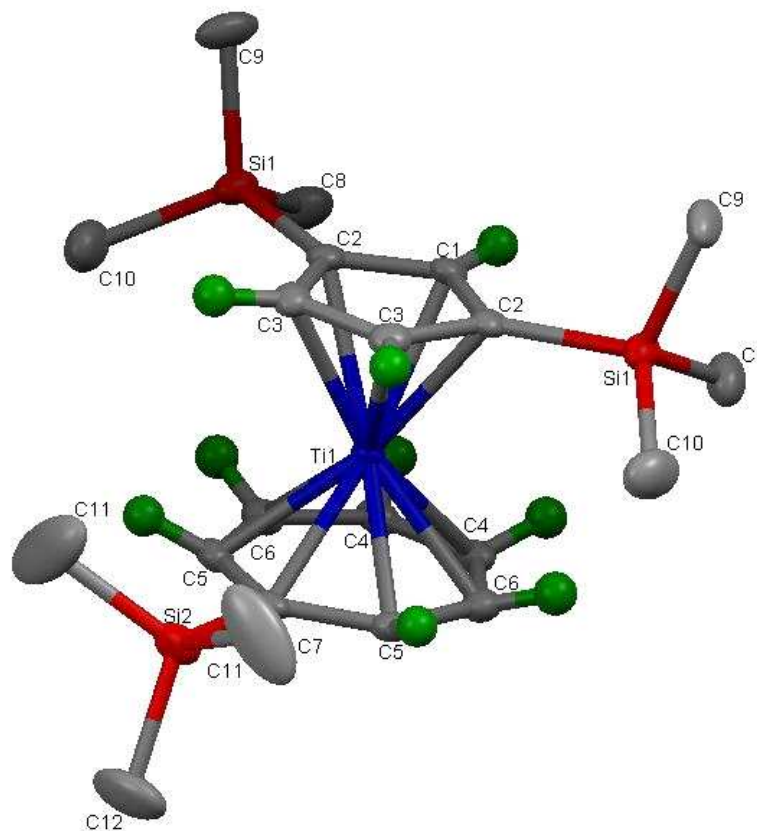


Figure 2.3.1.1. ORTEP drawing of **206d**.

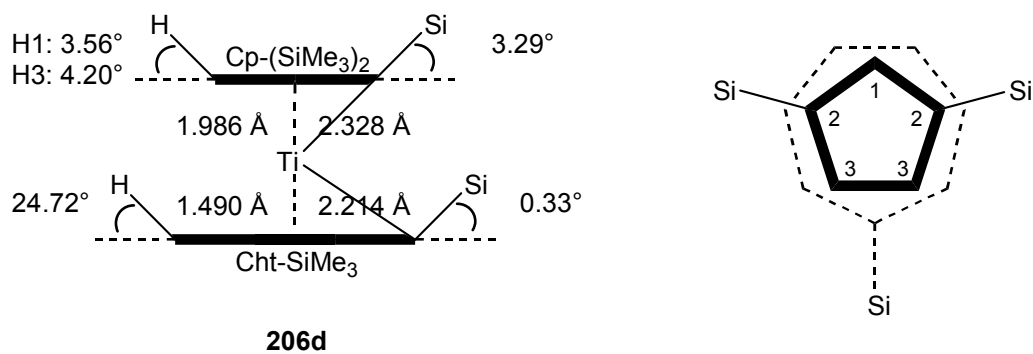


Figure 2.3.1.2. C-H and C-Si Bond Distortion Angles of **206d**.

The other trisubstituted derivative **204d** was also fully characterized. NMR spectroscopy (**Table 2.3.1.1**) and X-ray crystallography (**Table A.3.1 to A.3.5**) revealed

that, in this case, two trimethylsilyl groups are on the cycloheptatrienyl ring, and one is on the cyclopentadienyl ring. The ^1H NMR spectrum showed two pseudo triplets at δ 5.16 and δ 5.21 assigned to the **Cp**-Si(CH₃)₃ ring protons, and a multiplet at δ 5.60-5.72 was assigned to the **Cht**-(Si(CH₃)₃)₂ ring protons. The $^{13}\text{C}\{^1\text{H}\}$ NMR spectrum showed two distinct signals at δ 0.36 and δ 0.74 for the methyl carbons on Cp-Si(CH₃)₃ and Cht-(Si(CH₃)₃)₂, respectively, and the ^{29}Si DEPT NMR spectrum showed two signals at δ -8.24 and δ -2.44.

Blue crystals of **204d** grown from hexanes at -30 °C were characterized by X-ray crystallography (Table A.3.1 to A.3.5), and an ORTEP drawing is shown in Figure 2.3.1.3. There are 3 molecules (A, B, and C; molecule A is shown in Figure 2.3.1.4) in the asymmetric unit, and for all 3 molecules, both the Cht and Cp rings are approximately planar, deviating slightly from coplanarity (A: 2.00°; B: 2.13°; C: 1.16°), and they all have an approximately linear Centroid(Cht)-M-Centroid(Cp) angle (A: 177.68°; B: 178.02°; C: 178.71°).

As in the case of **206d**, the bond distortions on the Cht ligand of **204d** are more positive than those on the Cp ligand (Figure 2.3.1.5),^{270,271,275} with the cycloheptatrienyl ring protons having a more positive distortion (A: 25.57°; B: 25.69°; C: 26.21° average towards metal) compared to their silicon counterparts (A: 1.83°; B: 3.30°; C: 3.71° average towards metal). As for C-H and C-Si bond distortions on the Cp ligand, the former, for the most part, have less positive distortions (A: 4.50°; B: 4.54°; C: 4.64° average away from metal) than the latter (A: 3.85°; B: 3.86°; C: 4.60° average away from metal), and it is not clear why this is the case.

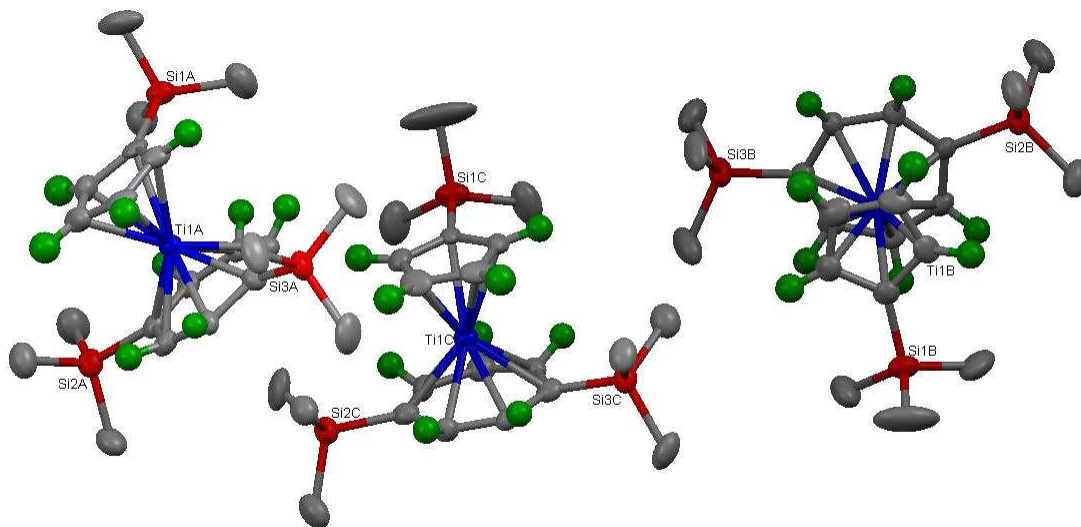


Figure 2.3.1.3. ORTEP drawing of **204d**.

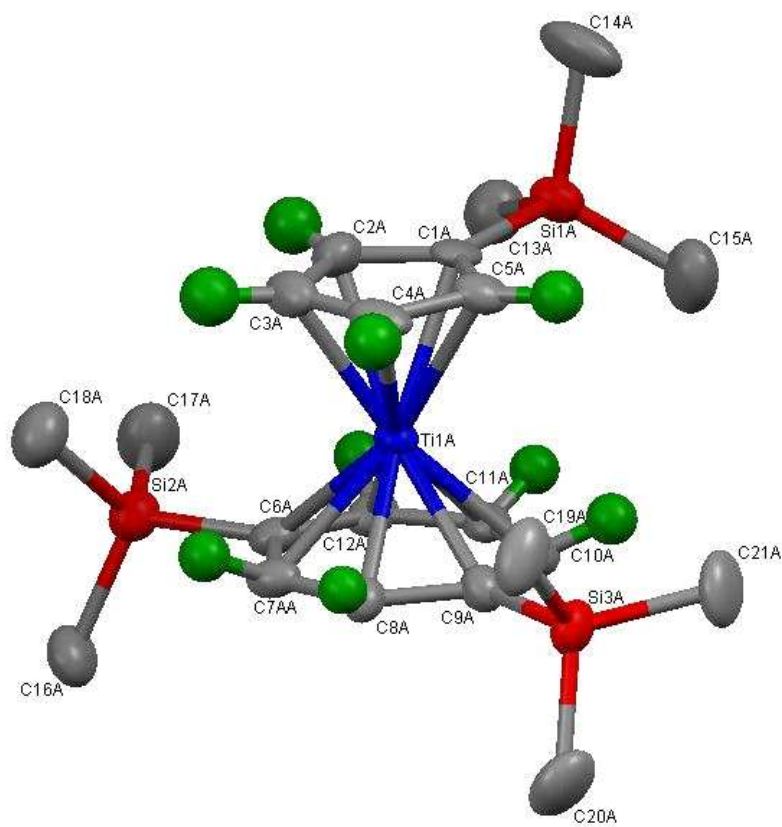


Figure 2.3.1.4. ORTEP drawing of **204d** molecule A.

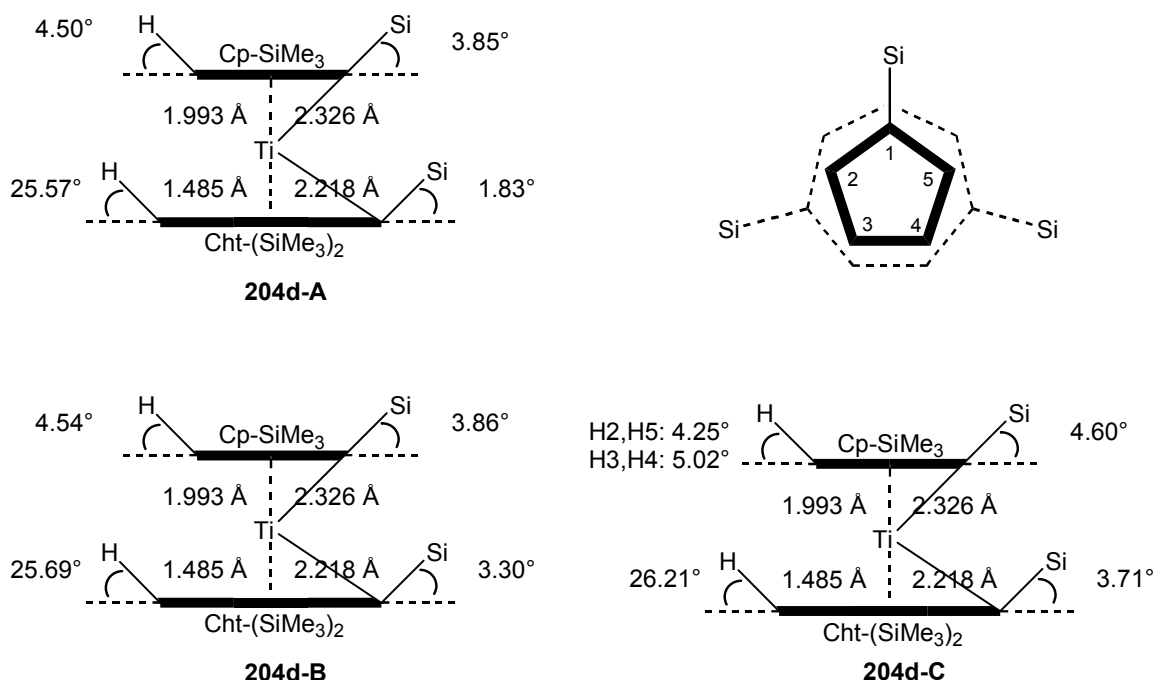


Figure 2.3.1.5. C-H and C-Si Bond Distortion Angles of **204d**.

The average Ti-C(Cht) bond length as well as the Ti-Centroid(Cht) distance of 2.218 Å and 1.485 Å, respectively are shorter than their cyclopentadienyl counterparts (c.f. average Ti-C(Cp) = 2.326 Å; average Ti-Centroid(Cp): 1.993 Å). Again, these differences in bond lengths and distances are consistent with those of other troticene derivatives and have been discussed previously (Section 2.1.2).^{7,221,269}

The tetrasubstituted derivative **207d** was similarly characterized (Table 2.3.1.1) (Table A.4.1 to A.4.5), with a molecular ion ($m/e = 492$) consistent with four trimethylsilyl groups. NMR spectroscopy and X-ray crystallography revealed that there are two trimethylsilyl groups on both the cycloheptatrienyl and cyclopentadienyl rings. The ^1H NMR spectrum showed two singlets at δ 0.19 and δ 0.44 for the methyl protons on Cp-(Si(CH₃)₃)₂ and Cht-(Si(CH₃)₃)₂ in a 1:1 ratio, respectively. The $^{13}\text{C}\{^1\text{H}\}$ NMR spectrum of **207d** showed two signals at δ 0.84 and δ 1.08 for the methyl carbons on Cp-

(Si(CH₃)₃)₂ and Cht-(Si(CH₃)₃)₂, respectively, while a ¹H coupled ¹³C NMR spectrum clearly showed the *ipso* carbons at δ 96.88 and δ 114.95 for **Cht**-(Si(CH₃)₃)₂ and **Cp**-(Si(CH₃)₃)₂, respectively. The ²⁹Si DEPT NMR spectrum showed two signals at δ -8.00 and δ 2.65 for Cp-(**Si**(CH₃)₃)₂ and Cht-(**Si**(CH₃)₃)₂, respectively.

Blue crystals of **207d** grown from hexanes at -30 °C were characterized by X-ray crystallography (Table A.4.1 to A.4.5), and an ORTEP drawing is shown in Figure 2.3.1.6. Both the Cht and Cp rings are approximately planar, deviating slightly from coplanarity by 5.72°, and have a Centroid(Cht)-M-Centroid(Cp) angle of 174.78°.

Unlike **206d** and **204d**, the C-Si bond distortions on both the cycloheptatrienyl and cyclopentadienyl rings of **207d** are less positive relative to their C-H bond counterparts (Figure 2.3.1.7), attributed to steric effects playing a large role in the bulky trimethylsilyl substituents, making further bending towards the metal center unfavorable. Also, the C-H and C-Si bond distortions on the cycloheptatrienyl ligand are more positive relative to their cyclopentadienyl ligand counterparts, attributed to the difference in ring size (see Section 2.1.2).^{270,271,275} All the cycloheptatrienyl ring protons have a more positive distortion (8.43° average towards metal) compared to their silicon counterparts (1.25° average towards metal). Similarly all the cyclopentadienyl ring protons have more positive distortions are bent slightly from the ring plane towards the metal center (C2-H2: 0.91° away from metal; C4-H4: 2.53° and C5-H5: 1.88° towards metal) compared to their silicon counterparts (7.29° away from metal).

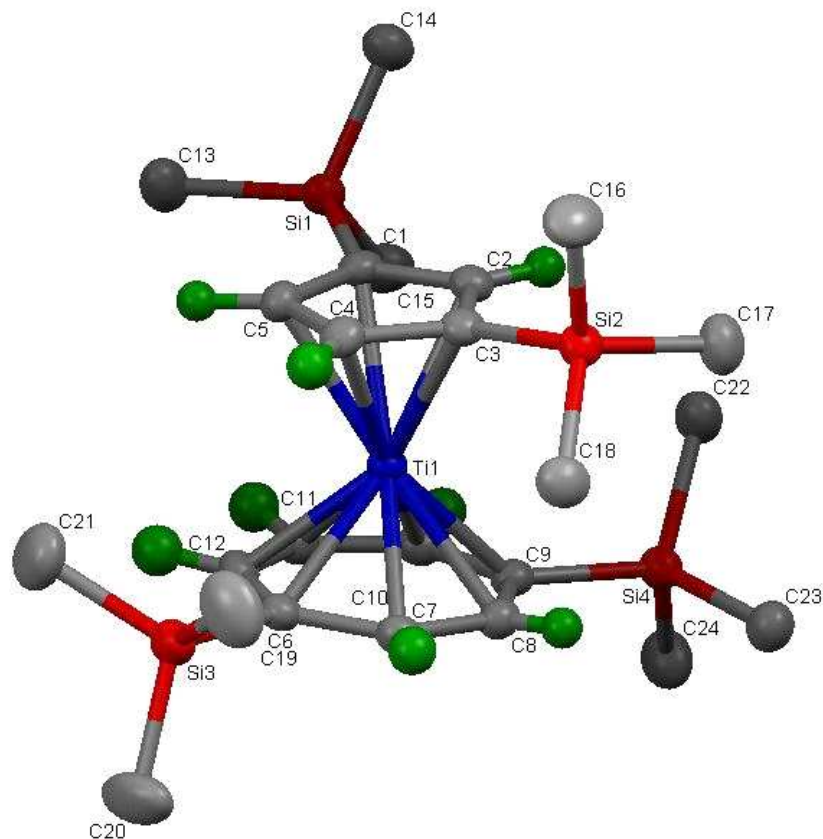


Figure 2.3.1.6. ORTEP drawing of **207d**.

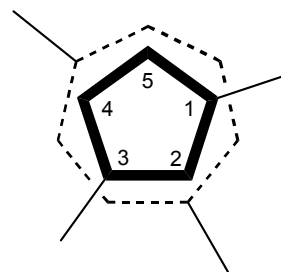
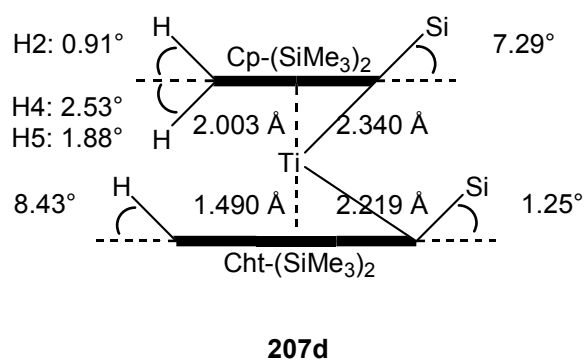
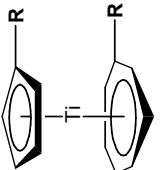
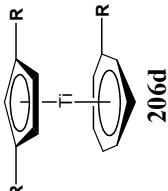
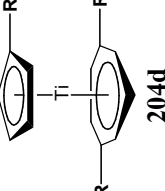
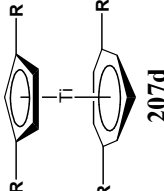


Figure 2.3.1.7. C-H and C-Si Bond Distortion Angles of **207d**.

The average Ti-C(Cht) bond length of 2.219 Å as well as the Ti-Centroid(Cht) distance of 1.490 Å are shorter than their cyclopentadienyl counterparts, with the average Ti-C(Cp) bond length of 2.340 Å and a Ti-Centroid(Cp) distance of 2.003 Å. These differences in bond lengths and distances are consistent with those of other troticene derivatives and have been discussed previously (**Section 2.1.2**).^{7,221,269}

Table 2.3.1.1. NMR Data^a for Isolated Products from Chlorotrimethylsilane-Quenched Polyolithiation of Tropicene.

| R = Si(CH ₃) ₃ | δ (¹ H) ^b | δ (¹³ C{ ¹ H}) ^b | δ (²⁹ Si DEPT) ^c |
|--|---|---|---|
|  203d | See 203d in Table 2.2.1 . | | |
|  206d | 0.17 (s, 18H, Cp-Si(CH ₃) ₃) ₂ , 0.38 (s, 9H, Cht-Si(CH ₃) ₃), 5.36 (t, 1H, Cp -Si(CH ₃) ₃) ₂ , 5.40 (d, 2H, Cp -Si(CH ₃) ₃) ₂ , 5.50-5.70 (m, 6H, Cht -Si(CH ₃) ₃) | 0.4 (Cp-Si(CH ₃) ₃) ₂ , 0.8 (Cht-Si(CH ₃) ₃), 96.8 (<i>ipso</i> C, Cht -Si(CH ₃) ₃), 87.3, 89.2, 91.0 (Cht -Si(CH ₃) ₃), 114.8 (<i>ipso</i> C, Cp -Si(CH ₃) ₃) ₂ , 106.2, 108.9 (Cp -Si(CH ₃) ₃) ₂) | -8.3 (Cp-(Si (CH ₃) ₃) ₂), 2.4 (Cht- Si (CH ₃) ₃) |
|  204d | 0.15 (s, 9H, Cp-Si(CH ₃) ₃), 0.39 (s, 18H, Cht-Si(CH ₃) ₃) ₂ , 5.16, 5.20 (t, 4H, Cp -Si(CH ₃) ₃), 5.58-5.72 (m, 5H, Cht -Si(CH ₃) ₃) ₂ | 0.4 (Cp-Si(CH ₃) ₃), 0.9 (Cht-Si(CH ₃) ₃) ₂ , 97.0 (<i>ipso</i> C, Cht -Si(CH ₃) ₃) ₂ , 91.8, 92.0, 92.9 (Cht -Si(CH ₃) ₃) ₂ , 111.8 (<i>ipso</i> C, Cp -Si(CH ₃) ₃), 100.7, 103.1 (Cp -Si(CH ₃) ₃) | -8.2 (Cp- Si (CH ₃) ₃), 2.4 (Cht-(Si (CH ₃) ₃) ₂) |
|  207d | 0.19 (s, 18H, Cp-Si(CH ₃) ₃) ₂ , 0.44 (s, 18H, Cht-Si(CH ₃) ₃) ₂ , 5.41 (t, 1H, Cp -Si(CH ₃) ₃) ₂ , 5.47 (d, 2H, Cp -Si(CH ₃) ₃) ₂ , 5.58-5.80 (m, 5H, Cht -Si(CH ₃) ₃) ₂) | 0.8 (Cp-Si(CH ₃) ₃) ₂ , 1.1 (Cht-Si(CH ₃) ₃) ₂ , 96.9 (<i>ipso</i> C, Cht -Si(CH ₃) ₃) ₂ , 91.07, 91.13, 94.0 (Cht -Si(CH ₃) ₃) ₂ , 114.9 (<i>ipso</i> C, Cp -Si(CH ₃) ₃) ₂ , 106.2, 109.5 (Cp -Si(CH ₃) ₃) ₂) | -8.0 (Cp-(Si (CH ₃) ₃) ₂), 2.6 (Cht-(Si (CH ₃) ₃) ₂) |

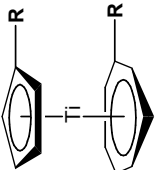
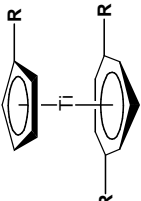
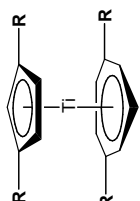
^a Solvent used: C₆D₆. ^b Internal reference: C₆D₆ (¹H NMR: δ 7.16 ppm; ¹³C NMR: δ 128.38 ppm).^c External reference: Tetramethylsilane (δ 0.0 ppm).

2.3.2. Dimethylsilyl Derivatives

The dimethylsilyl-substituted analogs of **207d** and **204d** (**207a** and **204a**, respectively) were similarly characterized. However, attempts to obtain crystals of **207a** and **204a** for X-ray crystallography were unsuccessful. The GC/MS of **207a** showed a molecular ion ($m/e = 436$) consistent with four dimethylsilyl groups. NMR spectroscopy revealed that there are two dimethylsilyl groups on both the cycloheptatrienyl and cyclopentadienyl rings. Except for a few key differences, the NMR spectra of the tetrasubstituted derivative **207a** shared common features with those of **207d**, indicative of two dimethylsilyl groups on both the cycloheptatrienyl and cyclopentadienyl rings (**Table 2.3.2.1**). The ^1H NMR spectra of **207a** showed two septets at δ 4.58 and δ 4.89 in a 1:1 ratio, assigned to the silyl protons on $\text{Cp}-(\text{SiH}(\text{CH}_3)_2)_2$ and $\text{Cht}-(\text{SiH}(\text{CH}_3)_2)_2$, respectively. Two doublets were observed at δ 0.197 and δ 0.204 for the methyl protons on $\text{Cp}-(\text{SiH}(\text{CH}_3)_2)_2$ due to the diastereotopic methyl groups of the dimethylsilyl substituents on the Cp ligand. While only one doublet can be seen at δ 0.45 for the methyl protons on $\text{Cht}-(\text{SiH}(\text{CH}_3)_2)_2$, the non-equivalent nature of the methyl groups of the dimethylsilyl substituents on the Cht ligand was confirmed by the $^{13}\text{C}\{^1\text{H}\}$ NMR spectrum which showed four methyl carbon signals: two at δ -2.54 and δ -2.24 for the methyl carbons on $\text{Cp}-(\text{SiH}(\text{CH}_3)_2)_2$, and two at δ -1.44 and δ -1.12 for the methyl carbons on $\text{Cht}-(\text{SiH}(\text{CH}_3)_2)_2$. A ^1H coupled ^{13}C NMR spectrum of **207a** clearly showed the *ipso* carbons at δ 93.8 and δ 111.5 for **Cht**-(SiH(CH₃)₂)₂ and **Cp**-(SiH(CH₃)₂)₂, respectively, and the ^{29}Si DEPT NMR showed two signals at δ -23.18 and δ -7.08 for the silicons on $\text{Cp}-(\text{SiH}(\text{CH}_3)_2)_2$ and $\text{Cht}-(\text{SiH}(\text{CH}_3)_2)_2$, respectively.

The GC/MS of **204a** showed a molecular ion ($m/e = 378$) consistent with three dimethylsilyl groups. The NMR spectra of trisubstituted derivative **204a** also shared common features with those of **204d**, indicative of two dimethylsilyl groups on the cycloheptatrienyl ring, and one on the cyclopentadienyl ring (**Table 2.3.2.1**). This was corroborated by the ^1H NMR spectrum which showed two septets at δ 4.54 and δ 4.86 for the silyl protons on $\text{Cp-SiH}(\text{CH}_3)_2$ and $\text{Cht}-(\text{SiH}(\text{CH}_3)_2)_2$ in a 1:2 ratio. One doublet at δ 0.18 can be seen for the methyl protons on $\text{Cp-SiH}(\text{CH}_3)_2$, while two doublets at δ 0.422 and δ 0.424 can be seen for the methyl protons on $\text{Cht}-(\text{SiH}(\text{CH}_3)_2)_2$ due to the non-equivalent methyl groups. This was confirmed by the $^{13}\text{C}\{^1\text{H}\}$ NMR spectrum which showed three methyl carbon signals: one signal at δ -2.51 for the methyl carbons on $\text{Cp-SiH}(\text{CH}_3)_2$, and two signals at δ -1.50 and δ -1.44 for the methyl carbons on $\text{Cht}-(\text{SiH}(\text{CH}_3)_2)_2$. A ^1H coupled ^{13}C NMR spectrum of **204a** clearly showed the *ipso* carbons at δ 93.8 and δ 107.9 for **Cht**-($\text{SiH}(\text{CH}_3)_2$)₂ and **Cp**- $\text{SiH}(\text{CH}_3)_2$, respectively, and the ^{29}Si DEPT NMR spectrum showed two signals at δ -23.36 and δ -7.09 for the silicons on $\text{Cp-SiH}(\text{CH}_3)_2$ and $\text{Cht}-(\text{SiH}(\text{CH}_3)_2)_2$, respectively.

Table 2.3.2.1. NMR Data^a for Isolated Products from Chlorodimethylsilane-Quenched Polyolithiation of Tropicene.

| R = SiH(CH ₃) ₂ | δ (¹ H) ^b | δ (¹³ C{ ¹ H}) ^b | δ (²⁹ Si DEPT) ^c |
|---|--|--|---|
|  203a | See 203a in Table 2.2.1 . | | |
|  204a | 0.18 (d, 6H, Cp-SiH(CH ₃) ₂), 0.422, 0.424 (2 d, 12H, Cht-(SiH(CH ₃) ₂) ₂), 4.54 (septet, 1H, Cp-SiH(CH ₃) ₂), 4.86 (septet, 2H, Cht-SiH(CH ₃) ₂), 5.17, 5.23 (t, 4H, Cp -(SiH(CH ₃) ₂) ₂), 5.59-5.72 (m, 5H, Cht -(SiH(CH ₃) ₂) ₂) | -2.5 (Cp-SiH(CH ₃) ₂), -1.5, -1.4 (Cht-(SiH(CH ₃) ₂) ₂), 93.8 (<i>ipso</i> C, Cht -(SiH(CH ₃) ₂) ₂), 92.5, 93.0, 94.7 (Cht -(SiH(CH ₃) ₂) ₂), 107.9 (<i>ipso</i> C, Cp -(SiH(CH ₃) ₂) ₂), 101.4, 104.4 (Cp -(SiH(CH ₃) ₂) ₂) | -23.4 (Cp-SiH(CH ₃) ₂), -7.1 (Cht-(SiH(CH ₃) ₂) ₂) |
|  207a | 0.197, 0.204 (2 d, 12H, Cp-(SiH(CH ₃) ₂) ₂), 0.45 (d, 12H, Cht-(SiH(CH ₃) ₂) ₂), 4.58 (septet, 2H, Cp-(SiH(CH ₃) ₂) ₂), 4.89 (septet, 2H, Cht-(SiH(CH ₃) ₂) ₂), 5.45 (d, 2H, Cp -(SiH(CH ₃) ₂) ₂), 5.47 (t, 1H, Cp -(SiH(CH ₃) ₂) ₂), 5.58-5.78 (m, 5H, Cht -(SiH(CH ₃) ₂) ₂) | -2.5, -2.2 (Cp-(SiH(CH ₃) ₂) ₂), -1.4, -1.1 (Cht-(SiH(CH ₃) ₂) ₂), 93.8 (<i>ipso</i> C, Cht -(SiH(CH ₃) ₂) ₂), 92.4, 93.2, 95.8 (Cht -(SiH(CH ₃) ₂) ₂), 111.5 (<i>ipso</i> C, Cp -(SiH(CH ₃) ₂) ₂), 107.4, 111.6 (Cp -(SiH(CH ₃) ₂) ₂) | -23.2 (Cp-(SiH(CH ₃) ₂) ₂), -7.1 (Cht-(SiH(CH ₃) ₂) ₂) |

^a Solvent used: C₆D₆. ^b Internal reference: C₆D₆ (¹H NMR: δ 7.16 ppm; ¹³C NMR: δ 128.38 ppm).

^c External reference: Tetramethylsilane (δ 0.0 ppm).

2.4. Summary

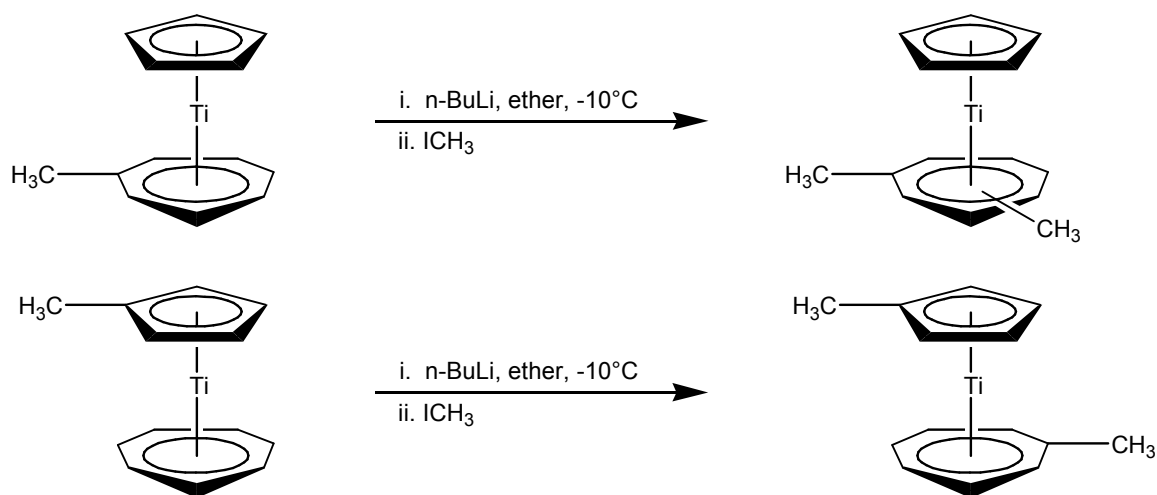
The preferential monolithiation of the cyclopentadienyl ligand of troticene using *n*-butyllithium was demonstrated. While the monolithiation of troticene at 0 °C has been shown to occur predominantly on the cycloheptatrienyl ligand,^{1,2} doing the reaction at room temperature leads to preferential monolithiation of the cyclopentadienyl ligand.

Temperature plays a big part in the monolithiation of troticene. While the monolithio-Cht troticene was preferentially formed at 0 °C, it was less stable than the monolithio-Cp troticene, particularly at higher temperatures. Warming up the reaction from 0 °C to room temperature resulted in a significant drop in the amount of monolithio-Cht troticene. Doing the reaction at room temperature also showed a faster drop in the amount of monolithio-Cht troticene over time compared to monolithio-Cp troticene. These results were taken to mean that the former is a kinetic product, while the latter is a thermodynamic product.

Troticene was readily dilithiated with 2.5 equiv. of *n*-butyllithium/TMEDA, and using a large excess of lithiating agent (8 equiv.) resulted in polyolithiation with up to 4 lithiums. Using an even larger excess of lithiating agent (24 equiv.) did not significantly increase the degree of lithiation beyond 4.

Chapter 3. Lithiation of Substituted (η^7 -Cycloheptatrienyl)(η^5 -cyclopentadienyl)titanium(II) Derivatives

The lithiation of substituted trocticene derivatives, to our knowledge, has only been reported once. Groenenboom and coworkers were able to add a second methyl group onto $\{\eta^7\text{-methylcycloheptatrienyl}\}\{\eta^5\text{-cyclopentadienyl}\}\text{titanium(II)}$ and $\{\eta^7\text{-cycloheptatrienyl}\}\{\eta^5\text{-methylcyclopentadienyl}\}\text{titanium(II)}$ via lithiation. In both cases, substitution occurred on the cycloheptatrienyl ligand (**Scheme 3.1**).¹ This chapter presents the lithiation of substituted trocticene derivatives and is a potential way for the preparation and characterization of some of the minor products from **Chapter 2**.

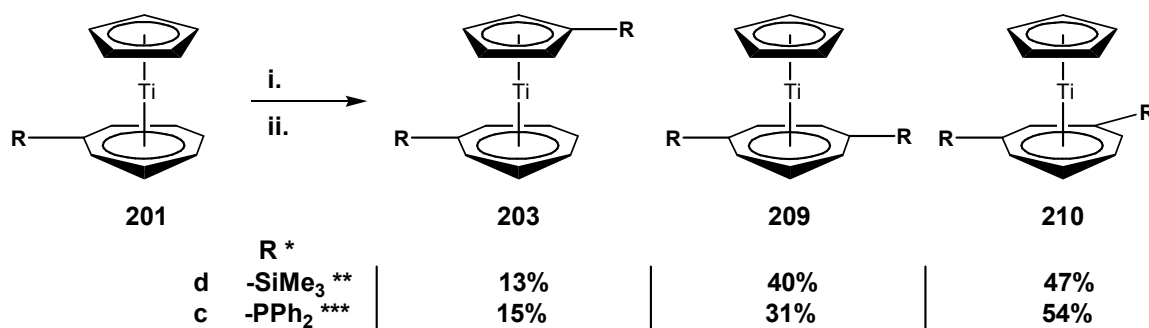


Scheme 3.1. Monolithiation of Methyltrocticene.¹

3.1. Monolithiation of Substituted Tropicene Derivatives

3.1.1. Monolithiation of the Cycloheptatrienyl ligand of Monosubstituted Tropicenes

Monolithiation of the trimethylsilyl-substituted cycloheptatrienyl ligand of **201d** was achieved by addition of 1.8 equiv. of *n*-BuLi to a stirred solution of **201d** in diethyl ether at -10 °C. Quenching with chlorotrimethylsilane gave a mixture of three *bis*(trimethylsilyl)tropicene isomers as major the product (71 % yield; blue oil) (**Scheme 3.1.1.1**), with ¹H NMR revealing an overall ratio of 13 % **203d**, 40 % **209d**, and 47 % **210d**.



i. excess *n*-BuLi, ether, -10 °C; ii. Cl-R (R = -SiMe₃, -PPh₂), -78°C - r.t.

* Product distribution determined from integration of ¹H NMR of crude product.

** Yield = 71% (**mixture**)

*** Yield = 37% (**210c**)

Scheme 3.1.1.1. Monolithiation of **201**.

A similar reaction with the diphenylphosphino-substituted complex (**201c**) and 5 equiv. of *n*-BuLi quenched with chlorodiphenylphosphine also produced three isomers of *bis*(diphenylphosphino)tropicene, with an overall ratio of 15 % **203c**,³ 31 % **209c**, and 54 % **210c** (**Scheme 3.1.1.1**). Complex **210c** was isolated as a pure solid via recrystallization from the crude product (37 % yield; blue solid).

In both reactions, one isomer (**203**) was derived from lithiation at the cyclopentadienyl ligand, and two isomers (**209** and **210**) were derived from lithiation at the cycloheptatrienyl ligand. This is consistent with the NMR data reported by Groenenboom and coworkers on the monolithiation of the methyl-substituted derivative.¹

While **210d** and **210c** definitely have a 1,3-substitution pattern on the Cht ligand, as evidenced by the crystal structure of **210c** (discussed later in this section), it is unlikely that **209d** and **209c** have a 1,2-substitution pattern because lithiation at the 2-position usually occurs only in the presence of *ortho*-lithiation directing groups,^{8,10,20,24,38,132,144,191,198-202} of which trimethylsilyl and diphenylphosphino groups are not. Thus, a 1,4-substitution pattern on **209d** and **209c** was considered much more likely.

Attempts to separate the three *bis*(trimethylsilyl)troticene isomers via column chromatography were unsuccessful. However, eluting the mixture through a long column of deactivated alumina with hexanes produced two portions with different isomer ratios, facilitating analysis of the NMR spectra. The mixture was characterized by GC/MS, ¹H, ¹³C {¹H}, ¹³C, and ²⁹Si DEPT NMR spectroscopy (Table 3.1.1.1). Complex **203d** showed two methyl proton singlets at δ 0.15 (Cp-Si(CH₃)₃) and δ 0.359 (Cht-Si(CH₃)₃), and two triplets at δ 5.09 and δ 5.18 for the Cp-Si(CH₃)₃ protons. In contrast, **209d** and **210d** each have only one methyl proton singlet at δ 0.370 and δ 0.356, respectively, and one Cp proton singlet at δ 4.95 and δ 4.96, respectively. The ¹³C {¹H} NMR signals of **209d** and **210d** have similar features, each with one signal for the Cht-(Si(CH₃)₃)₂ methyl carbons (δ 0.72 and δ 0.79, respectively) and the Cp ring carbons (δ 97.6 and δ 97.5, respectively). With the aid of a ¹H-coupled ¹³C NMR spectrum, the Cht-(Si(CH₃)₃)₂ *ipso*

carbons for **209d** and **210d** were identified at δ 97.0 and δ 99.4, respectively. The ^{29}Si DEPT NMR spectrum showed one signal each for **209d** and **210d** at δ 2.40 and δ 2.26, respectively, while **203d** has two signals at δ -8.2 and δ 2.45.

The mixture of *bis*(diphenylphosphino)troticene isomers (**203c**, **209c**, and **210c**) was similarly characterized using ^1H , $^{13}\text{C}\{^1\text{H}\}$, ^{13}C , and $^{31}\text{P}\{^1\text{H}\}$ NMR spectroscopy (Table 3.1.1.2), with **210c** being successfully isolated via recrystallization. In addition, the NMR signals of **209c** (^1H and $^{31}\text{P}\{^1\text{H}\}$) were deduced with the aid of a ^1H - ^1H COSY NMR spectrum of the mixture as well as the NMR spectra of pure samples of **203c** (obtained as minor product from preparation of **202c**, Section 2.1.2) and **210c**. ^1H NMR spectroscopy showed the *Cp* protons of **209c** and **210c** at δ 4.88 and δ 4.80, respectively (c.f. **201c**, δ 4.89), while **203c** has a multiplet at δ 5.01-5.09 for the *Cp*-PPh₂ protons. The $^{13}\text{C}\{^1\text{H}\}$ NMR spectrum of **210c** showed one signal at δ 100.3 for the *Cp* carbons and one signal (a doublet of doublets) at δ 96.7 for the *Cht*-(PPh₂)₂ *ipso* carbons (Figure 3.1.1.1). In comparison, **203c** has two *ipso* carbons at δ 94.8 (d, *Cht*-PPh₂) and δ 110.9 (d, *Cp*-PPh₂). $^{31}\text{P}\{^1\text{H}\}$ NMR spectroscopy showed one signal each for **209c** and **210c** at δ 17.5 and δ 19.6, respectively (c.f. **201c**, δ 17.8), while **203c** has two signals at δ -18.8 (*Cp*-PPh₂) and δ 17.4 (*Cht*-PPh₂).

Blue crystals of **210c** grown from toluene at room temperature were characterized by X-ray crystallography (Table A.5.1 to A.5.4), and an ORTEP drawing is shown in Figure 3.1.1.2. There is a plane of symmetry bisecting H1, C1, Ti1, C7, and H7. Both rings are approximately planar, deviating slightly from coplanarity by 1.65°, and have a Centroid(*Cht*)-Ti-Centroid(*Cp*) angle of 176.92°. The distortion angles of the C-H bonds on the cycloheptatrienyl ring are more positive than their C-P bond counterparts which lie

approximately on the ring plane, (**Figure 3.1.1.3**) attributed to steric effects playing a large role, making further bending of the bulky trimethylsilyl substituents towards the metal center unfavorable. The cycloheptatrienyl ring protons also have more positive distortions (25.28° average towards metal) than their cyclopentadienyl ring counterparts (4.67° average away from metal), attributed to the difference in ring size (see **Section 2.1.2**).^{270,271,275}

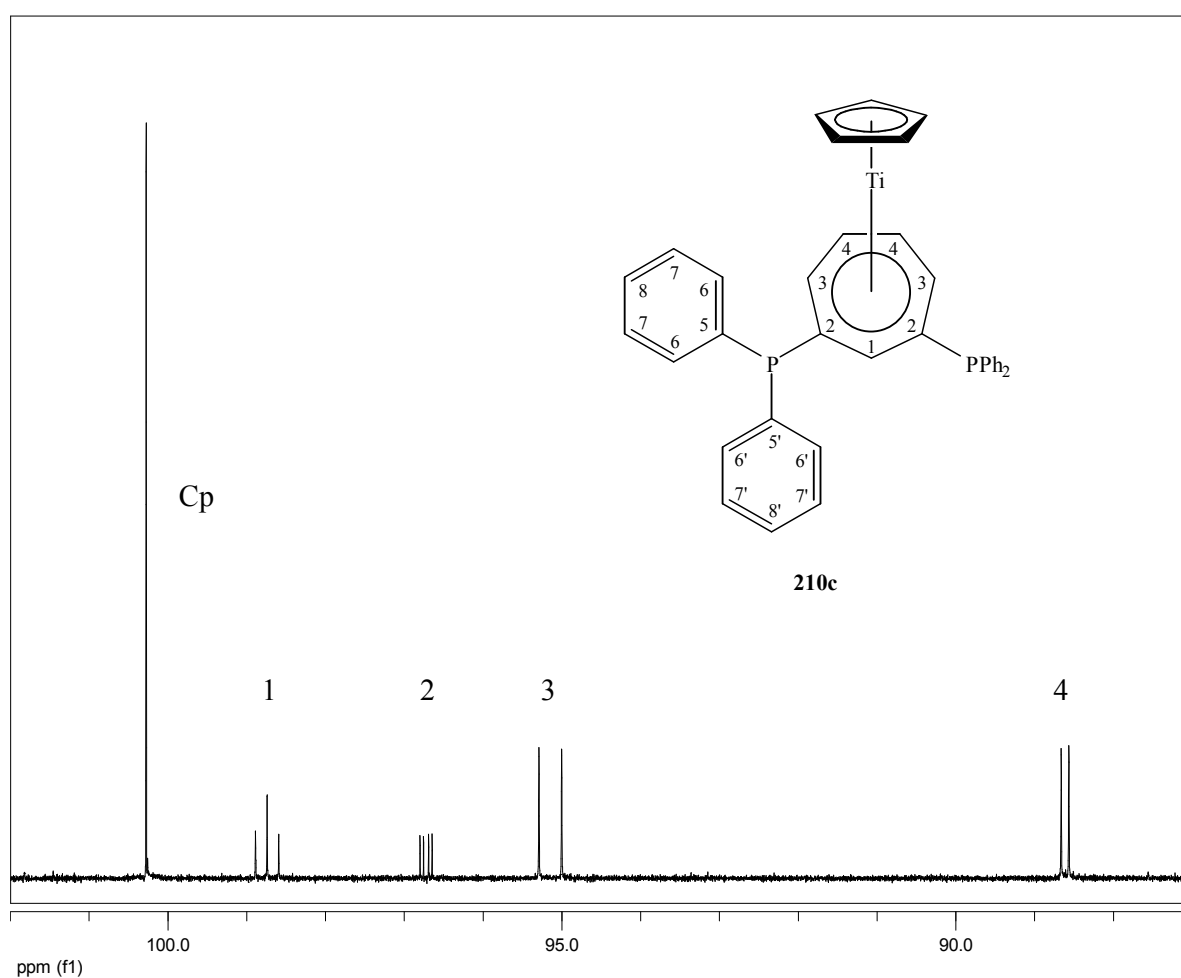


Figure 3.1.1.1. Cp and Cht $^{13}\text{C}\{^1\text{H}\}$ NMR Carbon Signals of **210c**.

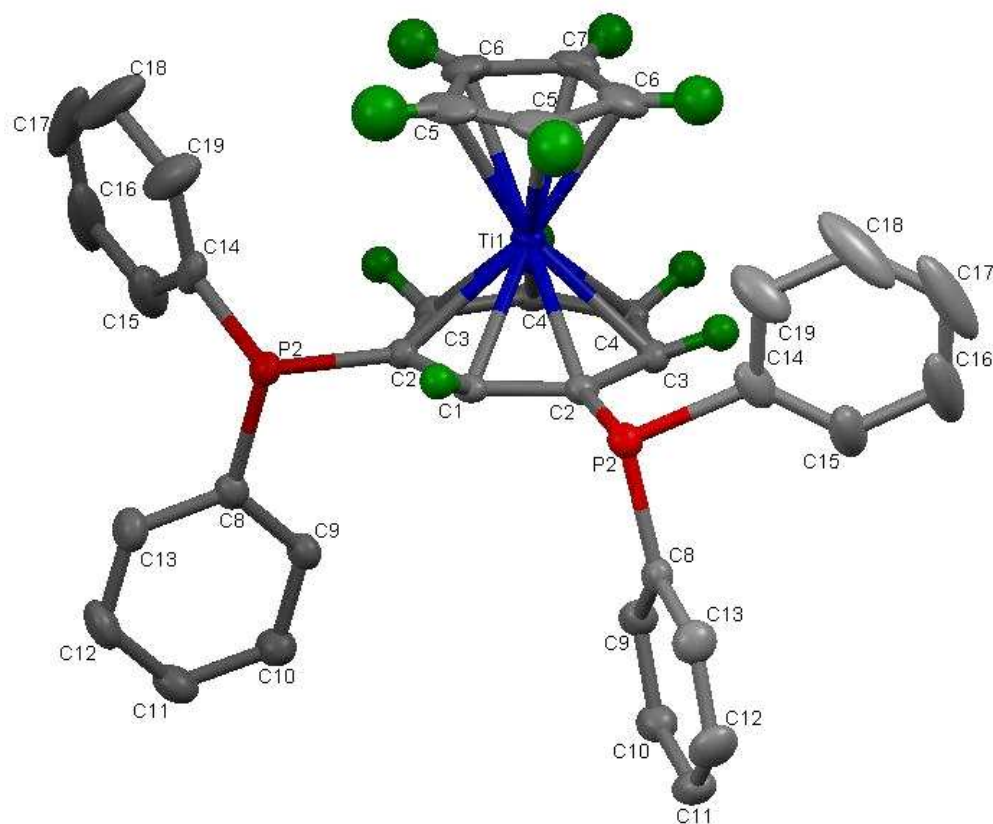


Figure 3.1.1.2. ORTEP drawing of **210c**.

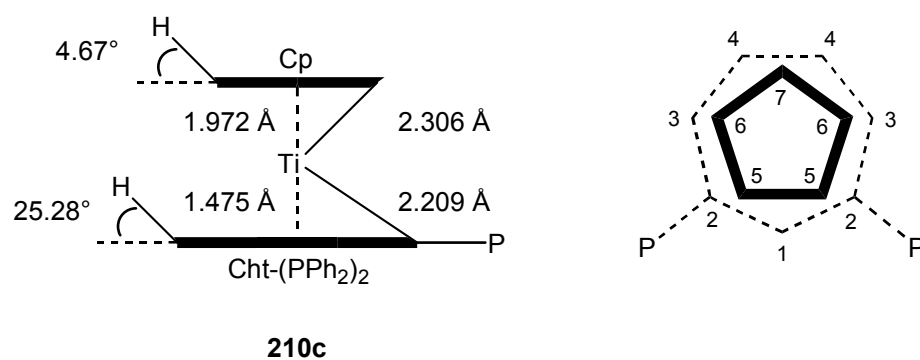
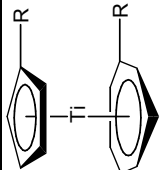
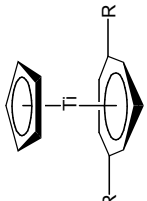
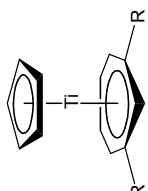


Figure 3.1.1.3. C-H and C-P Bond Distortion Angles of **210c**.

The average Ti-C(Cht) bond length of 2.209 Å as well as the Ti-Centroid(Cht) distance of 1.475 Å are shorter than their cyclopentadienyl counterparts, with an average Ti-C(Cp) bond length of 2.306 Å and a Ti-Centroid(Cp) distance of 1.972 Å. These differences in bond lengths and distances are consistent with those of other troticene derivatives and have been discussed previously (**Section 2.1.2**).^{7,221,269}

Monolithiation on the cyclopentadienyl ligand of a Cp-monosubstituted troticene derivative was not done due to the results obtained from the monolithiation of either ligand of **203d**, discussed in the following section.

Table 3.1.1.1. NMR Data^a for Major Products from Chlorotrimethylsilane-Quenched Monolithiation of **201d.**

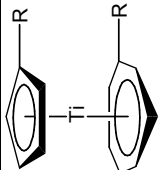
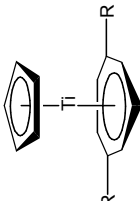
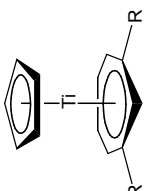
| R = Si(CH ₃) ₃ | δ (¹ H) ^b | δ (¹³ C{ ¹ H}) ^b | δ (²⁹ Si DEPT) ^c |
|--|---|---|--|
|  <p>203d^d</p> | See 203d in Table 2.2.1. | | |
|  <p>209d</p> | 0.370 (s, 12H, Cht-(Si(CH ₃) ₃) ₂), 4.95 (s, 5H, Cp), 5.55-5.70 (m, 5H, Cht -(Si(CH ₃) ₃) ₂) | 0.72 (Cht-(Si(CH ₃) ₃) ₂), 97.0 (<i>ipso</i> C, Cht -(Si(CH ₃) ₃) ₂), 91.30, 91.6, 93.7 (Cht -(Si(CH ₃) ₃) ₂), 97.6 (Cp) | 2.40 (Cht-(Si (CH ₃) ₃) ₂) |
|  <p>210d</p> | 0.356 (s, 12H, Cht-(Si(CH ₃) ₃) ₂), 4.96 (s, 5H, Cp), 5.50-5.70, 5.87-5.90 (m, 5H, Cht -(Si(CH ₃) ₃) ₂) | 0.79 (Cht-(Si(CH ₃) ₃) ₂), 99.4 (<i>ipso</i> C, Cht -(Si(CH ₃) ₃) ₂), 89.8, 91.32, 96.0 (Cht -(Si(CH ₃) ₃) ₂), 97.5 (Cp) | 2.26 (Cht-(Si (CH ₃) ₃) ₂) |

^a Solvent used: C₆D₆. ^b Internal reference: C₆D₆ (¹H NMR: δ 7.16 ppm; ¹³C NMR: δ 128.38 ppm).

^c External reference: Tetramethylsilane (δ 0.0 ppm).

^d Rausch, M. D.; Ogasa, M.; Rogers, R. D.; Rollins, A. N. *Organometallics* **1991**, 10, 2084-2086.

Table 3.1.1.2. NMR Data^a for Major Products from Chlorodiphenylphosphine-Quenched Monolithiation of **201d**.

| R = PPh ₂ | δ (¹ H) ^b | δ (¹³ C{ ¹ H}) ^b | δ (³¹ P{ ¹ H}) ^c |
|--|--|---|---|
|  <p>203c^d</p> | 5.01-5.09 (m, 4H, Cp -PPh ₂), 5.36-5.50, 5.76-5.86 (m, 6H, Cht -PPh ₂), 6.96-7.10, 7.28-7.54 (m, 20H, -PPh ₂) | 94.8 (d, <i>ipso</i> C, Cht -PPh ₂ , ¹ J _{C-P} = 11 Hz), 88.9 (Cht -PPh ₂), 89.7, 94.0 (d, Cht -PPh ₂), 110.9 (d, <i>ipso</i> C, Cp -PPh ₂ , ¹ J _{C-P} = 12 Hz), 101.7, 104.5 (d, Cp -PPh ₂), 140.1 (d, <i>ipso</i> C, Cp -PPh ₂ , ¹ J _{C-P} = 12 Hz), 141.2 (d, <i>ipso</i> C, Cht -PPh ₂ , ¹ J _{C-P} = 14 Hz), 129.0, 129.2 (-PPh ₂), 128.8, 128.9, 134.2, 134.45 (d, -PPh ₂) | -18.8 (Cp-PPh ₂), 17.4 (Cht-PPh ₂) |
|  <p>209c</p> | 4.88 (s, 5H, Cp), 5.37-5.45, 5.83-5.91 (m, 5H, Cht -PPh ₂), 7.05-7.18, 7.41-7.48, 7.59-7.66 (m, 20H, Cht -PPh ₂) | | 17.5 (Cht-(PPh ₂) ₂) |
|  <p>210c^e</p> | 4.80 (s, 5H, Cp), 5.38-5.46, 6.00-6.22 (m, 5H, Cht -PPh ₂), 6.94-7.10, 7.30-7.48 (m, 20H, Cht -PPh ₂) | 88.6 (d, C4, Cht -(PPh ₂) ₂), 95.2 (d, C3, Cht -(PPh ₂) ₂), 98.7 (t, C1, Cht -(PPh ₂) ₂), 96.7 (dd, <i>ipso</i> C, Cht -(PPh ₂) ₂ , ¹ J _{C-P} = 14 Hz), 100.3 (Cp), 128.7, 128.8, 128.86, 128.92, 129.2 (C7, C7', C8, C8', Cht -(PPh ₂) ₂), 134.1, 134.7 (d, C6, C6', Cht -(PPh ₂) ₂), 141.0, 141.6 (d, <i>ipso</i> C, C5, C5', Cht -(PPh ₂) ₂ , ¹ J _{C-P} = 14 Hz) | 19.6 (Cht-(PPh ₂) ₂) |

^a Solvent used: C₆D₆. ^b Internal reference: C₆D₆ (¹H NMR: δ 7.16 ppm; ¹³C NMR: δ 128.38 ppm).

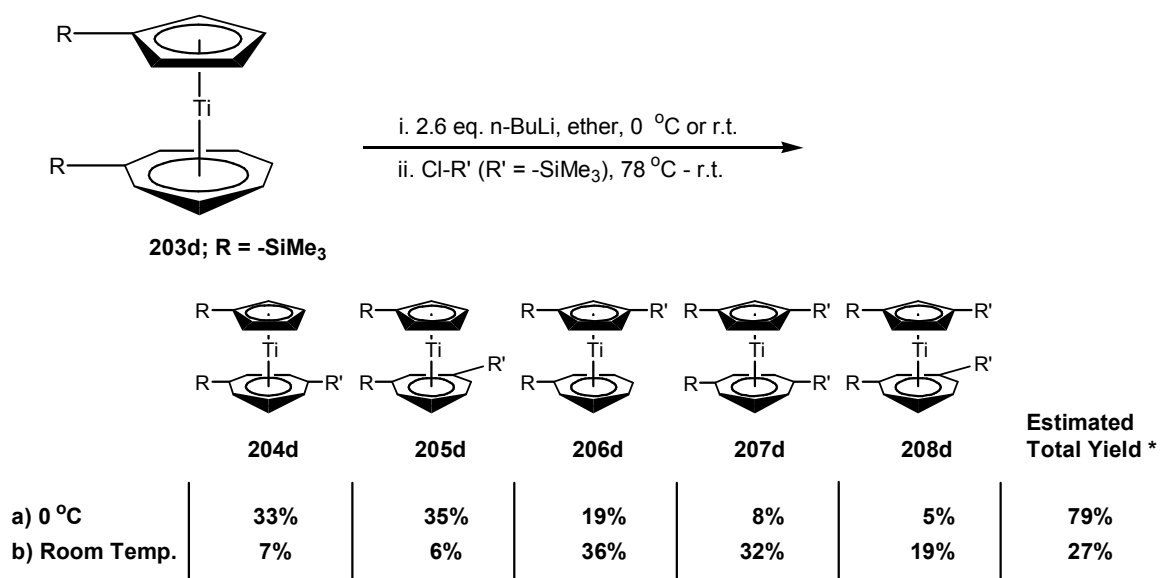
^c External reference: 85 % Phosphoric Acid (δ 0.0 ppm).

^d Kool, L. B.; Ogasa, M.; Rausch, M. D.; Rogers, R. D. *Organometallics* **1989**, 8, 1785-1790.

^e See **Figure 3.1.1.1** for ¹³C{¹H} NMR numbering scheme.

3.1.2. Monolithiation of *Bis*(trimethylsilyl)troticene **203d**

Monolithiation of the cycloheptatrienyl ligand of the *bis*(trimethylsilyl)-complex **203d** was achieved by adding 2.6 equiv. of *n*-BuLi to a stirred solution of **203d** in diethyl ether at 0 °C (**Scheme 3.1.2.1**). Quenching with chlorotrimethylsilane gave a blue oil product mixture consisting of **206d** (19 %), **204d** (33 %), **205d** (35 %), **207d** (8 %), and **208d** (5 %), with an estimated combined yield of 79 %. As in the case of **Scheme 3.1.1.1**, the majority of the products were derived from monolithiation on the cycloheptatrienyl ring (**204d** plus **205d**).



* Product distribution and yield estimated from integration of ¹H NMR of crude product.

Scheme 3.1.2.1. Monolithiation on either the Cht or Cp Ligand of **203d**.

In contrast, monolithiation of the cyclopentadienyl ligand of **203d** with 2.6 equiv. of *n*-BuLi at room temperature fared poorly (**Scheme 3.1.2.1**). Quenching with chlorotrimethylsilane gave a blue oil product mixture consisting of **206d** (36 %), **204d** (7

%), **205d** (6 %), **207d** (32 %), and **208d** (19 %), with an estimated combined yield of 27 %. While monolithiation occurred predominantly on the cyclopentadienyl ring (**206d** vs. **204d** plus **205d**), unlike the reaction at 0 °C, a significant portion of the products was derived from dilithiation. In addition, the reaction has a particularly low combined yield.

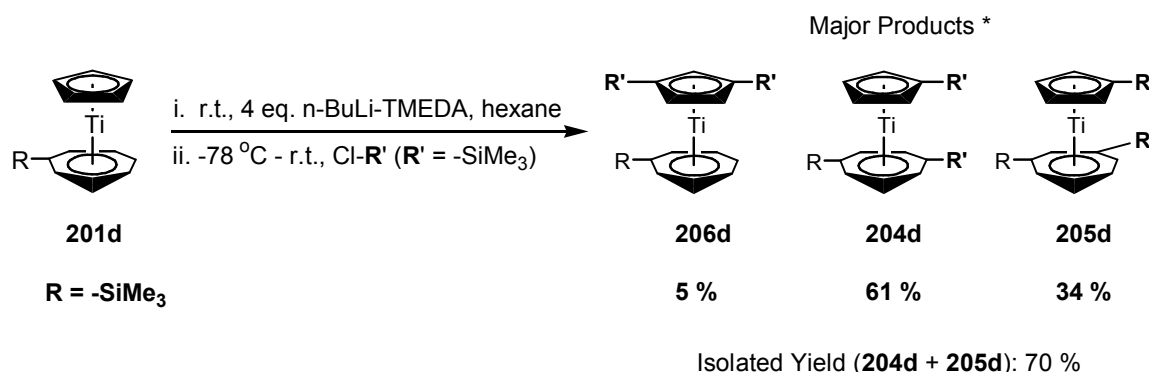
It is apparent that the cyclopentadienyl ligand of **203d** was more difficult to lithiate compared to the cycloheptatrienyl ligand, as evidenced by the much lower estimated yield obtained at room temperature compared with that at 0 °C. This is consistent with the assessment that the Cht ring protons are more acidic (thus more readily lithiated) than those of the Cp ring.^{1,2,211,212} Compared with troticene, the monolithiation of the substituted troticene derivatives **201d** and **203d** required more *n*-BuLi to push the reaction forward, attributed to a decrease in negative character of the ring ligands as more substituents are added to the ring.²¹²

3.2. Dilithiation of Substituted Tropicene Derivatives

3.2.1. Dilithiation of Monosubstituted Tropicene Derivatives **201d** and **202d**

Dilithiation of either **201d** or **202d** was achieved using excess *n*-BuLi-TMEDA. Addition of a solution of **201d** in hexane to 4 equiv. *n*-BuLi-TMEDA at room temperature followed by quenching with chlorotrimethylsilane gave a mixture of products derived from monolithiation (**203d**, **209d**, and **210d**; 7 %) and dilithiation (**206d**, **204d**, and **205d**; 93 %) of **201d** (Scheme 3.2.1.1) as determined from the integration of the ¹H NMR spectrum of the crude product mixture. As intended, the dilithiation products predominated, with the *tris*(trimethylsilyl)tropicene isomers having an overall ratio of 5 % **206d**, 61 % **204d** and 34 % **205d**. While a mixture of **204d** and

205d was isolated (70 % yield; blue oil), attempts to isolate them from each other via column chromatography failed.



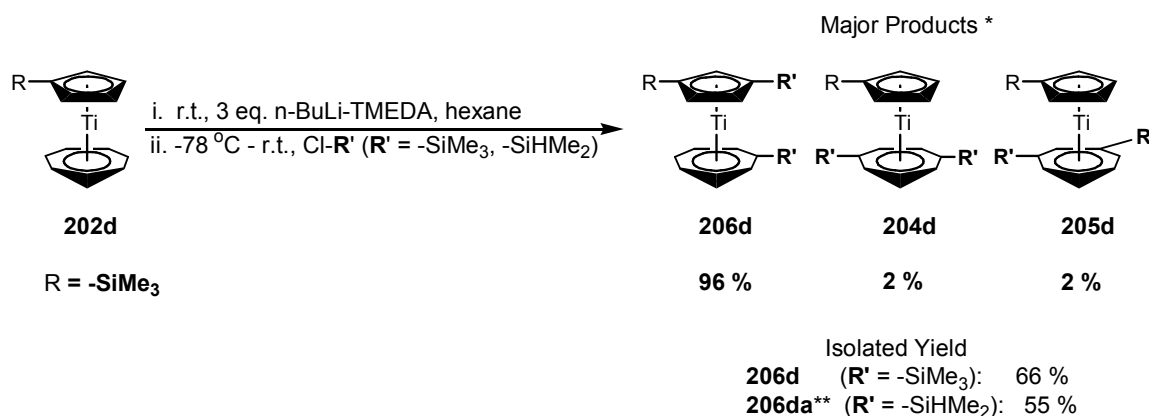
* Product distribution determined from integration of ^1H NMR of crude product.

Scheme 3.2.1.1. Major Product Distribution and Isolated Yield for the Dilithiation of **201d**.

The mixture of **204d** and **205d** was characterized by GC/MS, ^1H , $^{13}\text{C}\{^1\text{H}\}$, ^{13}C , and ^{29}Si DEPT NMR spectroscopy (**Table 3.2.1.1**), confirming that both isomers have two trimethylsilyl groups on the Cht ligand and only one on the Cp ligand. Analysis of the NMR spectra of the mixture was facilitated by comparison with those of isolated **204d** (from **Chapter 2**), making it possible to determine the NMR signals of **205d**. As expected, the NMR spectrum of **205d** have common features with those of **204d**, with the ^1H NMR spectrum of the mixture showing two singlets for **205d** at δ 0.16 (Cp-Si(CH_3) $_3$) and δ 0.37 (Cht-(Si(CH_3) $_3$) $_2$) in a 1:2 ratio, respectively (c.f. **204d**, δ 0.15 and δ 0.39). The $^{13}\text{C}\{^1\text{H}\}$ NMR spectrum of the mixture showed two signals for **205d** at δ 0.3 (Cp-Si(CH_3) $_3$) and δ 0.8 (Cht-(Si(CH_3) $_3$) $_2$) for the methyl carbons, and another two signals at δ 98.9 (Cht-(Si(CH_3) $_3$) $_2$) and δ 111.0 (Cp-Si(CH_3) $_3$) for the *ipso* carbons. The ^{29}Si DEPT

NMR of the mixture also showed two signals at δ -8.0 (Cp-**Si**(CH₃)₃) and δ -2.5 (Cht-**(Si**(CH₃)₃)₂) for **205d**.

The dilithiation of **202d** with 3 equiv. of *n*-BuLi-TMEDA followed by quenching with chlorotrimethylsilane also gave a mixture of products derived from monolithiation (**203d**; 4 %), dilithiation (**204d**, **205d**, and **206d**; 93 %), and trilithiation (**207d** and **208d**; 3 %) (**Scheme 3.2.1.2**) as determined from the integration of the ¹H NMR spectrum of the crude product mixture. As in the case of **Scheme 3.2.1.1**, the dilithiation products predominated, with the *tris*(trimethylsilyl)troticene isomers having an overall ratio of 96 % **206d**, 2 % **204d** and 2 % **205d**. Complex **206d** was isolated via column chromatography as a blue solid (66 % yield), with its identity confirmed by GC/MS and ¹H NMR spectroscopy as having two trimethylsilyl groups on the Cp ligand, and only one the Cht ligand (**Section 2.3.1**). A similar reaction quenched with chlorodimethylsilane produced **206da** as the major product (55 % yield; blue oil).



* Product distribution determined from integration of ¹H NMR of crude product.

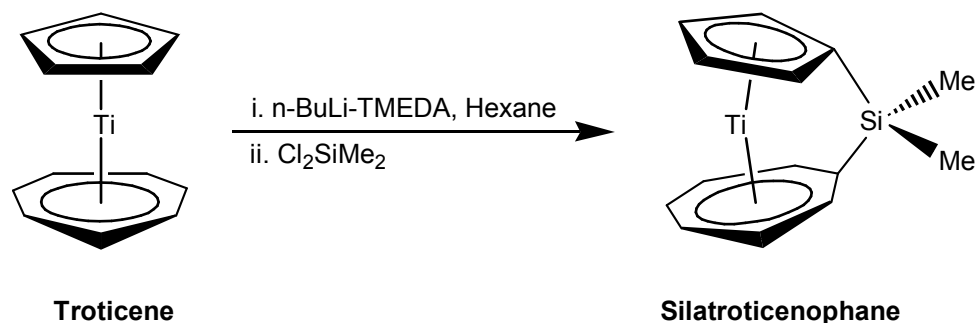
** Only **206da** was identified and isolated for R' = -SiHMe₂.

Scheme 3.2.1.2. Major Product Distribution and Isolated Yield for the Dilithiation of **202d**.

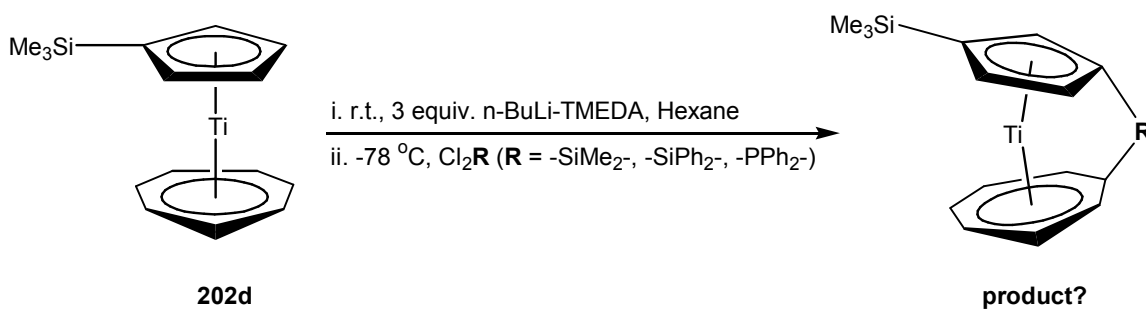
Complex **206da** was characterized by GC/MS, ^1H , $^{13}\text{C}\{^1\text{H}\}$, ^{13}C , and ^{29}Si DEPT NMR spectroscopy (Table 3.2.1.2), with a molecular ion ($m/e = 392$) consistent with one trimethylsilyl and two dimethylsilyl groups. This was confirmed by the ^1H NMR spectrum which showed two septets (just like **203a**) at δ 4.58 (Cp-(Si(CH₃)₃)(SiH(CH₃)₂)) and δ 4.88 (Cht-SiH(CH₃)₂) for the silyl protons, and a singlet at δ 0.16 for the trimethylsilyl methyl protons on Cp-(Si(CH₃)₃)(SiH(CH₃)₂). As expected, the $^{13}\text{C}\{^1\text{H}\}$ NMR spectrum of **206da** showed only one signal at δ 0.41 for the trimethylsilyl methyl carbons, and four signals for the dimethylsilyl methyl carbons: two signals at δ -2.55 and -2.47 (Cp-(Si(CH₃)₃)(SiH(CH₃)₂)), and two more signals at δ -1.33 and -1.32 (Cht-SiH(CH₃)₂). Two signals at δ 93.28 (Cht-SiH(CH₃)₂) and δ 110.38 (Cp-(Si(CH₃)₃)(SiH(CH₃)₂)) were observed for the *ipso* carbons adjacent to the dimethylsilyl groups, and one signal at δ 115.38 was observed for the *ipso* carbon adjacent to the trimethylsilyl group on Cp-(Si(CH₃)₃)(SiH(CH₃)₂). The ^{29}Si DEPT NMR spectrum of **206da**, optimized to either $^1J_{\text{Si-H}} = 180$ Hz or $^3J_{\text{Si-H}} = 8$ Hz, showed two signals at δ -23.22 (Cp-(Si(CH₃)₃)(SiH(CH₃)₂)) and δ -7.16 (Cht-SiH(CH₃)₂) for the dimethylsilyl silicons, and one signal at δ -8.24 for the trimethylsilyl silicon on Cp-(Si(CH₃)₃)(SiH(CH₃)₂).

The dilithiation of **202d**, which gave only one major product, is a promising route towards *ansa*-bridged troiticene complexes with an added solubilizing group. Tamm and coworkers were able to prepare silatroticenophane by quenching dilithio-troticene with dichlorodimethylsilane (Scheme 3.2.1.3), then obtained a polymer via ring-opening polymerization, though it was poorly characterized and of low molecular weight, partly due to poor solubility in common organic solvents.^{7,215} Our attempts to prepare *ansa*-bridged troiticene complexes by quenching the dilithiated **202d** with

dichlorodimethylsilane, dichlorodiphenylsilane, or dichlorophenylphosphine using similar reaction conditions were unsuccessful (**Scheme 3.2.1.4**), resulting in a dark blue-green oily crude product. Purification by either precipitation or sublimation was unsuccessful.

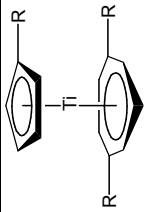
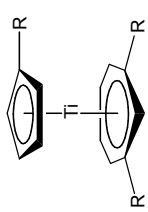


Scheme 3.2.1.3. Synthesis of Silatroticenophane.^{7,215}



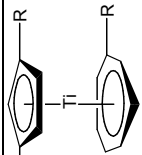
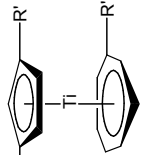
Scheme 3.2.1.4. Proposed Synthesis of Silatroticenophane via Dilithiation of **202d**.

Table 3.2.1.1. NMR Data^a for Major Products from Dilithiation of **201d**.

| R = Si(CH ₃) ₃ | δ (¹ H) ^b | δ (¹³ C { ¹ H}) ^b | δ (²⁹ Si DEPT) ^c |
|--|--|--|---|
|  204d | See 204d in Table 2.3.1.1 . | | |
|  205d | 0.16 (s, 9H, Cp-Si(CH ₃) ₃), 0.37 (s, 18H, Cht-Si(CH ₃) ₂), 5.10, 5.25 (t, 4H, Cp -Si(CH ₃) ₃), 5.61-5.81 (m, 5H, Cht -(Si(CH ₃) ₃) ₂) | 0.3 (Cp-Si(CH ₃) ₃), 0.8 (Cht-(Si(CH ₃) ₃) ₂), 98.9 (<i>ipso</i> C, Cht -(Si(CH ₃) ₃) ₂), 89.9, 92.0, 94.6 (Cht -(Si(CH ₃) ₃) ₂), 111.0 (<i>ipso</i> C, Cp -Si(CH ₃) ₃), 100.5, 103.4 (Cp -Si(CH ₃) ₃) | -8.0 (Cp- Si (CH ₃) ₃), 2.5 (Cht-(Si (CH ₃) ₃) ₂) |

^a Solvent used: C₆D₆. ^b Internal reference: C₆D₆ (¹H NMR: δ 7.16 ppm; ¹³C NMR: δ 128.38 ppm).^c External reference: Tetramethylsilane (δ 0.0 ppm).

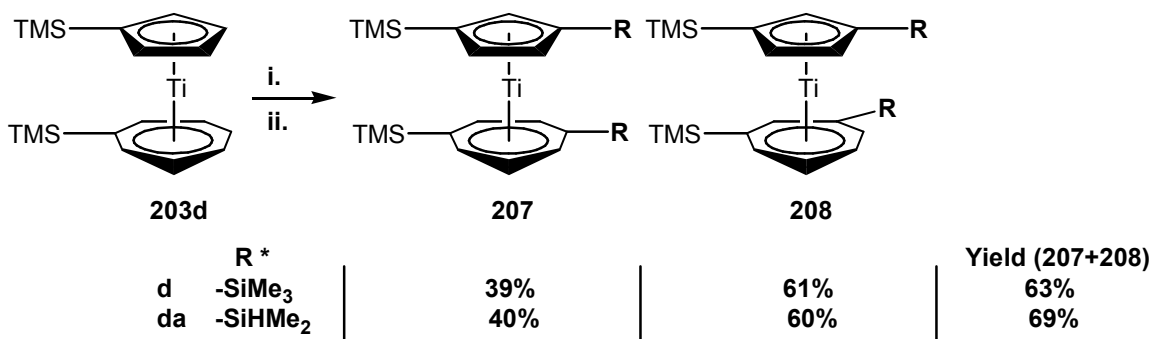
Table 3.2.1.2. NMR Data^a for Major Products from Dilithiation of **202d**.

| R = Si(CH ₃) ₃ R' = SiH(CH ₃) ₂ | δ (¹ H) ^b | δ (¹³ C{ ¹ H}) ^b | δ (²⁹ Si DEPT) ^c |
|---|--|---|--|
|  206d | See 206d in Table 2.3.1.1. | | |
|  206da | 0.16 (s, 9H, Cp-Si(CH ₃) ₃), 0.19, 0.20 (d, 6H, Cp-SiH(CH ₃) ₂), 0.43 (d, 6H, Cht-SiH(CH ₃) ₂), 4.58 (septet, 1H, Cp-SiH(CH ₃) ₂), 4.88 (septet, 1H, Cht-SiH(CH ₃) ₂), 5.32-5.44 (m, 3H, Cp-), 5.48-5.72 (m, 6H, Cht-) | -2.6, -2.5 (Cp-SiH(CH ₃) ₂), -1.33, -1.32 (Cht-SiH(CH ₃) ₂), 0.4 (Cp-Si(CH ₃) ₃), 93.3 (<i>ipso</i> C, Cht-SiH(CH ₃) ₂), 87.5, 87.7, 90.0, 90.4, 91.9, 92.9 (Cht-), 110.4 (<i>ipso</i> C, Cp-SiH(CH ₃) ₂), 115.4 (<i>ipso</i> C, Cp-Si(CH ₃) ₃), 106.7, 107.0, 110.0 (Cp-) | -23.2 (Cp-SiH(CH ₃) ₂), -8.2 (Cp-Si(CH ₃) ₃), -7.2 (Cht-SiH(CH ₃) ₂) |

^a Solvent used: C₆D₆. ^b Internal reference: C₆D₆ (¹H NMR: δ 7.16 ppm; ¹³C NMR: δ 128.38 ppm).^c External reference: Tetramethylsilane (δ 0.0 ppm).

3.2.2. Dilithiation of *Bis*(trimethylsilyl)troticene **203d**

Addition of a solution of **203d** in hexane to 8 equiv. *n*-BuLi-TMEDA in hexane at room temperature followed by quenching with chlorotrimethylsilane gave a mixture of two *tetrakis*(trimethylsilyl)troticene isomers as major product (63 % yield; blue oil) (Scheme 3.2.2.1), with ^1H NMR revealing an overall ratio of 39 % **207d** and 61 % **208d**. Attempts to isolate each isomer via column chromatography were unsuccessful. It is notable that unlike the 1-pot lithiation of troticene which gave **207** as the main tetrasubstituted product (Scheme 2.3), dilithiation of **203d** gave significant quantities of both **207** and **208**.



i. 8 equiv. *n*-BuLi/TMEDA, hexane, r.t; ii. Cl-R (R = -SiMe₃, -SiHMe₂), -78°C - r.t.

* Product distribution determined from integration of ^1H NMR of crude product.

Scheme 3.2.2.1. Major Products for the Dilithiation of **203d**.

A similar reaction quenched with chlorodimethylsilane also produced a mixture of two constitutional isomers as major product (69 % yield; blue oil), with ^1H NMR revealing an overall ratio of 40 % **207da**, and 60 % **208da** (Scheme 3.2.2.1). Having two different substituents on each ring ligand leads to the formation of diastereomers (Figure 3.2.2.1).

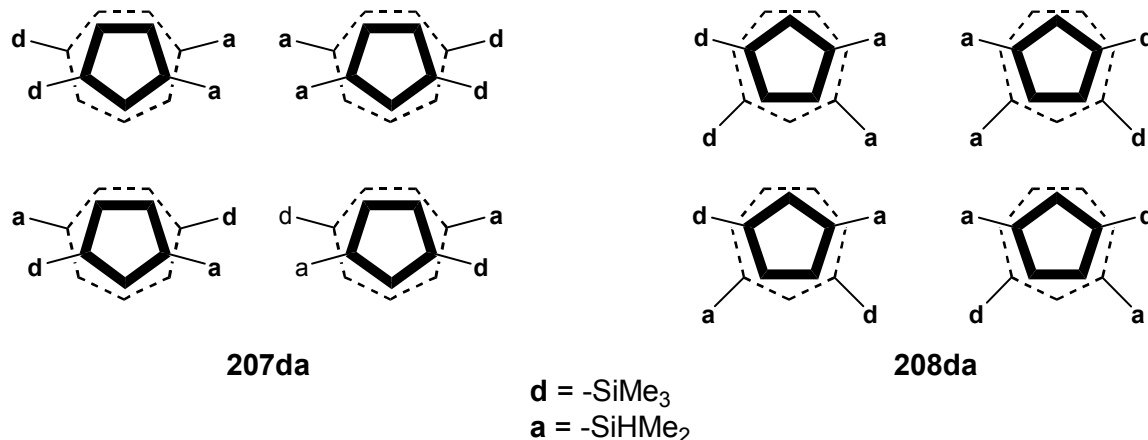


Figure 3.2.2.1. Isomers of **207da** and **208da**.

The mixture of **207d** and **208d** was characterized by GC/MS, ^1H , $^{13}\text{C}\{^1\text{H}\}$, and ^{29}Si DEPT NMR spectroscopy (**Table 3.2.2.2**), confirming that both isomers have two trimethylsilyl groups on each ring. Analysis of the NMR spectra of the mixture was facilitated by comparison with those of isolated **207d** (from **Chapter 2**), making it possible to determine the NMR signals associated with **208d**. As in the case of **207d**, the ^1H NMR spectrum of the mixture showed **208d** having two singlets at δ 0.21 ($\text{Cp}-(\text{Si}(\text{CH}_3)_3)_2$) and δ 0.45 ($\text{Cht}-(\text{Si}(\text{CH}_3)_3)_2$) for the methyl protons in a 1:1 ratio. The $^{13}\text{C}\{^1\text{H}\}$ NMR spectrum also showed **208d** having two signals at δ 0.9 ($\text{Cp}-(\text{Si}(\text{CH}_3)_3)_2$) and δ 1.3 ($\text{Cht}-(\text{Si}(\text{CH}_3)_3)_2$) for the methyl carbons, and another two signals at δ 100.1 ($\text{Cht}-(\text{Si}(\text{CH}_3)_3)_2$) and δ 114.7 ($\text{Cp}-(\text{Si}(\text{CH}_3)_3)_2$) for the *ipso* carbons. The ^{29}Si DEPT NMR spectrum showed two signals for **208d** at δ -7.77 ($\text{Cp}-(\text{Si}(\text{CH}_3)_3)_2$) and δ 2.39 ($\text{Cht}-(\text{Si}(\text{CH}_3)_3)_2$).

The mixture of **207da** and **208da** was also characterized by GC/MS, ^1H , $^{13}\text{C}\{^1\text{H}\}$, ^{13}C , and ^{29}Si DEPT NMR spectroscopy (**Table 3.2.2.3**). While attempts to isolate the

components of the mixture via column chromatography failed, eluting the mixture through a long column of deactivated alumina with hexanes produced two portions with different isomer ratios, facilitating the analysis of the NMR spectra of the mixture. GC/MS of the product mixture showed two peaks with a molecular ion ($m/e = 464$) consistent with two trimethylsilyl and two dimethylsilyl groups. In the ^1H NMR spectrum of the mixture, complex **207da** showed two singlets at δ 0.18 and δ 0.42 for the trimethylsilyl methyl protons on the Cp and Cht ligands, respectively, and two pairs of doublets for the dimethylsilyl methyl protons: one pair at δ 0.19 and δ 0.22 (Cp-(Si(CH₃)₃)(SiH(CH₃)₂)), and another pair at δ 0.475 and δ 0.482 (Cht-(Si(CH₃)₃)(SiH(CH₃)₂)). This pattern was repeated in the $^{13}\text{C}\{^1\text{H}\}$ NMR spectrum of the mixture, with complex **207da** having two signals at δ 0.64 and δ 0.93 for the trimethylsilyl methyl carbons on the Cp and Cht ligands, respectively, and two pairs of signals for the dimethylsilyl methyl carbons: one pair at δ -2.69 and δ -1.92 (Cp-(Si(CH₃)₃)(SiH(CH₃)₂)), and another pair at δ -1.48 and δ -0.93 (Cht-(Si(CH₃)₃)(SiH(CH₃)₂)). Two signals at δ 97.35 and δ 115.94 were assigned to the *ipso* carbons adjacent to the trimethylsilyl groups, and two more signals at δ 93.36 and δ 110.60 were assigned to the *ipso* carbons adjacent to the dimethylsilyl groups on the Cp and Cht ligands, respectively. The ^{29}Si DEPT NMR spectrum of the mixture, optimized to either $^1J_{\text{Si-H}} = 180$ Hz or $^3J_{\text{Si-H}} = 8$ Hz, showed two signals for **207da** δ -23.10 and δ -7.25 for the dimethylsilyl silicons, and another two signals at δ -7.85 and δ 2.83 for the trimethylsilyl silicons.

The NMR spectra assigned to **208da** have, for the most part, common features with those of **207da**, indicative of having a trimethylsilyl and a dimethylsilyl substituent

on both the Cht and Cp ligands (**Table 3.2.2.3**). A look at the *ipso* carbon signals of **207da** and **208da** points to the fact that the former is an analog of **207a** and **207d** with a 1,4-disubstitution pattern on the Cht ligand, while the latter is an analog of **208d** with a 1,3-disubstitution pattern on the Cht ligand (**Table 3.2.2.1**). This is corroborated by a key difference between the $^{13}\text{C}\{^1\text{H}\}$ NMR signals of **207da** and **208da** which point towards their different substitution patterns on the Cht ligand (**Figure 3.2.2.2**). Complex **207da** has two Cht carbon signals (C2 and C3) located in between its *ipso* carbon signals (C1 and C4), consistent with a 1,4-disubstituted Cht ligand. In contrast, complex **208da** has only one Cht carbon signal (C6) located in between its *ipso* carbon signals (C5 and C7), consistent with a 1,3-disubstituted Cht ligand. The Cp carbon signals of both isomers have similar patterns since both isomers have a 1,3-disubstituted Cp ligand.

Table 3.2.2.1. *Ipso*-Carbon Chemical Shifts of **207** and **208** Tropicene Derivatives.

| Complex | Cht- <i>ipso</i> carbons | | Cp- <i>ipso</i> carbons | |
|--------------|---------------------------------------|--|---------------------------------------|--|
| | Cht-Si(CH ₃) ₃ | Cht-SiH(CH ₃) ₂ | Cht-Si(CH ₃) ₃ | Cht-SiH(CH ₃) ₂ |
| 207a | N/A | 93.8 | N/A | 111.5 |
| 207d | 96.9 | N/A | 115.0 | N/A |
| 208d | 100.1 | N/A | 114.7 | N/A |
| 207da | 97.3 | 93.4 | 115.9 | 110.6 |
| 208da | 99.9 | 96.9 | 114.8 | 110.5 |

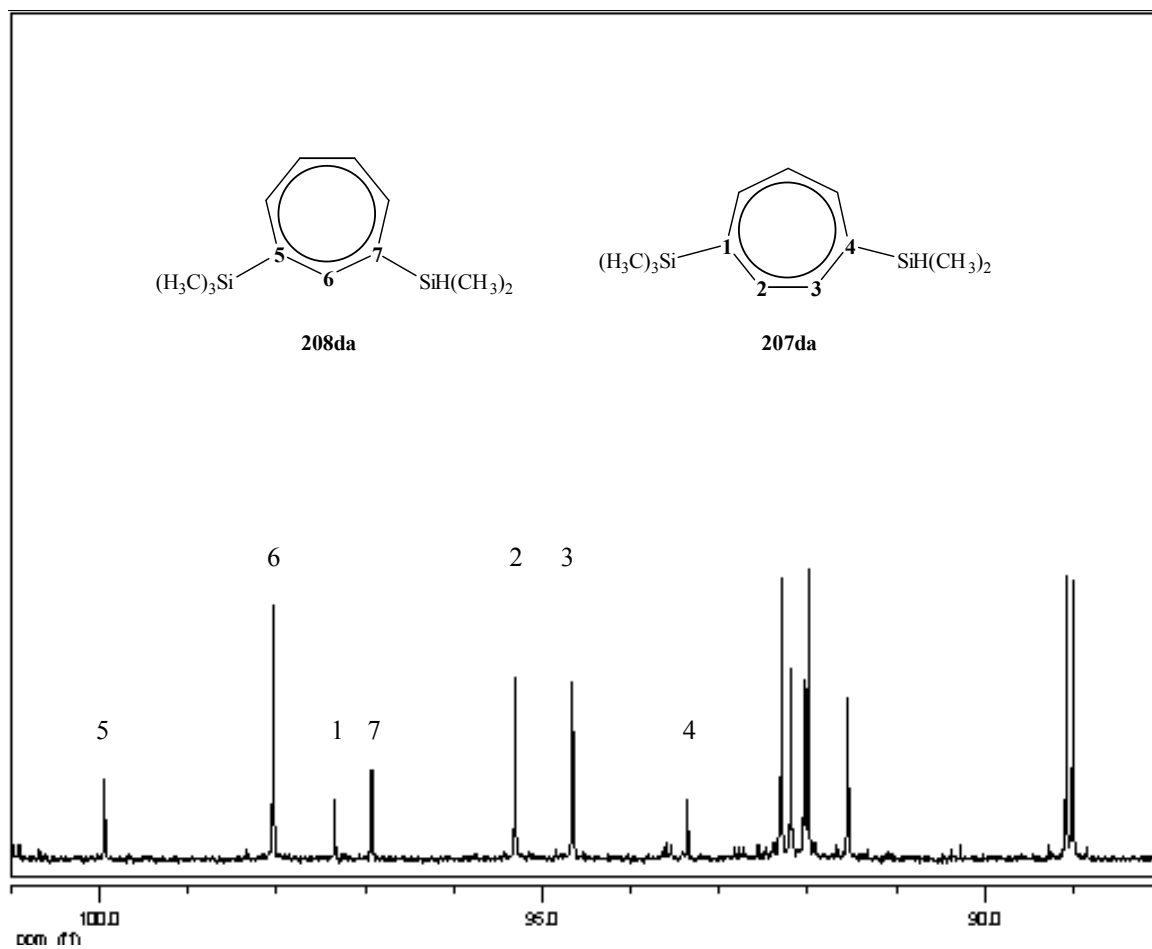
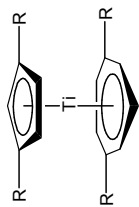
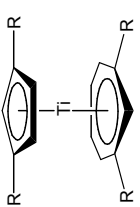


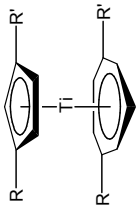
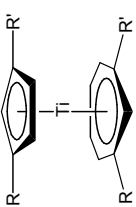
Figure 3.2.2.2. Cht $^{13}\text{C}\{^1\text{H}\}$ NMR Carbon Signals of **207da** and **208da**.

Table 3.2.2.2. NMR Data^a for Major Products from Chlorotrimethylsilane-Quenched Dilithiation of **203d**.

| R = Si(CH ₃) ₃ | δ (¹ H) ^b | δ (¹³ C{ ¹ H}) ^b | δ (²⁹ Si DEPT) ^c |
|--|--|---|---|
|  207d | See 207d in Table 2.3.1.1. | | |
|  208d | 0.21 (s, 18H, Cp-(Si(CH ₃) ₃) ₂), 0.45 (s, 18H, Cht-(Si(CH ₃) ₃) ₂), 5.34 (t, 1H, Cp -(Si(CH ₃) ₃) ₂), 5.40 (d, 2H, Cp -(Si(CH ₃) ₃) ₂), 5.46-5.52, 5.66-5.72, 6.06-6.12 (m, 5H, Cht -(Si(CH ₃) ₃) ₂) | 0.9 (Cp-(Si(CH ₃) ₃) ₂), 1.3 (Cht-(Si(CH ₃) ₃) ₂), 100.1 (<i>ipso</i> C, Cht -(Si(CH ₃) ₃) ₂), 87.7, 91.8, 97.4 (Cht -(Si(CH ₃) ₃) ₂), 114.7 (<i>ipso</i> C, Cp -(Si(CH ₃) ₃) ₂), 106.2, 110.1 (Cp -(Si(CH ₃) ₃) ₂) | -7.8 (Cp-(Si (CH ₃) ₃) ₂), 2.4 (Cht-(Si (CH ₃) ₃) ₂) |

^a Solvent used: C₆D₆. ^b Internal reference: C₆D₆ (¹H NMR: δ 7.16 ppm; ¹³C NMR: δ 128.38 ppm).^c External reference: Tetramethylsilane (δ 0.0 ppm).

Table 3.2.2.3. NMR Data^a for Major Products from Chlorodimethylsilane-Quenched Dilitiation of **203d**.

| R = Si(CH ₃) ₃ R' = SiH(CH ₃) ₃ | δ (H) ^b | δ (¹³ C{ ¹ H}) ^b | δ (²⁹ Si DEPT) ^c |
|---|--|--|--|
|  <p>207da</p> | 0.19, 0.22 (d, 6H, Cp-SiH(CH ₃) ₂), 0.475, 0.482 (d, 6H, Cht-SiH(CH ₃) ₂), 0.18 (s, 9H, Cp-Si(CH ₃) ₃), 0.42 (s, 9H, Cht-Si(CH ₃) ₃), 4.63 (septet, 1H, Cp-SiH(CH ₃) ₂), 4.94 (septet, 1H, Cht-SiH(CH ₃) ₂), 5.437, 5.441 (2 d, 1H, Cp-), 5.46 (t, 1H, Cp-), 5.487, 5.491 (2 d, 1H, Cp-), 5.640-5.668, 5.688-5.720, 5.768-5.778 (m, 5H, Cht-) | -2.7, -1.9 (Cp-SiH(CH ₃) ₂), -1.5, -0.9 (Cht-SiH(CH ₃) ₂), 0.6 (Cp-Si(CH ₃) ₃), 0.9 (Cht-Si(CH ₃) ₃), 93.4 (<i>ipso</i> C, Cht-), SiH(CH ₃) ₂), 97.3 (<i>ipso</i> C, Cht-), Si(CH ₃) ₃), 91.5, 92.04, 92.2, 94.7, 95.3 (Cht-), 110.6 (<i>ipso</i> C, Cp-), SiH(CH ₃) ₂), 115.9 (<i>ipso</i> C, Cp-), Si(CH ₃) ₃), 106.5, 106.9, 110.63 (Cp-) | -23.1 (Cp-SiH(CH ₃) ₂), -7.2 (Cht-SiH(CH ₃) ₂), -7.8 (Cp-Si(CH ₃) ₃), 2.8 (Cht-Si(CH ₃) ₃) |
|  <p>208da</p> | 0.16, 0.24 (d, 6H, Cp-SiH(CH ₃) ₂), 0.469, 0.473 (d, 6H, Cht-SiH(CH ₃) ₂), 0.19 (s, 9H, Cp-Si(CH ₃) ₃), 0.44 (s, 9H, Cht-Si(CH ₃) ₃), 4.74 (septet, 1H, Cp-SiH(CH ₃) ₂), 4.97 (septet, 1H, Cht-SiH(CH ₃) ₂), 5.356, 5.360 (2 d, 1H, Cp-), 5.39 (t, 1H, Cp-), 5.451, 5.455 (2 d, 1H, Cp-), 5.51-5.62, 5.670-5.702, 5.736-5.766, 6.00-6.02 (m, 5H, Cht-) | -2.9, -1.9 (Cp-SiH(CH ₃) ₂), -1.3, -0.9 (Cht-SiH(CH ₃) ₂), 0.5 (Cp-Si(CH ₃) ₃), 1.2 (Cht-Si(CH ₃) ₃), 96.9 (<i>ipso</i> C, Cht-), SiH(CH ₃) ₂), 99.9 (<i>ipso</i> C, Cht-), Si(CH ₃) ₃), 89.0, 89.1, 92.00, 92.3, 98.0 (Cht-), 110.5 (<i>ipso</i> C, Cp-), SiH(CH ₃) ₂), 114.8 (<i>ipso</i> C, Cp-), Si(CH ₃) ₃), 106.6, 107.1, 110.64 (Cp-) | -23.4 (Cp-SiH(CH ₃) ₂), -8.0 (Cht-SiH(CH ₃) ₂), -8.1 (Cp-Si(CH ₃) ₃), 2.6 (Cht-Si(CH ₃) ₃) |

^a Solvent used: C₆D₆. ^b Internal reference: C₆D₆ (¹H NMR: δ 7.16 ppm; ¹³C NMR: δ 128.38 ppm).^c External reference: Tetramethylsilane (δ 0.0 ppm).

3.3. Summary

The lithiation of substituted troticene derivatives was demonstrated. As in the case of troticene, monolithiation at lower temperatures (0 °C or -10 °C) resulted in preferential monolithiation at the Cht ligand. However, preferential monolithiation of the Cp ligand at room temperature was more difficult and gave a low yield of the desired product.

The dilithiation of substituted troticene derivatives occurred much more readily due to *n*-butyllithium/TMEDA being used instead of *n*-butyllithium alone. While the dilithiation of **201d** resulted in two major products (and one minor product) due to lithiation at either the 3- or 4- position of the Cht ligand, the dilithiation of **202d** resulted in only one major product (and 2 minor products), the latter promising a potential route towards *ansa*-bridged troticene complexes with an added solubilizing group. Attempts to prepare such product were hampered by difficulties encountered in purification of the crude product.

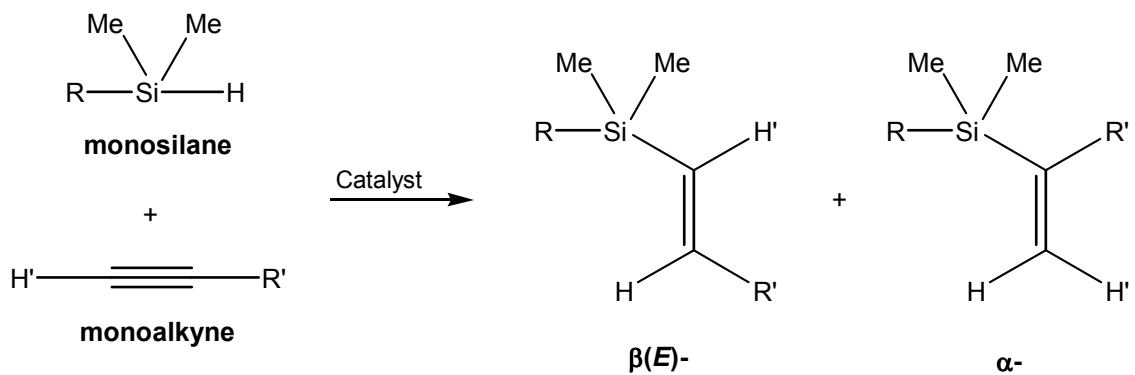
Unlike the 1-pot polyolithiation of troticene which gave one major tetrasubstituted product, the dilithiation of **203d** with *n*-butyllithium/TMEDA gave two major tetrasubstituted products (plus isomers), again due to lithiation at either the 3- or 4- position of the Cht ligand. The reaction resulted in multiple isomers, making it useless for any potential application as routes for preparing novel ligands.

Chapter 4. Poly{troticene-*bis*(silylenevinylene)(phenylene)}s

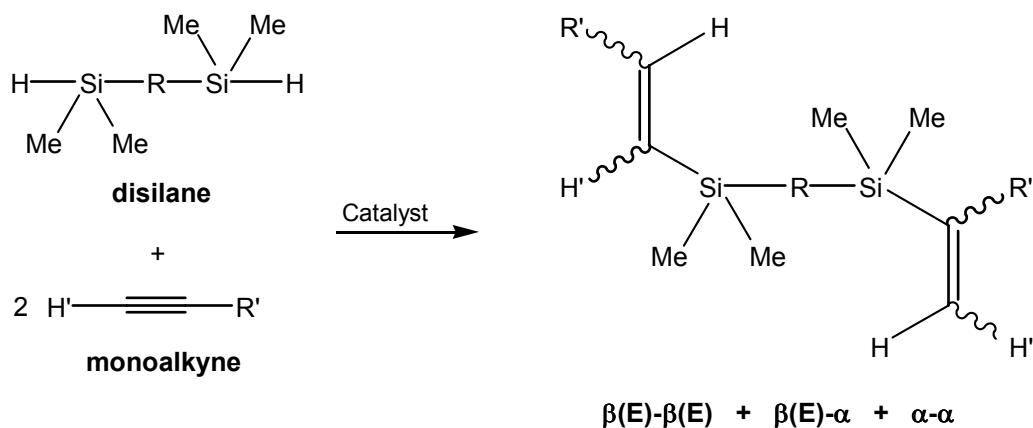
As mentioned in **Chapter 1**, Jain of our group studied the synthesis of polymers/oligomers (poly{ferrocene-*bis*(silylenevinylene)(phenylene)}s) as well as the corresponding model compounds via Pt-catalyzed hydrosilylation of the appropriate dimethylsilyl-ferrocene derivatives (**28** and **41**) and various alkynes (See **Chapter 1.2.6**).^{4,5}

This chapter presents the synthesis of poly{troticene-*bis*(silylenevinylene)(phenylene)}s via Pt-catalyzed hydrosilylation of 1,4- and 1,3-diethynylbenzene with { η^7 -(dimethylsilyl)cycloheptatrienyl} { η^5 -(dimethylsilyl)cyclopentadienyl} titanium(II) (**203a**) using Karstedt's catalyst. Polymers derived from either **203a** or *bis*(dimethylsilyl)ferrocene (**28**) and 2,5-*bis*(ethynyl)thiophene were also prepared.

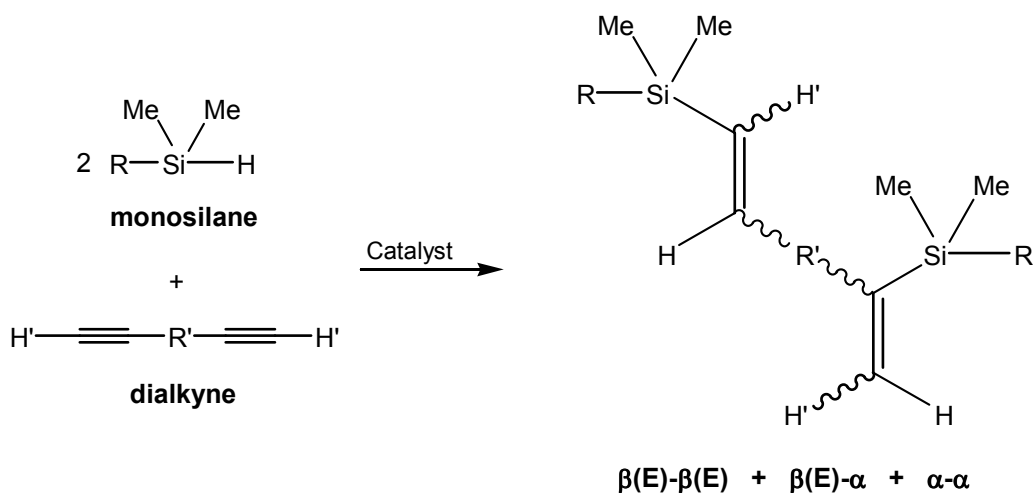
In addition, three types of model compounds were also prepared via Pt-catalyzed hydrosilylation to better characterize the polymeric systems: **Type 1** model compounds were prepared from one equiv. of a monosilane and a monoalkyne (**Scheme 4.1**); **Type 2** model compounds from one equiv. of a disilane and two equiv. of a monoalkyne (**Scheme 4.2**); and **Type 3** model compounds from two equiv. of a monosilane and one equiv. of a dialkyne (**Scheme 4.3**).



Scheme 4.1. General Scheme for Type 1 Model Compounds.



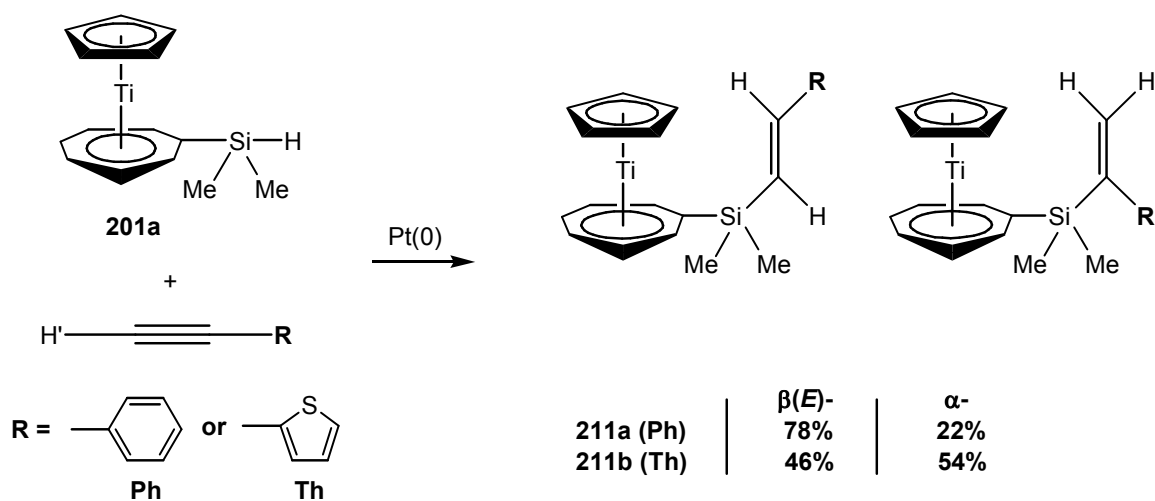
Scheme 4.2. General Scheme for Type 2 Model Compounds.



Scheme 4.3. General Scheme for Type 3 Model Compounds.

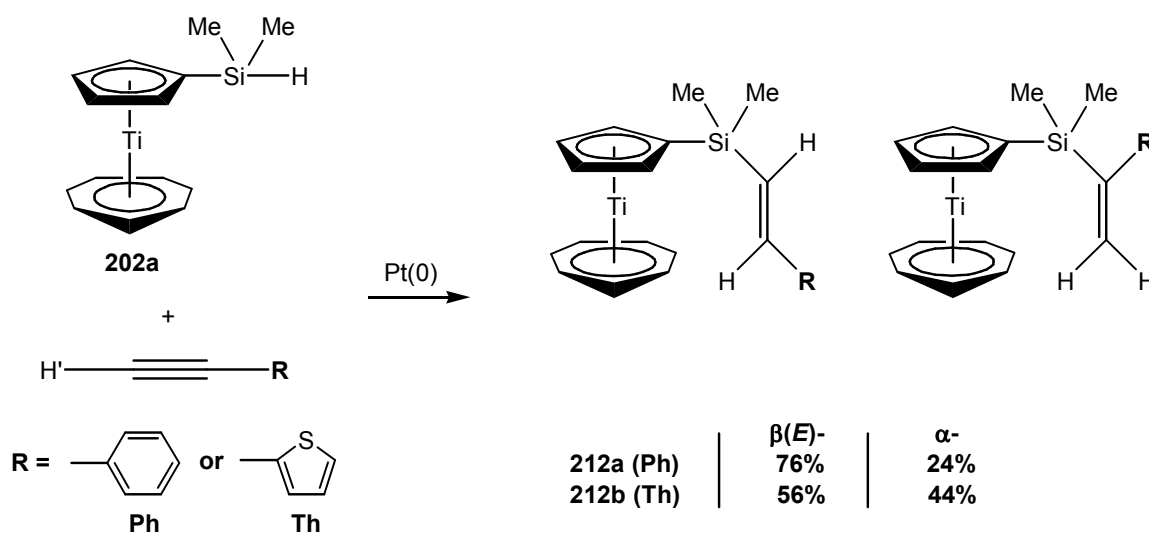
4.1. Type 1 Model Compounds

One pair of Type 1 model compounds was prepared using either **201a** or **202a** as the monosilane and phenylacetylene as the monoalkyne. Treatment of a mixture of one equiv. each of **201a** and phenylacetylene with Karstedt's catalyst in d_6 -benzene at room temperature gave a mixture of the $\beta(E)$ - and α - regioisomers²⁷⁶ of $[\eta^7\text{-}\{\text{dimethyl(phenylvinylene)silyl}\}\text{cycloheptatrienyl}](\eta^5\text{-cyclopentadienyl})\text{titanium(II)}$ (**211a**) (69 % yield; blue oil) (**Scheme 4.1.1**). An overall regiochemical distribution of 78 % $\beta(E)$ - / 22 % α - was estimated from integration of the ^1H NMR spectrum of the mixture. Another Type 1 model compound was similarly prepared using 2-ethynylthiophene, giving $[\eta^7\text{-}\{\text{dimethyl(thiophenevinylene)silyl}\}\text{cycloheptatrienyl}](\eta^5\text{-cyclopentadienyl})\text{titanium(II)}$ (**211b**) (94 % yield; blue oil) with a 46 % $\beta(E)$ - / 54 % α - ratio. Further hydrosilylation of the olefins in either model compound was not observed due to the unreactive internal alkene of the $\beta(E)$ - regioisomer, and the sterically encumbered alkene of the α - regioisomer.²⁴⁸



Scheme 4.1.1. Type 1 Model Compounds from **201a** and Monoalkynes.

A second pair of Type 1 model compound was prepared using **202a** as the monosilane, and either phenylacetylene or 2-ethynylthiophene (**Scheme 4.1.2**), the former giving $(\eta^7\text{-cycloheptatrienyl})[\eta^5\text{-}\{\text{dimethyl(phenylvinylene)silyl}\}\text{cyclopentadienyl}]$ titanium(II) (**212a**) (72 % yield; blue oil) with a 76 % $\beta(E)$ - / 24 % α -ratio, and the latter giving $[\eta^7\text{-}\{\text{dimethyl(thiophenevinylene)silyl}\}\text{cycloheptatrienyl}](\eta^5\text{-cyclopentadienyl})$ titanium(II) (**212b**) (93 % yield; blue oil) with a 56 % $\beta(E)$ - / 44 % α -ratio.

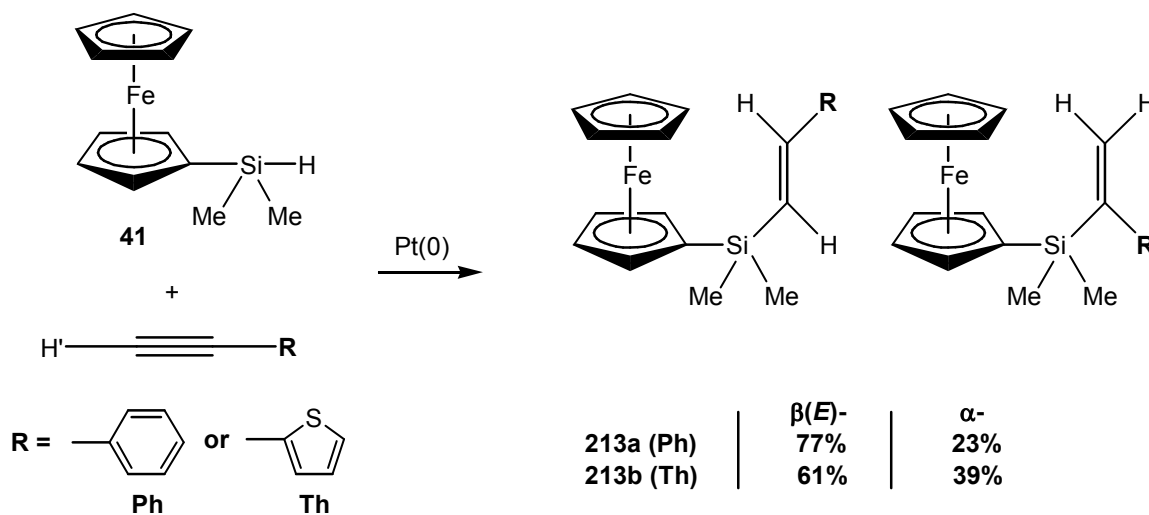


Scheme 4.1.2. Type 1 Model Compounds from **202a** and Monoalkynes.

It is notable that adducts from 2-ethynylthiophene have lower $\beta(E)$ - / α - ratios (approximately 1:1) compared to those from phenylacetylene (approximately 3:1), the latter being comparable with the Pt-complex-catalyzed hydrosilylation of phenylacetylene with Et_3SiH (approximately 80 % $\beta(E)$ - / 20 % α -).²²⁷ Similar observations were made by Lukevics and coworkers in the hydrosilylation of

phenylacetylene and 2-ethynylthiophene,²⁷⁷ and was attributed to the more electron withdrawing nature of the thiophene moiety relative to the phenyl group.

Type 1 model compounds prepared from dimethylsilylferrocene (**41**) and either 2-ethynylthiophene or phenylacetylene gave dimethyl(phenylenevinylene)silylferrocene (**213a**) (61 % yield; 77 % $\beta(E)$ - / 23 % α -; orange oil) and dimethyl(thienylvinylene)silylferrocene (**213b**) (55 % yield; 61 % $\beta(E)$ - / 39 % α -; orange oil), respectively (**Scheme 4.1.3**). It is evident that the observed regiochemical distributions have a lower $\beta(E)$ - to α - ratio when 2-ethynylthiophene was used, consistent with results from **Schemes 4.1.1** and **4.1.2**.



Scheme 4.1.3. Type 1 Model Compounds from **41a** and Monoalkynes.

The regioisomer mixture **211a** was characterized by GC/MS, ^1H , $^{13}\text{C}\{^1\text{H}\}$, ^{29}Si DEPT, and ^1H - ^1H COSY NMR (**Table 4.1.1**). The GC/MS of the mixture showed two peaks having a molecular ion (M^+) with $m/e = 364$, consistent with the two hydrosilylation adducts. The ^1H NMR spectrum showed two pairs of doublets, one pair at

δ 6.76 and 7.13 ($^3J_{\text{H-H}} = 19\text{Hz}$) assigned to the $\beta(\text{E})$ - regioisomer, and another pair at δ 5.73 (concealed by the Cht proton signals but revealed by ^1H - ^1H COSY NMR) and δ 5.98 ($^2J_{\text{H-H}} = 3\text{Hz}$) assigned to the α - regioisomer. The presence of two regioisomers was corroborated by the ^{29}Si DEPT NMR which showed two signals at δ -4.05 ($\beta(\text{E})$) and δ -2.25 (α).

Product **211b** was similarly characterized (Table 4.1.2), sharing common NMR spectral features with **211a**, indicating the presence of two regioisomers. The ^1H NMR spectrum showed two pairs of olefinic proton doublets ($\beta(\text{E})$: δ 6.61 and δ 7.17; α : δ 5.55 and δ 6.24), while the ^{29}Si DEPT NMR spectrum showed two signals at δ -4.3 ($\beta(\text{E})$) and δ -1.6 (α).

Both **212a** and **212b** were similarly characterized (Table 4.1.3 and 4.1.5), sharing common NMR spectral features with **211a** and **211b**, indicating the presence of two regioisomers in each. However, one key difference was that the olefinic proton signals of **212a** ($\beta(\text{E})$: δ 6.58 and 6.95; α : δ 5.46 and 5.78) and **212b** ($\beta(\text{E})$: δ 6.46 and δ 6.99; α : δ 5.26 and δ 6.06) were shifted upfield compared to those of **211a** and **211b**, respectively, attributed to the more electron donating (and more shielding) nature of the Cp ligand in **202a** compared with the Cht ligand in **201a**. This is also evident in the ^{29}Si DEPT NMR spectra of both model compounds, with **212a** having two signals at δ -14.61 ($\beta(\text{E})$) and δ -12.93 (α), and **212b** having two signals at δ -14.9 ($\beta(\text{E})$) and δ -12.1 (α).

The Type 1 model compound **213b** was also characterized by GC/MS, ^1H , $^{13}\text{C}\{^1\text{H}\}$, and ^{29}Si DEPT NMR (Table 4.1.6). The GC/MS of the mixture showed two peaks having a molecular ion (M^+) with $m/e = 352$, consistent with the two hydrosilylation adducts. This is reflected in the ^1H NMR spectrum which showed two

pairs of doublets for the olefinic protons, one pair at δ 6.55 and δ 7.11 (β (E); $^3J_{\text{H-H}} = 19.0$ Hz) and another pair at δ 5.47 and δ 6.12 (α ; $^2J_{\text{H-H}} = 2.0$ Hz). The ^{29}Si DEPT NMR of the mixture confirmed the presence of two regioisomers with two signals at δ -9.67 and δ -6.45 corresponding to the β (E)- and α - regioisomers, respectively.

Table 4.1.1. NMR Data^a for **211a**.

| Regioisomer | δ (¹ H) ^b | δ (¹³ C{ ¹ H}) ^b | δ (²⁹ Si DEPT) ^c |
|------------------------------|---|--|--|
| β(E) | 0.53 (s, 6H, β (E), <i>ChtSi</i> (CH ₃) ₂ -), 4.96 (s, 5H, β (E), <i>Cp</i>), 6.76, 7.13 (d, 2H, β (E), -C ₂ H ₂ -, ³ J _{H-H} = 19Hz) | -0.69 (β (E), <i>ChtSi</i> (CH ₃) ₂ -), 87.40, 89.43, 91.85 (β (E), <i>ChtSi</i> (CH ₃) ₂ -), 95.04 (β (E), <i>ipso C</i> , <i>ChtSi</i> (CH ₃) ₂ -), 97.64 (β (E), <i>Cp</i>) | -4.05 (β (E), <i>ChtSi</i> (CH ₃) ₂ -) |
| α | 0.50 (s, 6H, α , <i>ChtSi</i> (CH ₃) ₂ -), 4.87 (s, 5H, α , <i>Cp</i>), 5.73, 5.98 (d, 2H, α , -C ₂ H ₂ -, ² J _{H-H} = 3Hz) | -0.45 (α , <i>ChtSi</i> (CH ₃) ₂ -), 87.25, 89.34, 92.15 (α , <i>ChtSi</i> (CH ₃) ₂ -), 94.82 (α , <i>ipso C</i> , <i>ChtSi</i> (CH ₃) ₂ -), 97.75 (α , <i>Cp</i>) | -2.25 (α , <i>ChtSi</i> (CH ₃) ₂ -) |
| misc | 5.42-5.60, 5.68-5.78 (m, 2x6H, <i>ChtSi</i> (CH ₃) ₂ -), 7.00-7.40 (m, 2x5H, <i>Ph</i> -) | 127.09, 127.30, 127.88, 128.76, 128.83, 128.96, 129.22, 129.86 (<i>Ph</i> -), 139.06, 145.66, 153.53 (-C ₂ H ₂ -) | |

^a Solvent used: C₆D₆. ^b Internal reference: C₆D₆ (¹H NMR: δ 7.16 ppm; ¹³C NMR: δ 128.38 ppm). ^c External reference: Tetramethylsilane (δ 0.0 ppm).

Table 4.1.2. NMR Data^a for **211b**.^{*}

| Regioisomer | δ (¹ H) ^b | δ (¹³ C{ ¹ H}) ^b | δ (²⁹ Si DEPT) ^c |
|------------------------------|---|--|---|
| β(E) | 0.46 (s, 6H, β (E), ChtSi(CH ₃) ₂ -), 4.97 (s, 5H, β (E), Cp), 6.61, 7.17 (d, 2H, β (E), -C ₂ H ₂ -, ³ J _{H-H} = 19Hz) | -0.8 (β (E), ChtSi(CH ₃) ₂ -), 87.4, 89.5, 91.8 (β (E), ChtSi(CH ₃) ₂ -), 94.7 (β (E), ipso C, ChtSi(CH ₃) ₂ -), 97.7 (β (E), Cp) | -4.3 (β (E), ChtSi(CH ₃) ₂ -) |
| α | 0.53 (s, 6H, α , ChtSi(CH ₃) ₂ -), 4.89 (s, 5H, α , Cp), 5.55, 6.24 (d, 2H, α , -C ₂ H ₂ -, ² J _{H-H} = 3Hz) | -0.3 (α , ChtSi(CH ₃) ₂ -), 87.3, 89.3, 92.2 (α , ChtSi(CH ₃) ₂ -), 94.3 (α , ipso C, ChtSi(CH ₃) ₂ -), 97.8 (α , Cp) | -1.6 (α , ChtSi(CH ₃) ₂ -) |
| misc | 5.40-5.76 (m, 2x6H, ChtSi(CH ₃) ₂ -), 6.60-7.00 (m, 2x3H, Th-) | 124.2, 125.5, 126.1, 126.8, 128.0, 128.10, 128.11, 128.9 (Th-), 138.2, 144.8, 145.9, 147.8 (-C ₂ H ₂ -) | |

^a Solvent used: C₆D₆. ^b Internal reference: C₆D₆ (¹H NMR: δ 7.16 ppm; ¹³C NMR: δ 128.38 ppm). ^c External reference: Tetramethylsilane (δ 0.0 ppm).^{*} Th = Thiophene.

Table 4.1.3. NMR Data^a for **212a**.

| Regioisomer | $\delta (^1\text{H})$ ^b | $\delta (^{13}\text{C}\{^1\text{H}\})$ ^b | $\delta (^{29}\text{Si DEPT})$ ^c |
|-------------------------------------|--|---|--|
| $\beta(\text{E})$ | 0.33 (s, 6H, $\beta(\text{E})$, $\text{CpSi}(\text{CH}_3)_2$ -), 5.130-5.148, 5.170-5.188 (m, 4H, $\beta(\text{E})$, $\text{CpSi}(\text{CH}_3)_2$ -), 5.47 (s, 7H, $\beta(\text{E})$, <i>Ch</i> t), 6.58, 6.95 (d, 2H, $\beta(\text{E})$, $-\text{C}_2\text{H}_2$ -, $^3\text{J}_{\text{H-H}} = 19\text{Hz}$) | -1.21 ($\beta(\text{E})$, $\text{CpSi}(\text{CH}_3)_2$ -), 86.83 ($\beta(\text{E})$, <i>Ch</i> t), 100.66, 103.46 ($\beta(\text{E})$, $\text{CpSi}(\text{CH}_3)_2$ -), 108.50 ($\beta(\text{E})$, <i>ipso C</i> , $\text{CpSi}(\text{CH}_3)_2$ -) | -14.61 ($\beta(\text{E})$, $\text{CpSi}(\text{CH}_3)_2$ -) |
| α | 0.35 (s, 6H, α , $\text{CpSi}(\text{CH}_3)_2$ -), 5.040-5.056, 5.120-5.136 (m, 4H, α , $\text{CpSi}(\text{CH}_3)_2$ -), 5.40 (s, 7H, α , <i>Ch</i> t), 5.46, 5.78 (d, 2H, α , $-\text{C}_2\text{H}_2$ -, $^2\text{J}_{\text{H-H}} = 3\text{Hz}$) | -1.14 (α , $\text{CpSi}(\text{CH}_3)_2$ -), 86.88 (α , <i>Ch</i> t), 100.60, 103.88 (α , $\text{CpSi}(\text{CH}_3)_2$ -), 108.06 (α , <i>ipso C</i> , $\text{CpSi}(\text{CH}_3)_2$ -) | -12.93 (α , $\text{CpSi}(\text{CH}_3)_2$ -) |
| misc | 7.40-7.38 (m, 2x5H, <i>Ph</i> -) | 127.11, 127.23, 127.66, 128.31, 128.78, 128.83, 128.88, 129.26 (<i>Ph</i> -), 138.98, 145.38, 153.56 ($-\text{C}_2\text{H}_2$ -) | |

^a Solvent used: C_6D_6 . ^b Internal reference: C_6D_6 (^1H NMR: δ 7.16 ppm; ^{13}C NMR: δ 128.38 ppm). ^c External reference: Tetramethylsilane (δ 0.0 ppm).

Table 4.1.4. NMR Data^a for **212b**.^{*}

| Regioisomer | δ (¹ H) ^b | δ (¹³ C{ ¹ H}) ^b | δ (²⁹ Si DEPT) ^c |
|-------------|--|--|---|
| β (E) | 0.26 (s, 6H, β (E), CpSi(CH ₃) ₂ -), 5.08-5.16 (m, 4H, β (E), CpSi(CH ₃) ₂ -), 5.47 (s, 7H, β (E), <i>Ch</i> t), 6.46, 6.99 (d, 2H, β (E), -C ₂ H ₂ -, ³ J _{H-H} = 19Hz) | -1.3 (β (E), CpSi(CH ₃) ₂ -), 86.9 (β (E), <i>Ch</i> t), 100.7, 103.4 (β (E), CpSi(CH ₃) ₂ -), 108.2 (β (E), <i>ipso</i> C, CpSi(CH ₃) ₂ -) | -14.9 (β (E), CpSi(CH ₃) ₂ -) |
| α | 0.38 (s, 6H, α , CpSi(CH ₃) ₂ -), 5.06-5.13 (m, 4H, α , CpSi(CH ₃) ₂ -), 5.41 (s, 7H, α , <i>Ch</i> t), 5.26, 6.06 (d, 2H, α , -C ₂ H ₂ -, ² J _{H-H} = 3Hz) | -1.0 (α , CpSi(CH ₃) ₂ -), 87.0 (α , <i>Ch</i> t), 100.7, 104.0 (α , CpSi(CH ₃) ₂ -), 107.4 (α , <i>ipso</i> C, CpSi(CH ₃) ₂ -) | -12.1 (α , CpSi(CH ₃) ₂ -) |
| misc | 6.64-6.88 (m, 2x3H, <i>Th</i> -) | 124.4, 125.4, 125.7, 126.7, 127.5, 127.9, 128.1 (<i>Th</i> -), 137.8, 144.7, 145.8, 147.6 (-C ₂ H ₂ -) | |

^a Solvent used: C₆D₆. ^b Internal reference: C₆D₆ (¹H NMR: δ 7.16 ppm; ¹³C NMR: δ 128.38 ppm). ^c External reference: Tetramethylsilane (δ 0.0 ppm).^{*} Th = Thiophene.

Table 4.1.5. NMR Data^a for **213a**.

| Regioisomer | δ (¹ H) ^b |
|------------------------------|---|
| β(E) | 0.42 (s, 6H, -Si(CH ₃) ₂ -), 4.05 (s, 5H, Cp), 4.10, 4.23 (t, 4H, Cp -Si(CH ₃) ₂ -), 6.67, 7.06 (d, 2H, -C ₂ H ₂ -, ³ J _{H-H} = 19Hz) |
| α | 0.43 (s, 6H, -Si(CH ₃) ₂ -), 3.97 (s, 5H, Cp), 4.00, 4.17 (t, 4H, Cp -Si(CH ₃) ₂ -), 5.65, 5.85 (d, 2H, -C ₂ H ₂ -, ² J _{H-H} = 3Hz) |
| misc | 7.02-7.40 (m, 2x5H, -C ₂ H ₂ - Ph) |

^a Solvent used: C₆D₆. ^b Internal reference: C₆D₆ (¹H NMR: δ 7.16 ppm).

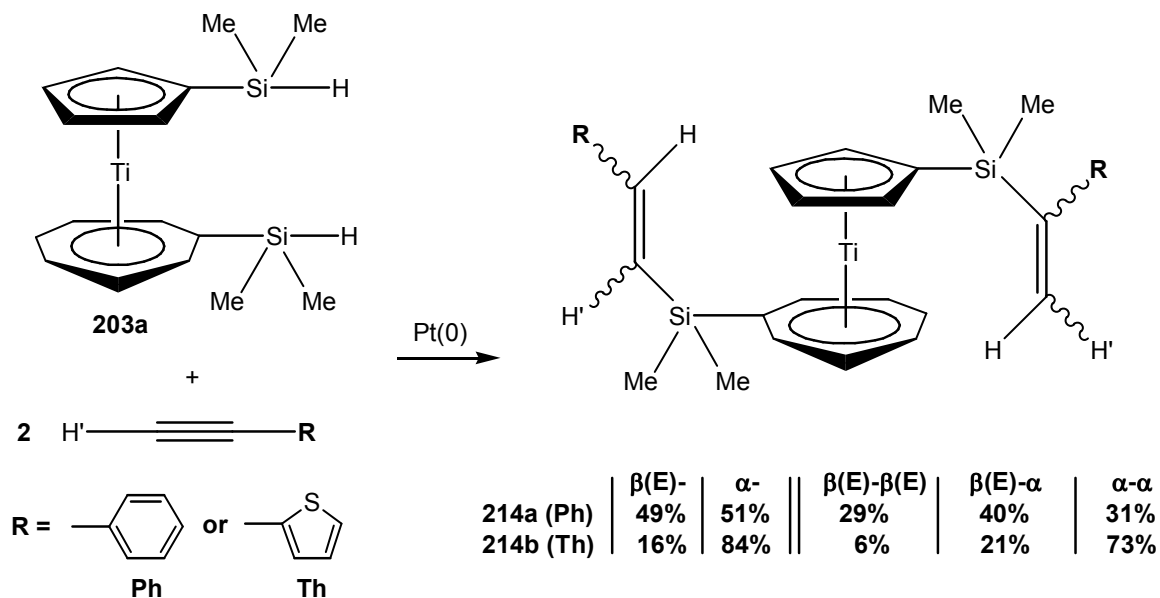
Table 4.1.6. NMR Data^a for **213b**.^{*}

| Regioisomer | δ (¹ H) ^b | δ (¹³ C{ ¹ H}) ^b | δ (²⁹ Si DEPT) ^c |
|------------------------------|--|---|---|
| β(E) | 0.35 (s, 6H, β (E), CpSi(CH ₃) ₂ -), 4.04 (s, 5H, β (E), Cp), 4.06, 4.20 (t, 4H, β (E), CpSi(CH ₃) ₂ -), 6.55, 7.11 (d, 2H, β (E), -C ₂ H ₂ -, ³ J _{H-H} = 19Hz) | -1.20 (β (E), CpSi(CH ₃) ₂ -), 68.96 (β (E), Cp), 71.76, 73.93 (β (E), CpSi(CH ₃) ₂ -), 70.22 (β (E), <i>ipso</i> C, CpSi(CH ₃) ₂ -) | -9.67 (β (E), CpSi(CH ₃) ₂ -) |
| α | 0.47 (s, 6H, α , CpSi(CH ₃) ₂ -), 3.98 (s, 5H, α , Cp), 4.03, 4.17 (t, 4H, α , CpSi(CH ₃) ₂ -), 5.47, 6.12 (d, 2H, α , -C ₂ H ₂ -, ² J _{H-H} = 3Hz) | -0.91 (α , CpSi(CH ₃) ₂ -), 69.07 (α , Cp), 71.81, 74.29 (α , CpSi(CH ₃) ₂ -), 69.88 (α , <i>ipso</i> C, CpSi(CH ₃) ₂ -) | -6.45 (α , CpSi(CH ₃) ₂ -) |
| misc | 6.64-6.82, 6.98-7.02 (m, 2x3H, <i>Th</i> -) | 124.28, 125.466, 125.474, 126.57, 127.25, 127.89, 128.05, 128.88 (<i>Th</i> -), 137.76, 144.99, 146.02, 147.91 (-C ₂ H ₂ -) | |

^a Solvent used: C₆D₆. ^b Internal reference: C₆D₆ (¹H NMR: δ 7.16 ppm; ¹³C NMR: δ 128.38 ppm). ^c External reference: Tetramethylsilane (δ 0.0 ppm).^{*} Th = Thiophene.

4.2. Type 2 Model Compounds

Type 2 Model compounds were prepared from the hydrosilylation of one equiv. of a disilane and two equiv. of a monoalkyne. Treating a mixture of one equiv. of **203a** and two equiv. of phenylacetylene with Karstedt's catalyst in d_6 -benzene at room temperature gave a mixture of four regioisomers of $[\eta^7\text{-}\{\text{dimethyl(phenylvinylene)silyl}\}\text{cycloheptatrienyl}] [\eta^5\text{-}\{\text{dimethyl(phenylvinylene)silyl}\}\text{cyclopentadienyl}]\text{titanium(II)}$ (**214a**) (73 % yield; blue oil) (Scheme 4.2.1). The mixture consisted of $\beta(\text{E})_{\text{Cht}}\text{-}\beta(\text{E})_{\text{Cp}}$ (29 %), $\beta(\text{E})_{\text{Cht}}\text{-}\alpha_{\text{Cp}}$ (21 %), $\alpha_{\text{Cht}}\text{-}\beta(\text{E})_{\text{Cp}}$ (19 %), and $\alpha_{\text{Cht}}\text{-}\alpha_{\text{Cp}}$ (31 %), with an overall regiochemical distribution of 49 % $\beta(\text{E})$ - and 51 % α -. This is consistent with the overall regiochemical distribution obtained by Jain from a similar reaction using 1,1'-bis(dimethylsilyl)ferrocene as the disilane (52 % $\beta(\text{E})$ - and 48 % α -).⁵



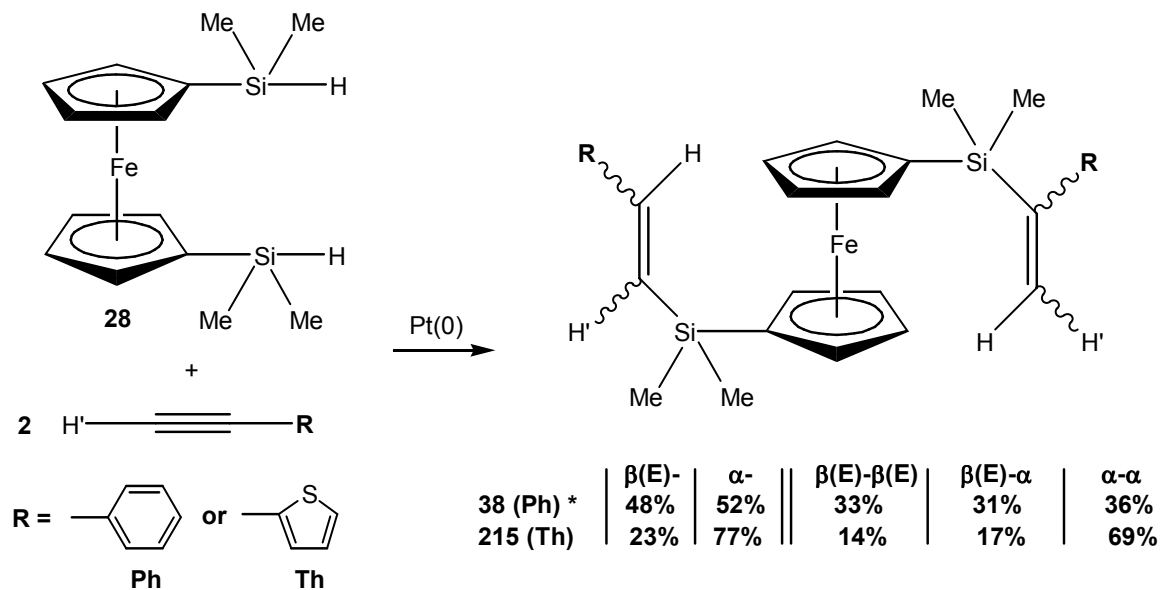
Scheme 4.2.1. Type 2 Model Compounds from **203a** and Monoalkynes.

Another Type 2 model compound was prepared from one equiv. of **203a** and two equiv. of 2-ethynylthiophene, again giving a mixture of four regioisomers of $[\eta^7\text{-}\{\text{dimethyl}(\text{thiophenevinylene})\text{silyl}\}\text{cycloheptatrienyl}] [\eta^5\text{-}\{\text{dimethyl}(\text{thiophenevinylene})\text{silyl}\}\text{cyclopentadienyl}]\text{titanium(II)}$ (**214b**) (95 % yield; blue oil) (**Scheme 4.2.1**). The mixture was comprised of 6 % $\beta(\text{E})_{\text{Cht}}\text{-}\beta(\text{E})_{\text{Cp}}$ / 11 % $\beta(\text{E})_{\text{Cht}}\text{-}\alpha_{\text{Cp}}$ / 10 % $\alpha_{\text{Cht}}\text{-}\beta(\text{E})_{\text{Cp}}$ / 73 % $\alpha_{\text{Cht}}\text{-}\alpha_{\text{Cp}}$, with an overall regiochemical distribution of 16 % $\beta(\text{E})\text{-}$ and 84 % $\alpha\text{-}$.

One equiv. of the disilane 1,1'-bis(dimethylsilyl)ferrocene (**28**) was similarly reacted with two equiv. of 2-ethynylthiophene, giving three regioisomers of a 1,1'-bis{dimethyl(thienylvinylene)silyl}ferrocene (**215**) (72 % yield; orange oil) (**Scheme 4.2.2**) composed of 14 % $\beta(\text{E})\text{-}\beta(\text{E})$ / 17 % $\beta(\text{E})\text{-}\alpha$ / 69 % $\alpha\text{-}\alpha$, with an overall regiochemical distribution of 23 % $\beta(\text{E})\text{-}$ and 77 % $\alpha\text{-}$. As in the case of the Type 1 model compounds, using 2-ethynylthiophene resulted in an increased preference for the α -adduct in **214b** and **215** relative to their phenylacetylene hydrosilylation counterparts (**214a**: 49 % $\beta(\text{E})\text{-}$ / 51 % $\alpha\text{-}$; **38**: 48 % $\beta(\text{E})\text{-}$ / 52 % $\alpha\text{-}$), attributed to the more electron withdrawing nature of the thiophene moiety relative to the phenyl group.²⁷⁷

The regioisomer mixture **214a** was characterized by ^1H , $^{13}\text{C}\{^1\text{H}\}$, ^{29}Si DEPT, and $^1\text{H}\text{-}^1\text{H}$ COSY NMR (**Table 4.2.1**). The ^1H NMR spectrum of the mixture showed a total of eight pairs of doublets for the olefin protons, two pairs for each regioisomer, with two pairs for the $\beta(\text{E})_{\text{Cht}}\text{-}\beta(\text{E})_{\text{Cp}}$ regioisomer at δ 6.574, 6.94 ($^3J_{\text{H-H}} = 19\text{Hz}$) and δ 6.77, 7.12 ($^3J_{\text{H-H}} = 19\text{Hz}$), two pairs for the $\alpha_{\text{Cht}}\text{-}\alpha_{\text{Cp}}$ regioisomer at δ 5.44, 5.78 ($^2J_{\text{H-H}} = 3\text{Hz}$) and δ 5.710, 5.96 ($^2J_{\text{H-H}} = 3\text{Hz}$), two pairs for the $\beta(\text{E})_{\text{Cht}}\text{-}\alpha_{\text{Cp}}$ regioisomer at δ 5.44, 5.77 ($^2J_{\text{H-H}} = 3\text{Hz}$) and δ 6.75, 7.11 ($^3J_{\text{H-H}} = 19\text{Hz}$), and two pairs for the $\alpha_{\text{Cht}}\text{-}\beta(\text{E})_{\text{Cp}}$ regioisomer at δ 5.711, 5.95 ($^2J_{\text{H-H}} = 3\text{Hz}$) and δ 6.565, 6.94 ($^3J_{\text{H-H}} = 19\text{Hz}$). Four pairs of singlets

observed in the methyl region corroborate the presence of four regioisomers (**Figure 4.2.1**), one pair for each regioisomer: $\{\delta\ 0.33\ \text{and}\ \delta\ 0.53\ (\beta(\text{E})_{\text{CHt}}-\beta(\text{E})_{\text{Cp}})\}$, $\{\delta\ 0.34\ \text{and}\ \delta\ 0.49\ (\alpha_{\text{CHt}}-\alpha_{\text{Cp}})\}$, $\{\delta\ 0.35\ \text{and}\ \delta\ 0.52\ (\beta(\text{E})_{\text{CHt}}-\alpha_{\text{Cp}})\}$, and $\{\delta\ 0.32\ \text{and}\ \delta\ 0.51\ (\alpha_{\text{CHt}}-\beta(\text{E})_{\text{Cp}})\}$.



* Jain, R.; Choi, H.; Lalancette, R. A.; Sheridan, J. B. *Organometallics* **2005**, *24*, 1468-1476.

Scheme 4.2.2. Type 2 Model Compounds from **28** and Monoalkynes.

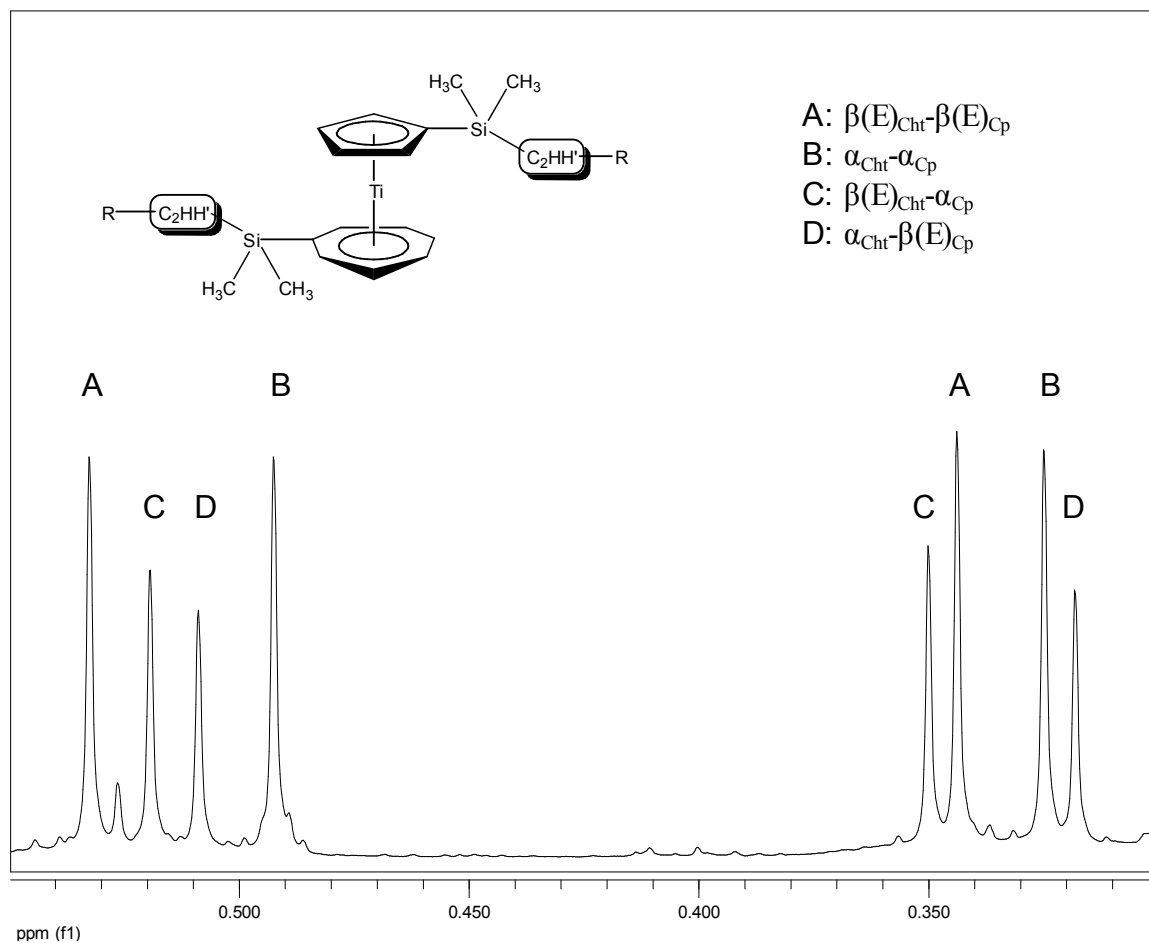


Figure 4.2.1. ^1H NMR of **214a** Methyl Protons.

The regioisomer mixture **214b** was similarly characterized (**Table 4.2.2**), with the ^1H NMR spectrum showing eight pairs of olefin signal doublets, indicative of four regioisomers having two pairs of doublets each. This was also corroborated by eight singlets in the methyl region between δ 0.25 to δ 0.56 ppm (**Figure 4.2.2**).

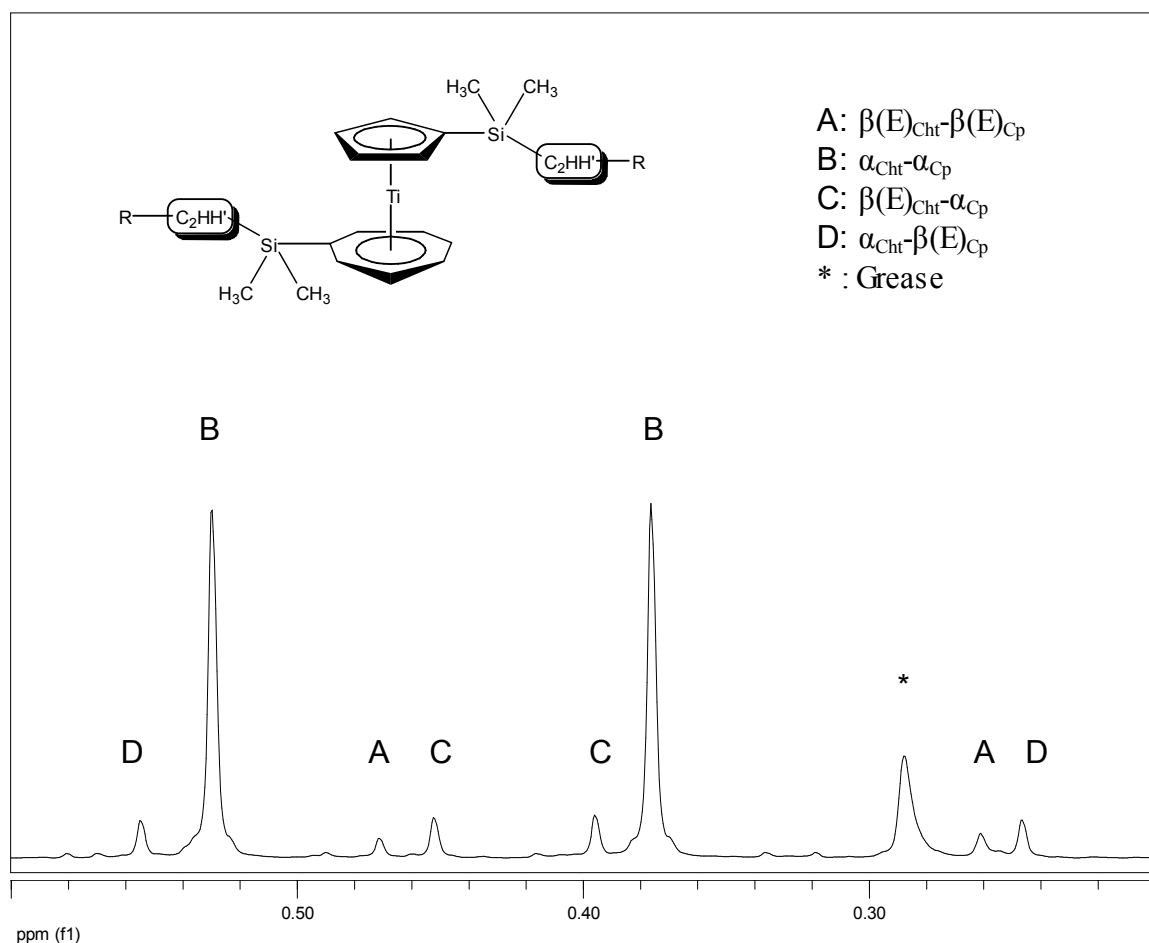


Figure 4.2.2. ¹H NMR of **214b** Methyl Protons.

The regioisomer mixture **215** was also similarly characterized (**Table 4.2.3**), but unlike **214a** or **214b**, the ¹H NMR spectrum showed only four pairs of doublets for the olefinic protons as expected, with one pair each for the $\beta(\text{E})$ - $\beta(\text{E})$ (δ 6.54 and δ 7.09) and α - α (δ 5.44 and δ 6.12) regioisomers, and two pairs for the $\beta(\text{E})$ - α (δ 6.52 and δ 7.08; δ 5.45 and δ 6.12) regioisomer. Four singlets observed in the methyl region corroborate the presence of three regioisomers, with one singlet each for the $\beta(\text{E})$ - $\beta(\text{E})$ (δ 0.36) and α - α (δ 0.45) regioisomers, and two singlets for the $\beta(\text{E})$ - α (δ 0.34 and δ 0.48) regioisomer (**Figure 4.2.3**). The ²⁹Si DEPT NMR showed four signals for the three regioisomers, one

signal each for the $\beta(E)$ - $\beta(E)$ (δ -9.43) and α - α (δ -6.32) regioisomers, and two signals for the $\beta(E)$ - α (δ -9.46 and δ -6.28) regioisomer.

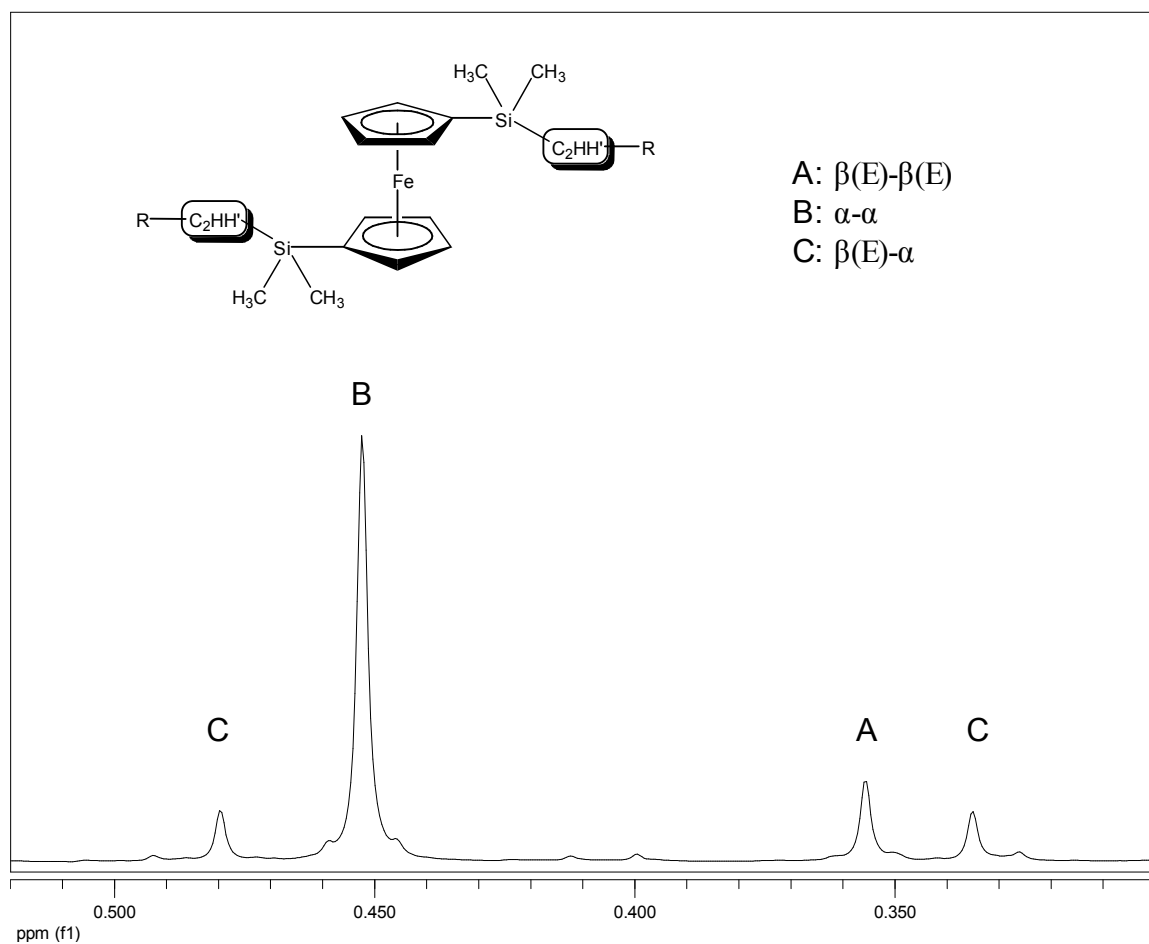


Figure 4.2.3. ^1H NMR Spectrum of **215** Methyl Protons.

The ^1H NMR spectra of the **Type 2** model compounds concurred with those of their respective **Type 1** model compounds, as shown in their olefinic proton signals (**Figure 4.2.4, 4.2.5 and 4.2.6**). However, one notable observation consistent in all three **Type 2** model compounds was their significantly *higher α - to $\beta(E)$ - ratio* compared to

their respective **Type 1** model compounds. This difference in regiochemical distributions is further explored in **Chapter 5**.

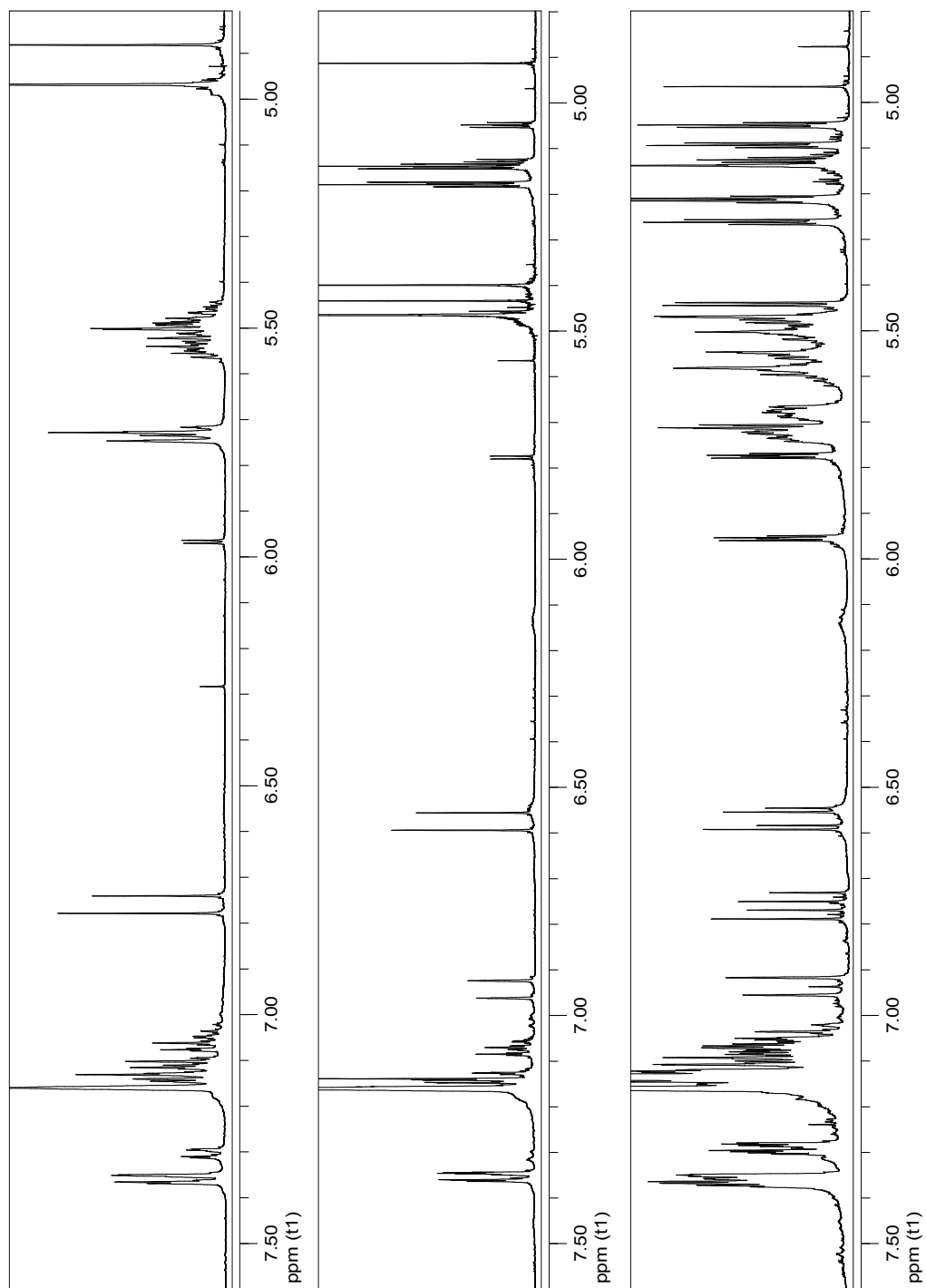


Figure 4.2.4. ^1H NMR Spectrum of **211a** (top), **212a** (mid), and **214a** (bot) Olefinic Protons.

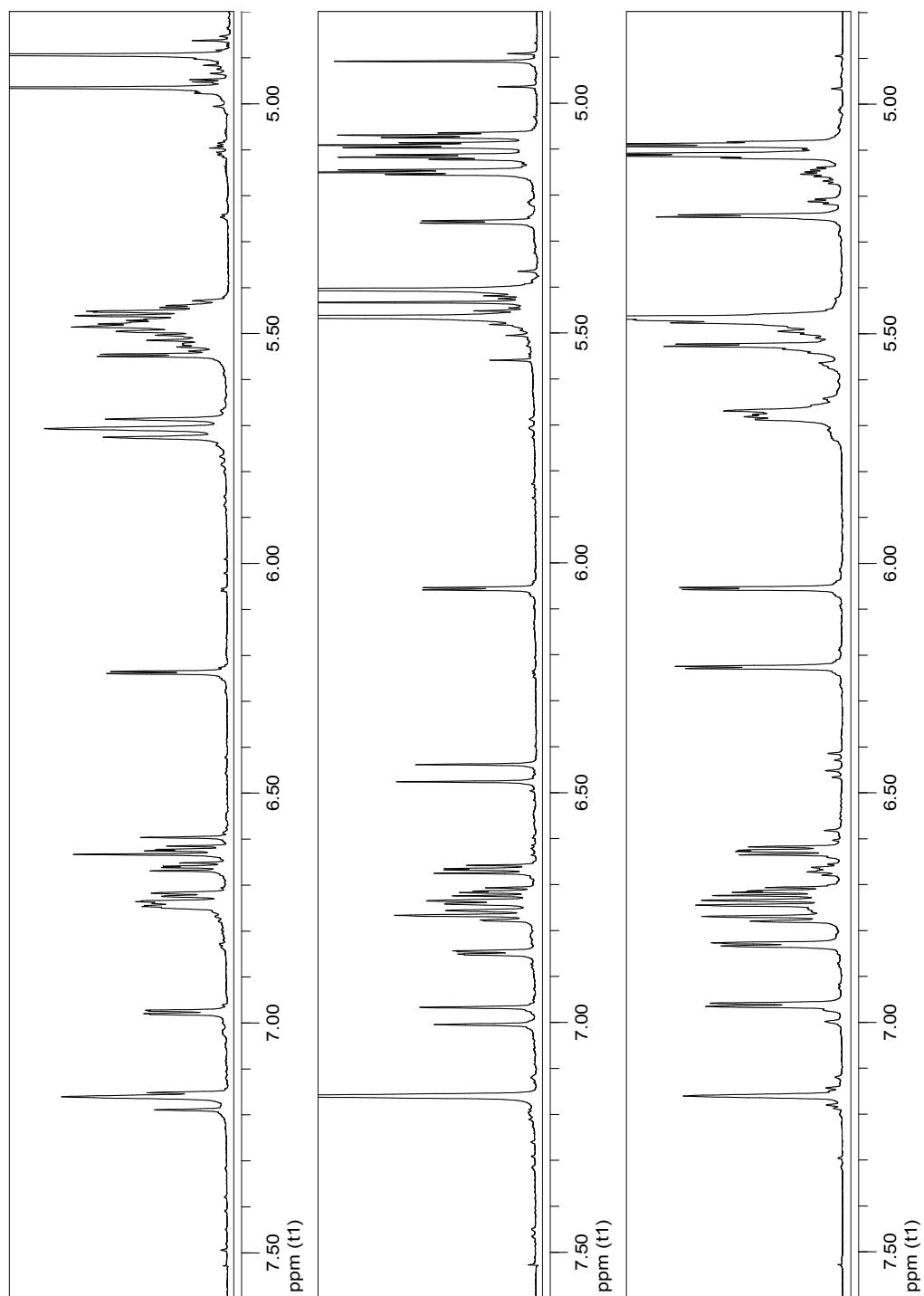


Figure 4.2.5. ^1H NMR Spectrum of **211b** (top), **212b** (mid), and **214b** (bot) Olefinic Protons.

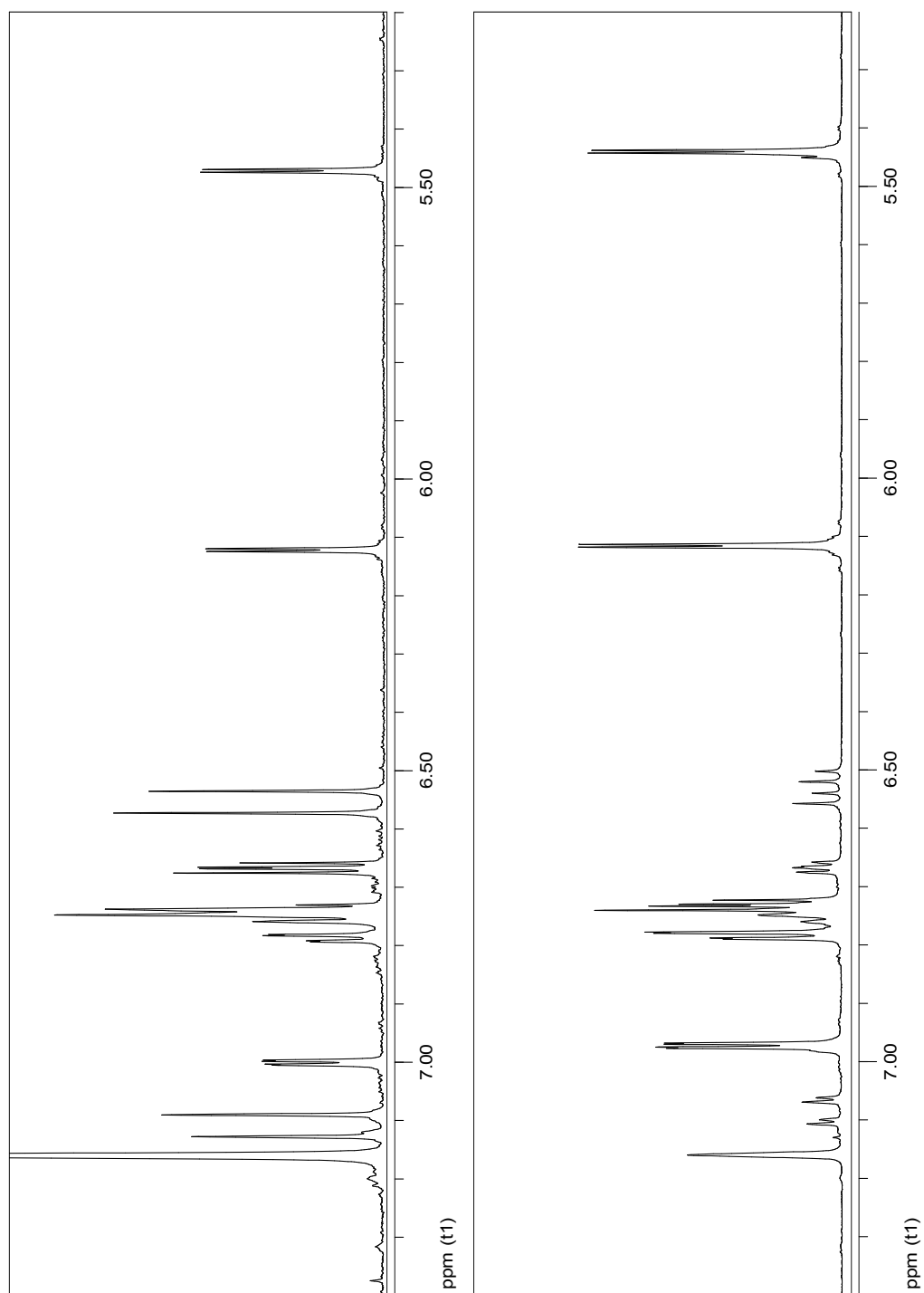


Figure 4.2.6. ^1H NMR Spectrum of **213** (top) and **215** (bot) Olefinic Protons.

Table 4.2.1. NMR Data^a for **214a**.

| Regioisomer | δ (¹ H) ^b | δ (¹³ C{ ¹ H}) ^b | δ (²⁹ Si DEPT) ^c |
|--|---|---|--|
| β(E)_{CHt-β(E)}Cp | 0.33 (s, 6H, CpSi(CH ₃) ₂ -), 0.53 (s, 6H, ChtSi(CH ₃) ₂ -), 6.574, 6.94 (d, 2H, CpSi(CH ₃) ₂ -C ₂ H ₂ -, ³ J _{H-H} = 19Hz), 6.77, 7.12 (d, 2H, ChtSi(CH ₃) ₂ -C ₂ H ₂ -, ³ J _{H-H} = 19Hz) | -1.17 (CpSi(CH ₃) ₂ -), -0.69 (ChtSi(CH ₃) ₂ -), 87.70, 89.64, 91.70 (ChtSi(CH ₃) ₂ -), 94.95 (<i>ipso</i> C, ChtSi(CH ₃) ₂ -), 100.91, 103.71 (CpSi(CH ₃) ₂ -), 109.16 (<i>ipso</i> C, CpSi(CH ₃) ₂ -) | -14.61 (CpSi(CH ₃) ₂ -), -4.02 (ChtSi(CH ₃) ₂ -) |
| α_{CHt-α}Cp | 0.34 (s, 6H, CpSi(CH ₃) ₂ -), 0.49 (s, 6H, ChtSi(CH ₃) ₂ -), 5.44, 5.78 (d, 2H, CpSi(CH ₃) ₂ -C ₂ H ₂ -, ² J _{H-H} = 3Hz), 5.710, 5.96 (d, 2H, ChtSi(CH ₃) ₂ -C ₂ H ₂ -, ² J _{H-H} = 3Hz) | -1.13 (CpSi(CH ₃) ₂ -), -0.54 (ChtSi(CH ₃) ₂ -), 87.70, 89.56, 92.02 (ChtSi(CH ₃) ₂ -), 94.68 (<i>ipso</i> C, ChtSi(CH ₃) ₂ -), 101.00, 104.24 (CpSi(CH ₃) ₂ -), 108.74 (<i>ipso</i> C, CpSi(CH ₃) ₂ -) | -12.92 (CpSi(CH ₃) ₂ -), -2.33 (ChtSi(CH ₃) ₂ -) |
| Continued on the next page. | | | |

^a Solvent used: C₆D₆. ^b Internal reference: C₆D₆ (¹H NMR: δ 7.16 ppm; ¹³C NMR: δ 128.38 ppm). ^c External reference: Tetramethylsilane (δ 0.0 ppm).

| Regioisomer | $\delta (^1\text{H})^b$ | $\delta (^{13}\text{C}\{\text{H}\})^b$ | $\delta (^{29}\text{Si DEPT})^c$ |
|---|---|---|---|
| $\beta(\text{E})_{\text{Cht}-\alpha_{\text{Cp}}}$ | 0.35 (s, 6H, $\text{CpSi}(\text{CH}_3)_{2-}$), 0.52 (s, 6H, $\text{ChtSi}(\text{CH}_3)_{2-}$), 5.44, 5.77 (d, 2H, $\text{CpSi}(\text{CH}_3)_{2-}\text{C}_2\text{H}_2$ -, $^2J_{\text{H-H}} = 3\text{Hz}$), 6.75, 7.11 (d, 2H, $\text{ChtSi}(\text{CH}_3)_{2-}\text{C}_2\text{H}_2$ -, $^3J_{\text{H-H}} = 19\text{Hz}$) | -1.13 ($\text{CpSi}(\text{CH}_3)_{2-}$), -0.70 ($\text{ChtSi}(\text{CH}_3)_{2-}$), 87.80, 89.67, 91.70 ($\text{ChtSi}(\text{CH}_3)_{2-}$), 94.95 (<i>ipso C</i> , $\text{ChtSi}(\text{CH}_3)_{2-}$), 100.85, 103.81 ($\text{CpSi}(\text{CH}_3)_{2-}$), 108.68 (<i>ipso C</i> , $\text{CpSi}(\text{CH}_3)_{2-}$) | -12.94 ($\text{CpSi}(\text{CH}_3)_{2-}$), -4.02 ($\text{ChtSi}(\text{CH}_3)_{2-}$) |
| $\alpha_{\text{Cht}-\beta(\text{E})_{\text{Cp}}}$ | 0.32 (s, 6H, $\text{CpSi}(\text{CH}_3)_{2-}$), 0.51 (s, 6H, $\text{ChtSi}(\text{CH}_3)_{2-}$), 5.711, 5.95 (d, 2H, $\text{ChtSi}(\text{CH}_3)_{2-}\text{C}_2\text{H}_2$ -, $^2J_{\text{H-H}} = 3\text{Hz}$), 6.565, 6.94 (d, 2H, $\text{CpSi}(\text{CH}_3)_{2-}\text{C}_2\text{H}_2$ -, $^3J_{\text{H-H}} = 19\text{Hz}$) | -1.17 ($\text{CpSi}(\text{CH}_3)_{2-}$), -0.49 ($\text{ChtSi}(\text{CH}_3)_{2-}$), 87.59, 89.52, 92.02 ($\text{ChtSi}(\text{CH}_3)_{2-}$), 94.72 (<i>ipso C</i> , $\text{ChtSi}(\text{CH}_3)_{2-}$), 101.05, 104.14 ($\text{CpSi}(\text{CH}_3)_{2-}$), 109.25 (<i>ipso C</i> , $\text{CpSi}(\text{CH}_3)_{2-}$) | -14.61 ($\text{CpSi}(\text{CH}_3)_{2-}$), -2.29 ($\text{ChtSi}(\text{CH}_3)_{2-}$) |
| misc | 5.03-5.28 (multiplet, 4x4H, <i>Cp</i> -), 5.45-5.75 (multiplet, 4x6H, <i>Cht</i> -), 7.00-7.40 (multiplet, 4x10H, <i>Ph</i> -) | 127.07, 127.09, 127.11, 127.13, 127.25, 127.32, 127.64, 127.86, 127.87, 128.76, 128.78, 128.79, 128.82, 128.84, 128.86, 128.87, 129.21, 129.26, 129.78, 129.80 (<i>Ph</i> -), 138.94, 138.96, 139.06, 139.08, 145.33, 145.46, 145.49, 145.61, 145.63, 145.71, 145.75, 153.54, 153.61, 153.62 (<i>C</i> ₂ H ₂ -) | |

^a Solvent used: C₆D₆. ^b Internal reference: C₆D₆ (¹H NMR: δ 7.16 ppm; ¹³C NMR: δ 128.38 ppm). ^c External reference: Tetramethylsilane (δ 0.0 ppm).

Table 4.2.2. NMR Data^a for **214b**.^{*}

| Regioisomer | $\delta(^1\text{H})^b$ | $\delta(^{13}\text{C}\{^1\text{H}\})^b$ | $\delta(^{29}\text{Si DEPT})^c$ |
|---|--|---|---|
| $\beta(\text{E})_{\text{Cht}}\text{-}\beta(\text{E})_{\text{Cp}}$ | 0.26 (s, 6H, $\beta(\text{E})\text{-}\beta(\text{E})$, $\text{CpSi}(\text{CH}_3)_{2-}$), | -1.23 ($\beta(\text{E})\text{-}\beta(\text{E})$, $\text{CpSi}(\text{CH}_3)_{2-}$), -0.77 ($\beta(\text{E})\text{-}\beta(\text{E})$), | -14.77 ($\beta(\text{E})\text{-}\beta(\text{E})$), |
| | 0.47 (s, 6H, $\beta(\text{E})\text{-}\beta(\text{E})$, $\text{ChtSi}(\text{CH}_3)_{2-}$), | $\text{ChtSi}(\text{CH}_3)_{2-}$, 87.72, 89.69, 91.67 ($\beta(\text{E})\text{-}\beta(\text{E})$), | $\text{CpSi}(\text{CH}_3)_{2-}$, -4.18 |
| | 6.44, 6.980 (d, 2H, $\beta(\text{E})\text{-}\beta(\text{E})$, | $\text{ChtSi}(\text{CH}_3)_{2-}$, 94.61 ($\beta(\text{E})\text{-}\beta(\text{E})$, <i>ipso</i> C, | ($\beta(\text{E})\text{-}\beta(\text{E})$, |
| | $\text{CpSi}(\text{CH}_3)_{2-}\text{-C}_2\text{H}_2\text{-}$, $^3J_{\text{H-H}} = 19\text{Hz}$), 6.62, | $\text{ChtSi}(\text{CH}_3)_{2-}$, 100.98, 103.73 ($\beta(\text{E})\text{-}\beta(\text{E})$, | $\text{ChtSi}(\text{CH}_3)_{2-}$) |
| | 7.17 (d, 2H, $\beta(\text{E})\text{-}\beta(\text{E})$, $\text{ChtSi}(\text{CH}_3)_{2-}\text{-C}_2\text{H}_2\text{-}$, $^3J_{\text{H-H}} = 19\text{Hz}$) | $\text{CpSi}(\text{CH}_3)_{2-}$, 108.89 ($\beta(\text{E})\text{-}\beta(\text{E})$, <i>ipso</i> C, | |
| $\alpha_{\text{Cht}}\text{-}\alpha_{\text{Cp}}$ | 0.38 (s, 6H, $\alpha\text{-}\alpha$, $\text{CpSi}(\text{CH}_3)_{2-}$), 0.53 (s, | -0.96 ($\alpha\text{-}\alpha$, $\text{CpSi}(\text{CH}_3)_{2-}$), -0.34 ($\alpha\text{-}\alpha$, | -12.00 ($\alpha\text{-}\alpha$, |
| | 6H, $\alpha\text{-}\alpha$, $\text{ChtSi}(\text{CH}_3)_{2-}$), 5.247, 6.048 (d, | $\text{ChtSi}(\text{CH}_3)_{2-}$, 87.83, 89.67, 92.15 ($\alpha\text{-}\alpha$, | $\text{CpSi}(\text{CH}_3)_{2-}$), -1.53 |
| | 2H, $\alpha\text{-}\alpha$, $\text{CpSi}(\text{CH}_3)_{2-}\text{-C}_2\text{H}_2\text{-}$, $^2J_{\text{H-H}} =$ | $\text{ChtSi}(\text{CH}_3)_{2-}$, 94.20 ($\alpha\text{-}\alpha$, <i>ipso</i> C, $\text{ChtSi}(\text{CH}_3)_{2-}$), | ($\alpha\text{-}\alpha$, $\text{ChtSi}(\text{CH}_3)_{2-}$) |
| | 3Hz), 5.525, 6.218 (d, 2H, $\alpha\text{-}\alpha$, | 101.14, 104.45 ($\alpha\text{-}\alpha$, $\text{CpSi}(\text{CH}_3)_{2-}$), 108.22 ($\alpha\text{-}\alpha$, | |
| Continued on the next page. | | | |

^a Solvent used: C_6D_6 . ^b Internal reference: C_6D_6 (^1H NMR: δ 7.16 ppm; ^{13}C NMR: δ 128.38 ppm). ^c External reference: Tetramethylsilane (δ 0.0 ppm).^{*} Th = Thiophene.

| Regioisomer | δ (^1H) ^b | δ ($^{13}\text{C}\{\text{H}\}$) ^b | δ ($^{29}\text{Si DEPT}$) ^c |
|--|--|---|--|
| $\beta(\text{E})_{\text{Cht-}\alpha\text{Cp}}$ | 0.40 (s, 6H, $\beta(\text{E})-\alpha$, CpSi(CH ₃) ₂ -), 0.45 (s, 6H, $\beta(\text{E})-\alpha$, ChtSi(CH ₃) ₂ -), 5.252, 6.046 (d, 2H, $\beta(\text{E})-\alpha$, CpSi(CH ₃) ₂ -C ₂ H ₂ -, ² J _{H-H} = 3Hz), 6.60, 7.16 (d, 2H, $\beta(\text{E})-\alpha$, ChtSi(CH ₃) ₂ -C ₂ H ₂ -, ³ J _{H-H} = 19Hz) | -0.94 ($\beta(\text{E})-\alpha$, CpSi(CH ₃) ₂ -), -0.79 ($\beta(\text{E})-\alpha$, ChtSi(CH ₃) ₂ -), 87.68, 89.79, 91.75 ($\beta(\text{E})-\alpha$, ChtSi(CH ₃) ₂ -), 94.72 ($\beta(\text{E})-\alpha$, ipso C, ChtSi(CH ₃) ₂ -), 101.13, 104.29 ($\beta(\text{E})-\alpha$, CpSi(CH ₃) ₂ -), 108.06 ($\beta(\text{E})-\alpha$, ipso C, CpSi(CH ₃) ₂ -) | -12.01 ($\beta(\text{E})-\alpha$, CpSi(CH ₃) ₂ -), -4.16 ($\beta(\text{E})-\alpha$, ChtSi(CH ₃) ₂ -) |
| $\alpha_{\text{Cht-}\beta(\text{E})\text{Cp}}$ | 0.25 (s, 6H, $\alpha-\beta(\text{E})$, CpSi(CH ₃) ₂ -), 0.56 (s, 6H, $\alpha-\beta(\text{E})$, ChtSi(CH ₃) ₂ -), 5.528, 6.215 (d, 2H, $\alpha-\beta(\text{E})$, ChtSi(CH ₃) ₂ -C ₂ H ₂ -, ² J _{H-H} = 3Hz), 6.43, 6.977 (d, 2H, $\alpha-\beta(\text{E})$, CpSi(CH ₃) ₂ -C ₂ H ₂ -, ³ J _{H-H} = 19Hz) | -1.24 ($\alpha-\beta(\text{E})$, CpSi(CH ₃) ₂ -), -0.32 ($\alpha-\beta(\text{E})$, ChtSi(CH ₃) ₂ -), 87.87, 89.56, 92.08 ($\alpha-\beta(\text{E})$, ChtSi(CH ₃) ₂ -), 94.12 ($\alpha-\beta(\text{E})$, ipso C, ChtSi(CH ₃) ₂ -), 100.99, 103.87 ($\alpha-\beta(\text{E})$, CpSi(CH ₃) ₂ -), 109.07 ($\alpha-\beta(\text{E})$, ipso C, CpSi(CH ₃) ₂ -) | -14.75 ($\alpha-\beta(\text{E})$, CpSi(CH ₃) ₂ -), -1.53 ($\alpha-\beta(\text{E})$, ChtSi(CH ₃) ₂ -) |
| misc | 5.08-5.23 (m, 4x4H, Cp-), 5.44-5.74 (m, 4x6H, Cht-), 6.62-6.98 (m, 4x6H, Th-). | 124.2, 124.3, 124.4, 124.44, 125.4, 125.5, 125.6, 125.7, 125.74, 126.0, 126.7, 126.8, 126.83, 127.6, 127.9, 127.94, 128.0, 128.09, 128.1, 128.12, 128.2, 128.8 (Th-), 137.9, 138.0, 138.2, 138.3, 144.6, 144.7, 144.8, 144.9, 145.75, 145.8, 145.9, 146.0, 147.5, 147.6, 147.8, 147.83 (-C ₂ H ₂ -) | |

^a Solvent used: C₆D₆. ^b Internal reference: C₆D₆ (^1H NMR: δ 7.16 ppm; ^{13}C NMR: δ 128.38 ppm). ^c External reference: Tetramethylsilane (δ 0.0 ppm).

* Th = Thiophene.

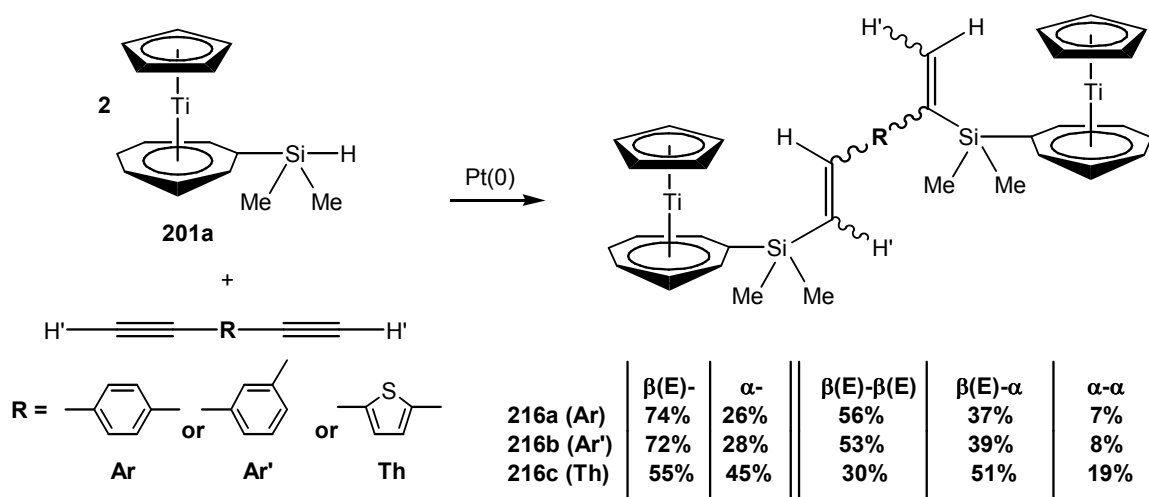
Table 4.2.3. NMR Data^a for **215**.^{*}

| Regioisomer | δ (¹ H) ^b | δ (¹³ C{ ¹ H}) ^b | δ (²⁹ Si DEPT) ^c |
|---|--|--|---|
| β(E) -β(E) | 0.36 (s, 12H, β (E)- β (E), CpSi(CH ₃) ₂ -), 4.09, 4.29 (t, 8H, β (E)- β (E), CpSi(CH ₃) ₂ -), 6.54, 7.09 (d, 4H, β (E)- β (E), -C ₂ H ₂ -, ³ J _{H-H} = 19Hz) | -1.13 (β (E)- β (E), CpSi(CH ₃) ₂ -), 70.57 (β (E)- β (E), <i>ipso</i> C, CpSi(CH ₃) ₂ -), 72.28, 74.02 (β (E)- β (E), CpSi(CH ₃) ₂ -) | -9.43 (β (E)- β (E), CpSi(CH ₃) ₂ -) |
| α-α | 0.45 (s, 12H, α - α , CpSi(CH ₃) ₂ -), 4.02, 4.19 (t, 8H, α - α , CpSi(CH ₃) ₂ -), 5.44, 6.12 (d, 4H, α - α , -C ₂ H ₂ -, ² J _{H-H} = 3Hz) | -0.85 (α - α , CpSi(CH ₃) ₂ -), 70.30 (α - α , <i>ipso</i> C, CpSi(CH ₃) ₂ -), 72.49, 74.50 (α - α , CpSi(CH ₃) ₂ -) | -6.32 (α - α , CpSi(CH ₃) ₂ -) |
| β(E)-α | 0.34, 0.48 (s, 12H, β (E)- α , CpSi(CH ₃) ₂ -), 4.04, 4.07, 4.21, 4.27 (t, 8H, β (E)- α , CpSi(CH ₃) ₂ -), 5.45, 6.12 (d, 2H, β (E)- α , -C ₂ H ₂ -, ² J _{H-H} = 3Hz), 6.52, 7.08 (d, 2H, β (E)- α , -C ₂ H ₂ -, ³ J _{H-H} = 19Hz) | -1.16, -0.83 (β (E)- α , CpSi(CH ₃) ₂ -), 70.18, 70.70 (β (E)- α , <i>ipso</i> C, CpSi(CH ₃) ₂ -), 72.35, 72.43, 74.10, 74.40 (β (E)- α , CpSi(CH ₃) ₂ -) | -9.46 (β (E)- α , CpSi(CH ₃) ₂ -), -6.28 (β (E)- α , CpSi(CH ₃) ₂ -)) |
| misc | 6.64-6.80, 6.96-7.00 (multiplet, 3x6H, <i>Th</i> -) | 124.29, 124.33, 125.50, 125.52, 125.55, 126.62, 126.65, 127.25, 127.89, 128.05, 128.06, 128.72 (C ₄ SH ₃ -), 137.79, 137.84, 144.76, 144.82, 145.91, 145.95, 147.81, 147.83 (-C ₂ H ₂ -) | |

^a Solvent used: C₆D₆. ^b Internal reference: C₆D₆ (¹H NMR: δ 7.16 ppm; ¹³C NMR: δ 128.38 ppm). ^c External reference: Tetramethylsilane (δ 0.0 ppm). ^{*} Th = Thiophene.

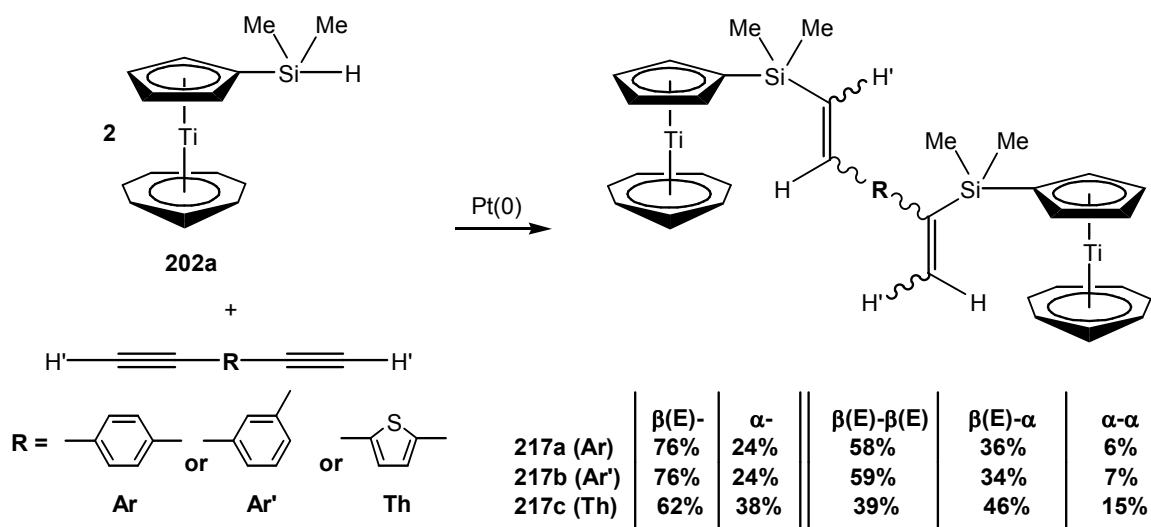
4.3. Type 3 Model Compounds

Type 3 model compounds were prepared from the hydrosilylation of two equiv. of a monosilane and one equiv. of a dialkyne. One set utilized **201a** as the monosilane (**Scheme 4.3.1**). Using 1,4-diethynylbenzene gave a mixture of three regioisomers of *bis*{(dimethyl)silylenevinylene}-1,4-phenylene bridged *bis*(tropicene) (**216a**) (61 % yield; blue oil) composed of 56 % β (E)- β (E) / 37 % β (E)- α / 7 % α - α with an overall regiochemical distribution of 74 % β (E)- and 26 % α -, while 1,3-diethynylbenzene gave a mixture of three regioisomers of *bis*{(dimethyl)silylenevinylene}-1,3-phenylene bridged *bis*(tropicene) (**216b**) (74 % yield; blue oil) composed of 53 % β (E)- β (E) / 39 % β (E)- α / 8 % α - α and an overall regiochemical distribution of 72 % β (E)- and 28 % α -. With 2,5-diethynylthiophene as the dialkyne, a mixture of three regioisomers of *bis*{(dimethyl)silylenevinylene}-2,5-thiophene bridged *bis*(tropicene) (**216c**) was obtained as product (73 % yield; blue oil) composed of 30 % β (E)- β (E) / 51 % β (E)- α / 19 % α - α and an overall regiochemical distribution of 55 % β (E)- and 45 % α -.



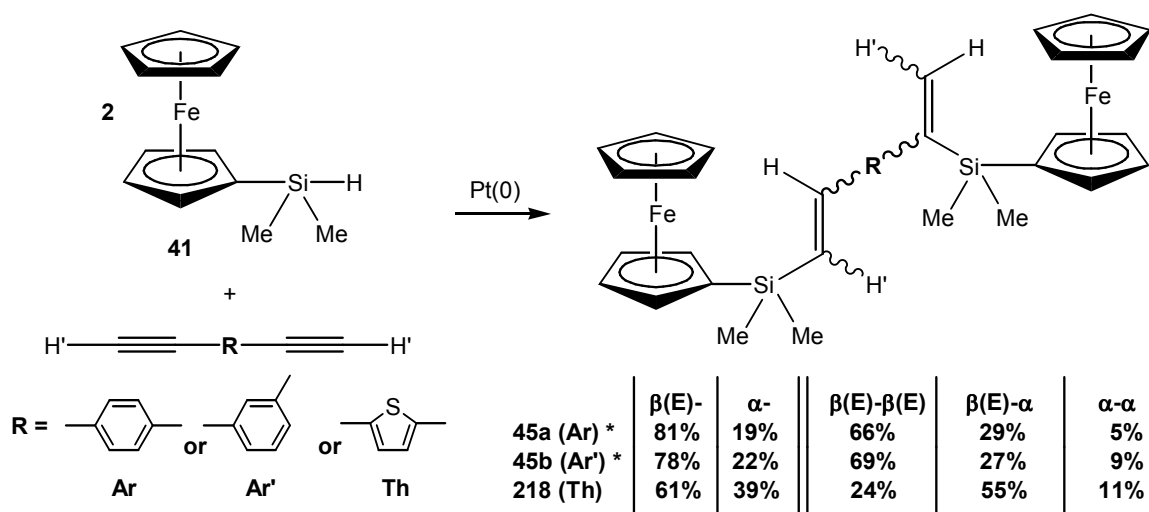
Scheme 4.3.1. Type 3 Model Compounds from **201a** and Dialkynes.

Another set of Type 3 model compounds was prepared with **202a** as the monosilane (**Scheme 4.3.2**). Using 1,4-diethynylbenzene gave a mixture of three regioisomers of *bis*{(dimethyl)silylenevinylene}-1,4-phenylene bridged *bis*(troticene) (**217a**) (68 % yield; blue oil) composed of 58 % β (E)- β (E) / 36 % β (E)- α / 6 % α - α with an overall regiochemical distribution of 76 % β (E)- and 24 % α -, while 1,3-diethynylbenzene gave a mixture of three regioisomers of *bis*{(dimethyl)silylenevinylene}-1,3-phenylene bridged *bis*(troticene) (**217b**) (68 % yield; blue oil) composed of 59 % β (E)- β (E) / 34 % β (E)- α / 7 % α - α , with an overall regiochemical distribution of 76 % β (E)- and 24 % α -. Using 2,5-diethynylthiophene as the dialkyne similarly gave a mixture of three regioisomers of *bis*{(dimethyl)silylenevinylene}-2,5-thiophene bridged *bis*(troticene) (**217c**) (73 % yield; blue oil) composed of 39 % β (E)- β (E) / 46 % β (E)- α / 15 % α - α , with an overall regiochemical distribution of 62 % β (E)- and 38 % α -.



Scheme 4.3.2. Type 3 Model Compounds from **202a** and Dialkynes.

A similar reaction was carried out using two equiv. of dimethylsilylferrocene (**41**) and one equiv. of 2,5-*bis*(ethynyl)thiophene, giving a mixture of three regioisomers of 1,1'-*bis*{(dimethyl) silylenevinylene}-2,5-thienylene bridged biferrocene (**218**) (95 % yield; orange oil) (**Scheme 4.3.3**) composed of 34 % β (E)- β (E) / 55 % β (E)- α / 11 % α - α , with an overall regiochemical distribution of 61 % β (E)- and 39 % α .



* Jain, R.; Choi, H.; Lalancette, R. A.; Sheridan, J. B. *Organometallics* **2005**, 24, 1468-1476.

Scheme 4.3.3. Type 3 Model Compounds from **41** and Dialkynes.

It is notable that the overall regiochemical distributions of the Type 3 model compounds are comparable with that of their Type 1 model counterparts (**Scheme 4.1.1** to **4.1.3**). In contrast, their Type 2 model counterparts have a relatively lower β (E)- to α -ratio observed in both the phenylene- and thienylene- containing model compounds (**Scheme 4.2.1** and **4.2.2**), an observation consistent with results obtained by Jain and coworkers (**Chapter 1.2.6**).^{4,5} This difference in regiochemical distributions between the model compounds is further explored in **Chapter 5**.

The regioisomer mixture **216a** was characterized by ^1H , $^{13}\text{C}\{^1\text{H}\}$, ^{29}Si DEPT, and ^1H - ^1H COSY NMR (Table 4.3.1). The ^1H NMR spectrum showed four pairs of doublets for the olefinic protons, with one pair each for the $\beta(\text{E})$ - $\beta(\text{E})$ (δ 6.78 and δ 7.11) and α - α (δ 5.71 and δ 5.98) regioisomers, and two pairs for the $\beta(\text{E})$ - α (δ 6.71 and δ 7.10; δ 5.74 and δ 6.00) regioisomer. The $^{13}\text{C}\{^1\text{H}\}$ NMR spectrum corroborates the presence of three regioisomers with four methyl carbon signals ($\beta(\text{E})$ - $\beta(\text{E})$: δ -0.70 ppm; α - α : δ -0.25 ppm; $\beta(\text{E})$ - α : δ -0.63 ppm and δ -0.48 ppm) as well as four Cp carbon signals ($\beta(\text{E})$ - $\beta(\text{E})$: δ 95.65 ppm; α - α : δ 97.76 ppm; $\beta(\text{E})$ - α : δ 97.63 ppm and δ 97.78 ppm). Four signals were also observed in the ^{29}Si DEPT NMR spectrum, with one signal each for the $\beta(\text{E})$ - $\beta(\text{E})$ (δ -4.02) and α - α (δ -2.11) regioisomers, and two signals for the $\beta(\text{E})$ - α (δ -4.05 and δ -2.30) regioisomer.

Products **216b** and **216c** were similarly characterized (Table 4.3.2 and Table 4.3.3), sharing common NMR spectral features with **216a** indicating the presence of three regioisomers. The ^{29}Si DEPT NMR spectra of **216b** confirmed the presence of three regioisomers with four signals, one signal each for the $\beta(\text{E})$ - $\beta(\text{E})$ (δ -4.15) and α - α (δ -2.35) regioisomers, and two signals for the $\beta(\text{E})$ - α (δ -4.19 and δ -2.52) regioisomer. The ^{29}Si DEPT NMR spectra of **216c** also showed four signals, one signal each for the $\beta(\text{E})$ - $\beta(\text{E})$ (δ -4.34) and α - α (δ -1.60) regioisomers, and two signals for the $\beta(\text{E})$ - α (δ -4.38 and δ -1.60) regioisomer.

The second set of Type 3 model compounds from Scheme 4.3.2 (**217a**, **217b**, and **217c**) was also similarly characterized by (Table 4.3.4, 4.3.5 and 4.3.6, respectively), sharing common NMR spectral features with their Scheme 4.3.1 counterparts (**216a**, **216b**, and **216c**) indicating the presence of three regioisomers in each. As in the case of

the Type 1 model compounds, one key difference was that the methyl and olefinic proton signals of **217a**, **217b**, and **217c** were more upfield compared to **216a**, **216b**, and **216c**, respectively, attributed to the more electron donating (and more shielding) nature of the Cp ligand compared with the Cht ligand. This is also evident in both the $^{13}\text{C}\{^1\text{H}\}$ NMR methyl carbon signals and ^{29}Si DEPT NMR silicon signals of the products.

The regioisomer mixture **218** was characterized by ^1H , $^{13}\text{C}\{^1\text{H}\}$, ^{29}Si DEPT, and ^1H - ^1H COSY NMR (Table 4.3.7). As in the case of the troticene-based model compounds, the ^1H NMR spectrum showed four pairs of doublets for the olefinic protons, indicating the presence of three regioisomers, with one pair for each of the $\beta(\text{E})$ - $\beta(\text{E})$ (δ 6.58 and δ 7.05) and α - α (δ 5.469 and δ 6.16) regioisomers, and two pairs for the $\beta(\text{E})$ - α (δ 6.56 and δ 7.08; δ 5.465 and δ 6.14) regioisomer. This was corroborated by four signals observed in the ^{29}Si DEPT NMR spectrum, one signal for each of the $\beta(\text{E})$ - $\beta(\text{E})$ (δ -9.59) and α - α (δ -6.44) regioisomers, and two signals for the $\beta(\text{E})$ - α (δ -9.69 and δ -6.36) regioisomer.

The overall regiochemical distributions obtained from the reactions involving either 1,4- or 1,3- diethynylbenzene as the dialkyne are consistent with other similar Pt-catalyzed hydrosilylation reactions reported in the literature, showing a clear preference for the $\beta(\text{E})$ - adduct (See Scheme 1.2.6.3).^{5,276} Examples include results obtained by Hiyami and coworkers²²⁷ from the Pt-complex-catalyzed hydrosilylation of phenylacetylene with Et_3SiH ($\beta(\text{E})$ - / α : 80 / 20), as well as by Kim and coworkers^{253,254} from the Pt-catalyzed hydrosilylation polymerization of 3- or 4- (dimethylsilyl)phenylacetylene ($\beta(\text{E})$ - / α : 70 / 30), clearly favoring the $\beta(\text{E})$ - form which has been attributed to steric effects playing a big role in the regioselectivity.^{227,247}

In general, the thiophene-containing model compounds have a lower $\beta(\text{E})$ - to α - ratio relative to their phenyl-containing counterparts, attributed to the more electron withdrawing nature of the thiophene moiety compared to the phenyl group.²⁷⁷ However, an observation consistent among the thiophene- and phenyl- containing model compounds is the decreased $\beta(\text{E})$ - to α - ratio in the reactions involving the disilane sandwich complexes relative to the reactions involving their monosilane counterparts. This observation is explored further in **Chapter 5**. The following section describes the syntheses and characterization of polymeric systems relevant to the model compounds described in this chapter.

Table 4.3.1. NMR Data^a for **216a**.^{*}

| Regioisomer | δ (¹ H) ^b | δ (¹³ C{ ¹ H}) ^b | δ (²⁹ Si DEPT) ^c |
|--|---|---|--|
| β(E)_{Chr}-β(E)_{Chr} | 0.54 (s, 12H, ChtSi(CH ₃) ₂ -), 4.97 (s, 10H, Cp), 6.78, 7.11 (d, 4H, -C ₂ H ₂ -, ³ J _{H-H} = 19Hz) | -0.70 (ChtSi(CH ₃) ₂ -), 87.43, 89.46, 91.87 (ChtSi(CH ₃) ₂ -), 94.99 (<i>ipso</i> C, ChtSi(CH ₃) ₂ -), 97.65 (Cp) | -4.02 (ChtSi(CH ₃) ₂ -) |
| α_{Chr}-α_{Chr} | 0.49 (s, 12H, ChtSi(CH ₃) ₂ -), 4.87 (s, 10H, Cp), 5.71, 5.98 (d, 4H, -C ₂ H ₂ -, ² J _{H-H} = 3Hz) | -0.25 (ChtSi(CH ₃) ₂ -), 87.21, 89.31, 92.21 (ChtSi(CH ₃) ₂ -), 95.04 (<i>ipso</i> C, ChtSi(CH ₃) ₂ -), 97.76 (Cp) | -2.11 (ChtSi(CH ₃) ₂ -) |
| β(E)_{Chr}-α_{Chr} / α_{Chr}-β(E)_{Chr} | 0.51, 0.52 (s, 12H, ChtSi(CH ₃) ₂ -), 4.90, 4.96 (s, 10H, Cp), 5.74, 6.00 (d, 2H, -C ₂ H ₂ -, ² J _{H-H} = 3Hz), 6.71, 7.10 (d, 2H, -C ₂ H ₂ -, ³ J _{H-H} = 19Hz) | -0.63, -0.48 (ChtSi(CH ₃) ₂ -), 87.31, 87.37, 89.38, 89.41, 91.88, 92.18 (ChtSi(CH ₃) ₂ -), 94.80, 95.28 (<i>ipso</i> C, ChtSi(CH ₃) ₂ -), 97.63, 97.78 (Cp) | -4.05, -2.30 (ChtSi(CH ₃) ₂ -) |
| misc | 5.42-5.58, 5.68-5.78 (m, 3x12H, Cht-), 7.27- 7.35 (m, 3x4H, -Ph-) | 127.26, 127.64, 127.81, 129.32, 129.52 (-Ph-), 137.38, 138.94, 143.81, 145.18, 145.47, 145.53, 152.93, 153.23 (-C ₂ H ₂ -) | |

^a Solvent used: C₆D₆. ^b Internal reference: C₆D₆ (¹H NMR: δ 7.16 ppm; ¹³C NMR: δ 128.38 ppm). ^c External reference: Tetramethylsilane (δ 0.0 ppm).

Table 4.3.2. NMR Data^a for **216b**.

| Regioisomer | $\delta(^1\text{H})^b$ | $\delta(^{13}\text{C}\{^1\text{H}\})^b$ | $\delta(^{29}\text{Si DEPT})^c$ |
|---|--|--|--|
| $\beta(\text{E})_{\text{Chr}}-\beta(\text{E})_{\text{Cht}}$ | 0.532 (s, 12H, $\text{ChtSi}(\text{CH}_3)_2$ -), 4.960 (s, 10H, <i>Cp</i>), 6.80, 7.12 (d, 4H, $-\text{C}_2\text{H}_2$ -, $^3J_{\text{H-H}} = 19\text{Hz}$) | -0.65 ($\text{ChtSi}(\text{CH}_3)_2$ -), 87.41, 89.47, 91.86 (<i>ChtSi</i> (CH_3) ₂ -), 94.98 (<i>ipso C</i> , <i>ChtSi</i> (CH_3) ₂ -), 97.65 (<i>Cp</i>) | -4.15 ($\text{ChtSi}(\text{CH}_3)_2$ -) |
| $\alpha_{\text{Chr}}-\alpha_{\text{Cht}}$ | 0.480 (s, 12H, $\text{ChtSi}(\text{CH}_3)_2$ -), 4.884 (s, 10H, <i>Cp</i>), 5.71, 5.95 (d, 4H, $-\text{C}_2\text{H}_2$ -, $^2J_{\text{H-H}} = 3\text{Hz}$) | -0.34 ($\text{CpSi}(\text{CH}_3)_2$ -), 87.22, 89.36, 92.22 (<i>ChtSi</i> (CH_3) ₂ -), 94.93 (<i>ipso C</i> , <i>ChtSi</i> (CH_3) ₂ -), 97.74 (<i>Cp</i>) | -2.35 ($\text{ChtSi}(\text{CH}_3)_2$ -) |
| $\beta(\text{E})_{\text{Chr}}-\alpha_{\text{Cht}} / \alpha_{\text{Chr}}-\beta(\text{E})_{\text{Cht}}$ | 0.483, 0.527 (s, 12H, $\text{ChtSi}(\text{CH}_3)_2$ -), 4.882, 4.962 (s, 10H, <i>Cp</i>), 5.73, 5.96 (d, 2H, $-\text{C}_2\text{H}_2$ -, $^2J_{\text{H-H}} = 3\text{Hz}$), 6.65, 7.11 (d, 2H, $-\text{C}_2\text{H}_2$ -, $^3J_{\text{H-H}} = 19\text{Hz}$) | -0.67, -0.61 ($\text{ChtSi}(\text{CH}_3)_2$ -), 87.33, 87.35, 89.44, 91.94, 92.15 (<i>ChtSi</i> (CH_3) ₂ -), 94.75, 95.28 (<i>ipso C</i> , <i>ChtSi</i> (CH_3) ₂ -), 97.66, 97.76 (<i>Cp</i>) | -4.19, -2.52 ($\text{C}_7\text{H}_6\text{Si}(\text{CH}_3)_2$ -) |
| misc | 5.42-5.78 (m, 3x12H, <i>Cht</i> -), 7.01-7.61 (m, 3x4H, $-\text{Ph}$ -). | 125.79, 126.06, 126.09, 126.14, 126.92, 127.81, 128.63, 128.94, 129.09, 129.47, 129.51, 129.63, 129.86 ($-\text{Ph}$ -), 138.99, 139.47, 145.48, 145.56, 145.69, 146.04, 153.63, 153.66 ($-\text{C}_2\text{H}_2$ -) | |

^a Solvent used: C_6D_6 . ^b Internal reference: C_6D_6 (^1H NMR: δ 7.16 ppm; ^{13}C NMR: δ 128.38 ppm). ^c External reference: Tetramethylsilane (δ 0.0 ppm).

Table 4.3.3. NMR Data^a for **216c**.^{*}

| Regioisomer | δ (¹ H) ^b | δ (¹³ C{ ¹ H}) ^b | δ (²⁹ Si DEPT) ^c |
|--|---|--|--|
| β(E)_{Chl}-β(E)_{Chl} | 0.454 (s, 12H, β (E)- β (E), ChtSi(CH ₃) ₂ -), 4.96 (s, 10H, β (E)- β (E), Cp), 6.63, 7.10 (d, 4H, β (E)- β (E), -C ₂ H ₂ -, ³ J _{H-H} = 19Hz), 6.58 (s, 2H, β (E)- β (E), -Th-) | -0.82 (β (E)- β (E), ChtSi(CH ₃) ₂ -), 87.41, 89.48, 91.82 (β (E)- β (E), ChtSi(CH ₃) ₂ -), 94.59 (β (E)- β (E), ipso C, ChtSi(CH ₃) ₂ -), 97.69 (β (E)- β (E), Cp) | -4.34 (β (E)- β (E), ChtSi(CH ₃) ₂ -) |
| α_{Chl}-α_{Chl} | 0.52 (s, 12H, α - α , ChtSi(CH ₃) ₂ -), 4.896 (s, 10H, α - α , Cp), 5.52, 6.25 (d, 4H, α - α , -C ₂ H ₂ -, ² J _{H-H} = 3Hz), 6.83 (s, 2H, α - α , -Th-) | -0.11 (α - α , ChtSi(CH ₃) ₂ -), 87.30, 89.31, 92.27 (α - α , ChtSi(CH ₃) ₂ -), 94.47 (α - α , ipso C, ChtSi(CH ₃) ₂ -), 97.84 (α - α , Cp) | -1.60 (α - α , ChtSi(CH ₃) ₂ -) |
| β(E)_{Chl}-α_{Chl} / α_{Chl}-β(E)_{Chl} | 0.452, 0.53 (s, 12H, β (E)- α , ChtSi(CH ₃) ₂ -), 4.904, 4.97 (s, 10H, β (E)- α , Cp), 5.52, 6.24 (d, 2H, β (E)- α , -C ₂ H ₂ -, ² J _{H-H} = 3Hz), 6.59, 7.09 (d, 2H, β (E)- α , -C ₂ H ₂ -, ³ J _{H-H} = 19Hz), 6.57, 6.88 (d, 2H, β (E)- α , -Th-) | -0.75, -0.23 (β (E)- α , ChtSi(CH ₃) ₂ -), 87.37, 87.38, 89.36, 89.45, 91.87, 92.22 (β (E)- α , ChtSi(CH ₃) ₂ -), 94.19, 94.92 (β (E)- α , ipso C, ChtSi(CH ₃) ₂ -), 97.68, 97.86 (β (E)- α , Cp) | -4.38, -1.60 (β (E)- α , ChtSi(CH ₃) ₂ -) |
| misc | 5.40-5.56, 5.67-5.73 (m, 3x12H, Chl-) | 127.02, 127.05, 127.69, 127.70, 127.94, 128.79, 129.73 (-Th-), 138.21, 138.38, 144.16, 144.77, 144.92, 145.40, 146.18, 147.65 (-C ₂ H ₂ -) | |

^a Solvent used: C₆D₆. ^b Internal reference: C₆D₆ (¹H NMR: δ 7.16 ppm; ¹³C NMR: δ 128.38 ppm). ^c External reference: Tetramethylsilane (δ 0.0 ppm).^{*} Th = Thiophene.

Table 4.3.4. NMR Data^a for **217a**.

| Regioisomer | δ (¹ H) ^b | δ (¹³ C{ ¹ H}) ^b | δ (²⁹ Si DEPT) ^c |
|--|---|--|---|
| β(E)_{Cp}-β(E)_{Cp} | 0.35 (s, 12H, CpSi(CH ₃) ₂ -), 5.47 (s, 14H, <i>Ch</i> t), 6.60, 6.93 (d, 4H, -C ₂ H ₂ -, ³ J _{H-H} = 19Hz) | -1.23 (CpSi(CH ₃) ₂ -), 86.86 (<i>Ch</i> t), 100.69, 103.48 (CpSi(CH ₃) ₂ -), 108.41 (<i>ipso</i> C, CpSi(CH ₃) ₂ -) | -14.53 (CpSi(CH ₃) ₂ -) |
| α_{Cp}-α_{Cp} | 0.370 (s, 12H, CpSi(CH ₃) ₂ -), 5.40 (s, 14H, <i>Ch</i> t), 5.47, 5.84 (d, 4H, -C ₂ H ₂ -, ² J _{H-H} = 3Hz) | -0.92 (CpSi(CH ₃) ₂ -), 86.86 (<i>Ch</i> t), 100.60, 103.90 (CpSi(CH ₃) ₂ -), 108.18 (<i>ipso</i> C, CpSi(CH ₃) ₂ -) | -12.86 (CpSi(CH ₃) ₂ -) |
| β(E)_{Cp}-α_{Cp} / α_{Cp}-β(E)_{Cp} | 0.334, 0.373 (s, 12H, CpSi(CH ₃) ₂ -), 5.41, 5.47 (s, 14H, <i>Ch</i> t), 5.48, 5.81 (d, 2H, -C ₂ H ₂ -, ² J _{H-H} = 3Hz), 6.57, 6.95 (d, 2H, -C ₂ H ₂ -, ³ J _{H-H} = 19Hz) | -1.16, -1.09 (CpSi(CH ₃) ₂ -), 86.84, 86.91 (<i>Ch</i> t), 100.65, 103.48, 103.89 (CpSi(CH ₃) ₂ -), 107.94, 108.60 (<i>ipso</i> C, CpSi(CH ₃) ₂ -) | -14.59, -12.90 (CpSi(CH ₃) ₂ -) |
| misc | 5.04-5.20 (m, 3x8H, Cp-), 7.12-7.35 (m, 3x4H, - <i>Ph</i> -) | 127.13, 127.53, 127.60, 127.85, 128.01, 128.74, 128.80 (- <i>Ph</i> -), 137.33, 138.91, 143.58, 144.84, 145.08, 145.39, 153.01, 153.21 (-C ₂ H ₂ -) | |

^a Solvent used: C₆D₆. ^b Internal reference: C₆D₆ (¹H NMR: δ 7.16 ppm; ¹³C NMR: δ 128.38 ppm). ^c External reference: Tetramethylsilane (δ 0.0 ppm).

Table 4.3.5. NMR Data^a for **217b**.

| Regioisomer | δ (¹ H) ^b | δ (¹³ C{ ¹ H}) ^b | δ (²⁹ Si DEPT) ^c |
|--|---|--|---|
| β(E)_{Cp}-β(E)_{Cp} | 0.34 (s, 12H, CpSi(CH ₃) ₂ -), 5.46 (s, 14H, <i>Ch</i> t), 6.63, 6.95 (d, 4H, -C ₂ H ₂ -, ³ J _{H-H} = 19Hz) | -1.22 (CpSi(CH ₃) ₂ -), 86.85 (<i>Ch</i> t), 100.70, 103.48 (CpSi(CH ₃) ₂ -), 108.38 (<i>ipso</i> C, CpSi(CH ₃) ₂ -) | -14.63 (CpSi(CH ₃) ₂ -) |
| α_{Cp}-α_{Cp} | 0.38 (s, 12H, CpSi(CH ₃) ₂ -), 5.41 (s, 14H, <i>Ch</i> t), 5.49, 5.84 (d, 4H, -C ₂ H ₂ -, ² J _{H-H} = 3Hz) | -0.99 (CpSi(CH ₃) ₂ -), 86.91 (<i>Ch</i> t), 100.60, 103.89 (CpSi(CH ₃) ₂ -), 108.09 (<i>ipso</i> C, CpSi(CH ₃) ₂ -) | -12.98 (CpSi(CH ₃) ₂ -) |
| β(E)_{Cp}-α_{Cp} / α_{Cp}-β(E)_{Cp} | 0.33, 0.36 (s, 12H, CpSi(CH ₃) ₂ -), 5.40, 5.47 (s, 14H, <i>Ch</i> t), 5.49, 5.79 (d, 2H, -C ₂ H ₂ -, ² J _{H-H} = 3Hz), 6.61, 6.98 (d, 2H, -C ₂ H ₂ -, ³ J _{H-H} = 19Hz) | -1.30, -1.16 (CpSi(CH ₃) ₂ -), 86.85, 86.91 (<i>Ch</i> t), 100.64, 100.66, 103.47, 103.92 (CpSi(CH ₃) ₂ -), 107.99, 108.54 (<i>ipso</i> C, CpSi(CH ₃) ₂ -) | -14.69, -13.06 (CpSi(CH ₃) ₂ -) |
| misc | 5.04-5.19 (m, 3x8H, Cp-), 7.03-7.60 (m, 3x4H, -Ph-). | 125.57, 125.86, 125.90, 125.95, 126.96, 127.67, 128.45, 128.75, 128.89, 128.91, 129.02, 129.09, 129.57 (-Ph-), 138.88, 139.41, 145.13, 145.20, 145.33, 145.45, 145.88, 153.62, 153.70 (-C ₂ H ₂ -) | |

^a Solvent used: C₆D₆. ^b Internal reference: C₆D₆ (¹H NMR: δ 7.16 ppm; ¹³C NMR: δ 128.38 ppm). ^c External reference: Tetramethylsilane (δ 0.0 ppm).

Table 4.3.6. NMR Data^a for **217c**.^{*}

| Regioisomer | δ (¹ H) ^b | δ (¹³ C{ ¹ H}) ^b | δ (²⁹ Si DEPT) ^c |
|--|--|---|---|
| β(E)_{Cp}-β(E)_{Cp} | 0.26 (s, 12H, β (E)- β (E), CpSi(CH ₃) ₂ -), 5.465 (s, 14H, β (E)- β (E), <i>Ch</i> t), 6.51, 6.93 (d, 4H, β (E)- β (E), -C ₂ H ₂ -, ³ J _{H-H} = 19Hz), 6.61 (s, 2H, β (E)- β (E), - <i>Th</i> -) | -1.29 (β (E)- β (E), CpSi(CH ₃) ₂ -), 86.89 (β (E)- β (E), <i>Ch</i> t), 100.68, 103.40 (β (E)- β (E), CpSi(CH ₃) ₂ -), 108.03 (β (E)- β (E), <i>ipso</i> C, CpSi(CH ₃) ₂ -) | -14.78 (β (E)- β (E), CpSi(CH ₃) ₂ -) |
| α_{Cp}-α_{Cp} | 0.41 (s, 12H, α - α , CpSi(CH ₃) ₂ -), 5.413 (s, 14H, α - α , <i>Ch</i> t), 5.26, 6.09 (d, 4H, α - α , -C ₂ H ₂ -, ² J _{H-H} = 3Hz), 6.80 (s, 2H, α - α , - <i>Th</i> -) | -0.84 (α - α , CpSi(CH ₃) ₂ -), 87.00 (α - α , <i>Ch</i> t), 100.70, 104.01 (α - α , CpSi(CH ₃) ₂ -), 107.49 (α - α , <i>ipso</i> C, CpSi(CH ₃) ₂ -) | -12.10 (α - α , CpSi(CH ₃) ₂ -) |
| β(E)_{Cp}-α_{Cp} / α_{Cp}-β(E)_{Cp} | 0.27, 0.40 (s, 12H, β (E)- α , CpSi(CH ₃) ₂ -), 5.408, 5.469 (s, 14H, β (E)- α , <i>Ch</i> t), 5.27, 6.08 (d, 2H, β (E)- α , -C ₂ H ₂ -, ² J _{H-H} = 3Hz), 6.46, 6.95 (d, 2H, β (E)- α , -C ₂ H ₂ -, ³ J _{H-H} = 19Hz), 6.68, 6.76 (d, 2H, β (E)- α , - <i>Th</i> -) | -1.25, -0.94 (β (E)- α , CpSi(CH ₃) ₂ -), 86.87, 87.00 (β (E)- α , <i>Ch</i> t), 100.66, 100.74, 103.44, 103.98 (β (E)- α , CpSi(CH ₃) ₂ -), 107.24, 108.26 (β (E)- α , <i>ipso</i> C, CpSi(CH ₃) ₂ -) | -14.87, -12.04 (β (E)- α , CpSi(CH ₃) ₂ -) |
| misc | 5.08-5.17 (m, 3x8H, <i>Cp</i> -) | 126.11, 126.24, 127.33, 127.42, 127.66, 127.89, 128.33, 129.18 (- <i>Th</i> -), 137.83, 137.96, 144.24, 144.63, 144.79, 145.39, 146.16, 147.58 (-C ₂ H ₂ -) | |

^a Solvent used: C₆D₆. ^b Internal reference: C₆D₆ (¹H NMR: δ 7.16 ppm; ¹³C NMR: δ 128.38 ppm). ^c External reference: Tetramethylsilane (δ 0.0 ppm).^{*} Th = Thiophene.

Table 4.3.7. NMR Data^a for **218**.^{*}

| Regioisomer | δ (¹ H) ^b | δ (¹³ C{ ¹ H}) ^b | δ (²⁹ Si DEPT) ^c |
|--|---|--|---|
| β(E)-β(E) | 0.35 (s, 12H, β (E)- β (E), CpSi(CH ₃) ₂ -), 4.04 (s, 10H, β (E)- β (E), Cp), 6.58, 7.05 (d, 4H, β (E)- β (E), -C ₂ H ₂ -, ³ J _{H-H} = 19Hz), 6.60 (s, 2H, β (E)- β (E), -Th-) | -1.19 (β (E)- β (E), CpSi(CH ₃) ₂ -), 68.98 (β (E)- β (E), Cp), 70.11 (β (E)- β (E), <i>ipso</i> C, CpSi(CH ₃) ₂ -), 71.78, 73.92 (β (E)- β (E), CpSi(CH ₃) ₂ -) | -9.59 (β (E)- β (E), CpSi(CH ₃) ₂ -) |
| α-α | 0.49 (s, 12H, α - α , CpSi(CH ₃) ₂ -), 3.99 (s, 10H, α - α , Cp), 5.469, 6.16 (d, 4H, α - α , -C ₂ H ₂ -, ² J _{H-H} = 3Hz), 6.96 (s, 2H, α - α , -Th-) | -0.75 (α - α , CpSi(CH ₃) ₂ -), 69.09 (α - α , Cp), 69.99 (α - α , <i>ipso</i> C, CpSi(CH ₃) ₂ -), 71.83, 74.33 (α - α , CpSi(CH ₃) ₂ -) | -6.44 (α - α , CpSi(CH ₃) ₂ -) |
| β(E)-α | 0.36, 0.48 (s, 12H, β (E)- α , CpSi(CH ₃) ₂ -), 3.98, 4.05 (s, 10H, β (E)- α , Cp), 5.465, 6.14 (d, 2H, β (E)- α , -C ₂ H ₂ -, ² J _{H-H} = 3Hz), 6.56, 7.08 (d, 2H, β (E)- α , -C ₂ H ₂ -, ³ J _{H-H} = 19Hz), 6.69, 6.91 (d, 2H, β (E)- α , -Th-) | -1.14, -0.84 (β (E)- α , CpSi(CH ₃) ₂ -), 68.98, 69.09 (β (E)- α , Cp), 69.76, 70.29 (β (E)- α , <i>ipso</i> C, CpSi(CH ₃) ₂ -), 71.75, 71.87, 73.94, 74.30 (β (E)- α , CpSi(CH ₃) ₂ -) | -9.69, -6.36 (β (E)- α , CpSi(CH ₃) ₂ -) |
| misc | 4.02-4.09, 4.16-4.22 (m, 3x8H, Cp-) | 126.30, 126.35, 127.02, 127.34, 127.47, 127.51, 128.91, 129.65 (-Th-), 137.84, 137.98, 144.31, 144.91, 145.04, 145.41, 146.31, 147.65 (-C ₂ H ₂ -) | |

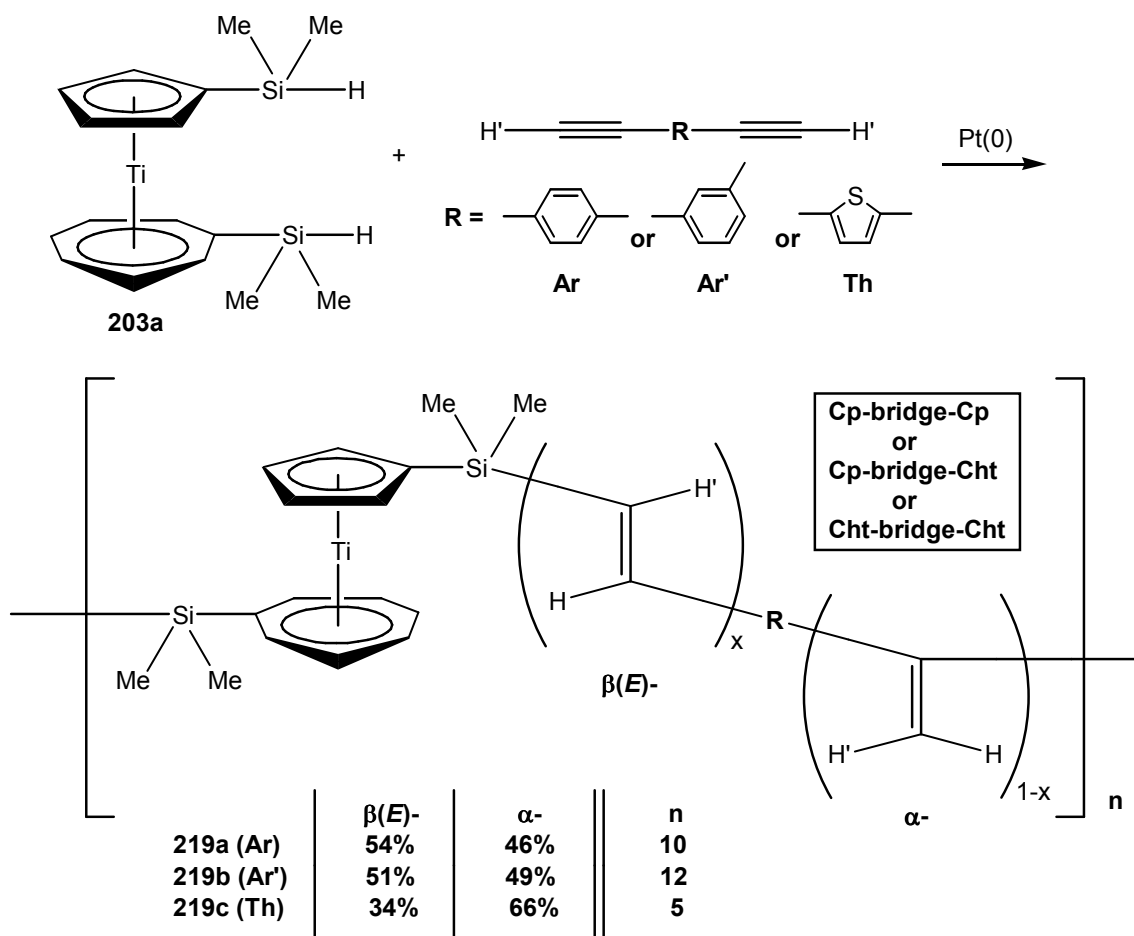
^a Solvent used: C₆D₆. ^b Internal reference: C₆D₆ (¹H NMR: δ 7.16 ppm; ¹³C NMR: δ 128.38 ppm). ^c External reference: Tetramethylsilane (δ 0.0 ppm).^{*} Th = Thiophene.

4.4. Synthesis and Characterization of poly{troticene-*bis*(silylenevinylene)(phenylene)}s using Karstedt's catalyst.

Two methods of polymerization have been used in the literature to synthesize polymers via hydrosilylation. The first method involves a monomeric species containing both a silane and an alkyne/ene moiety (**Scheme 1.2.4.1**).^{250,254,278,279} The second method involves a disilane (or similar molecule) along with a dialkyne/ene (**Scheme 1.2.4.2**).^{252,253,276,280-284} While the second method generally results in lower molecular weight species due to stoichiometric imbalances, the monomers are easier to synthesize compared to the silyl-alkynyl monomers used in the first method. It is for this reason that the second approach was employed for the hydrosilylation polymerizations presented in this section, using dialkynes with either $\{\eta^7\text{-(dimethylsilyl)cycloheptatrienyl}\}\{\eta^5\text{-(dimethylsilyl)cyclopentadienyl}\}$ titanium(II) (**203a**) or 1,1'-*bis*(dimethylsilyl)ferrocene as the disilane. Reaction progress was monitored by ^1H NMR, with any stoichiometric imbalances being remedied by addition of the necessary monomer. In general, the reactions proceeded to completion after 4 to 5 days at room temperature, while heating to 70 °C to 79 °C significantly sped up the reaction to completion in 18 to 24 hours.

Treatment of equimolar amounts of **203a** and 1,4-diethynylbenzene with Karstedt's catalyst in d_6 -benzene gave a viscous blue-green liquid (**Scheme 4.4.1**). The product, poly{troticene-*bis*(silylenevinylene)}-1,4-phenylene (**219a**), was isolated via precipitation into cold hexanes as a blue green solid (84 %). The precipitated product **219a** was insoluble in any of the various organic solvents utilized such as dichloromethane, tetrahydrofuran, benzene, and hexanes. However, samples taken

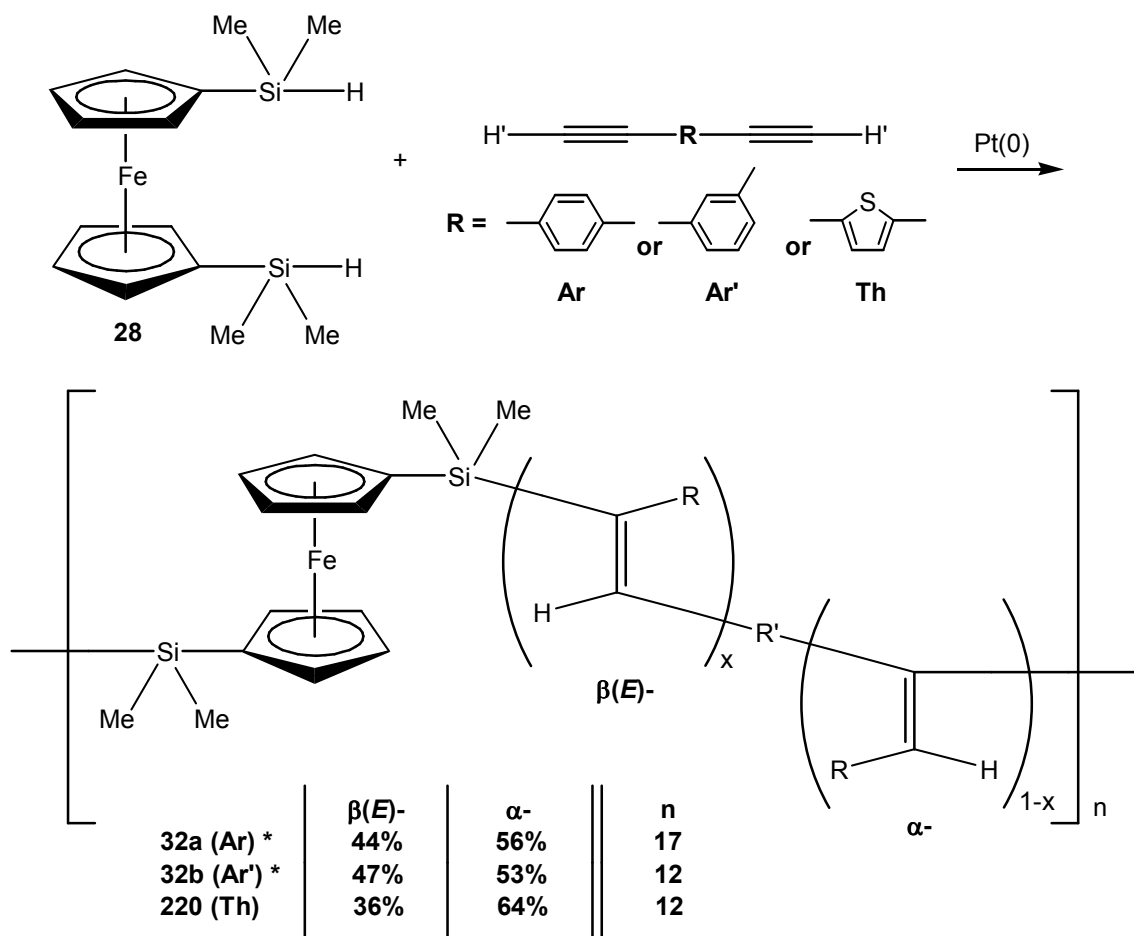
directly from the viscous crude product were soluble in THF, enabling analysis with MALDI-TOF/TOF.



Scheme 4.4.1. Polymers/Oligomers from **203a** and Dialkynes.

Another polymer/oligomer was prepared in a similar fashion using 1,3-diethynylbenzene as dialkyne (**Scheme 4.4.1**), giving poly{troticene-*bis*(silylenevinylene)}-1,3-phenylene (**219b**) as a blue green solid (83 %) after precipitation. The precipitated product was similarly insoluble in any of the organic solvents used for **219a**.

The same polymerization protocol was used for the reaction between either **203a** or 1,1'-bis(dimethylsilyl)ferrocene (**28**) and 2,5-bis(ethynyl)thiophene (**Scheme 4.4.2**). The former gave a blue green solid upon precipitation (poly{troticene-bis(silylenevinylene)}-2,5-thiophene (**219c**); 34 %), and the latter gave an orange solid upon precipitation (poly{ferrocene-bis(silylenevinylene)}-2,5-thienylene (**220**); 32 %). Both products were similarly insoluble in any of the various organic solvents utilized such as dichloromethane, tetrahydrofuran, benzene, and hexanes, requiring the use of the crude unprecipitated product for either MALDI-TOF/TOF or GPC analysis.



* Jain, R.; Lalancette, R. A.; Sheridan, J. B. *Organometallics* 2005, 24, 1458-1467.

Scheme 4.4.2. Polymers/Oligomers from **28** and Dialkynes.

Both polymers/oligomers **219a** and **219b** were characterized by ^1H , $^{13}\text{C}\{^1\text{H}\}$, and ^{29}Si DEPT NMR, as well as MALDI-TOF/TOF (**Table 4.4.1** and **Table 4.4.2**, respectively). Both contained randomly arranged $\beta(\text{E})$ - and α - regioisomeric structures, consistent with other polymers/oligomers prepared via Pt-catalyzed hydrosilylation polymerizations in the literature.^{227,250,253,254,285} Based on the integration of their ^1H NMR spectra, **219a** has an overall regiochemical distribution of 54 % $\beta(\text{E})$ - / 46 % α - (49 % / 51 % at reaction temperature of 70 °C to 79 °C), while **219b** has 51 % $\beta(\text{E})$ - / 49 % α -, both consistent with that of the Type 2 model compound **214a** (49 % $\beta(\text{E})$ - / 51 % α) (**Scheme 4.2.1**), but have higher $\beta(\text{E})$ - to α - ratios compared to that of the corresponding Type 1 (**Scheme 4.1.1** and **4.1.2**) and Type 3 model compounds (**Scheme 4.3.1** and **4.3.2**). Similar regiochemical distributions were reported by Jain and coworkers in reactions using 1,1'-*bis*(dimethylsilyl)ferrocene as the disilane (**32a** and **32b**; **Scheme 1.2.6.1**),^{4,5} implying that the identity of the disilane sandwich complex has little bearing on the resulting regiochemical distribution of the reaction.

The ^1H NMR spectrum of **219a** showed broad peaks around δ 5.78-5.90 and δ 5.94-6.08 for the α - olefinic protons, and δ 6.48-6.67, δ 6.87-7.04, and δ 6.67-6.87 for the $\beta(\text{E})$ - olefinic protons, concurring with the **Type 1**, **2**, and **3** model compounds (**Figure 4.2.4** and **Figure 4.4.1**). Peaks corresponding to the $-\text{SiH}(\text{CH}_3)_2$ (δ 0.10-0.20), $\text{CpSiH}(\text{CH}_3)_2$ (δ 4.48-4.56), $\text{ChtSiH}(\text{CH}_3)_2$ (δ 4.80-4.88), and $-\text{C}\equiv\text{CH}$ (δ 2.70-2.80) end groups were also observed, indicating an AB-type polymeric structure. While the presence of cyclic structures cannot be ruled out,^{280,281,286} the presence of both types of end groups, as well as the use of rigid dialkynes (which can conceivably impose

geometrical constraints) as opposed to dialkenes (which could impart flexibility after hydrosilylation) point towards a non-cyclic structure.²⁸⁷ The MALDI-TOF/TOF spectrum showed the repeat unit to be ≈ 447 mass units, corresponding to the sum of the monomeric masses, with the heaviest species detected corresponding to $n = 10$ ($m/z = 4469.0$) (**Figure 4.4.2**).

The ^1H NMR spectrum of **219b** shared similar features with that of **219a**, indicative of an AB-type polymeric structure. Broad olefinic peaks around δ 5.76-5.86 and δ 5.92-6.14 for the α -olefinic protons, and δ 6.55-6.70, δ 6.88-7.00, and δ 6.74-6.88 for the $\beta(\text{E})$ -olefinic protons concurred with the **Type 1**, **2**, and **3** model compounds (**Figure 4.2.4** and **Figure 4.4.3**). The MALDI-TOF/TOF spectrum showed the repeat unit to be ≈ 447 mass units, corresponding to the sum of the monomeric masses, with the heaviest species detected corresponding to $n = 12$ ($m/z = 5358.1$) which is slightly higher than that of **219a** (**Figure 4.4.4**).

Both polymers/oligomers **219c** and **220** were similarly characterized (**Table 4.4.3** and **Table 4.4.4**, respectively), both having randomly arranged $\beta(\text{E})$ - and α -regioisomeric structures, with the overall regiochemical distribution of **219c** (34 % $\beta(\text{E})$ - / 66 % α) and **220** (36 % $\beta(\text{E})$ - / 64 % α) favoring the α -adduct (**Scheme 4.4.1** and **Scheme 4.4.2**) just like their corresponding **Type 2** model compounds **214b** (16 % $\beta(\text{E})$ - / 84 % α) (**Scheme 4.2.1**) and **215** (23 % $\beta(\text{E})$ - / 77 % α) (**Scheme 4.2.2**). In contrast, their corresponding **Type 1** (**Scheme 4.1.1 + 4.1.2** and **Scheme 4.1.3**, respectively) and **Type 3** (**Scheme 4.3.1 + 4.3.2** and **Scheme 4.3.3**, respectively) model compounds have higher $\beta(\text{E})$ - to α -ratios.. This observation is consistent in all four polymers (and their

corresponding model compounds) presented in this section, and will be explored further in **Chapter 5**.

The ^1H NMR spectrum of **219c** showed broad peaks for the α - ($\text{Cp}\sim\text{C}_2\text{H}_2$: δ 5.23-5.28 and δ 6.04-6.19; $\text{Cht}\sim\text{C}_2\text{H}_2$: δ 5.61-5.56 and δ 6.19-6.36) and $\beta(\text{E})$ - olefinic protons ($\text{Cp}\sim\text{C}_2\text{H}_2$: δ 6.38-6.53 and δ 6.94-7.05; $\text{Cht}\sim\text{C}_2\text{H}_2$: δ 6.53-6.64 and δ 7.05-7.16), concurring with the Type 1, 2, and 3 model compounds. (**Figure 4.2.5** and **Figure 4.4.5**). As in the case of **219a** and **219b**, peaks corresponding to $\text{CpSiH}(\text{CH}_3)_2$ (δ 0.14-0.20), $\text{CpSiH}(\text{CH}_3)_2$ (δ 4.48-4.54), $\text{ChtSiH}(\text{CH}_3)_2$ (δ 4.80-4.86), and $-\text{C}\equiv\text{CH}$ (δ 2.87-2.94) end groups were observed, indicative of an AB-type polymeric structure. The MALDI-TOF/TOF spectrum showed the repeat unit to be ≈ 453 mass units, corresponding to the sum of the monomeric masses, with the heaviest species detected corresponding to $n = 5$ ($m/z = 2262.7$) which is lower than that of either **219a** ($n = 10$) or **219b** ($n = 12$) (**Figure 4.4.6**). This can be attributed to decomposition or polymerization of the 2,5-diethynylthiophene, with the thermal instability of 1-alkynes being well documented in the literature.^{288,289}

The ^1H NMR spectrum of **220** similarly showed broad peaks for the α - (δ 5.40-5.50 and δ 6.12-6.20) and $\beta(\text{E})$ - olefinic protons (δ 6.50-6.60 and δ 7.00-7.10) that concurred with the olefinic proton signals of the corresponding model compounds (**Figure 4.2.6** and **Figure 4.4.7**). Visible peaks for the dimethylsilyl ($\text{CpSiH}(\text{CH}_3)_2$: δ 0.14-0.26; $\text{CpSiH}(\text{CH}_3)_2$: δ 4.64-4.72) and ethynyl ($-\text{C}\equiv\text{CH}$: 2.88-2.94) end groups were indicative of an AB-type polymeric structure. The MALDI-TOF/TOF spectrum showed the repeat unit to be ≈ 435 mass units, corresponding to the sum of the monomeric masses, with the heaviest species detected corresponding to $n = 12$ ($m/z = 5214.3$) which,

while the same as that of **32b** ($n = 12$), is lower than that of **32a** ($n = 17$) (**Figure 4.4.8**).⁴ Just like **219c**, this can be attributed to decomposition or polymerization of the 2,5-diethynylthiophene, making it unavailable for hydrosilylation.^{288,289}

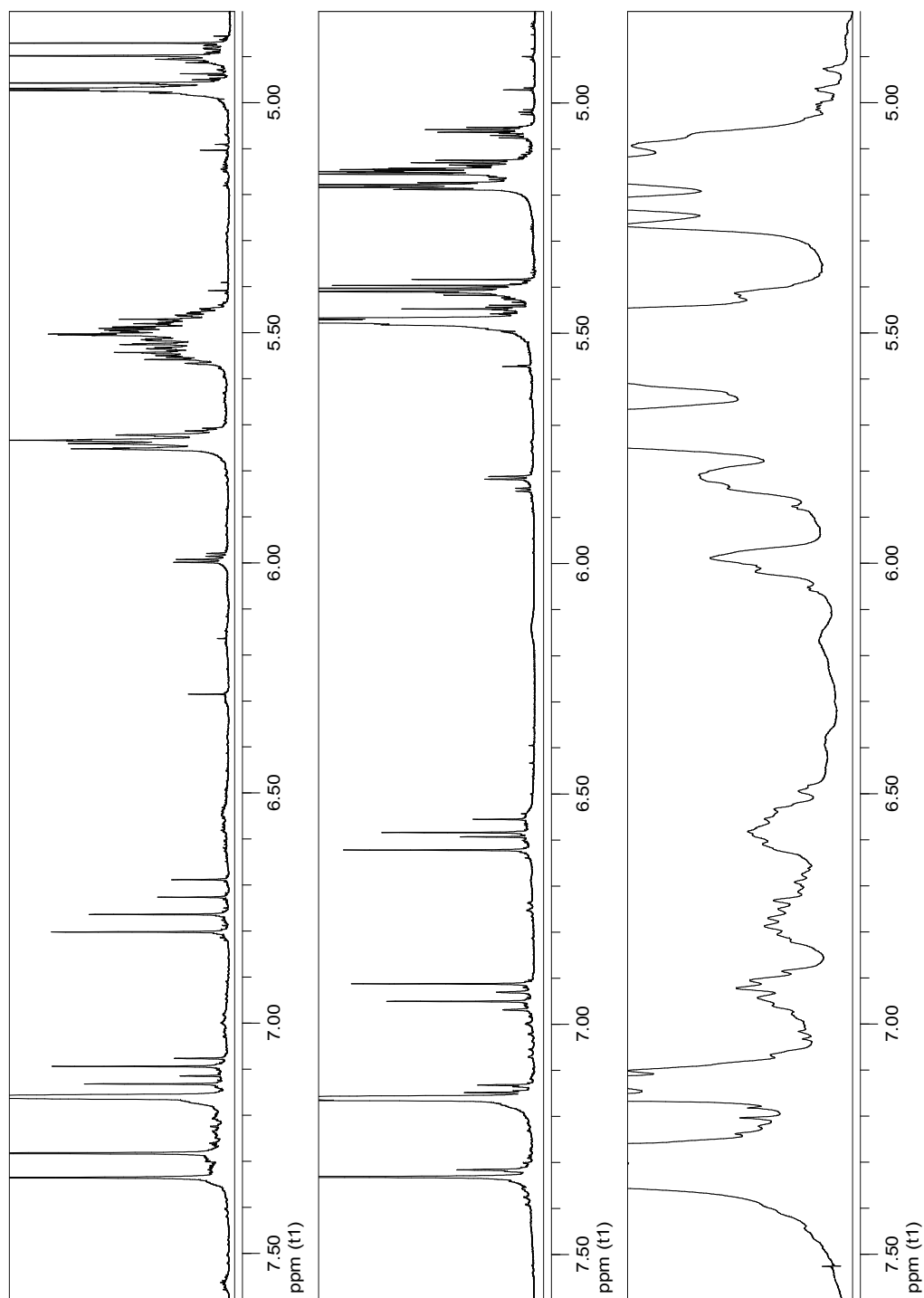


Figure 4.4.1. ^1H NMR Spectrum of **216a** (top), **217a** (mid), and **219a** (bot) Olefinic Protons.

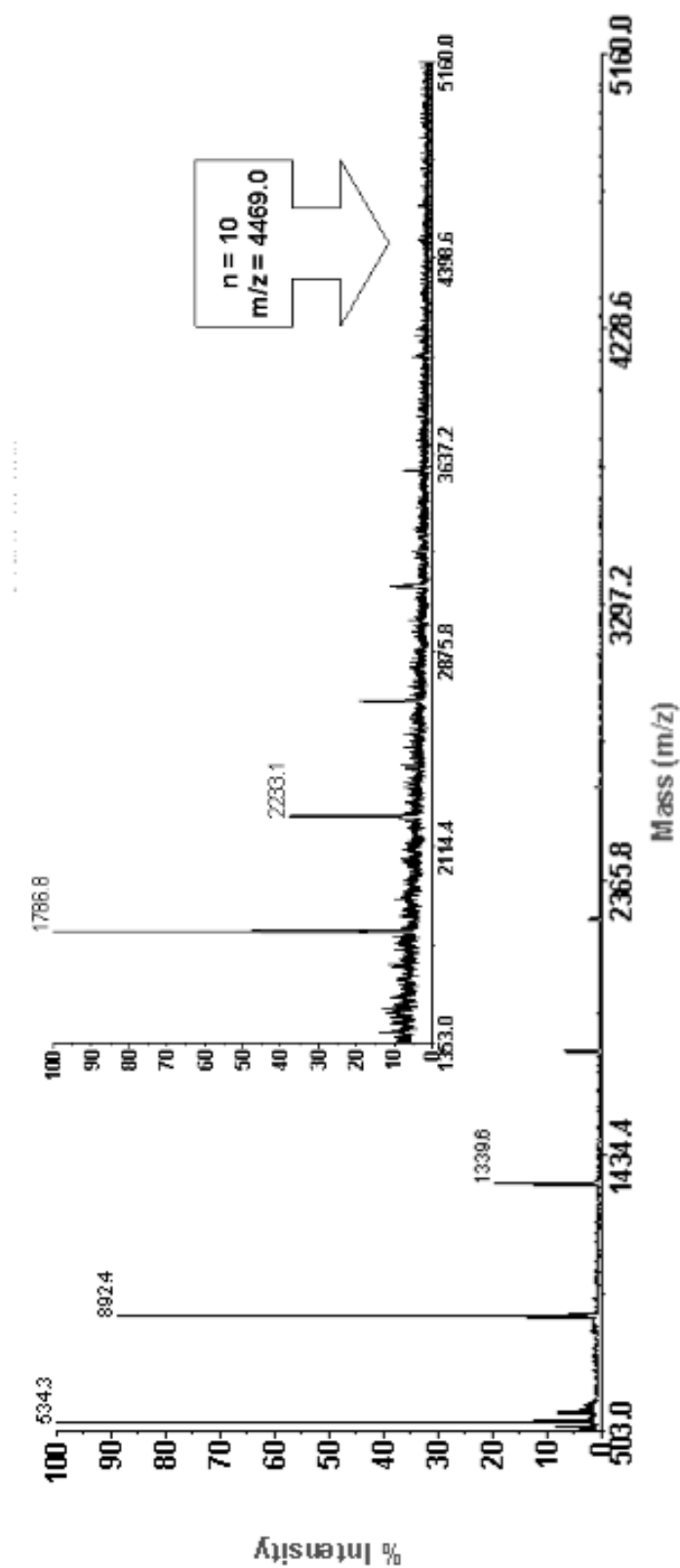


Figure 4.4.2. MALDI-TOF/TOF Spectrum of 219a.

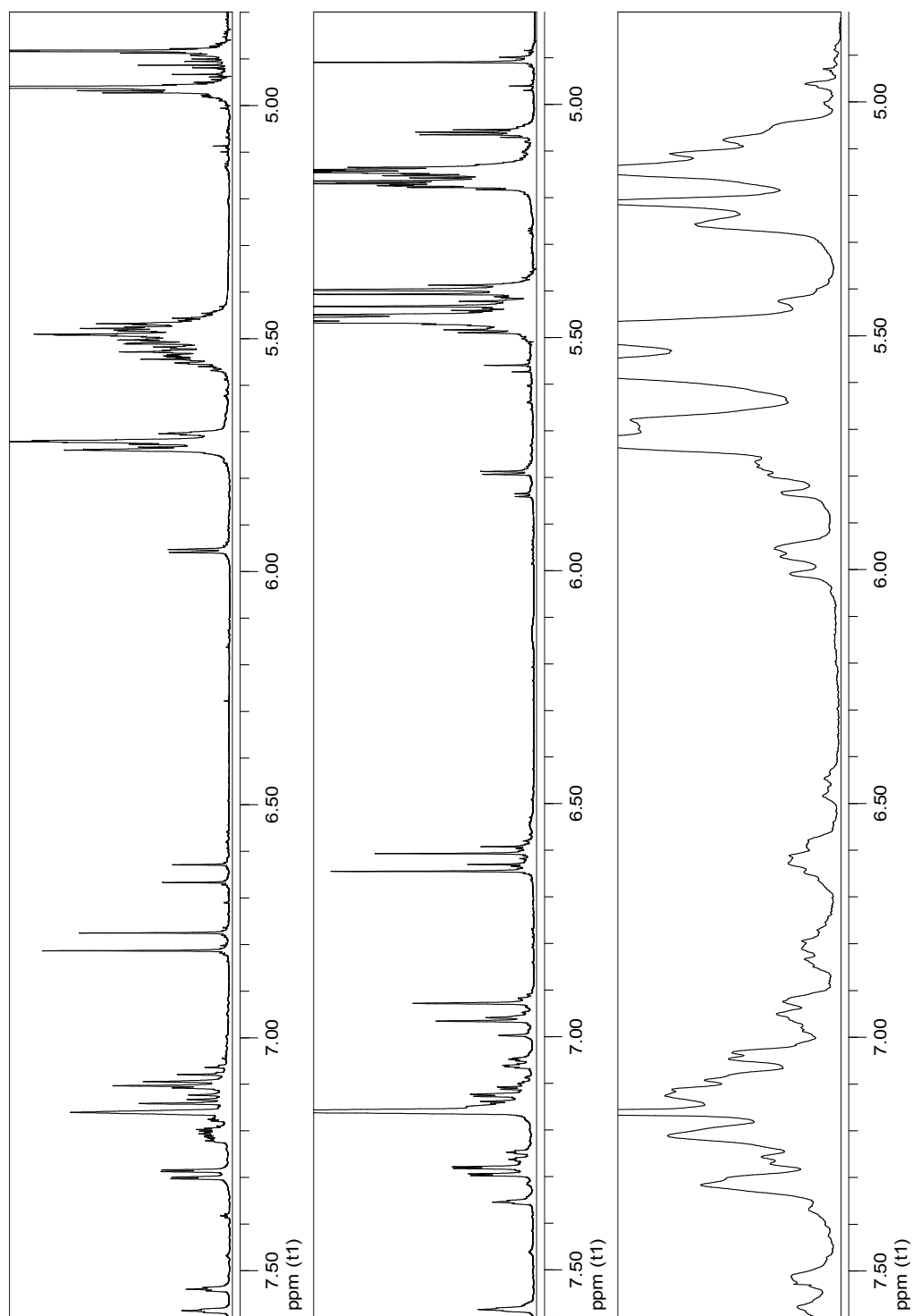


Figure 4.4.3. ^1H NMR Spectrum of **216b** (top), **217b** (mid), and **219b** (bot) Olefinic Protons.

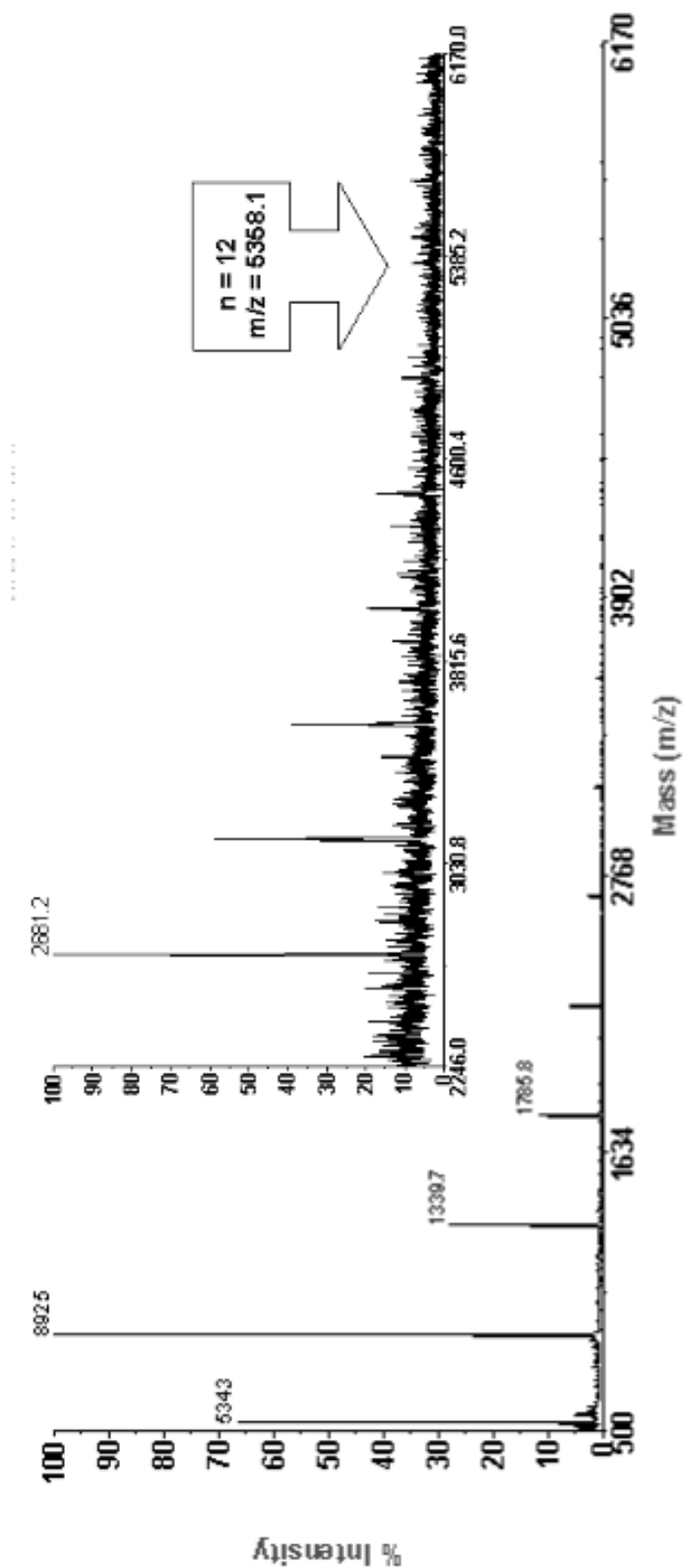


Figure 4.4.4. MALDI-TOF/TOF Spectrum of 219b.

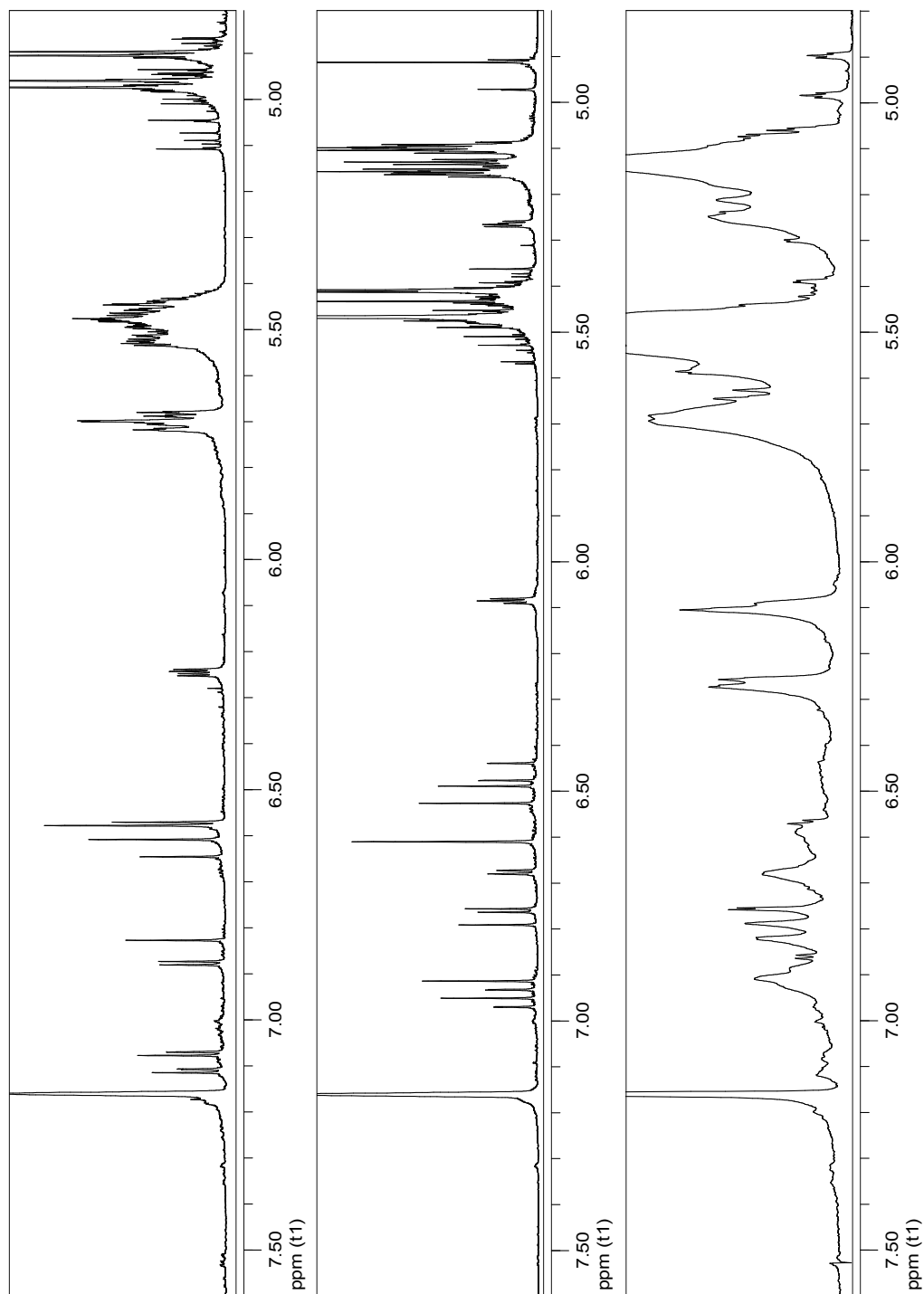


Figure 4.4.5. ^1H NMR Spectrum of **216c** (top), **217c** (mid), and **219c** (bot) Olefinic Protons.

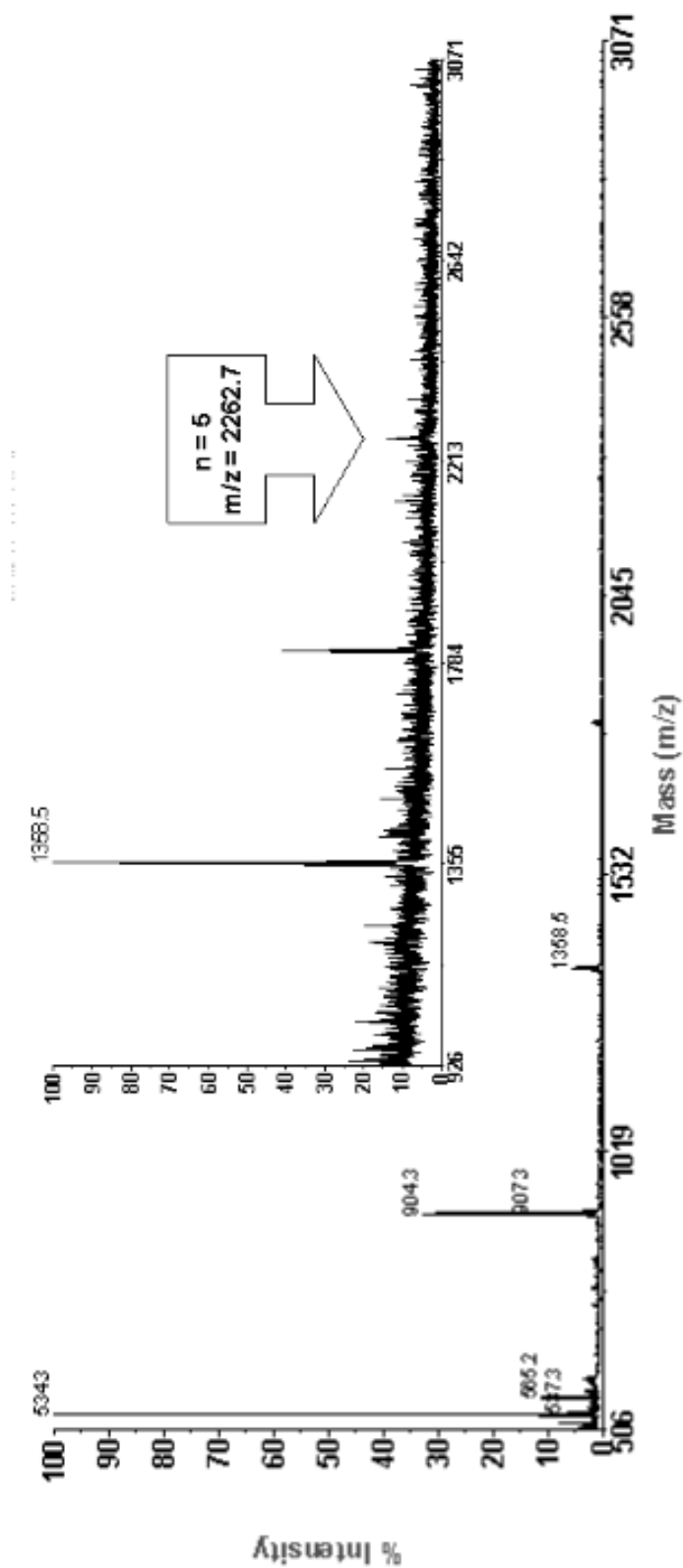


Figure 4.4.6. MALDI-TOF/TOF Spectrum of 219c.

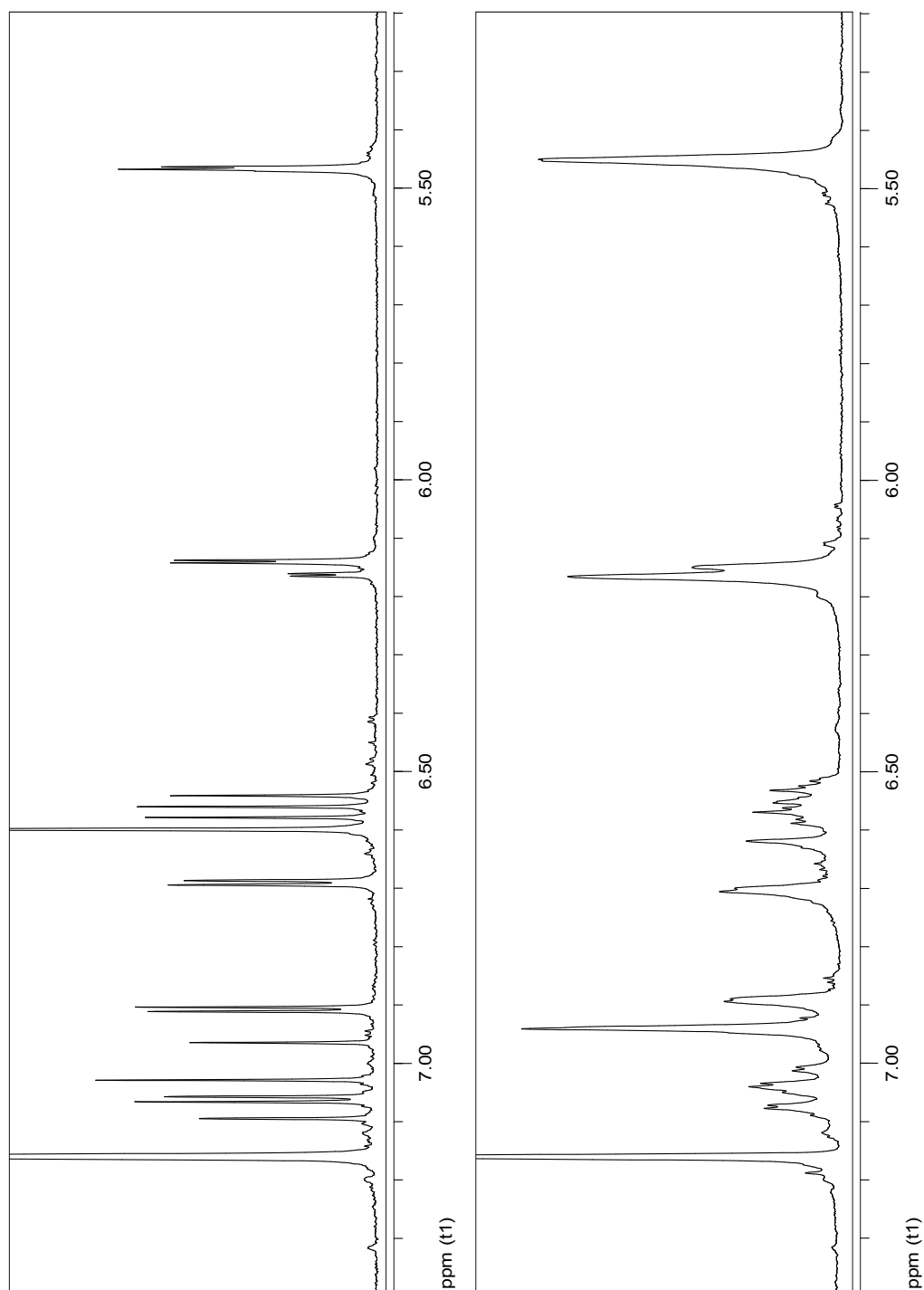


Figure 4.4.7. ^1H NMR Spectrum of **218** (top) and **220** (bot) Olefinic Protons.

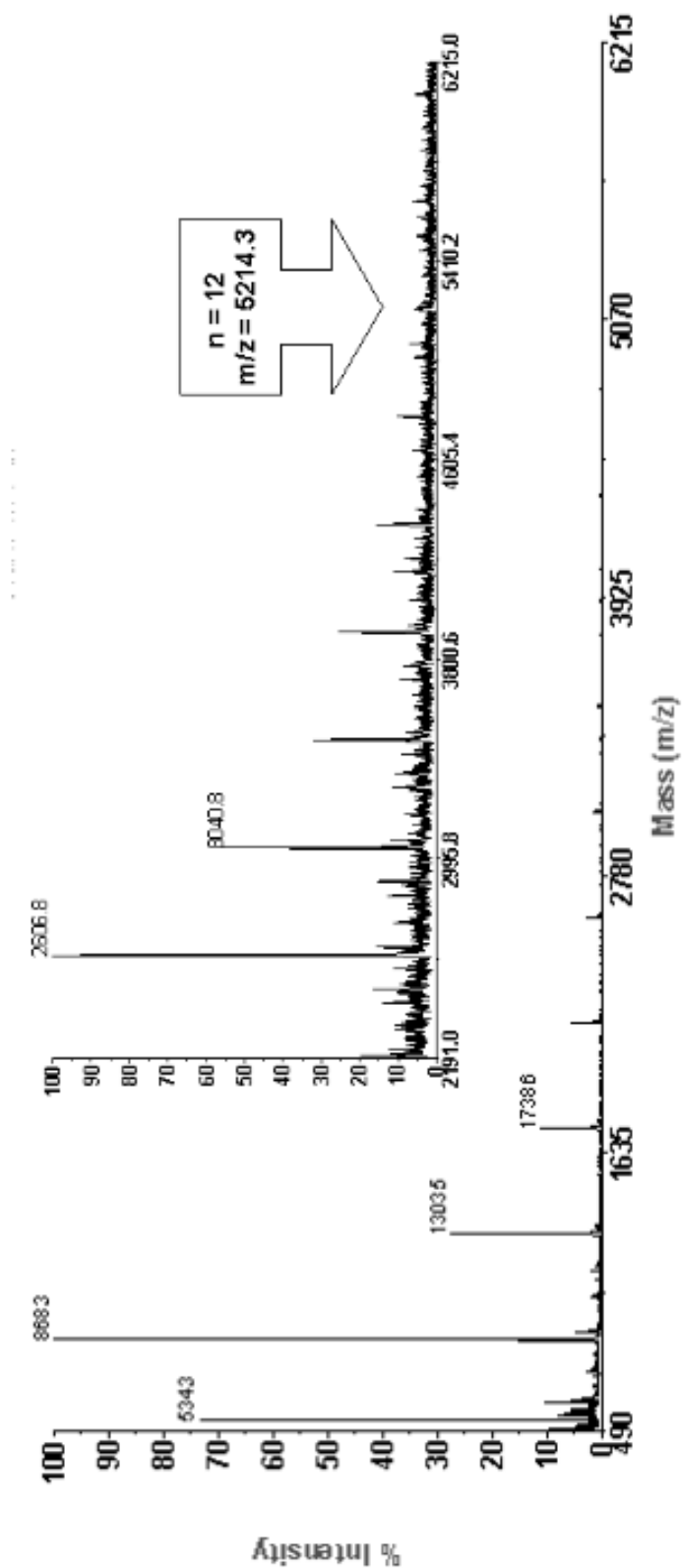


Figure 4.4.8. MALDI-TOF/TOF Spectrum of 220.

Table 4.4.1. NMR Data^a for Polymer/Oligomer **219a**.

| Product | δ (¹ H) ^b | δ (¹³ C{ ¹ H}) ^b | δ (²⁹ Si DEPT) ^c |
|-------------------|--|--|--|
| 219a | 0.24-0.45 (m, 6H, CpSi(CH ₃) ₂ -), 0.45-0.61 (m, 6H, ChtSi(CH ₃) ₂ -), 5.00-5.36 (m, 4H, CpSi(CH ₃) ₂ -), 5.36-5.78 (m, 6H, ChtSi(CH ₃) ₂ -), 5.40-5.50 (m, 2H, α , CpSi(CH ₃) ₂ -C ₂ H ₂ -), 5.66-5.76, 5.94-6.08 (m, 1H, α , C ₂ H ₂ -), 6.48-6.67, 6.87-7.04 (m, 2H, ChtSi(CH ₃) ₂ -C ₂ H ₂ -), 6.67-6.87, 7.04-7.18 β (E), CpSi(CH ₃) ₂ -C ₂ H ₂ -), 7.04-7.50 (m, 1H, β (E), ChtSi(CH ₃) ₂ -C ₂ H ₂ -), 7.04-7.50 (m, 4H, -Ph-) | -1.3- -0.8 (CpSi(CH ₃) ₂ -), -0.8- -0.1 (ChtSi(CH ₃) ₂ -), 87.3-88.1, 89.2-90.0, 91.5-92.4 (ChtSi(CH ₃) ₂ -), 94.4-95.4 (<i>ipso</i> C, ChtSi(CH ₃) ₂ -), 100.6-101.4, 103.4-104.6 (CpSi(CH ₃) ₂ -), 108.4-109.6 (<i>ipso</i> C, CpSi(CH ₃) ₂ -), 127.0-129.8 (-Ph-), 137.1-137.6, 138.7-139.2, 143.3-144.0, 144.8-145.8, 152.8-153.5 (-C ₂ H ₂ -) | -14.8- -14.3 (β (E), CpSi(CH ₃) ₂ -), -13.1- -12.7 (α , CpSi(CH ₃) ₂ -), -4.2- -3.8 (β (E), ChtSi(CH ₃) ₂ -), -2.5- -2.0 (α , ChtSi(CH ₃) ₂ -) |
| End groups | 0.10-0.20 (CpSiH(CH ₃) ₂), 2.70-2.80 (-C \equiv CH), 4.48-4.56 (CpSiH(CH ₃) ₂), 4.80-4.88 (ChtSiH(CH ₃) ₂) | | |

^a Solvent used: C₆D₆. ^b Internal reference: C₆D₆ (¹H NMR: δ 7.16 ppm; ¹³C NMR: δ 128.38 ppm). ^c External reference: Tetramethylsilane (δ 0.0 ppm).

Table 4.4.2. NMR Data^a for Polymer/Oligomer **219b**.

| Product | δ (¹ H) ^b | δ (¹³ C{ ¹ H}) ^b | δ (²⁹ Si DEPT) ^c |
|-------------------|---|---|--|
| 219b | 0.26-0.44 (m, 6H, CpSi(CH ₃) ₂ -), 0.44-0.62 (m, 6H, ChtSi(CH ₃) ₂ -), 5.00-5.35 (m, 4H, CpSi(CH ₃) ₂ -), 5.35-5.76 (m, 6H, ChtSi(CH ₃) ₂ -), 5.41-5.50, 5.75-5.87 (m, 2H, α , CpSi(CH ₃) ₂ -C ₂ H ₂ -), 5.69-5.83, 5.92-6.06 (m, 2H, α , ChtSi(CH ₃) ₂ -C ₂ H ₂ -), 6.42-6.68, 6.91-7.02 (m, 2H, β (E), CpSi(CH ₃) ₂ -C ₂ H ₂ -), 6.61-6.88, 7.02-7.19 (m, 2H, β (E), ChtSi(CH ₃) ₂ -C ₂ H ₂ -), 7.00-7.62 (m, 4H, -Ph-) | -1.4- -0.9 (CpSi(CH ₃) ₂ -), -0.9- -0.3 (ChtSi(CH ₃) ₂ -), 87.2-88.2, 89.0-90.0, 91.4-92.4 (ChtSi(CH ₃) ₂ -), 94.2-95.4 (<i>ipso</i> C, ChtSi(CH ₃) ₂ -), 100.6-101.4, 103.4-104.6 (CpSi(CH ₃) ₂ -), 108.2-109.6 (<i>ipso</i> C, CpSi(CH ₃) ₂ -), 125.4-130.0 (- <i>Ph</i> -), 138.6-139.6, 145.0-146.2, 153.2-154.0 (-C ₂ H ₂ -) | -14.8- -14.4 (β (E), CpSi(CH ₃) ₂ -), -13.1- -12.7 (α , CpSi(CH ₃) ₂ -), -4.1- -3.8 (β (E), ChtSi(CH ₃) ₂ -), -2.6- -2.2 (α , ChtSi(CH ₃) ₂ -) |
| End groups | 0.10-0.20 (CpSiH(CH ₃) ₂), 2.68-2.76 (-C \equiv CH), 4.48-4.56 (CpSiH(CH ₃) ₂), 4.80-4.88 (ChtSiH(CH ₃) ₂) | | |

^a Solvent used: C₆D₆. ^b Internal reference: C₆D₆ (¹H NMR: δ 7.16 ppm; ¹³C NMR: δ 128.38 ppm). ^c External reference: Tetramethylsilane (δ 0.0 ppm).

Table 4.4.3. NMR Data^a for Polymer/Oligomer **219c**.^{*}

| Product | δ (¹ H) ^b | δ (¹³ C{ ¹ H}) ^b | δ (²⁹ Si DEPT) ^c |
|-------------------|---|---|--|
| 219c | 0.30-0.46 (m, 6H, CpSi(CH ₃) ₂ -), 0.46-0.64 (m, 6H, ChtSi(CH ₃) ₂ -), 5.02-5.35 (m, 4H, CpSi(CH ₃) ₂ -), 5.35-5.80 (m, 6H, ChtSi(CH ₃) ₂ -), 5.20-5.42, 6.04-6.16 (m, 2H, α , CpSi(CH ₃) ₂ -C ₂ H ₂ -), 5.50-5.68, 6.22-6.32 (m, 2H, α , ChtSi(CH ₃) ₂ -C ₂ H ₂ -), 6.38-6.50, 6.88-7.00 (m, 2H, β (E), CpSi(CH ₃) ₂ -C ₂ H ₂ -), 6.48-6.66, 7.06-7.18 (m, 2H, β (E), ChtSi(CH ₃) ₂ -C ₂ H ₂ -), 6.64-6.94 (m, 4H, -Th-) | -1.0- -0.5 (CpSi(CH ₃) ₂ -), -0.4-0.1 (ChtSi(CH ₃) ₂ -), 87.5-88.2, 89.4-90.0, 91.6-92.4 (ChtSi(CH ₃) ₂ -), 93.9-94.6 (<i>ipso</i> C, ChtSi(CH ₃) ₂ -), 100.8-101.6, 103.4-105.0 (CpSi(CH ₃) ₂ -), 107.9-108.6 (<i>ipso</i> C, CpSi(CH ₃) ₂ -), 126.0-129.5 (-Th-), 137.8-138.7, 144.0-145.0, 145.7-146.8, 147.2-148.0 (-C ₂ H ₂ -) | -15.0- -14.5 (β (E), CpSi(CH ₃) ₂ -), -12.2- -11.8 (α , CpSi(CH ₃) ₂ -), -4.3- -4.0 (β (E), ChtSi(CH ₃) ₂ -), -1.7- -1.3 (α , ChtSi(CH ₃) ₂ -) |
| End groups | 0.14-0.20 (CpSiH(CH ₃) ₂), 2.87-2.94 (-C \equiv CH), 4.48-4.54 (CpSiH(CH ₃) ₂), 4.80-4.86 (ChtSiH(CH ₃) ₂) | | |

^a Solvent used: C₆D₆. ^b Internal reference: C₆D₆ (¹H NMR: δ 7.16 ppm; ¹³C NMR: δ 128.38 ppm). ^c External reference: Tetramethylsilane (δ 0.0 ppm).^{*} Th = Thiophene.

Table 4.4.4. NMR Data^a for Polymer/Oligomer **220**.^{*}

| Product | δ (¹ H) ^b | δ (¹³ C{ ¹ H}) ^b | δ (²⁹ Si DEPT) ^c |
|-------------------|--|--|---|
| 220 | 0.32-0.53 (m, 12H, C ₅ H ₄ Si(CH ₃) ₂ -), 4.00-4.35 (m, 8H, CpSi(CH ₃) ₂ -), 5.40-5.50, 6.12-6.20 (m, 4H, α , CpSi(CH ₃) ₂ -C ₂ H ₂ -), 6.50-6.60, 7.00-7.10 (m, 4H, β (E), CpSi(CH ₃) ₂ -C ₂ H ₂ -), 6.60-7.00 (m, 4H, -Th-) | -1.2- -0.5 (CpSi(CH ₃) ₂ -), 70.0-70.8 (<i>ipso</i> C, CpSi(CH ₃) ₂ -), 72.0-72.8, 73.8-74.8 (CpSi(CH ₃) ₂ -), 126.1-129.7 (-Th-), 137.7-138.2, 144.1-144.5, 144.5-145.0, 145.3-145.5, 146.1-146.4, 147.5-147.8 (-C ₂ H ₂ -) | δ -9.6- -9.0 (β (E), CpSi(CH ₃) ₂ -), -6.5- -6.1 (α , CpSi(CH ₃) ₂ -) |
| End groups | 0.14-0.26 (CpSiH(CH ₃) ₂), 2.88-2.94 (-C \equiv CH), 4.64-4.72 (CpSiH(CH ₃) ₂) | | |

^a Solvent used: C₆D₆. ^b Internal reference: C₆D₆ (¹H NMR: δ 7.16 ppm; ¹³C NMR: δ 128.38 ppm). ^c External reference: Tetramethylsilane (δ 0.0 ppm).

* Th = Thiophene.

4.5. Cyclic Voltammetry

The Type 3 model compounds presented in **Chapter 4.3** can be viewed as two troiticene units with a *bis*(silylenevinylene)phenylene/thienylene bridge. Examples of metallocenes (such as ferrocene) linked by a conjugated bridge have been previously reported and studied for their redox behavior.^{4,5,255,256,261,262,290-292}

Cyclic voltammetry was employed to probe for metal-metal interaction in the Type 3 model compounds. Results were inconclusive as to whether there is any metal-metal interaction in the Type 3 model compounds tested.

4.6. Summary

Dimethylsilyl troiticene derivatives were used in the preparation of troiticene-based polymers/oligomers containing silylenevinylene/phenylene/thienylene bridges between the metallocene units along with the corresponding model compounds. The ¹H NMR spectra of the polymers/oligomers concurred with those of the model compounds and have an AB-type polymeric structure containing randomly arranged β (E)- and α -regioisomeric structures. The results were consistent with regiochemical distributions obtained by Jain and coworkers using *bis*(dimethylsilyl)ferrocene.^{4,5} Low molecular weights were obtained due to astringent 1:1 stoichiometric requirement as well as the step-growth hydrosilylation polymerization protocol which is susceptible to chain termination reactions, most likely the loss of the Si-H functionality. Results from cyclic voltammetry were inconclusive as to whether there is any metal-metal interaction between the metallocene units.

Chapter 5. Comparison of the Hydrosilylation of Alkynes with Various Silanes

There are two notable observations made from the reactions presented in **Chapter 4**. One observation is the lower $\beta(\text{E})$ - to α - ratio of hydrosilylation reactions that utilized alkynes with the thienyl moiety, as opposed to a phenyl moiety. Similar observations were made by Lukevics and colleagues when they compared the $\beta(\text{E})$ - to α - ratio in the hydrosilylation of phenylacetylene and 2-ethynylthiophene, and was attributed to the more electron withdrawing nature of the thiophene moiety relative to the phenyl group.²⁷⁷

Another observation is the lower $\beta(\text{E})$ - to α - ratio of hydrosilylation reactions that utilized a *bis*(dimethylsilyl)-sandwich complex, as opposed to a mono(dimethylsilyl)-sandwich complex. This is consistent with results obtained by Jain and coworkers, and was attributed to the effect of the different silanes on silyl migration patterns without further elaboration.^{4,5} This section further explores the observed product distribution discrepancy between the hydrosilylation reactions involving a *bis*(dimethylsilyl)-sandwich complex and its mono dimethylsilyl-sandwich complex counterpart.

5.1. Effect of Alkyne Substituent on Hydrosilylation

In an effort to ascertain whether or not the observed discrepancies in the product distribution were due to an effect of the alkyne used, three sets of alkyne hydrosilylations were compared using four different silanes (dimethylsilylbenzene, dimethylsilylferrocene, 1,4-*bis*(dimethylsilyl)benzene, and 1,1'-

bis(dimethylsilyl)ferrocene), chosen to compare sandwich with non-sandwich dimethylsilyl complexes.

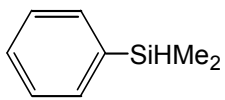
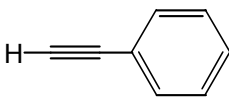
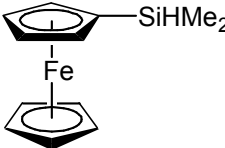
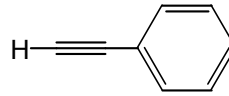
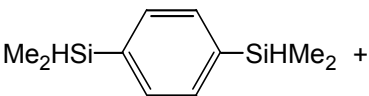
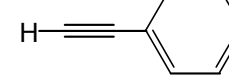
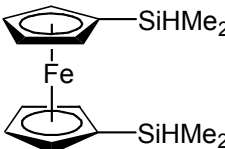
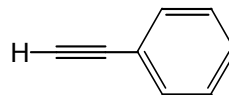
The first set of hydrosilylation reactions used phenylacetylene as the alkyne, with yields and regiochemical distributions (from ^1H NMR integrations) shown in **Table 5.1.1**. The products obtained were characterized by ^1H NMR (**Table 5.1.4**), with the spectra sharing common features with the **Type 1** (**221** and **222**) and **Type 2** (**223** and **224**) model compounds presented in **Chapter 4**. It can be seen that while the first three reactions have similar regiochemical distributions, the $\beta(\text{E})$ - to α - ratio of **224** is relatively low. Similar observations were made when comparing hydrosilylation reactions using either dimethylsilyltroticene or *bis*(dimethylsilyl)troticene (**Chapter 4.1** and **4.2**).

To confirm this, two other sets of reactions were done using two more alkynes. One set used 4-ethynyltoluene (**Table 5.1.2**), and another set used 2-ethynylthiophene (**Table 5.1.3**). Products from both sets of reactions were characterized by ^1H NMR (**Table 5.1.5** and **Table 5.1.6**, respectively) from which the $\beta(\text{E})$ - to α - ratios were estimated via integration of the spectra. Compared with the other two sets of reactions, those that used ethynylthiophene have a lower $\beta(\text{E})$ - to α - ratio, attributed to its more electron withdrawing nature, and is consistent with the observations and explanation made by Lukevics and colleagues.²⁷⁷ On the other hand, the reactions that used 4-ethynyltoluene have a higher $\beta(\text{E})$ - to α - ratio, which can be attributed to either its less electron withdrawing nature or a bulkier alkyne substituent.

One feature consistent in all three sets of reactions is the lower $\beta(\text{E})$ - to α - ratio observed in the reactions that used 1,1'-*bis*(dimethylsilyl)ferrocene compared with the other reactions in a particular set. With the hydrosilylation reactions using either

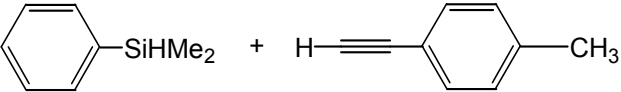
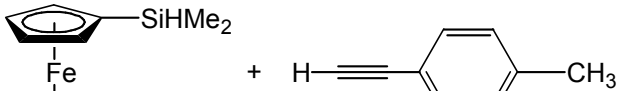
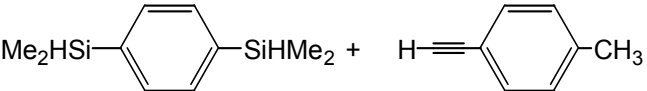
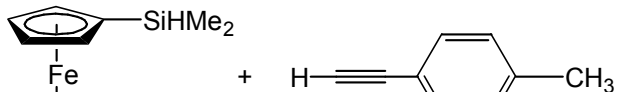
dimethylsilylbenzene, 1,4-*bis*(dimethylsilyl)benzene, or dimethylsilylferrocene giving similar $\beta(\text{E})$ - to α - ratios, it is apparent that the discrepancy with that of 1,1'-*bis*(dimethylsilyl)ferrocene is not due to an electronic effect of the ferrocene moiety on the silane. One possible source of this discrepancy is the fact that, unlike those of 1,4-*bis*(dimethylsilyl)benzene, the two dimethylsilyl groups on 1,1'-*bis*(dimethylsilyl)ferrocene are attached to ligands that can rotate about an axis, bringing the two dimethylsilyl groups into close proximity of each other which somehow affects the regioselectivity of the hydrosilylation reaction. This possibility is explored further in the next section.

Table 5.1.1. Hydrosilylation of Phenylacetylene Using Various Silanes.

| Reactants (Alkynes in Excess) | Regiochemical Distribution | | Yield |
|--|-------------------------------|------------|-------------------|
| | $\beta(E)$ - | α - | |
|  +  221^c | 77 % | 23 % | 71 % |
|  +  222 | 75 % | 25 % | 63 % |
|  +  223^d | 75 % | 25 % | 72 % ^a |
|  +  224^e | 53 % | 47 % | 66 % ^b |

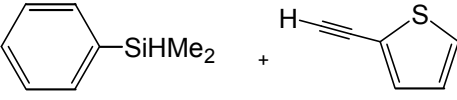
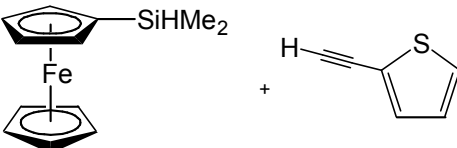
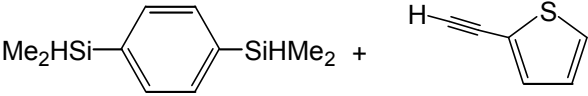
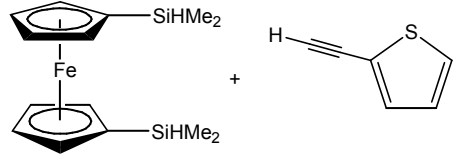
^a Product Distribution: $\beta(E)$ - $\beta(E)$: 56 %; $\beta(E)$ - α : 37 %; α - α : 7 %.^b Product Distribution: $\beta(E)$ - $\beta(E)$: 35 %; $\beta(E)$ - α : 35 %; α - α : 30 %.^c Previously reported with various catalysts. a) Iovel, I. G.; Goldberg, Y. S.; Shymanska, M. V.; Lukevics, E. *Organometallics* **1987**, 6, 1410-1413. b) Caseri, W.; Pregosin, P. S. *Organometallics* **1988**, 7, 1373-1380. c) Jimenez, R.; Lopez, J. M.; Cervantes, J. *Canadian Journal of Chemistry* **2000**, 78, 1491-1495.^d Previously reported with various catalysts. a) Mori, A.; Takahisa, E.; Kajiro, H.; Nishihara, Y.; Hiyama, T. *Macromolecules* **2000**, 33, 1115-1116. b) Mori, A.; Takahisa, E.; Yamamura, Y.; Kato, T.; Mudalige, A. P.; Kajiro, H.; Hirabayashi, K.; Nishihara, Y.; Hiyama, T. *Organometallics* **2004**, 23, 1755-1765.^e Previously reported with various catalysts. Jain, R.; Choi, H.; Lalancette, R. A.; Sheridan, J. B. *Organometallics* **2005**, 24, 1468-1476.

Table 5.1.2. Hydrosilylation of 4-Ethynyltoluene Using Various Silanes.

| Reactants (Alkynes in Excess) | Regiochemical Distribution | | Yield |
|---|-------------------------------|------------|-------------------|
| | $\beta(E)$ - | α - | |
|  225^c | 81 % | 19 % | 51 % |
|  226 | 79 % | 21 % | 54 % |
|  227 | 80 % | 20 % | 83 % ^a |
|  228 | 58 % | 42 % | 83 % ^b |

^a Product Distribution: $\beta(E)$ - $\beta(E)$: 65 %; $\beta(E)$ - α : 30 %; α - α : 5 %.^b Product Distribution: $\beta(E)$ - $\beta(E)$: 42 %; $\beta(E)$ - α : 31 %; α - α : 27 %.^c Previously reported with various catalysts. a) Katayama, H.; Taniguchi, K.; Kobayashi, M.; Sagawa, T.; Minami, T.; Ozawa, F. *Journal of Organometallic Chemistry* **2002**, 645, 192-200. b) Nagao, M.; Asano, K.; Umeda, K.; Katayama, H.; Ozawa, F. *Journal of Organic Chemistry* **2005**, 70, 10511-10514.

Table 5.1.3. Hydrosilylation of 2-Ethynylthiophene Using Various Silanes.

| Reactants (Alkynes in Excess) | Regiochemical Distribution | | Yield |
|---|-------------------------------|------------|-------------------|
| | $\beta(\text{E})$ - | α - | |
|  229^c | 61 % | 39 % | 47 % |
|  230 | 63 % | 37 % | 55 % |
|  231 | 60 % | 40 % | 57 % ^a |
|  232 | 32 % | 68 % | 47 % ^b |

^a Product Distribution: $\beta(\text{E})$ - $\beta(\text{E})$: 36 %; $\beta(\text{E})$ - α : 16 %; α - α : 48 %.^b Product Distribution: $\beta(\text{E})$ - $\beta(\text{E})$: 23 %; $\beta(\text{E})$ - α : 59 %; α - α : 18 %.^c Previously reported with various catalysts. Lukevics, E.; Sturkovich, R. Y.; Pudova, O. A. *Journal of Organometallic Chemistry* **1985**, 292, 151-158.

Table 5.1.4. ¹H NMR^a data for products from reactions in Table 5.1.1.

| Product | δ (¹ H) ^b |
|------------------------|---|
| 221^c | β(E): 0.38 (s, 6H, -Si(CH ₃) ₂ -), 6.58, 7.01 (d, 2H, -C ₂ H ₂ -, ³ J _{H-H} = 19Hz) α: 0.36 (s, 6H, -Si(CH ₃) ₂ -), 5.64, 5.97 (d, 2H, -C ₂ H ₂ -, ² J _{H-H} = 3Hz) misc: 6.94-7.62 (m, 2x10H, Ph -Si(CH ₃) ₂ -C ₂ H ₂ - Ph) |
| 222 | See Table 4.1.5. |
| 223^c | β(E)-β(E): 0.43 (s, 12H, -Si(CH ₃) ₂ -), 6.62, 7.04 (d, 4H, -C ₂ H ₂ -, ³ J _{H-H} = 19Hz) α-α: 0.37 (s, 12H, -Si(CH ₃) ₂ -), 5.65, 5.98 (d, 4H, -C ₂ H ₂ -, ² J _{H-H} = 3Hz) β(E)-α: 0.40 (s, 6H, β (E)- α -Si(CH ₃) ₂ -), 0.41 (s, 6H, β(E) - α -, -Si(CH ₃) ₂ -), 5.68, 6.00 (d, 2H, β (E)- α -C ₂ H ₂ -, ² J _{H-H} = 3Hz), 6.58, 7.09 (d, 2H, β(E) - α -, -C ₂ H ₂ -, ³ J _{H-H} = 19Hz) misc: 6.96-7.34 (m, 3x10H, Ph(-Si(CH ₃) ₂ -C ₂ H ₂ - Ph) ₂), 7.56-7.70 (m, 3x4H, Ph (SiCH ₃) ₂ -C ₂ H ₂ -Ph) ₂) |
| 224^c | β(E)-β(E): 0.42 (s, 12H, -Si(CH ₃) ₂ -), 4.14, 4.32 (t, 8H, Cp -Si(CH ₃) ₂ -), 6.67, 7.04 (d, 4H, -C ₂ H ₂ -, ³ J _{H-H} = 19Hz) α-α: 0.43 (s, 12H, -Si(CH ₃) ₂ -), 3.98, 4.18 (t, 8H, Cp -Si(CH ₃) ₂ -), 5.62, 5.84 (d, 4H, -C ₂ H ₂ -, ² J _{H-H} = 3Hz) β(E)-α: 0.40 (s, 6H, β(E) - α -, -Si(CH ₃) ₂ -), 0.44 (s, 6H, β (E)- α -, -Si(CH ₃) ₂ -), 4.05, 4.22 (t, 4H, β (E)- α -Cp-Si(CH ₃) ₂ -), 4.07, 4.28 (t, 8H, β(E) - α -, Cp-Si(CH ₃) ₂ -), 5.63, 5.85 (d, 2H, β (E)- α -, -C ₂ H ₂ -, ² J _{H-H} = 3Hz), 6.65, 7.03 (d, 2H, β(E) - α -, -C ₂ H ₂ -, ³ J _{H-H} = 19Hz) misc: 7.02-7.40 (m, 3x10H, Fe(-Si(CH ₃) ₂ -C ₂ H ₂ - Ph) ₂) |

^a Solvent used: C₆D₆. ^b Internal reference: C₆D₆ (¹H NMR: δ 7.16 ppm).^c See Table 5.1.1 for references.

Table 5.1.5. ¹H NMR^a data for products from reactions in Table 5.1.2.

| Product | δ (¹ H) ^b |
|------------------------|--|
| 225^c | <p>β(E): 0.40 (s, 6H, -Si(CH₃)₂-), 2.10 (s, 3H, -PhCH₃), 6.57, 7.04 (d, 2H, -C₂H₂-, ³J_{H-H} = 19Hz)</p> <p>α: 0.39 (s, 6H, -Si(CH₃)₂-), 2.07 (s, 3H, -PhCH₃), 5.64, 6.02 (d, 2H, -C₂H₂-, ²J_{H-H} = 3Hz)</p> <p>misc: 6.86-7.30 (m, 2x4H, -PhCH₃), 7.12-7.64 (m, 2x5H, Ph-Si(CH₃)₂-)</p> |
| 226 | <p>β(E): 0.43 (s, 6H, -Si(CH₃)₂-), 2.10 (s, 3H, -PhCH₃), 4.06 (s, 5H, Cp), 4.12, 4.23 (t, 4H, Cp-Si(CH₃)₂-), 6.66, 7.08 (d, 2H, -C₂H₂-, ³J_{H-H} = 19Hz)</p> <p>α: 0.46 (s, 6H, -Si(CH₃)₂-), 2.12 (s, 3H, -PhCH₃), 3.98 (s, 5H, Cp), 4.03, 4.18 (t, 4H, Cp-Si(CH₃)₂-), 5.65, 5.90 (d, 2H, -C₂H₂-, ²J_{H-H} = 3Hz)</p> <p>misc: 6.92-7.38 (m, 2x4H, -PhCH₃)</p> |
| 227 | <p>β(E)-β(E): 0.444 (s, 12H, -Si(CH₃)₂-), 2.09 (s, 6H, -PhCH₃), 6.61, 7.07 (d, 4H, -C₂H₂-, ³J_{H-H} = 19Hz)</p> <p>α-α: 0.406 (s, 12H, -Si(CH₃)₂-), 2.07 (s, 6H, -PhCH₃), 5.66, 6.03 (d, 4H, -C₂H₂-, ²J_{H-H} = 3Hz)</p> <p>β(E)-α: 0.411 (s, 6H, β(E)-α, -Si(CH₃)₂-), 0.436 (s, 6H, β(E)-α, -Si(CH₃)₂-), 2.05 (s, 3H, β(E)-α, -PhCH₃), 2.10 (s, 3H, β(E)-α, -PhCH₃), 5.69, 6.05 (d, 2H, β(E)-α, -C₂H₂-, ²J_{H-H} = 3Hz), 6.58, 7.05 (d, 2H, β(E)-α, -C₂H₂-, ³J_{H-H} = 19Hz)</p> <p>misc: 6.86-7.32 (m, 3x8H, -PhCH₃), 7.58-7.70 (m, 3x4H, Ph(SiCH₃)₂-C₃H₂-PhCH₃)₂</p> |
| 228 | <p>β(E)-β(E): 0.44 (s, 12H, -Si(CH₃)₂-), 2.10 (s, 6H, -PhCH₃), 4.16, 4.33 (t, 8H, Cp-Si(CH₃)₂-), 6.66, 7.07 (d, 4H, -C₂H₂-, ³J_{H-H} = 19Hz)</p> <p>α-α: 0.45 (s, 12H, -Si(CH₃)₂-), 2.12 (s, 6H, -PhCH₃), 4.02, 4.20 (t, 8H, Cp-Si(CH₃)₂-), 5.628, 5.891 (d, 4H, -C₂H₂-, ²J_{H-H} = 3Hz)</p> <p>β(E)-α: 0.42 (s, 6H, β(E)-α, -Si(CH₃)₂-), 0.48 (s, 6H, β(E)-α, -Si(CH₃)₂-), 2.10 (s, 3H, β(E)-α, -PhCH₃), 2.12 (s, 3H, β(E)-α, -PhCH₃), 4.087, 4.24 (t, 4H, β(E)-α, Cp-Si(CH₃)₂-), 4.093, 4.29 (t, 8H, β(E)-α, Cp-Si(CH₃)₂-), 5.635, 5.893 (d, 2H, β(E)-α, -C₂H₂-, ²J_{H-H} = 3Hz), 6.64, 7.06 (d, 2H, β(E)-α, -C₂H₂-, ³J_{H-H} = 19Hz)</p> <p>misc: 6.92-7.38 (m, 3x8H, -PhCH₃)</p> |

^a Solvent used: C₆D₆. ^b Internal reference: C₆D₆ (¹H NMR: δ 7.16 ppm).^c See Table 5.1.2 for references.

Table 5.1.6. ^1H NMR^a data for products from reactions in **Table 5.1.3**.^{*}

| Product | δ (^1H) ^b |
|------------------------|---|
| 229^c | $\beta(\text{E})$: 0.32 (s, 6H, $-\text{Si}(\text{CH}_3)_2-$), 6.46, 7.05 (d, 2H, $-\text{C}_2\text{H}_2-$, $^3J_{\text{H-H}} = 19\text{Hz}$) α: 0.38 (s, 6H, $-\text{Si}(\text{CH}_3)_2-$), 5.46, 6.22 (d, 2H, $-\text{C}_2\text{H}_2-$, $^2J_{\text{H-H}} = 2\text{Hz}$) misc: 6.54-6.82 (m, 2x3H, Th -), 7.12-7.58 (m, 2x5H, Ph -) |
| 230 | See Table 4.1.6 . |
| 231 | $\beta(\text{E})$-$\beta(\text{E})$: 0.35 (s, 12H, $-\text{Si}(\text{CH}_3)_2-$), 6.49, 7.08 (d, 4H, $-\text{C}_2\text{H}_2-$, $^3J_{\text{H-H}} = 19\text{Hz}$) α-α: 0.39 (s, 12H, $-\text{Si}(\text{CH}_3)_2-$), 5.47, 6.22 (d, 4H, $-\text{C}_2\text{H}_2-$, $^2J_{\text{H-H}} = 2\text{Hz}$) $\beta(\text{E})$-α: 0.32 (s, 6H, $\beta(\text{E})$ - α , $-\text{Si}(\text{CH}_3)_2-$), 0.42 (s, 6H, $\beta(\text{E})$ - α , $-\text{Si}(\text{CH}_3)_2-$), 5.50, 6.25 (d, 2H, $\beta(\text{E})$ - α , $-\text{C}_2\text{H}_2-$, $^2J_{\text{H-H}} = 2\text{Hz}$), 6.45, 7.06 (d, 2H, $\beta(\text{E})$ - α , $-\text{C}_2\text{H}_2-$, $^3J_{\text{H-H}} = 19\text{Hz}$) misc: 6.54-6.84 (m, 3x6H, $\text{Ph}(-\text{Si}(\text{CH}_3)_2-\text{C}_2\text{H}_2-\text{Th})_2$), 7.50-7.62 (m, 3x4H, Ph ($\text{Si}(\text{CH}_3)_2-\text{C}_2\text{H}_2-\text{Th})_2$) |
| 232 | See Table 4.2.3 . |

^a Solvent used: C_6D_6 . ^b Internal reference: C_6D_6 (^1H NMR: δ 7.16 ppm). ^{*} Th = Thiophene.

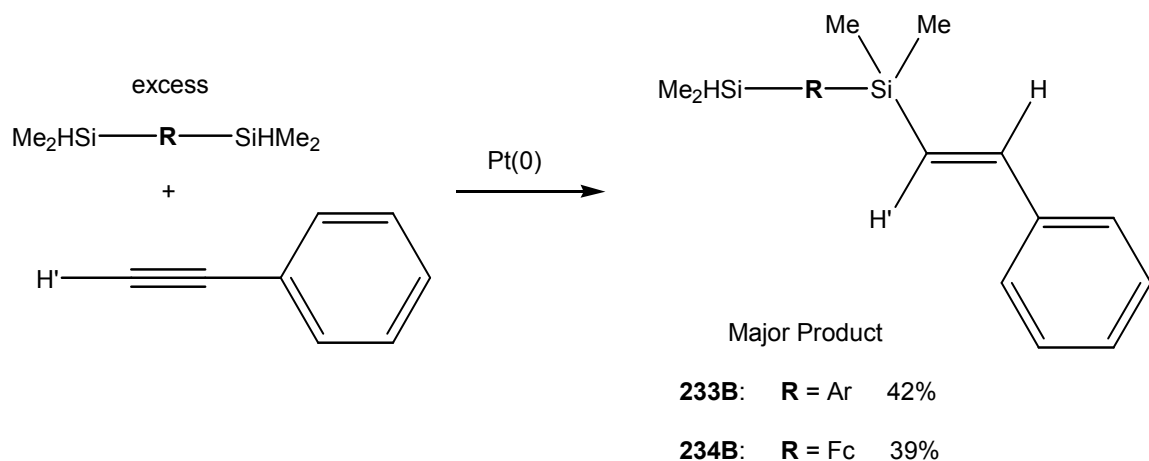
^c See **Table 5.1.3** for references.

5.2. Comparison of 1,4-*bis*(dimethylsilyl)benzene and 1,1'-*bis*(dimethylsilyl)ferrocene

To explore the possibility of a 'cooperative effect' between the two dimethylsilyl groups of 1,1'-*bis*(dimethylsilyl)ferrocene, the hydrosilylation of phenylacetylene with *bis*-silanes 1,1'-*bis*(dimethylsilyl)ferrocene or 1,4-*bis*(dimethylsilyl)benzene were compared. This was done in two steps. The first step is to compare the hydrosilylation of the mono-hydrosilylated adducts of either *bis*-silane (**Section 5.2.1** and **5.2.2**). The second step is to monitor the hydrosilylation of either *bis*-silane over time via ^1H NMR (**Section 5.2.3**). From these experiments, it is hoped that a clearer picture of the hydrosilylation of alkynes with 1,1'-*bis*(dimethylsilyl)ferrocene emerges, and how it differs from that of 1,4-*bis*(dimethylsilyl)benzene.

5.2.1. Preparation of Mono-Hydrosilylated *Bis*-Silanes

Karstedt's catalyst was employed in an effort to produce mono-hydrosilylated *bis*-silane adducts from phenylacetylene with either 1,4-*bis*(dimethylsilyl)benzene or 1,1'-*bis*(dimethylsilyl)ferrocene. Using the protocol described in the experimental section, excess 1,4-*bis*(dimethylsilyl)benzene was reacted with phenylacetylene (**Scheme 5.2.1.1**). Purification via column chromatography gave the mono- β (E)- adduct 1-{dimethyl(phenylvinylene)silyl}-4-dimethylsilyl-benzene (**233B**, 42 %, colorless/pale yellow oil) as major product. A similar reaction using 1,1'-*bis*(dimethylsilyl)ferrocene (**Scheme 5.2.1.1**) gave the mono- β (E)- adduct 1-{dimethyl(phenylvinylene)silyl}-1'-dimethylsilyl-ferrocene (**234B**, 39 %, orange oil) as major product. In both reactions no mono- α - adduct (**233A** and **234A**, respectively) was isolated.



Scheme 5.2.1.1. Synthesis of **233B**.

Complex **233B** was characterized by GC/MS, ^1H , $^{13}\text{C}\{^1\text{H}\}$, and ^{29}Si DEPT NMR (**Table 5.2.1.1**), showing a molecular ion (M^+) with $m/e = 296$, consistent with a mono-adduct. The ^1H NMR spectra of **233B** showed one pair of olefinic proton doublets at δ 6.60 and δ 7.03 ($\beta(\text{E})$ -, $^3J_{\text{H-H}} = 19$ Hz) along with a $-\text{SiH}(\text{CH}_3)_2$ silane proton at δ 4.67. The presence of a reacted and an unreacted dimethylsilyl group was confirmed by ^{29}Si DEPT NMR, optimized to either $^1J_{\text{Si-H}} = 180$ Hz or $^3J_{\text{Si-H}} = 8$ Hz, showing one signal at δ -16.8 for the $-\text{SiH}(\text{CH}_3)_2$ silicon and another signal at δ -10.1 for the $-\text{Si}(\text{CH}_3)_2(\text{CHCHPh})$ silicon, respectively.

Complex **234B** was also characterized by GC/MS, ^1H , $^{13}\text{C}\{^1\text{H}\}$, and ^{29}Si DEPT NMR (**Table 5.2.1.2**), showing a molecular ion (M^+) with $m/e = 404$, consistent with a mono-adduct. The NMR spectra of **234B** shared common features with those of **233B**, indicative of a hydrosilylation mono-adduct. This was confirmed by ^{29}Si DEPT NMR, optimized to either $^1J_{\text{Si-H}} = 180$ Hz or $^3J_{\text{Si-H}} = 8$ Hz, showing one signal at δ -18.2 for the -

SiH(CH₃)₂ silicon and another signal at δ -9.3 for the ***-Si***(CH₃)₂(CHCHPh) silicon, respectively.

Table 5.2.1.1. NMR^a data for **233B**.

| Product | δ (¹ H) ^b | δ (¹³ C{ ¹ H}) ^b | δ (²⁹ Si DEPT) ^c |
|-------------|---|--|---|
| 233B | 0.26 (d, 6H, -Ph-SiH(CH ₃) ₂), 0.41 (s, 6H, -Ph-Si(CH ₃) ₂ (C ₂ H ₂ Ph)), 4.67 (septet, 1H, -SiH(CH ₃) ₂), 6.60, 7.03 (d, 2H, β (E), -C ₂ H ₂ Ph, ³ J _{H-H} = 19Hz), 7.02-7.34 (m, 5H, -C ₂ H ₂ Ph), 7.52-7.64 (m, 4H, - Ph -Si(CH ₃) ₂ (C ₂ H ₂ Ph)) | -3.4 (-SiH(CH ₃) ₂), -2.1 (-Si(CH ₃) ₂ C ₂ H ₂ Ph)), 127.3, 127.5, 128.8, 140.2 (-C ₂ H ₂ Ph), 129.1, 146.5 (-C ₂ H ₂ Ph), 134.19, 134.20, 138.8, 139.0 (- Ph -) | -16.8 (- Si H(CH ₃) ₂), -10.1 (- Si (CH ₃) ₂ (C ₂ H ₂ Ph)) |

^a Solvent used: C₆D₆. ^b Internal reference: C₆D₆ (¹H NMR: δ 7.16 ppm; ¹³C NMR: δ 128.38 ppm). ^c External reference: Tetramethylsilane (δ 0.0 ppm).

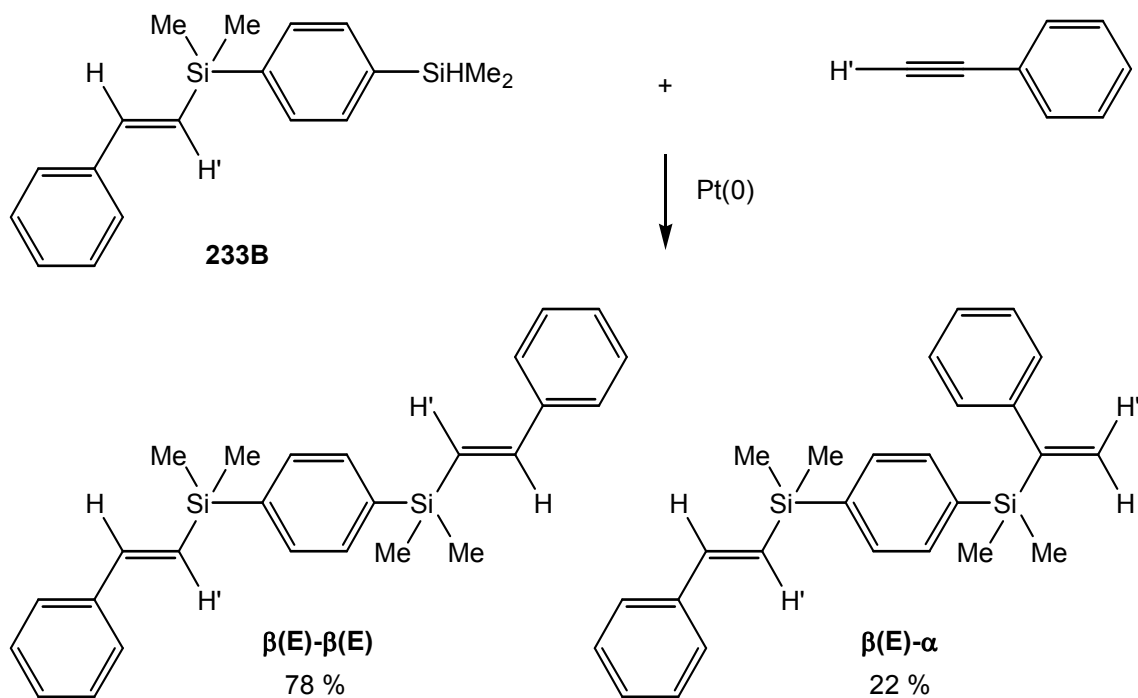
Table 5.2.1.2. NMR^a data for **234B**.

| Product | δ (¹ H) ^b | δ (¹³ C{ ¹ H}) ^b | δ (²⁹ Si DEPT) ^c |
|-------------|--|--|--|
| 234B | 0.26 (d, 6H, CpSiH(CH ₃) ₂), 0.43 (s, 6H, CpSi(CH ₃) ₂ (C ₂ H ₂ Ph)), 4.09, 4.25 (t, 4H, Cp SiH(CH ₃) ₂), 4.10, 4.27 (t, 4H, Cp Si(CH ₃) ₂ (C ₂ H ₂ Ph)), 4.69 (septet, 1H, -SiH(CH ₃) ₂), 6.68, 7.04 (d, 2H, β (E), -C ₂ H ₂ Ph, ³ J _{H-H} = 19Hz), 7.04-7.40 (m, 5H, -C ₂ H ₂ Ph) | -2.5 (CpSiH(CH ₃) ₂), -1.1 (CpSi(CH ₃) ₂ C ₂ H ₂ Ph)), 68.6 (<i>ipso</i> C, Cp SiH(CH ₃) ₂), 70.9 (<i>ipso</i> C, Cp Si(CH ₃) ₂ (C ₂ H ₂ Ph)), 72.24, 74.19 (Cp SiH(CH ₃) ₂), 72.25, 74.23 (Cp Si(CH ₃) ₂ (C ₂ H ₂ Ph)), 127.3, 128.7, 128.9, 139.2 (-C ₂ H ₂ Ph), 129.2, 145.3 (-C ₂ H ₂ Ph) | -18.2 (Cp Si H(CH ₃) ₂), -9.3 (Cp Si (CH ₃) ₂ (C ₂ H ₂ Ph)) |

^a Solvent used: C₆D₆. ^b Internal reference: C₆D₆ (¹H NMR: δ 7.16 ppm; ¹³C NMR: δ 128.38 ppm). ^c External reference: Tetramethylsilane (δ 0.0 ppm).

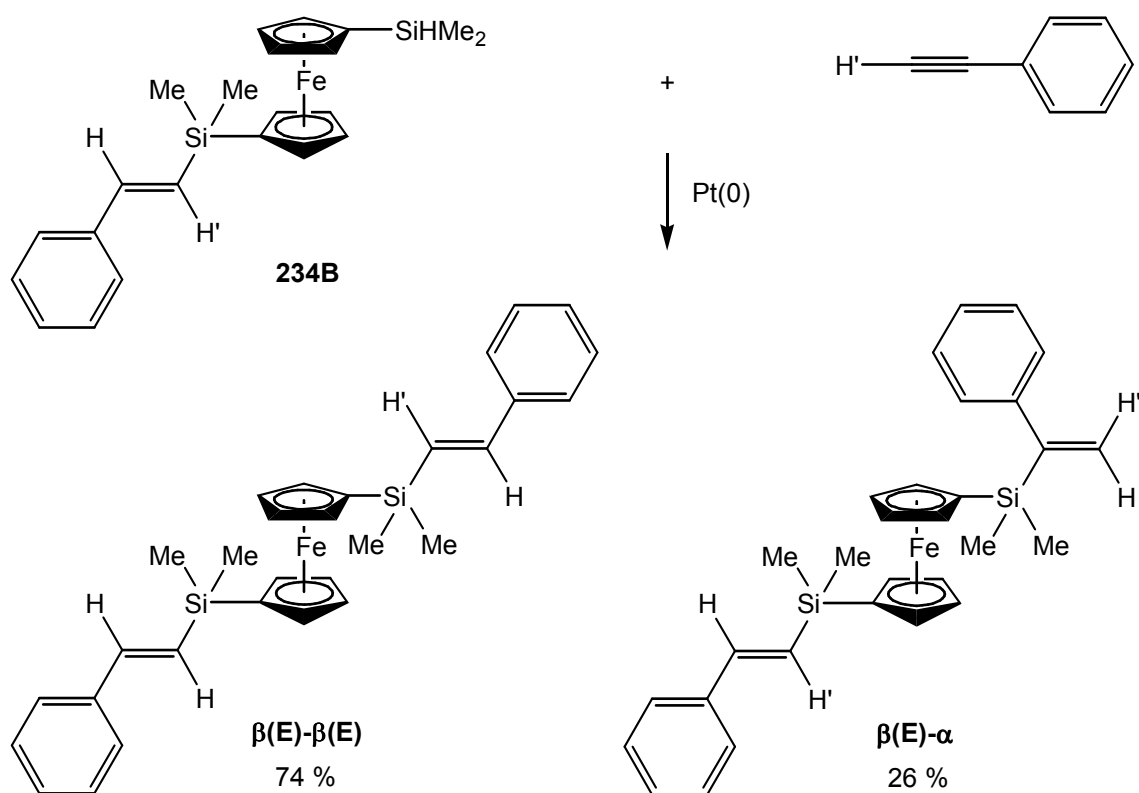
5.2.2. Hydrosilylation of Phenylacetylene with Mono-Hydrosilylated *Bis*-Silanes

Phenylacetylene was hydrosilylated with either of the mono- β (E)-hydrosilylated *bis*-silanes (**233B** or **234B**) presented in the previous section. Treating a mixture of the mono- β (E)- complex **233B** and phenylacetylene with Karstedt's catalyst in d_6 -benzene gave a mixture of the β (E)- β (E) and β (E)- α regioisomers in a 78 % to 22 % ratio (**Scheme 5.2.2.1**) (84 % yield; colorless / very pale yellow oil). In other words, 78 % of the mono- β (E)- complex **233B** became β (E)- β (E), and 22 % became β (E)- α . The GC/MS of the product showed two peaks having a molecular ion (M^+) with $m/e = 398$, consistent with the two hydrosilylation adducts. This was confirmed in its ^1H NMR spectrum which is almost identical to that of **223**, except for the α - α regioisomer signals being absent.



Scheme 5.2.2.1. Hydrosilylation of Phenylacetylene with **233B**.

A similar reaction using the mono- $\beta(\text{E})$ - complex **234B** gave a mixture of the $\beta(\text{E})$ - $\beta(\text{E})$ and $\beta(\text{E})$ - α regioisomers in a 74 % to 26 % ratio (**Scheme 5.2.2.2**) (83 % yield; orange oil), with the GC/MS showing two peaks having a molecular ion (M^+) with $m/e = 506$, consistent with the two hydrosilylation adducts. The ^1H NMR spectrum of the product was also almost identical with that of **224**, except for the α - α regioisomer signals being absent.



Scheme 5.2.2.2. Hydrosilylation of Phenylacetylene with **234B**.

Given the fact that the hydrosilylation of phenylacetylene with either 1,4-*bis*(dimethylsilyl)benzene or 1,1'-*bis*(dimethylsilyl)ferrocene resulted in disparate regiochemical distributions (**Table 5.1.1**; **223** vs. **224**), it is interesting to note that the

hydrosilylation reactions using their respective mono- β (E)-hydrosilylated adducts (**233B** and **234B**) gave comparable product distributions, preferring the β (E)- configuration for the second hydrosilylation reaction. This selectivity is consistent with those of **221** and **222**, both of which showed preference for the β (E)- adduct. Based on these results, it can be reasonably posited that the low β (E)- to α - ratios observed in hydrosilylation reactions using 1,1'-*bis*(dimethylsilyl)ferrocene as well as its trolicene analog can be attributed to the reactivity of the mono- α - adduct. This is explored further in the next two sections, wherein reactions **223** and **224** were monitored by ^1H NMR.

5.2.3. ^1H NMR Monitored Hydrosilylation of Phenylacetylene

A repeat of reactions **223** and **224** was monitored by ^1H NMR, with product distributions being estimated from integration of the obtained spectra. **Table 5.2.3.1** and **Table 5.2.3.2** show the relative amounts of the various hydrosilylation adducts (the 3 *bis*-adducts and 2 mono-adducts) from the hydrosilylation of phenylacetylene with either 1,4-*bis*(dimethylsilyl)benzene or 1,1'-*bis*(dimethylsilyl)ferrocene, respectively, the three *bis*-adducts being β (E)- β (E), β (E)- α , and α - α , and the two mono-adducts being mono- β (E)- and mono- α - (See **Figures 5.2.3.1 to 5.2.3.8**).

Table 5.2.3.1. Reaction 223 Monitored by ^1H NMR.^a

| Time (hr) | <i>Bis</i> -Adducts | | | Mono-Adducts | |
|-----------|---------------------------------------|--------------------------------|---------------------|-------------------|----------|
| | $\beta(\text{E})$ - $\beta(\text{E})$ | $\beta(\text{E})$ - α^b | α - α | $\beta(\text{E})$ | α |
| 3 | 16 | 12 (5/7) | 3 | 49 | 20 |
| | 50 | 40 (14/26) | 10 | 71 | 29 |
| 5 | 19 | 15 (5/10) | 3 | 45 | 18 |
| | 52 | 39 (15/24) | 9 | 72 | 28 |
| 20 | 41 | 31 (12/19) | 6 | 16 | 6 |
| | 53 | 40 (15/25) | 7 | 72 | 28 |
| Complete | 53 | 40 (15/25) | 7 | 0 | 0 |
| | $\beta(\text{E})$: 73 | | α : 27 | | |

^a Product distribution for mono- and *bis*- adducts in the non-shaded area; Only for the *bis*- adducts in the lightly shaded area; Only the mono- adducts in the heavily shaded area.

^b Ratio in parenthesis indicates ratio of the $\beta(\text{E})$ - $\alpha_{(\text{Path } \beta(\text{E})-)}$ / $\beta(\text{E})$ - $\alpha_{(\text{Path } \alpha-)}$.

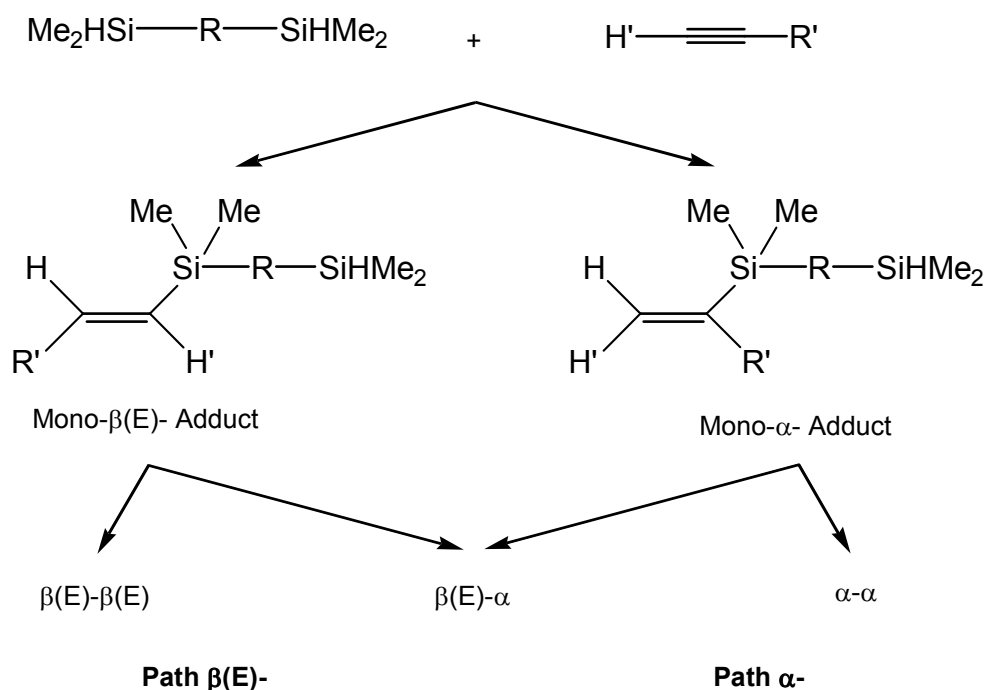
Table 5.2.3.2. Reaction 224 Monitored by ^1H NMR.^a

| Time (hr) | <i>Bis</i> -Adducts | | | Mono-adducts | |
|-----------|---------------------------------------|--------------------------------|---------------------|-------------------|----------|
| | $\beta(\text{E})$ - $\beta(\text{E})$ | $\beta(\text{E})$ - α^b | α - α | $\beta(\text{E})$ | α |
| 0.5 | 15 | 21 (5/16) | 27 | 31 | 6 |
| | 24 | 33 (8/25) | 43 | 85 | 15 |
| 1 | 15 | 22 (5/17) | 28 | 30 | 5 |
| | 24 | 33 (8/25) | 43 | 86 | 14 |
| 1.5 | 16 | 20 (6/14) | 28 | 31 | 5 |
| | 24 | 32 (8/24) | 44 | 85 | 15 |
| 2 | 16 | 23 (6/17) | 28 | 29 | 4 |
| | 23 | 34 (8/26) | 43 | 88 | 12 |
| 5 | 16 | 23 (6/17) | 30 | 27 | 4 |
| | 24 | 33 (8/25) | 43 | 88 | 12 |
| 8 | 16 | 24 (6/18) | 31 | 26 | 3 |
| | 23 | 33 (8/25) | 44 | 89 | 11 |
| 12 | 19 | 27 (7/20) | 30 | 20 | 4 |
| | 25 | 36 (9/27) | 39 | 84 | 16 |
| 16 | 23 | 29 (8/21) | 30 | 15 | 3 |
| | 28 | 35 (10/25) | 37 | 83 | 17 |
| Complete | 36 | 33 (13/20) | 31 | 0 | 0 |
| | $\beta(\text{E})$: 52 | | α : 48 | | |

^a Product distribution for mono- and *bis*- adducts in the non-shaded area; Only for the *bis*- adducts in the lightly shaded area; Only the mono- adducts in the heavily shaded area.

^b Ratio in parenthesis indicates ratio of the $\beta(\text{E})$ - $\alpha_{(\text{Path } \beta(\text{E})-)}$ / $\beta(\text{E})$ - $\alpha_{(\text{Path } \alpha-)}$.

Logically, the $\beta(\text{E})$ - $\beta(\text{E})$ *bis*-adduct is derived from a mono- $\beta(\text{E})$ - adduct, and the α - α *bis*-adduct is derived from a mono- α - adduct. On the other hand, the $\beta(\text{E})$ - α can be derived from both the mono- $\beta(\text{E})$ - and mono- α - adducts (**Scheme 5.2.3.1**; **Path $\beta(\text{E})$ -** and **Path α -**, respectively). The problem is determining how much of the $\beta(\text{E})$ - α *bis*-adduct is derived from either the mono- $\beta(\text{E})$ - or mono- α - adduct. As shown in **Table 5.2.3.1** and **5.2.3.2**, the relative amounts of $\beta(\text{E})$ - $\beta(\text{E})$, $\beta(\text{E})$ - α , and α - α have been determined by integration of the ^1H NMR spectra of the reactions. Using the selectivity of the mono- $\beta(\text{E})$ - adducts from **Scheme 5.2.2.1** and **5.2.2.2**, it is possible to determine how much of the *total* $\beta(\text{E})$ - α is derived from the mono- $\beta(\text{E})$ - adduct, with the rest of the $\beta(\text{E})$ - α being derived from the mono- α - adduct.



Scheme 5.2.3.1. Products from Pt-Catalyzed Hydrosilylation of a *Bis*-Hydrosilane and a Mono-Alkyne.

As an example, at 3 hours in **Table 5.2.3.1**, the relative amounts of the *bis*-adducts is 50 % $\beta(E)\text{-}\beta(E)$ / 40 % $\beta(E)\text{-}\alpha$ / 10 % $\alpha\text{-}\alpha$. From **Scheme 5.2.2.1**, it was estimated that 78 % of mono- $\beta(E)$ - adducts turn into $\beta(E)\text{-}\beta(E)$ and 22 % turn into $\beta(E)\text{-}\alpha$. Given the amount of $\beta(E)\text{-}\beta(E)$ at 50 % from **Table 5.2.3.1**, the estimated amount of $\beta(E)\text{-}\alpha$ that has been formed from the mono- $\beta(E)$ - adduct is 14 out of 40, which means that 26 out of 40 is from the mono- α - adduct. Comparing the 26 $\beta(E)\text{-}\alpha$ (from the mono- α - adduct) with the 10 $\alpha\text{-}\alpha$ (also from the mono- α - adduct) means that majority of the mono- α - adduct led to $\beta(E)\text{-}\alpha$ (72 %) and the rest formed $\alpha\text{-}\alpha$ (28 %). This preference for the $\beta(E)$ -configuration can be seen all throughout the duration of the reaction (**Table 5.2.3.3**), and is consistent with the selectivity observed in **221**, **222**, and **223** (**Table 5.1.1**). It can be reasonably posited that the two dimethylsilyl groups of 1,4-*bis*(dimethylsilyl)benzene are independent of each other, with the hydrosilylation selectivity of one dimethylsilyl moiety having no effect on the other, both of which show similar selectivity for the $\beta(E)$ -configuration consistent with those of those of the mono-silanes dimethylsilylbenzene and dimethylsilylferrocene.

In contrast, the same cannot be said for reaction **224**. Referring to **Table 5.2.3.2** and applying the same method for determining the amount of $\beta(E)\text{-}\alpha$ that is formed from either **Path $\beta(E)$** - or **Path α** -, it was determined that most of the mono- α - adduct went on to become $\alpha\text{-}\alpha$ rather than $\beta(E)\text{-}\alpha$. As an example, at 0.5 hours in **Table 5.2.3.2**, the relative amounts of the *bis*-adducts is 24 % $\beta(E)\text{-}\beta(E)$ / 33 % $\beta(E)\text{-}\alpha$ / 43 % $\alpha\text{-}\alpha$. From **Scheme 5.2.2.2**, it was estimated that 74 % of the mono- $\beta(E)$ - adduct turned into $\beta(E)\text{-}\beta(E)$ and 26 % formed $\beta(E)\text{-}\alpha$. Given the amount of $\beta(E)\text{-}\beta(E)$ at 24 % from **Table 5.2.3.2**, the estimated amount of $\beta(E)\text{-}\alpha$ that came from the mono- $\beta(E)$ - adduct is 8 out of

33, which means that 25 out of 33 was derived from the mono- α - adduct. Comparing the 25 $\beta(\text{E})$ - α (from the mono- α - adduct) with the 43 α - α (also from the mono- α - adduct) means that, unlike reaction **223**, the majority of the mono- α - adduct went on to become α - α (63 %) and the rest became $\beta(\text{E})$ - α (37 %). While the mono- $\beta(\text{E})$ - adduct shows preference for the $\beta(\text{E})$ - configuration in the second hydrosilylation reaction similar to dimethylsilylbenzene, dimethylsilylferrocene, and 1,4-*bis*(dimethylsilyl)benzene, the mono- α - adduct *does not*. This preference for the α - configuration in the second hydrosilylation of the mono- α - adduct is seen all throughout the duration of the reaction (**Table 5.2.3.4**), and can account for the difference in regiochemical distribution of reactions **223** and **224**.

In addition to the difference in selectivity of the mono- α - adducts in reactions **223** and **224**, another notable observation is the relative amounts of mono-adducts in both reactions. The ratio of mono- $\beta(\text{E})$ - to mono- α - in reaction **223** (**Table 5.2.3.1**) is noticeably lower than that of reaction **224** (**Table 5.2.3.2**). This can be attributed to the mono- α - adduct being converted to *bis*-adducts *at a faster rate* than the mono- $\beta(\text{E})$ - adduct in reaction **224** compared to reaction **223**. This is reflected the relative amounts of *bis*-adducts obtained via **Path $\beta(\text{E})$ -** or **Path α -**. **Table 5.2.3.5** shows that for reaction **223**, majority of the *bis*-adducts were obtained via **Path $\beta(\text{E})$ -**, with the trend remaining constant throughout the reaction. In contrast, **Table 5.2.3.6** shows that initially, for reaction **224**, the majority of the *bis*-adducts were obtained from **Path α -**, with **Path $\beta(\text{E})$ -** catching up only as the silane is depleted at around 16 hours (determined from ^1H NMR). With no unreacted *bis*-silane left to produce fresh mono- α - adduct, the majority of the *bis*-adducts produced after 16 hours would naturally be obtained via **Path $\beta(\text{E})$ -**.

Table 5.2.3.3. Product Distribution of Reaction **223** *Bis*-Adducts via Path $\beta(\text{E})$ - or α -.

| Time (hr) | Product Distribution of <i>Bis</i> - Adducts | | | |
|-----------|--|------------------------------|------------------------------|---------------------|
| | Path $\beta(\text{E})$ - ^a | | Path α - | |
| | $\beta(\text{E})$ - $\beta(\text{E})$ | $\beta(\text{E})$ - α | $\beta(\text{E})$ - α | α - α |
| 3 | 78 | 22 | 72 | 28 |
| 5 | | | 73 | 27 |
| 20 | | | 78 | 22 |
| Complete | | | 78 | 22 |

^a Product distribution from Scheme 5.2.2.1.**Table 5.2.3.4.** Product Distribution of Reaction **224** *Bis*-Adducts via Path $\beta(\text{E})$ - or α -.

| Time (hr) | Product Distribution of <i>Bis</i> - Adducts | | | |
|-----------|--|------------------------------|------------------------------|---------------------|
| | Path $\beta(\text{E})$ - ^a | | Path α - | |
| | $\beta(\text{E})$ - $\beta(\text{E})$ | $\beta(\text{E})$ - α | $\beta(\text{E})$ - α | α - α |
| 0.5 | 74 | 26 | 37 | 63 |
| 1 | | | 37 | 63 |
| 1.5 | | | 35 | 65 |
| 2 | | | 38 | 62 |
| 5 | | | 37 | 63 |
| 8 | | | 36 | 64 |
| 12 | | | 41 | 59 |
| 16 | | | 40 | 60 |
| Complete | | | 39 | 61 |

^a Product distribution from Scheme 5.2.2.2.

The difference between the hydrosilylation of phenylacetylene with either 1,4-*bis*(dimethylsilyl)benzene (reaction **223**) or 1,1'-*bis*(dimethylsilyl)ferrocene (reaction **224**) can be summarized as follows: **1)** The mono- $\beta(\text{E})$ - adducts of reactions **223** and **224** both preferentially lead to the $\beta(\text{E})$ - $\beta(\text{E})$ *bis*-adduct, consistent with results found in the

literature; **2)** The mono- α - adduct from reaction **223** preferentially leads to the β (E)- α *bis*-adduct, while the mono- α - adduct from reaction **224** preferentially leads to the α - α *bis*-adduct; **3)** The mono- α - adduct from reaction **224** appears to react faster with another equivalent of phenylacetylene to produce the *bis*-adducts compared to the mono- α -adduct from reaction **223**.

Table 5.2.3.5. Distribution of **223** *Bis*-Adducts via Path β (E)- or α - from **Table 5.2.3.1**.

| Time (hr) | Product Distribution of <i>Bis</i> -Adducts | |
|-----------|---|-----------------|
| | Path β (E)- | Path α - |
| 3 | 64 | 36 |
| 5 | 67 | 33 |
| 20 | 68 | 32 |
| Complete | 68 | 32 |

Table 5.2.3.6. Distribution of **224** *Bis*-Adducts via Path β (E)- or α - from **Table 5.2.3.2**.

| Time (hr) | Product Distribution of <i>Bis</i> -Adducts | |
|-----------|---|-----------------|
| | Path β (E)- | Path α - |
| 0.5 | 32 | 68 |
| 1 | 32 | 68 |
| 1.5 | 32 | 68 |
| 2 | 31 | 69 |
| 5 | 32 | 68 |
| 8 | 31 | 69 |
| 12 | 34 | 66 |
| 16 | 38 | 62 |
| Complete | 49 | 51 |

The difference between the hydrosilylation of phenylacetylene with either 1,4-*bis*(dimethylsilyl)benzene (reaction **223**) or 1,1'-*bis*(dimethylsilyl)ferrocene (reaction **224**) can be summarized as follows: **1)** The mono- β (E)- adducts of reactions **223** and **224** both preferentially lead to the β (E)- β (E) *bis*-adduct, consistent with results found in the literature; **2)** The mono- α - adduct from reaction **223** preferentially leads to the β (E)- α *bis*-adduct, while the mono- α - adduct from reaction **224** preferentially leads to the α - α *bis*-adduct; **3)** The mono- α - adduct from reaction **224** appears to react faster with another equivalent of phenylacetylene to produce the *bis*-adducts compared to the mono- α - adduct from reaction **223**.

Unlike 1,4-*bis*(dimethylsilyl)benzene, rotation about the Cp-M-Cp axis metallocenes such as 1,1'-*bis*(dimethylsilyl)ferrocene allows for the possibility of the two dimethylsilyl-groups interacting with the same Pt center. We propose two possibilities to explain the preference of the mono- α - adduct **234A** for more α - as well as its rapid conversion into *bis*-adducts compared to the mono- β (E)- adduct **234B**. The first one is that the mono- α - adduct olefins bind better than the mono- β (E)- adduct olefins to the Pt catalyst. The second is that, unlike **234B** which has two bulky groups (red circles) which hinder the approach of the unreacted dimethylsilyl-group via rotation about the Cp-Fe-Cp axis, **234A** has a “clear” area of approach (green circle) with less steric hindrance (**Figure 5.2.3.1**).

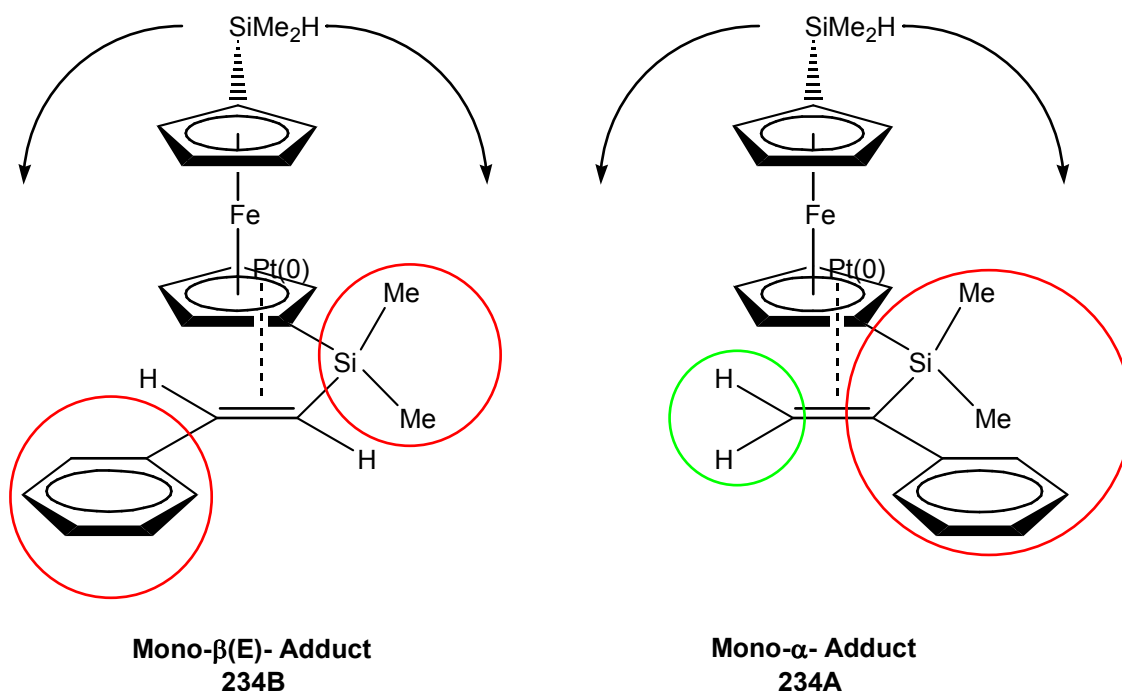
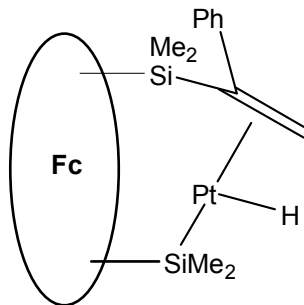
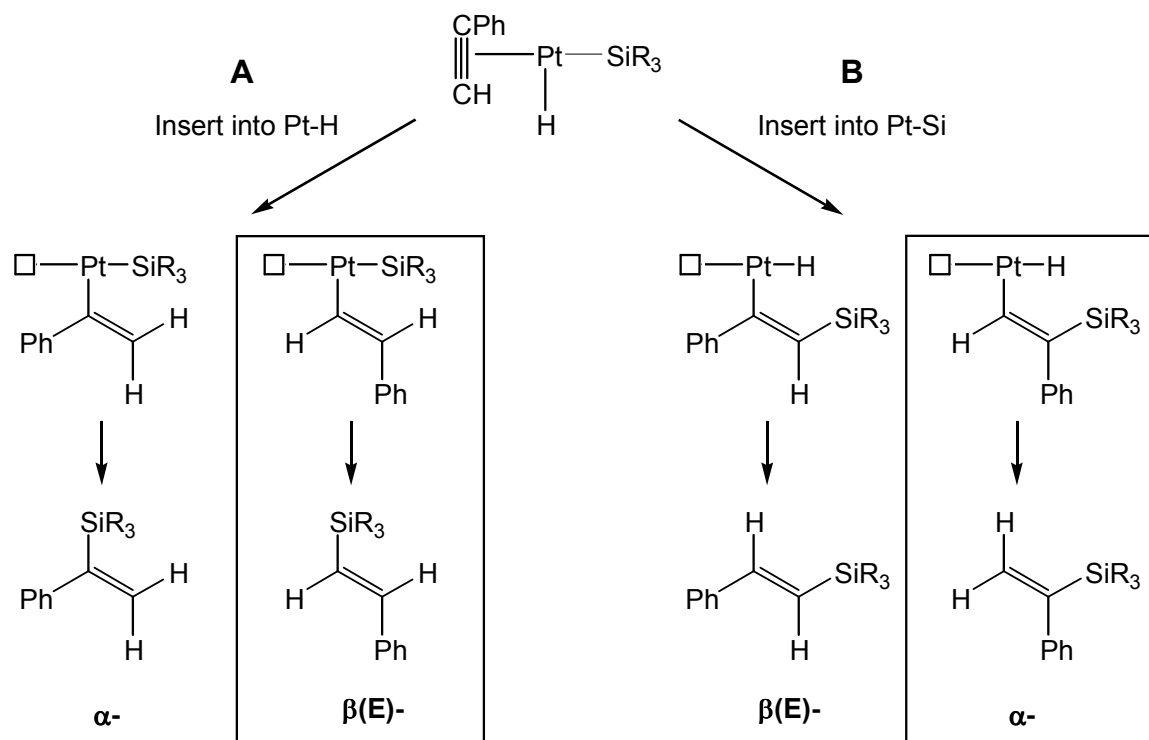


Figure 5.2.3.1. Mono-β(E)- vs. Mono-α- Hydrosilylation.

Either way results in having the Pt catalyst near at hand, allowing for the oxidative addition of the unreacted dimethylsilyl-group onto the bound Pt catalyst before it is released. This has two effects on the reaction. The first effect is the faster conversion of the mono-α- adduct **234A** into *bis*-adducts, as evidenced by the relatively small quantities of mono-α- adduct **234A** seen in the ¹H NMR spectra of the reaction in progress. The second effect is a cooperative effect between the two dimethylsilyl-groups wherein the olefin is positioned *trans*- to the Pt-Si bond (**Figure 5.2.3.2**), weakening that bond due to a *trans*- influence and making alkyne insertion into that bond more favorable.

**234A****Figure 5.2.3.2. 234A-Chelated Pt-catalyst.**

We also propose that alkyne insertion into the Pt-Si bond in turn steers the regioselectivity of the hydrosilylation towards more α -. The hydrosilylation reactions of mono-adducts **233A**, **233B**, and **234B** proceed via insertion into the Pt-H bond which leads to more β (E)- by virtue of steric constraints making the bulky Ph-group move away from the Pt catalyst (**Scheme 5.2.3.2**). In contrast, the hydrosilylation reaction of **234A** proceeds via alkyne insertion into the Pt-Si bond which leads to more α -, again by virtue of steric constraints making the bulky Ph-group move away from the Pt catalyst.



Scheme 5.2.3.2. β(E)- and α- Regioisomers from Insertion of Alkyne into Pt-H and Pt-Si.

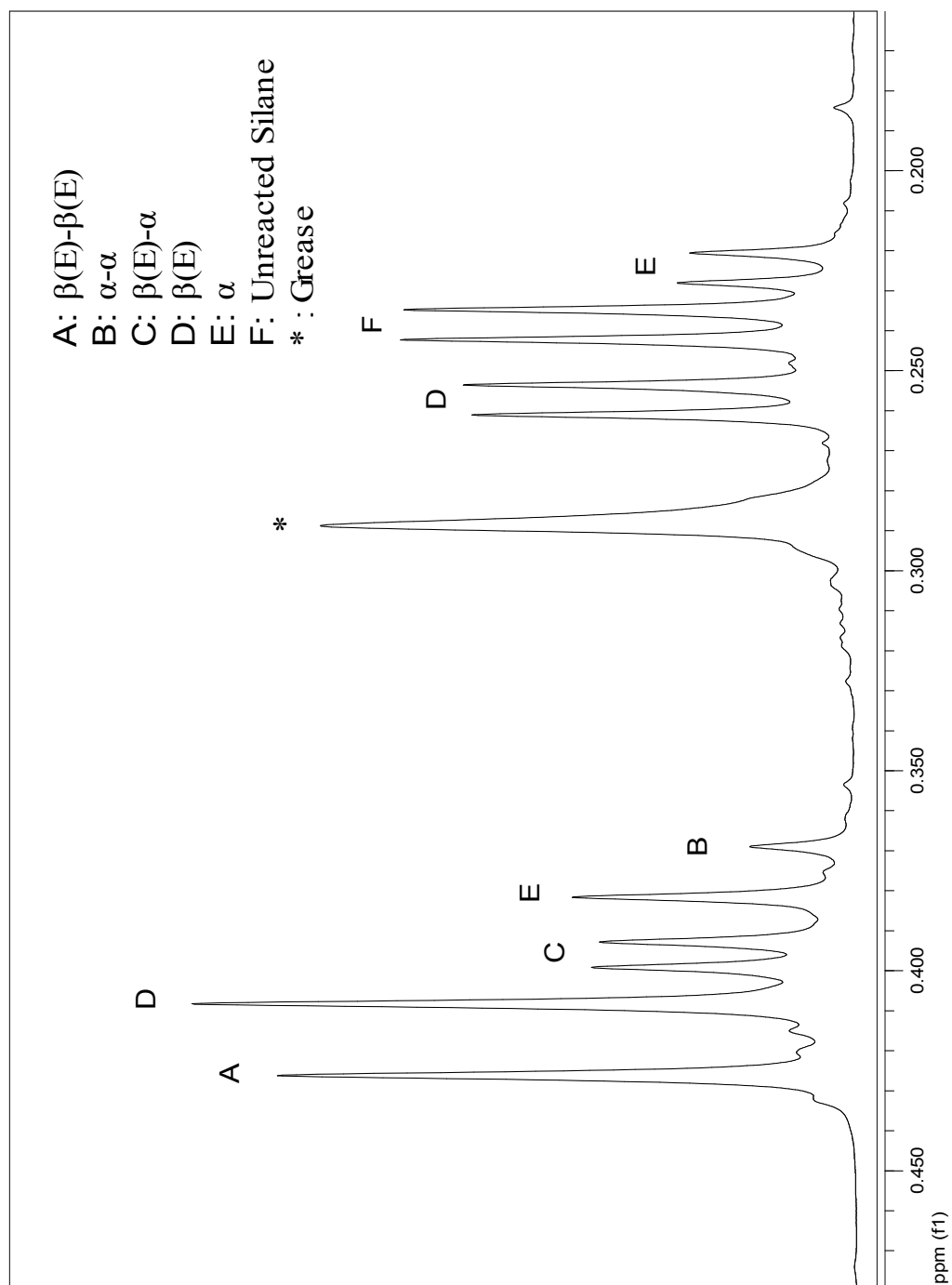


Figure 5.2.3.3. ^1H NMR Spectra of Reaction 223 Methyl Protons after 5 Hours.

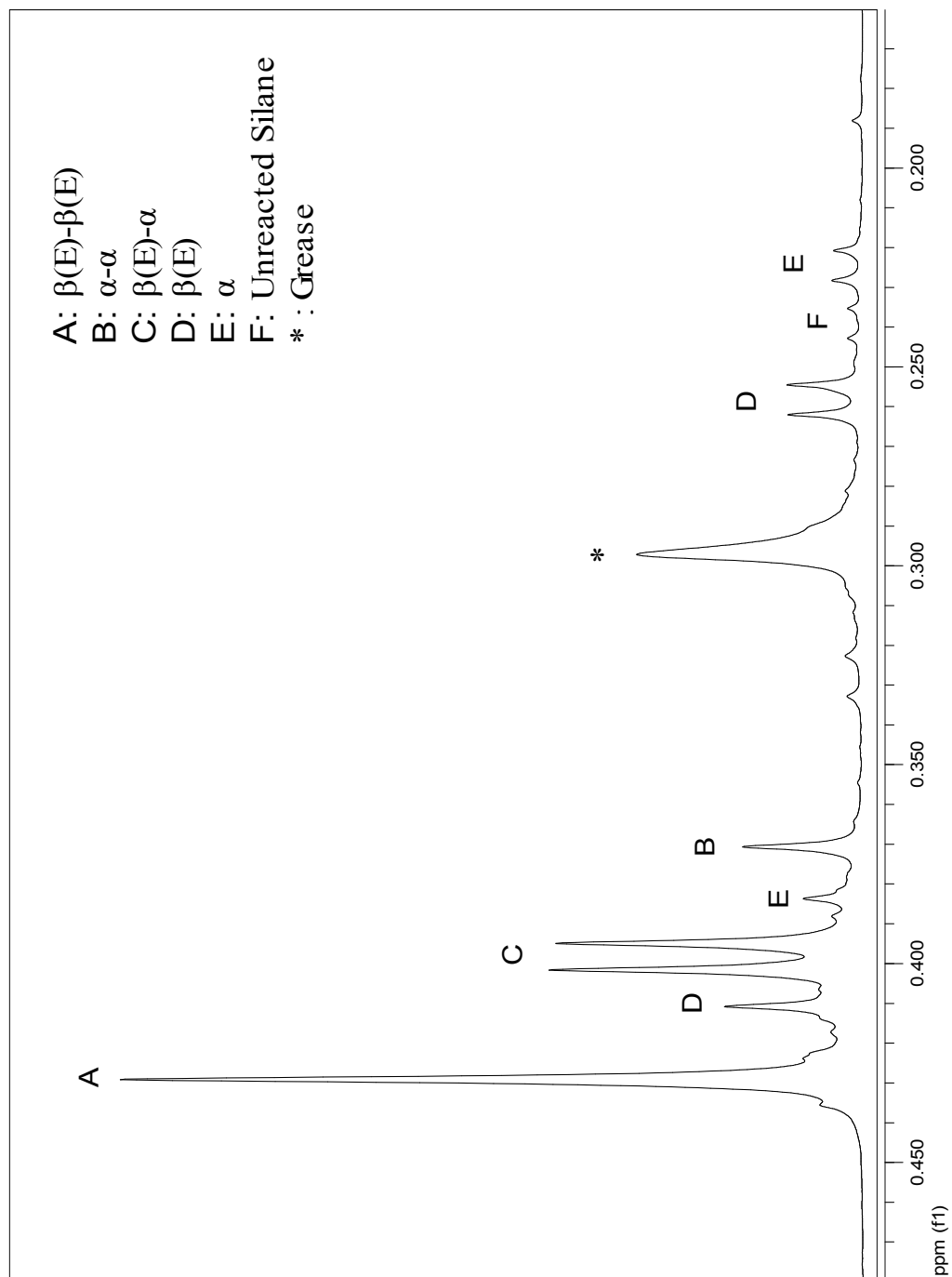


Figure 5.2.3.4. ^1H NMR Spectra of Reaction 223 Methyl Protons after 20 Hours.

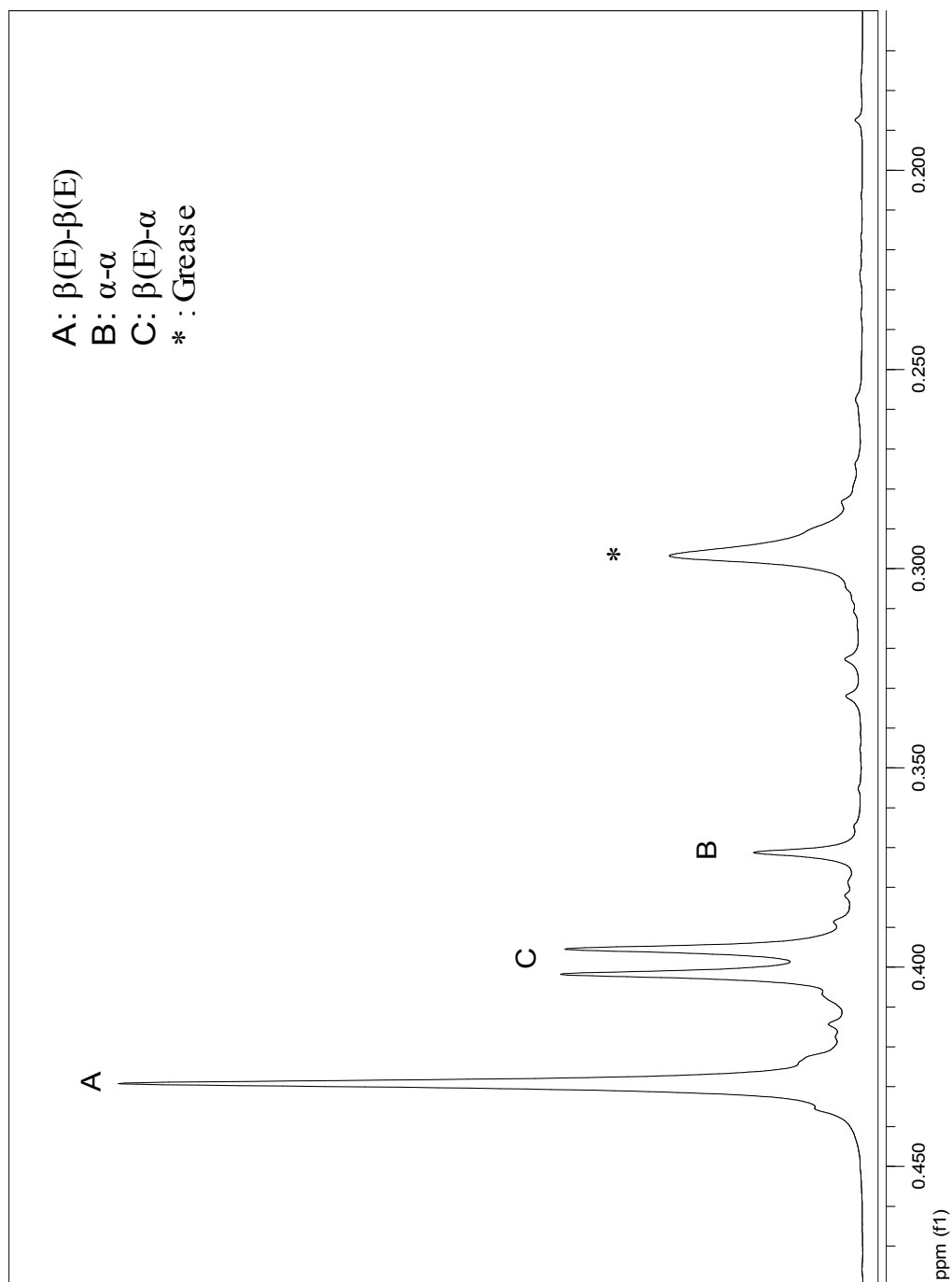


Figure 5.2.3.5. ^1H NMR Spectra of Reaction 223 Methyl Protons after Completion.

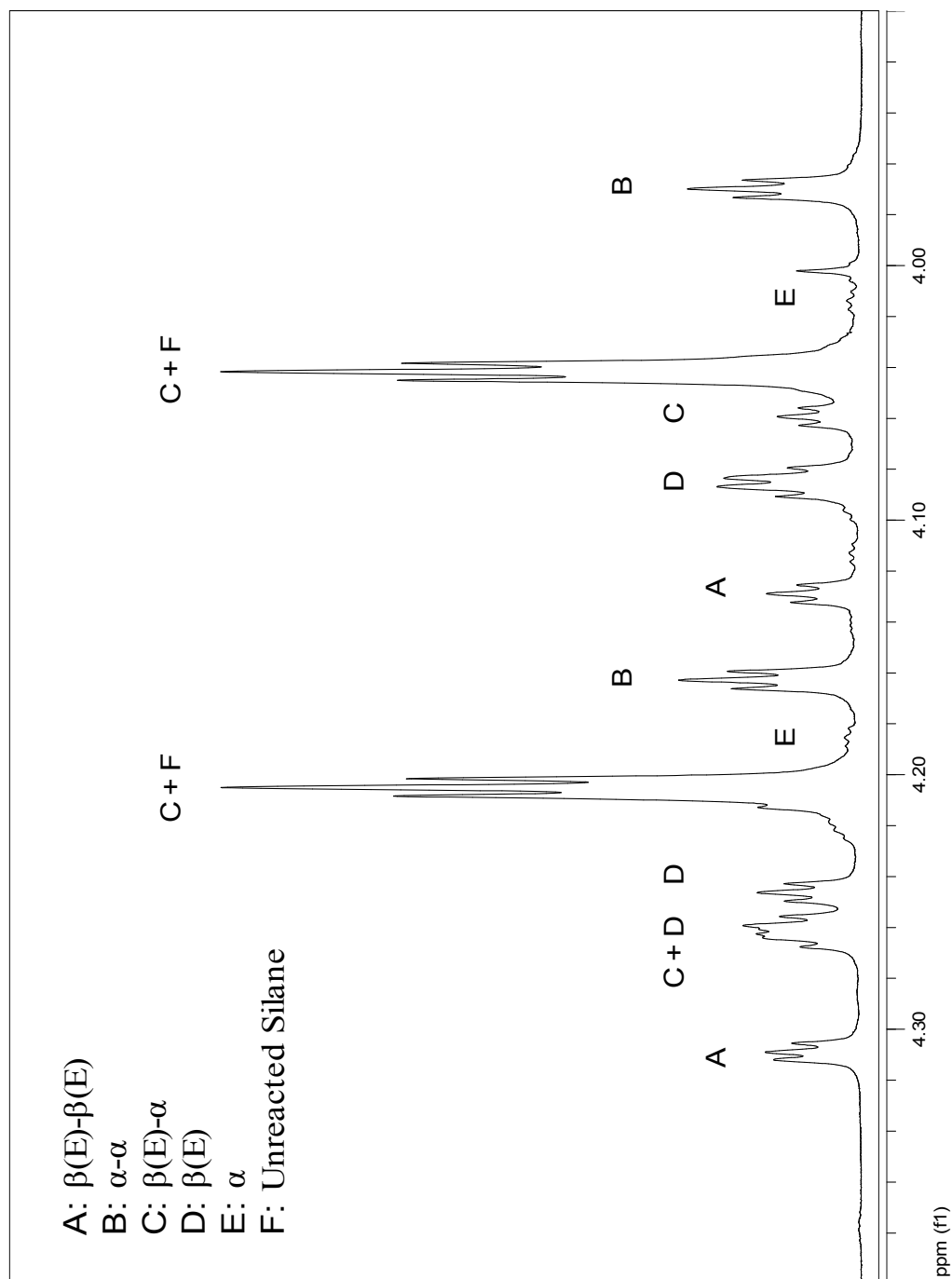


Figure 5.2.3.6. ^1H NMR Spectra of Reaction 224 Cp Protons after 1 Hour.

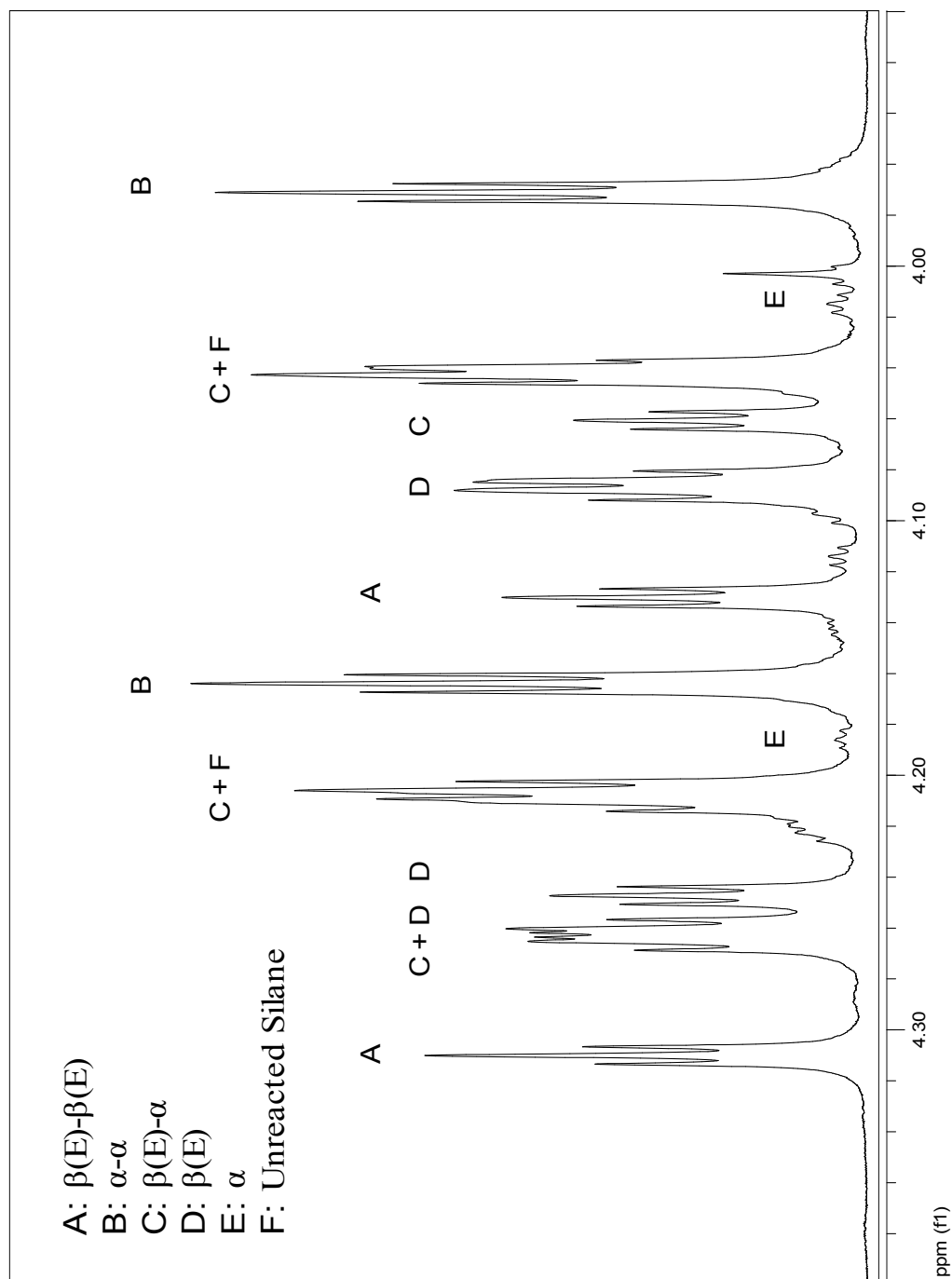


Figure 5.2.3.7. ^1H NMR Spectra of Reaction 224 Cp Protons after 5 Hours.

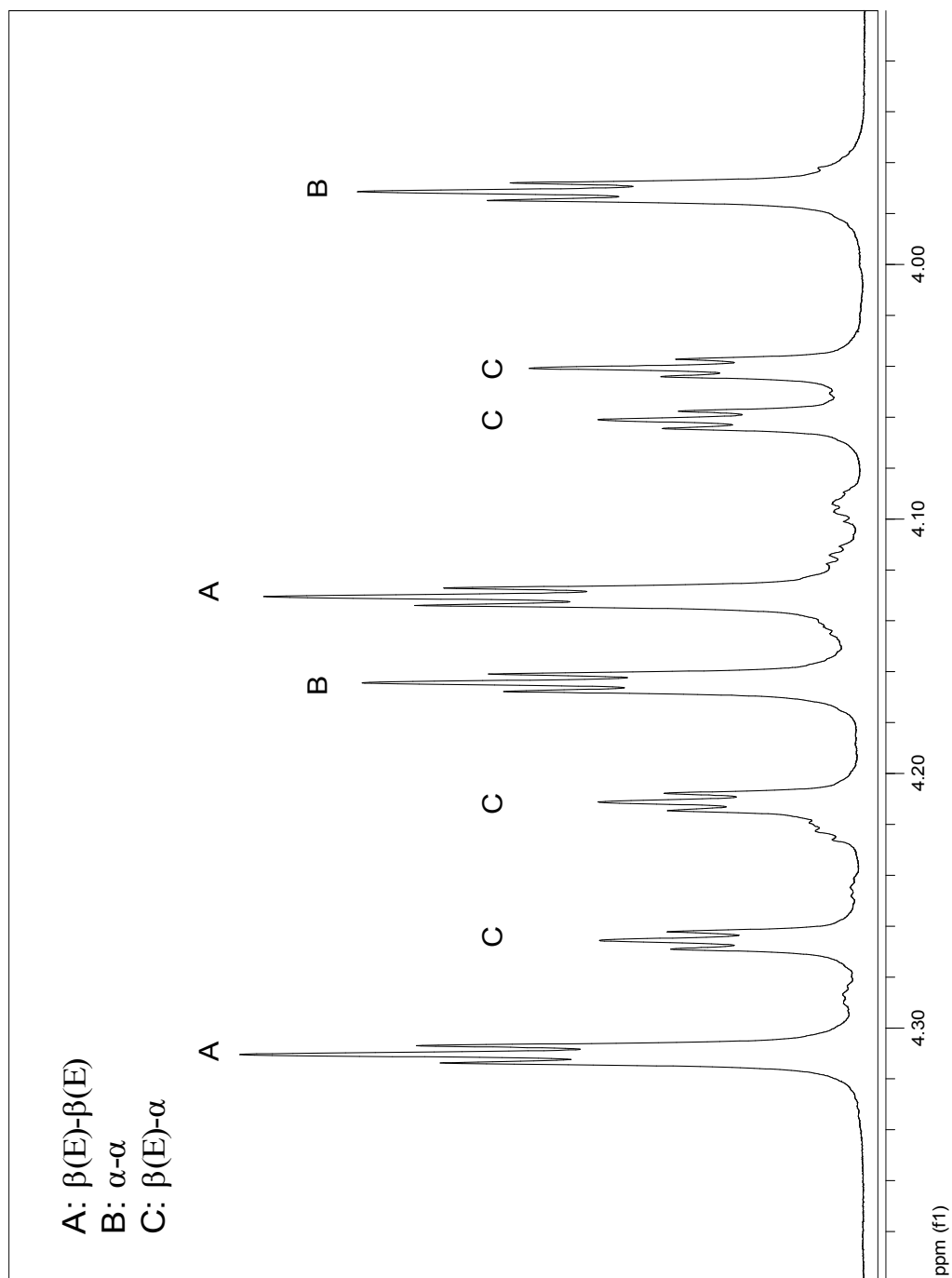


Figure 5.2.3.8. ^1H NMR Spectra of Reaction 224 Cp Protons after Completion.

5.3. Summary

One notable observation was the lower $\beta(\text{E})$ - to α - olefinic proton ratio in hydrosilylation reactions of *bis*(dimethylsilyl)- ferrocene or troticene derivatives compared to dimethylsilyl- ferrocene or troticene derivatives. On the other hand, both the hydrosilylation reactions of either 1,4-*bis*(dimethylsilyl)benzene or dimethylsilylbenzene gave results consistent with that of dimethylsilylferrocene. It was inferred from these results that the discrepancy in regiochemical distribution was not due to an electronic effect of the ferrocene moiety on the silane, but rather the fact that, unlike those of 1,4-*bis*(dimethylsilyl)benzene, the two dimethylsilyl groups on 1,1'-*bis*(dimethylsilyl)ferrocene are attached to ligands that can rotate along an axis, bringing the two dimethylsilyl groups into close proximity of each other which somehow affects the regioselectivity of the hydrosilylation reaction.

A comparison between the hydrosilylation of 1,1'-*bis*(dimethylsilyl)ferrocene and 1,4-*bis*(dimethylsilyl)benzene was aided by comparing the hydrosilylation reactions of the mono- $\beta(\text{E})$ -adducts of both silanes. It was shown the hydrosilylation of both the mono- $\beta(\text{E})$ - and mono- α - adducts of *bis*(dimethylsilyl)benzene preferentially led to a $\beta(\text{E})$ - configuration. On the other hand, while the mono- $\beta(\text{E})$ - adduct of *bis*(dimethylsilyl)ferrocene preferentially led to a $\beta(\text{E})$ - configuration, the mono- α - adduct preferentially led to an α - configuration. In addition, the mono- α - adduct of ferrocene appeared to be consumed faster than the mono- $\beta(\text{E})$ - adduct. These factors led to an increased amount of α -olefinic protons in hydrosilylation reactions of 1,1'-*bis*(dimethylsilyl)ferrocene.

Experimental Section

General Methods. All operations were performed under nitrogen using Schlenk techniques or in a Braun MB150 inert atmosphere glovebox. NMR spectroscopy was performed on a Varian VXR-400S (400 MHz) and a Varian Unity Inova (500 MHz) NMR FT spectrometers. All ^1H and ^{13}C NMR spectra were referenced internally to d_6 -benzene solvent (δ 7.16 ppm and δ 128.38 ppm, respectively). ^{29}Si DEPT, ^{119}Sn , and ^{31}P NMR were referenced externally to tetramethylsilane (δ 0.0 ppm), tetraethyltin (δ 1.0 ppm), and 85 % phosphoric acid (δ 0.0 ppm), respectively. Gas Chromatography-Mass Spectrometry (GC/MS) was performed on a Hewlett Packard HP 6890 series Gas Chromatograph with a HP 7683 series injector and a HP 5973 mass selective detector. Gel Permeation Chromatography (GPC) was performed on a Waters Breeze system with a Waters 717plus Autosampler, a Waters 1525 Binary HPLC Pump, a Waters 2487 Dual λ Absorbance Detector, and a Waters 2414 Refractive Index Detector. MALDI-TOF-TOF measurements were performed by Dr. Anand Sundararaman on an Applied Biosystems 4700 Proteomics Analyzer. Cyclic voltammetry was performed on a BAS CV-50W voltammetric analyzer using $[\text{Bu}_4\text{N}][\text{B}(\text{C}_6\text{F}_5)_4]$ as supporting electrolyte and either ferrocene or decamethylferrocene as internal standard. Elemental analyses were performed by Robertson Microlit Laboratories, Inc. (Madison, NJ). X-ray structures were done by Dr. Roger A. Lalancette (Rutgers-Newark) (**202c**, **206d** and **210c**) and Dr. Alan J. Lough (University of Toronto) (**206d**, **204d** and **207d**) (See details below).

X-ray Crystal Structure Determination.

For 202c: Crystals of **202c** were mounted on a glass fiber using cyanoacrylate cement. Intensity data were collected on a Siemens P4 diffractometer at 293 K using a graphite monochromated Mo K α radiation ($\lambda = 0.71073$ Å). Lorentz, polarization, and empirical absorption corrections were applied to the data set. The structure was solved by direct methods. Non-hydrogen atoms were refined anisotropically by full-matrix least-squares methods to minimize $\Sigma w(F_o - F_c)^2$, where $w^{-1} = \sigma^2(F) + g(F)^2$. Hydrogen atoms were included in calculated positions. Crystal data, data collection, and least-squares parameters for **202c** are listed in **Table A.1.***. All calculations were performed and graphics created using SHELXTL v6.14²⁹³ and Mercury v1.4.1.²⁹⁴

For 206d and 210c: Crystals were mounted on a Cryoloop using Paratone-N. Intensity data were collected on a Bruker Apex 2 CCD area-detector diffractometer at 100 K using Cu K α radiation ($\lambda = 1.54178$ Å). Data were collected using both ω and ϕ scans.²⁹⁵ Lorentz, polarization, numerical absorption, and empirical absorption corrections were applied to the data set.^{296,297} The structures were solved by direct methods. Non-hydrogen atoms were refined anisotropically by full-matrix least-squares methods to minimize $\Sigma w(F_o - F_c)^2$, where $w^{-1} = \sigma^2(F) + g(F)^2$. Hydrogen atoms were found in electron density maps, but were placed in geometrically idealized positions and constrained to ride on their parent C atoms (the methyl hydrogen atoms were put in ideally staggered positions). Crystal data, data collection, and least-squares parameters for **206d** and **210c** are listed in **Table A.2.*** and **Table A.5.***, respectively. All calculations were performed and graphics created using SHELXTL v6.14²⁹³ and Mercury v1.4.1.²⁹⁴

For 204d and 207d: Data were collected on a Bruker-Nonius Kappa-CCD diffractometer using monochromated Mo K α , and were measured using a combination of ϕ scans with ω scans with κ offsets, to fill the Ewald sphere. The data were processed using Denzo-SMN package.²⁹⁸ Absorption corrections were carried out using SORTAV.²⁹⁹ The structure was solved and refined by full-matrix least-squares methods to minimize $\Sigma w(F_o - F_c)^2$, where $w^{-1} = \sigma^2(F) + g(F)^2$. Crystal data, data collection, and least-squares parameters for **204d** and **207d** are listed in **Table A.3.*** and **Table A.4.***, respectively. All calculations were performed and graphics created using SHELXTL v6.1³⁰⁰ and Mercury v1.4.1.²⁹⁴

Materials. Solvents were dried over sodium/benzophenone (ether, tetrahydrofuran, and toluene), or calcium hydride (dichloromethane and hexane), and distilled prior to use. Column chromatography was performed on silica (standard grade, 60 Å, 32-63 μ , from Sorbent Technologies), neutral Alumina (~150 mesh, from Aldrich Chemical Company, Inc.), or Florisil[®] (100-200 mesh, from Fisher Scientific), with the latter two being deactivated with 5% (by weight) water prior to use. Celite[®] used for filtrations was purchased from Aldrich Chemical Company, Inc. NMR solvents were purchased from Cambridge Isotope Laboratories, Inc. Reagents were purchased from Acros Organics, Aldrich Chemical Company Inc., GFS Chemicals Inc. and Strem Chemicals Inc. Karstedt's catalyst (platinum-divinyltetramethyldisiloxane complex; 3-3.5% Pt concentration in vinyl terminated polydimethylsiloxane), and 1,4-*bis*-(dimethylsilyl)benzene was purchased from Gelest, Inc. Dimethylsilylbenzene was purchased from Aldrich Chemical Company, Inc. 1,3-Diethynylbenzene, ethynylbenzene,

and 4-ethynyltoluene were purchased from GFS Chemicals, Inc. (η^7 -Cycloheptatrienyl)(η^5 -cyclopentadienyl)titanium(II),³⁰¹ $\{\eta^7$ -(lithio)cycloheptatrienyl} $\{\eta^5$ -cyclopentadienyl}titanium(II),^{1,2} $\{\eta^7$ -(lithio)cycloheptatrienyl} $\{\eta^5$ -(lithio)cyclopentadienyl}titanium(II)·2TMEDA,^{3,210,214} $\{\eta^7$ -(trimethylsilyl)cycloheptatrienyl} $\{\eta^5$ -cyclopentadienyl}titanium(II),²⁰⁷ (η^7 -cycloheptatrienyl) $\{\eta^5$ -(trimethylsilyl)cyclopentadienyl}titanium(II),²⁶⁷ $\{\eta^7$ -(trimethylsilyl)cycloheptatrienyl} $\{\eta^5$ -(trimethylsilyl)cyclopentadienyl}titanium(II),²¹⁰ $\{\eta^7$ -(dimethylphosphino)cycloheptatrienyl} $\{\eta^5$ -cyclopentadienyl}titanium(II),^{208,209} dimethylsilylferrocene,⁴ 1,1'-bis(dimethylsilyl)ferrocene,³⁰² 1,4-diethynylbenzene,³⁰³ 2,5-diethynylthiophene,³⁰⁴ and 2-ethynylthiophene³⁰⁴ were prepared using literature procedures.

Troticene Derivatives via Lithiation.

General Procedure for Monosubstitution at the η^7 -Cycloheptatrienyl Ligand of Troticene and Troticene Derivatives. The procedure was modified from the synthesis of (η^7 -methylcycloheptatrienyl)(η^5 -cyclopentadienyl)titanium(II).^{1,2} *n*-Butyllithium (1 equiv.) was added dropwise over 30 minutes to a stirred slurry of troticene (1 equiv.) in diethylether (10 ml ether per 0.10 g troticene) at 0 °C. The reaction mixture turned from blue to brown/black in color after being stirred at 0 °C for 6 hours. Cooling to -78°C (acetone/dry ice) and addition of a slight excess of the appropriate quenching agent dropwise over 15 minutes was followed by warming slowly to room temperature overnight. All volatile components were then removed under vacuum and the residue extracted with hexane, filtered through Celite®, and filtered again through a small amount of deactivated alumina (2.20 g) in a pipet to give a crude product mixture.

Components and product distribution of the crude product mixture were determined using GC/MS and ^1H NMR spectroscopy, and the desired product isolated using column chromatography on deactivated alumina or Florisil[®]. Tropicene derivatives required more equivalents of *n*-butyllithium.

General Procedure for Monosubstitution on the η^5 -Cyclopentadieny Ligand of Tropicene and Tropicene Derivatives. *n*-Butyllithium (1 equiv.) was added dropwise over 30 minutes to a stirred slurry of tropicene (1 equiv.) in diethylether (10 ml ether per 0.10 g tropicene) at room temperature. The reaction mixture turned from blue to brown/black in color after being stirred at room temperature for 6 hours. Cooling to -78°C (acetone/dry ice) and addition of a slight excess of the appropriate quenching agent dropwise over 15 minutes was followed by warming slowly to room temperature overnight. All volatile components were then removed under vacuum and the residue extracted with hexane, filtered through Celite[®], and filtered again through a small amount of deactivated alumina (2.20 g) in a pipet to give a crude product mixture. Components and product distribution of the crude product mixture were determined using GC/MS and ^1H NMR spectroscopy, and the desired product isolated using column chromatography on deactivated alumina or Florisil[®]. Tropicene derivatives required more equivalents of *n*-butyllithium.

General Procedure for Disubstitution and Tetrasubstitution of Tropicene and Tropicene Derivatives. The procedure was modified from the synthesis of $\{\eta^7\text{-(diphenylphosphino)cycloheptatrienyl}\}$ $\{\eta^5\text{-(diphenylphosphino)cyclopentadienyl}\}$ titanium(II).^{3,210,214} A slurry of tropicene (1 equiv.) in hexane (6 ml hexane per 0.10 g tropicene) was added slowly over 15 minutes to a stirred mixture of hexane (6 ml hexane

per 0.10 g troticene), *n*-butyllithium (2.5 equiv.), and TMEDA (*n*-BuLi : TMEDA mole ratio = 1 : 1.2) at room temperature. The reaction mixture turned from blue to brown/black in color immediately, and was stirred at room temperature for 24 hours. Cooling to -78 °C (acetone/dry ice) and addition of a slight excess of the appropriate quenching agent dropwise over 15 minutes was followed by warming slowly to room temperature overnight. All volatile components were then removed under vacuum and the residue extracted with hexane, filtered through Celite[®], and filtered again through a small amount of deactivated alumina (2.20 g) in a pipet to give a crude product mixture. Components and product distribution of the crude product mixture were determined using GC/MS and ¹H NMR spectroscopy, and isolated using column chromatography on deactivated alumina or Florisil[®]. Tropicene derivatives required more equivalents of *n*-BuLi-TMEDA.

General Procedure for Purification via Column Chromatography. Column chromatography was performed on deactivated Alumina or Florisil[®] (5% water by weight). It was observed that the products were more stable, particularly the Sn-containing compounds, on deactivated Florisil[®] compared to deactivated Alumina. Hexanes with 0.5% triethylamine by volume was flushed through the columns prior to sample loading. In general, the crude product was dissolved in a minimum amount of hexanes, loaded onto the column, and eluted with hexanes (with 0.5% triethylamine by volume) to give a broad blue band. Multiple fractions were collected and analyzed by GC/MS and ¹H NMR spectroscopy. The sequence of elution is as follows: tetrasubstituted (1,4-disubstituted Cht) (**207**) eluted first, then followed sequentially by tetrasubstituted (1,3-disubstituted Cht) (**208**), trisubstituted (1,4-disubstituted Cht) (**204**),

trisubstituted (1,3-disubstituted Cht) (**205**), trisubstituted (1,3-disubstituted Cp) (**206**), disubstituted (monosubstituted Cht and Cp) (**203**), monosubstituted (Cht) (**201**), monosubstituted (Cp) (**202**), and troticene. Fractions containing a mixture of the products were rechromatographed as necessary. In the case of the diphenylphosphine substituted derivative, the solvent used was a mixture of hexanes (with 0.5% triethylamine by volume) and toluene (90 % hexanes/10 % toluene). In that case, the unreacted starting material eluted first, followed by the (η^7 -cycloheptatrienyl) monosubstituted product, then the (η^5 -cyclopentadienyl) monosubstituted product, with the disubstituted product eluting last.

(η^7 -Cycloheptatrienyl) Monosubstituted Derivatives.

{ η^7 -(Dimethylsilyl)cycloheptatrienyl}{ η^5 -cyclopentadienyl}titanium(II)

(201a). Complex **201a** was prepared from troticene (0.600 g; 2.939 mmol), *n*-BuLi (1.84 ml of 1.6 M solution in hexane; 2.944 mmol), and chlorodimethylsilane (0.36 ml; 0.306 g, 96 %; 3.105 mmol) as described in the general procedure above and was isolated as a blue oil. Product distribution of crude product: **201a** (85 %), **202a** (10 %), **203a** (5 %). **201a Yield:** 0.402 g, 1.533 mmol, 52 %. **201a:** ^1H NMR (399.8 MHz, C_6D_6), ^{13}C { ^1H } NMR (100.5 MHz, C_6D_6), ^{29}Si DEPT NMR (79.4 MHz, C_6D_6): See **Table 2.1.1.1**. *m/e* = 262 (M^+). Elemental Analysis Calculated for $\text{C}_{14}\text{H}_{18}\text{SiTi}$: C, 64.10; H, 6.93. Found: C, 63.12; H, 6.58.

{ η^7 -(Trimethylstannyl)cycloheptatrienyl}{ η^5 -cyclopentadienyl}titanium(II)

(201b). Complex **201b** was prepared from troticene (0.600 g; 2.939 mmol), *n*-BuLi (1.84 ml of 1.6 M solution in hexane; 2.944 mmol), and chlorotrimethylstannane (0.620 g, 98

%; 3.049 mmol; dissolved in 10ml hexane) as described in the general procedure above and was isolated as a blue solid. Product distribution of crude product: **201b** (79 %), **202b** (13 %), **203b** (8 %). **201b Yield:** 0.378 g, 1.030 mmol, 35 %. **201b:** ^1H NMR (499.9 MHz, C_6D_6), ^{13}C $\{^1\text{H}\}$ NMR (125.7 MHz, C_6D_6), ^{119}Sn $\{^1\text{H}\}$ NMR (186.4 MHz, C_6D_6): See **Table 2.1.1.1**. $m/e = 368$ (M^+).

$\{\eta^7\text{-(Diphenylphosphino)cycloheptatrienyl}\}(\eta^5\text{-cyclopentadienyl})\text{titanium(II)}$ (201c**).**^{208,209} Complex **3A0B** was prepared from troiticene (0.50 g; 2.449 mmol), *n*-BuLi (1.54 ml of 1.6 M solution in hexane; 2.464 mmol), and chlorodiphenylphosphine (0.48 ml, 0.590 g, 95 %; 2.540 mmol) as described in the general procedure. The crude product was dissolved in hot toluene then cooled to -30°C , from which complex **201c** was isolated as a blue solid. **201c Yield:** 0.631 g, 1.625 mmol, 66 %. **201c:** ^1H NMR (499.9 MHz, C_6D_6), ^{13}C $\{^1\text{H}\}$ NMR (125.7 MHz, C_6D_6), ^{31}P $\{^1\text{H}\}$ NMR (202.4 MHz, C_6D_6): See **Table 2.1.1.1**. $m/e = 388$ (M^+).

$\{\eta^7\text{-(Trimethylsilyl)cycloheptatrienyl}\}(\eta^5\text{-cyclopentadienyl})\text{titanium(II)}$ (201d**).**²⁰⁷ Complex **201d** was prepared from troiticene (0.600 g; 2.939 mmol), *n*-BuLi (1.84 ml of 1.6 M solution in hexane; 2.944 mmol), and chlorotrimethylsilane (0.40 ml; 0.340 g, 98 %; 3.067 mmol) as described in the general procedure above and was isolated as a blue solid. Product distribution of crude product: **201d** (91 %), **202d** (6 %), **203d** (3 %). **201d Yield:** 0.498 g, 1.802 mmol, 61 %. **201d:** ^1H NMR (499.9 MHz, C_6D_6), ^{13}C $\{^1\text{H}\}$ NMR (125.7 MHz, C_6D_6), ^{29}Si DEPT NMR (79.4 MHz, C_6D_6): See **Table 2.1.1.1**. $m/e = 276$ (M^+).

(η^5 -Cyclopentadienyl) Monosubstituted Derivatives.

(η^7 -Cycloheptatrienyl){ η^5 -(dimethylsilyl)cyclopentadienyl}titanium(II)

(202a). Complex **202a** was prepared from troticene (0.600 g; 2.939 mmol), *n*-BuLi (1.84 ml of 1.6 M solution in hexane; 2.944 mmol), and chlorodimethylsilane (0.36 ml; 0.306 g, 96 %; 3.105 mmol) as described in the general procedure above and was isolated as a blue solid. Product distribution of crude product: **201a** (4 %), **202a** (75 %), **203a** (21 %). **202a Yield:** 0.318 g, 1.212 mmol, 41 %. **202a:** ^1H NMR (499.9 MHz, C_6D_6), ^{13}C { ^1H } NMR (125.7 MHz, C_6D_6), ^{29}Si DEPT NMR (99.3 MHz, C_6D_6): See **Table 2.1.2.1**. $m/e = 262$ (M^+). Elemental Analysis Calculated for $\text{C}_{14}\text{H}_{18}\text{SiTi}$: C, 64.10; H, 6.93. Found: C, 63.13; H, 6.78.

(η^7 -Cycloheptatrienyl){ η^5 -(trimethylstannyl)cyclopentadienyl}titanium(II)

(202b). Complex **202b** was prepared from troticene (0.600 g; 2.939 mmol), *n*-BuLi (1.84 ml of 1.6 M solution in hexane; 2.944 mmol), and chlorotrimethylstannane (0.620 g, 98 %; 3.049 mmol; dissolved in 10ml hexane) as described in the general procedure above and was isolated as a blue solid. Product distribution of crude product: **201b** (6 %), **202b** (72 %), **203b** (22 %). **202b Yield:** 0.346 g, 0.943 mmol, 32 %. **202b:** ^1H NMR (499.9 MHz, C_6D_6), ^{13}C { ^1H } NMR (125.7 MHz, C_6D_6), ^{119}Sn { ^1H } NMR (186.4 MHz, C_6D_6): See **Table 2.1.2.1**. $m/e = 368$ (M^+).

(η^7 -Cycloheptatrienyl){ η^5 -(diphenylphosphino)cyclopentadienyl}titanium(II)

(202c). Complex **202c** was prepared from troticene (0.600 g; 2.939 mmol), *n*-BuLi (1.84 ml of 1.6 M solution in hexane; 2.944 mmol), and chlorodiphenylphosphine (0.58 ml; 0.713 g, 95 %; 3.069 mmol) as described in the general procedure above and was isolated as a blue solid. Product distribution of crude product: **201c** (5 %), **202c** (75 %), **203c** (20

%). **202c Yield:** 0.402 g, 1.035 mmol, 35 %. Recrystallization from toluene at -30 °C produced blue crystals. **202c:** ^1H NMR (499.9 MHz, C_6D_6), ^{13}C $\{^1\text{H}\}$ NMR (125.7 MHz, C_6D_6), ^{31}P $\{^1\text{H}\}$ NMR (202.4 MHz, C_6D_6): See **Table 2.1.2.1**. $m/e = 388$ (M^+). Elemental Analysis Calculated for $\text{C}_{24}\text{H}_{21}\text{PTi}$: C, 74.23; H, 5.46. Found: C, 74.22; H, 5.27.

(η^7 -Cycloheptatrienyl){ η^5 -(trimethylsilyl)cyclopentadienyl}titanium(II)

(202d).²⁶⁷ Complex **202d** was prepared from troticene (0.600 g; 2.939 mmol), *n*-BuLi (1.84 ml of 1.6 M solution in hexane; 2.944 mmol), and chlorotrimethylsilane (0.40 ml; 0.340 g, 98 %; 3.067 mmol) as described in the general procedure above and was isolated as a blue solid. Product distribution of crude product: **201d** (6 %), **202d** (68 %), **203d** (26 %). **202d Yield:** 0.324 g, 1.172 mmol, 40 %. **202d:** ^1H NMR (499.9 MHz, C_6D_6), ^{13}C $\{^1\text{H}\}$ NMR (125.7 MHz, C_6D_6), ^{29}Si DEPT NMR (79.4 MHz, C_6D_6): See **Table 2.1.2.1**. $m/e = 276$ (M^+).

Monolithiation of Tropicene at either 0 °C or Room Temperature. (≈ 25 °C).

Lithiation at 0 °C. Monolithiation of troticene (0.200 g; 0.980 mmol) was carried out at 0 °C with 0.8 equivalents *n*-BuLi (0.50 ml of 1.6 M solution in hexane; 0.800 mmol) as described in the general procedure above, with a small amount of hexamethylbenzene (0.020 g; 0.123 mmol) added as an internal standard. One aliquot (**I**) ($\approx 1/4$ of total reaction mixture) was drawn after 6 hours then quenched at -78°C with chlorotrimethylsilane (0.06 ml; 0.051 g, 98 %; 0.460 mmol for each aliquot). Two more aliquots were drawn after 20 hours, one of which was kept at 0°C (**II**) and the other was warmed up to room temperature (**III**) for another four hours, then quenched at -78°C with chlorotrimethylsilane. The remaining reaction mixture was allowed to react for 48 hours

(IV) before quenching with chlorotrimethylsilane. The crude product mixtures were isolated as described in the general procedure above. Low vacuum (≈ 200 mm Hg) was used to remove the solvent during isolation of the crude product, which was never left under vacuum for extended periods of time to minimize any loss of the hexamethylbenzene internal standard via sublimation. Product distributions were determined relative to hexamethylbenzene from integration of the ^1H NMR spectra of the crude products. Results are shown on **Scheme 2.1.3.1**.

Lithiation at Room Temperature (≈ 25 °C). Monolithiation of troiticene (0.200 g; 0.980 mmol) was carried out at room temperature (≈ 25 °C) with 0.8 equivalents *n*-BuLi (0.50 ml of 1.6 M solution in hexane; 0.800 mmol) as described in the general procedure above, with a small amount of hexamethylbenzene (0.010 g; 0.062 mmol) added as an internal standard. Aliquots were drawn using a cannula after 3 (**I**), 6 (**II**), and 12 (**III**) hours then quenched with excess chlorotrimethylsilane (0.06 ml; 0.051 g, 98 %; 0.460 mmol for each aliquot). The crude product mixture was isolated as described in the general procedure above. Low vacuum (≈ 200 mm Hg) was used to evaporate solvent during isolation of the crude product, which was never left under vacuum for extended periods of time to minimize any loss of the hexamethylbenzene internal standard via sublimation. Product distributions were determined relative to hexamethylbenzene from integration of the ^1H NMR spectra of the crude products. Results are shown on **Scheme 2.1.3.2**.

Disubstituted Derivatives.

$\{\eta^7\text{-(Dimethylsilyl) cycloheptatrienyl}\} \{\eta^5\text{-(dimethylsilyl) cyclopentadienyl}\}$ titanium(II) (203a). Complex **203a** was prepared from troticene (0.800 g; 3.919 mmol), *n*-BuLi (6.14 ml of 1.6 M solution in hexane; 9.824 mmol), TMEDA (1.82 ml; 1.401 g, 99 %; 11.939 mmol), and chlorodimethylsilane (1.40 ml; 1.190 g, 96 %; 12.074 mmol) as described in the general procedure above and was isolated as a blue oil. **203a Yield:** 0.929 g, 2.899 mmol, 74 %. **203a:** ^1H NMR (399.9 MHz, C_6D_6), ^{13}C $\{^1\text{H}\}$ NMR (100.5 MHz, C_6D_6), ^{29}Si DEPT NMR (79.4 MHz, C_6D_6): See **Table 2.2.1**. $m/e = 320$ (M^+). Elemental Analysis Calculated for $\text{C}_{16}\text{H}_{24}\text{Si}_2\text{Ti}$: C, 59.96; H, 7.56. Found: C, 58.64; H, 6.78.

$\{\eta^7\text{-(Trimethylstannyl)cycloheptatrienyl}\} \{\eta^5\text{-(trimethylstannyl) cyclopentadienyl}\}$ titanium(II) (203b). Complex **203b** was prepared from troticene (0.400 g; 1.959 mmol), *n*-BuLi (3.06 ml of 1.6 M solution in hexane; 4.896 mmol), TMEDA (0.92 ml; 0.708 g, 99 %; 6.035 mmol), and chlorotrimethylstannane (1.228 g, 98 %; 6.040 mmol; dissolved in 10ml hexane) as described in the general procedure above and was isolated as a blue solid. **203b Yield:** 0.644 g, 1.216 mmol, 62 %. **203b:** ^1H NMR (499.9 MHz, C_6D_6), ^{13}C $\{^1\text{H}\}$ NMR (125.7 MHz, C_6D_6), ^{119}Sn $\{^1\text{H}\}$ NMR (186.4 MHz, C_6D_6): See **Table 2.2.1**. $m/e = 530$ (M^+). Elemental Analysis Calculated for $\text{C}_{18}\text{H}_{28}\text{Sn}_2\text{Ti}$: C, 40.81; H, 5.34. Found: C, 40.64; H, 5.16.

$\{\eta^7\text{-(Trimethylsilyl)cycloheptatrienyl}\} \{\eta^5\text{-(trimethylsilyl) cyclopentadienyl}\}$ titanium(II) (203d).²¹⁰ Complex **203d** was prepared from troticene (0.400 g; 1.959 mmol), *n*-BuLi (3.06 ml of 1.6 M solution in hexane; 4.896 mmol), TMEDA (0.92 ml; 0.708 g, 99 %; 6.035 mmol), and chlorotrimethylsilane (0.80 ml; 0.680 g, 98 %; 6.134

mmol) as described in the general procedure above and was isolated as a blue solid. **203d**
Yield: 0.484 g, 1.389 mmol, 71 %. **203d:** ^1H NMR (499.9 MHz, C_6D_6), ^{13}C $\{^1\text{H}\}$ NMR (125.7 MHz, C_6D_6), ^{29}Si DEPT NMR (79.4 MHz, C_6D_6): See **Table 2.2.1**. $m/e = 348$ (M^+).

Trisubstituted and Tetrasubstituted Derivatives via 1-Pot Reaction.

$\{\eta^7\text{-(Trimethylsilyl)cycloheptatrienyl}\}$ $[\eta^5\text{-}\{1,3\text{-bis(trimethylsilyl)}\}$
 $\text{cyclopentadienyl}]\text{titanium(II)}$ (**206d**), $[\eta^7\text{-}\{1,4\text{-Bis(trimethylsilyl)}\}$ cycloheptatrienyl]
 $\{\eta^5\text{-(trimethylsilyl)cyclopentadienyl}\}\text{titanium(II)}$ (**204d**), $[\eta^7\text{-}\{1,4\text{-Bis(trimethylsilyl)}\}$
 $\text{cycloheptatrienyl}][\eta^5\text{-}\{1,3\text{-bis(trimethylsilyl)}\}\text{cyclopentadienyl}]\text{titanium(II)}$ (**207d**).
 Complexes **206d**, **204d**, and **207d** were prepared from troticene (0.200 g; 0.980 mmol),
 $n\text{-BuLi}$ (4.90 ml of 1.6 M solution in hexane; 7.840 mmol), TMEDA (1.44 ml; 1.109 g,
 99 %; 9.446 mmol), and chlorotrimethylsilane (1.24 ml; 1.054 g, 98 %; 9.508 mmol) as
 described in the general procedure above. Product distribution of crude product: **203d** (24
 %), **206d** (7 %), **204d** (18 %), **205d** (3 %), **207d** (44 %), **208d** (4 %). Attempts to isolate
205d and **208d** were unsuccessful. **203d**, **206d**, **204d**, and **207d** were isolated as blue
 solids. **203d Yield:** 0.061 g, 0.175 mmol, 18 %; **206d Yield:** 0.016 g, 0.038 mmol, 4 %;
204d Yield: 0.052 g, 0.124 mmol, 13 %; **207d Yield:** 0.161 g, 0.327 mmol, 33 %.
 Recrystallization of **206d**, **204d**, and **207d** from hexanes at $-30\text{ }^\circ\text{C}$ produced blue crystals.
 The reaction was repeated with 24 equiv. of $n\text{-BuLi}$ -TMEDA using troticene (0.060 g,
 .294 mmol), $n\text{-BuLi}$ (4.42 ml of 1.6 M solution in hexane, 7.072 mmol), TMEDA (1.30
 ml; 1.001 g, 99 %; 8.528 mmol), and chlorotrimethylsilane (1.12 ml; 0.952 g, 98 %;
 8.588 mmol) as described in the general procedure above. Product distribution of crude

product: **203d** (15 %), **206d** (8 %), **204d** (13 %), **205d** (2 %), **207d** (59 %), **208d** (3 %). **207d** was isolated as blue solid. **207d Yield:** 0.056 g, 0.114 mmol, 39 %. Recrystallization of **207d** from hexanes at -30 °C produced blue crystals. **203d:** (See disubstitution of trocticene for NMR data). **206d:** ^1H NMR (499.9 MHz, C_6D_6), ^{13}C $\{^1\text{H}\}$ NMR (125.7 MHz, C_6D_6), ^{29}Si DEPT NMR (99.3 MHz, C_6D_6): See **Table 2.3.1.1**. $m/e = 420$ (M^+). Elemental Analysis Calculated for $\text{C}_{21}\text{H}_{36}\text{Si}_3\text{Ti}$: C, 59.94; H, 8.64. Found: C, 58.23; H, 8.67. **204d:** ^1H NMR (499.9 MHz, C_6D_6), ^{13}C $\{^1\text{H}\}$ NMR (125.7 MHz, C_6D_6), ^{29}Si DEPT NMR (99.3 MHz, C_6D_6): See **Table 2.3.1.1**. $m/e = 420$ (M^+). Elemental Analysis Calculated for $\text{C}_{21}\text{H}_{36}\text{Si}_3\text{Ti}$: C, 59.94; H, 8.64. Found: C, 59.67; H, 8.63. **207d:** ^1H NMR (499.9 MHz, C_6D_6), ^{13}C $\{^1\text{H}\}$ NMR (125.7 MHz, C_6D_6), ^{29}Si DEPT NMR (99.3 MHz, C_6D_6): See **Table 2.3.1.1**. $m/e = 492$ (M^+). Elemental Analysis Calculated for $\text{C}_{24}\text{H}_{44}\text{Si}_4\text{Ti}$: C, 58.47; H, 9.02. Found: C, 58.20; H, 9.37.

$[\eta^7\text{-}\{1,4\text{-Bis(dimethylsilyl)}\}\text{cycloheptatrienyl}]$ $\{\eta^5\text{-(dimethylsilyl)}\}$ $\text{cyclopentadienyl}\}$ titanium(II) (**204a**), $[\eta^7\text{-}\{1,4\text{-Bis(dimethylsilyl)}\}\text{cycloheptatrienyl}]$ $[\eta^5\text{-}\{1,3\text{-bis(dimethylsilyl)}\}\text{cyclopentadienyl}]\}$ titanium(II) (**207a**). Complexes **204a** and **207a** were prepared from trocticene (0.200 g; 0.980 mmol), *n*-BuLi (4.90 ml of 1.6 M solution in hexane; 7.840 mmol), TMEDA (1.44 ml; 1.109 g, 99 %; 9.446 mmol), and chlorodimethylsilane (1.10 ml; 0.935 g, 96 %; 9.486 mmol) as described in the general procedure above. Product distribution of crude product: **203a** (24 %), **206a** (3 %), **204a** (21 %), **205a** (3 %), **207a** (46 %), **208a** (3 %). Attempts to isolate **206a**, **205a** and **208a** were unsuccessful. **203a**, **204a**, and **207a** were isolated as blue oils. **203a Yield:** 0.053 g, 0.165 mmol, 17 %; **204a Yield:** 0.042 g, 0.111 mmol, 11 %; **207a Yield:** 0.139 g, 0.318 mmol, 32 %. **203a:** See **Table 2.2.1** for NMR data. **204a:** ^1H NMR (499.9 MHz, C_6D_6),

^{13}C $\{^1\text{H}\}$ NMR (125.7 MHz, C_6D_6), ^{29}Si DEPT NMR (99.3 MHz, C_6D_6): See **Table 2.3.2.1**. $m/e = 378$ (M^+). **207a**: ^1H NMR (499.9 MHz, C_6D_6), ^{13}C $\{^1\text{H}\}$ NMR (125.7 MHz, C_6D_6), ^{29}Si DEPT NMR (99.3 MHz, C_6D_6): See **Table 2.3.2.1**. $m/e = 436$ (M^+). Elemental Analysis Calculated for $\text{C}_{20}\text{H}_{36}\text{Si}_4\text{Ti}$: C, 54.99; H, 8.32. Found: C, 54.71; H, 8.02.

Monosubstitution of Substituted Tropicene Derivatives

Monosubstitution of $\{\eta^7\text{-(trimethylsilyl)cycloheptatrienyl}\}\{\eta^5\text{-cyclopentadienyl}\}\text{titanium(II)}$ to produce $\{\eta^7\text{-(trimethylsilyl)cycloheptatrienyl}\}\{\eta^5\text{-(trimethylsilyl)cyclopentadienyl}\}\text{titanium(II)}$ (**203d**), $[\eta^7\text{-}\{1,4\text{-bis(trimethylsilyl)}\}\text{cycloheptatrienyl}]\{\eta^5\text{-cyclopentadienyl}\}\text{titanium(II)}$ (**209d**), and $[\eta^7\text{-}\{1,3\text{-bis(trimethylsilyl)}\}\text{cycloheptatrienyl}]\{\eta^5\text{-cyclopentadienyl}\}\text{titanium(II)}$ (**210d**).

Monosubstitution of the Cht ligand of **201d** was done using **201d** (0.101 g; 0.365 mmol), $n\text{-BuLi}$ (0.42 ml of 1.6 M solution in hexane; 0.672 mmol), and chlorotrimethylsilane (0.10 ml; 0.085 g, 98 %; 0.767 mmol) as described in the general procedure above, except that lithiation was done at -10°C . The ^1H NMR spectrum of the crude product revealed 12 % starting material (**201d**), 84 % disubstituted tropicenes (**203d**, **209d**, and **210d**), and only 4 % trisubstituted tropicenes (**206d**, **204d**, and **205d**). Product distribution of disubstituted tropicenes: **203d** (13 %), **209d** (40 %), and **210d** (47 %). Attempts to isolate each isomer by column chromatography were unsuccessful. The mixture of **203d**, **209d**, and **210d** was isolated as a blue oil. **Yield**: 0.091 g, 0.261 mmol, 71 %. **203d**: See **Table 2.2.1** for NMR data. **209d**: ^1H NMR (499.9 MHz, C_6D_6), $^{13}\text{C}\{^1\text{H}\}$ NMR (125.7 MHz, C_6D_6), ^{29}Si DEPT NMR (99.3 MHz, C_6D_6): See **Table**

3.1.1.1. $m/e = 348$ (M^+). 210d: ^1H NMR (499.9 MHz, C_6D_6), ^{13}C $\{^1\text{H}\}$ NMR (125.7 MHz, C_6D_6), ^{29}Si DEPT NMR (99.3 MHz, C_6D_6): See **Table 3.1.1.1. $m/e = 348$ (M^+).**

Monosubstitution of $\{\eta^7\text{-(diphenylphosphino)cycloheptatrienyl}\}(\eta^5\text{-cyclopentadienyl})\text{titanium(II)}$ to produce $\{\eta^7\text{-(diphenylphosphino)cycloheptatrienyl}\}\{\eta^5\text{-(diphenylphosphino)cyclopentadienyl}\}\text{titanium(II)}$ (203c), $[\text{Kool, 1989 \#14; } \eta^7\text{-}\{1,4\text{-bis(diphenylphosphino)}\}\text{cycloheptatrienyl}] (\eta^5\text{-cyclopentadienyl})\text{titanium(II)}$ (209c), and $[\eta^7\text{-}\{1,3\text{-bis(diphenylphosphino)}\}\text{cycloheptatrienyl}](\eta^5\text{-cyclopentadienyl})\text{titanium(II)}$ (210c). Monosubstitution of the Cht ligand of **201c** was done using **201c** (0.481 g; 1.239 mmol), *n*-BuLi (3.88 ml of 1.6 M solution in hexane; 6.208 mmol), and chlorodiphenylphosphine (1.20 ml; 1.475 g, 95 %; 6.350 mmol) as described in the general procedure above, except that lithiation was done at -10°C .. Only disubstituted troticenes can be identified in the crude product. Product distribution of disubstituted troticenes: **203c** (15 %), **209c** (31 %), and **210c** (54 %). The crude product was dissolved in hot toluene then cooled slowly to room temperature, from which only complex **210c** was isolated via crystallization as a blue solid. The isolated product was further purified by recrystallization in toluene. **210c Yield:** 0.261 g, 0.456 mmol, 37 %. **203c:** ^1H NMR (499.9 MHz, C_6D_6), ^{13}C $\{^1\text{H}\}$ NMR (125.7 MHz, C_6D_6), ^{31}P $\{^1\text{H}\}$ NMR (202.4 MHz, C_6D_6): See **Table 3.1.1.2. 209c:** ^1H NMR (499.9 MHz, C_6D_6), ^{31}P $\{^1\text{H}\}$ NMR (202.4 MHz, C_6D_6): See **Table 3.1.1.2. 210c:** ^1H NMR (499.9 MHz, C_6D_6), ^{13}C $\{^1\text{H}\}$ NMR (125.7 MHz, C_6D_6), ^{31}P $\{^1\text{H}\}$ NMR (202.4 MHz, C_6D_6): See **Table 3.1.1.2. $m/e = 572$ (M^+).**

Monosubstitution of the cycloheptatrienyl ligand of $\{\eta^7\text{-(Trimethylsilyl)cycloheptatrienyl}\}(\eta^5\text{-(trimethylsilyl)cyclopentadienyl})\text{titanium(II)}$ (203d).

Monosubstitution of the Cht ligand of **203d** was done using **203d** (0.101 g; 0.290 mmol), *n*-BuLi (0.47 ml of 1.6 M solution in hexane; 0.752 mmol), and chlorotrimethylsilane (0.12 ml; 0.102 g, 98 %; 0.920 mmol) as described in the general procedure above. No attempts were made to isolate each component of the product mixture. Product distribution of crude product: **206d** (19 %), **204d** (33 %), **205d** (35 %), **207d** (8 %), **208d** (5 %). **Total crude product yield:** 0.110 g, 90 % (11 % starting material plus 79 % total products; calculated from ^1H NMR).

Monosubstitution of the cyclopentadienyl ligand of $\{\eta^7\text{-(Trimethylsilyl)cycloheptatrienyl}\}\{\eta^5\text{-(trimethylsilyl)cyclopentadienyl}\}\text{titanium(II)}$ (203d**).**

Monosubstitution of the Cp ligand of **203d** was done using **203d** (0.155 g; 0.445 mmol), *n*-BuLi (0.71 ml of 1.6 M solution in hexane; 1.136 mmol), and chlorotrimethylsilane (0.15 ml; 0.128 g, 98 %; 1.150 mmol) as described in the general procedure above. No attempts were made to isolate each component of the product mixture. Product distribution of crude product: **206d** (36 %), **204d** (7 %), **205d** (6 %), **207d** (32 %), **208d** (19 %). **Total crude product yield:** 0.114 g, 65 % (38 % starting material plus 27 % total products; calculated from ^1H NMR).

Disubstitution of Substituted Troiticene Derivatives.

Disubstitution of $\{\eta^7\text{-(Trimethylsilyl)cycloheptatrienyl}\}\{\eta^5\text{-cyclopentadienyl}\}\text{titanium(II)}$ (201d**) to produce $[\eta^7\text{-}\{1,4\text{-Bis(trimethylsilyl)}\}\text{cycloheptatrienyl}]\{\eta^5\text{-(trimethylsilyl)cyclopentadienyl}\}\text{titanium(II)}$ (**204d**), and $[\eta^7\text{-}\{1,3\text{-Bis(trimethylsilyl)}\}\text{cycloheptatrienyl}]\{\eta^5\text{-(trimethylsilyl)cyclopentadienyl}\}\text{titanium(II)}$ (**205d**).** Disubstitution of **201d** was done using **201d** (0.088 g; 0.318 mmol),

n-BuLi (0.80 ml of 1.6 M solution in hexane; 1.280 mmol), TMEDA (0.24 ml, 0.135 g, 99 %, 1.574 mmol), and chlorotrimethylsilane (0.22 ml, 0.187 g, 98 %, 1.687 mmol) as described in the general procedure above. The ^1H NMR spectrum of the crude product revealed 1 % starting material (**201d**), 7 % disubstituted troticenes (**203d**, **209d**, and **210d**), and 92 % trisubstituted troticenes (**206d**, **204d**, and **205d**). Product distribution of trisubstituted troticenes: **206d** (5 %), **204d** (61 %) and **205d** (34 %). Attempts to isolate each isomer by column chromatography were unsuccessful. The mixture of **204d** and **205d** was isolated as a blue oil. **Yield**: 0.094 g, 0.223 mmol, 70 %. **204d**: See **Table 2.3.1.1** for NMR data. **205d**: ^1H NMR (499.9 MHz, C_6D_6), $^{13}\text{C}\{^1\text{H}\}$ NMR (125.7 MHz, C_6D_6), ^{29}Si DEPT NMR (99.3 MHz, C_6D_6): See **Table 3.2.1.1**. $m/e = 420$ (M^+).

Disubstitution of $(\eta^7\text{-Cycloheptatrienyl})\{\eta^5\text{-(trimethylsilyl)cyclopentadienyl}\}$ titanium(II) (202d**) to produce $\{\eta^7\text{-(Trimethylsilyl)cycloheptatrienyl}\}[\eta^5\text{-}\{1,3\text{-bis(trimethylsilyl)cyclopentadienyl}\}]$ titanium(II) (**206d**).** Complex **206d** was prepared from **202d** (0.087 g, 0.315 mmol), *n*-BuLi (0.60 ml of 1.6 M solution in hexane; 0.960 mmol), TMEDA (0.18 ml, 0.139 g, 99 %, 1.181 mmol), and chlorotrimethylsilane (0.16 ml, 0.136 g, 98 %, 1.227 mmol) as described in the general procedure above. The ^1H NMR spectrum of the crude product revealed 2 % starting material (**202d**), 4 % disubstituted troticene (**203d**), 91 % trisubstituted troticenes (**204d**, **205d**, and **206d**), and 3 % tetrasubstituted troticenes (**207d**, and **208d**). Product distribution of trisubstituted troticenes: **206d** (96 %), **204d** (2 %) and **205d** (2 %). **206d** was isolated via column chromatography as a blue solid. Alternatively, **206d** can be crystallized directly from the crude product in hexanes at -30°C . **Yield**: 0.087 g, 0.207 mmol, 66 %. **206d**: See **Table 2.3.1.1** for NMR data.

Disubstitution of $\{\eta^7\text{-Cycloheptatrienyl}\}\{\eta^5\text{-(trimethylsilyl)cyclopentadienyl}\}$ titanium(II) (202d) to produce $\{\eta^7\text{-(Dimethylsilyl)cycloheptatrienyl}\}\{\eta^5\text{-(1-trimethylsilyl-3-dimethylsilyl)cyclopentadienyl}\}$ titanium(II) (206da). Complex **206da** was prepared from **202d** (0.079 g; 0.286 mmol), *n*-BuLi (0.54 ml of 1.6 M solution in hexane; 0.864 mmol), TMEDA (0.16 ml, 0.123 g, 99 %, 1.050 mmol), and chlorodimethylsilane (0.14 ml, 0.119 g, 96 %, 1.207 mmol) as described in the general procedure above. **206da** was isolated via column chromatography as a blue oil. **Yield:** 0.062 g, 0.158 mmol, 55 %. **206da:** ^1H NMR (499.9 MHz, C_6D_6), $^{13}\text{C}\{^1\text{H}\}$ NMR (125.7 MHz, C_6D_6), ^{29}Si NMR (99.3 MHz, C_6D_6): See **Table 3.2.1.2**. $m/e = 392$ (M^+).

Disubstitution of $\{\eta^7\text{-(Trimethylsilyl)cycloheptatrienyl}\}\{\eta^5\text{-(trimethylsilyl)cyclopentadienyl}\}$ titanium(II) (203d) to produce $[\eta^7\text{-}\{1,4\text{-Bis(trimethylsilyl)}\}\text{cycloheptatrienyl}][\eta^5\text{-}\{1,3\text{-bis(trimethylsilyl)}\}\text{cyclopentadienyl}]\text{titanium(II)}$ (207d), $[\eta^7\text{-}\{1,3\text{-bis(Trimethylsilyl)}\}\text{cycloheptatrienyl}][\eta^5\text{-}\{1,3\text{-bis(trimethylsilyl)}\}\text{cyclopentadienyl}]\text{titanium(II)}$ (208d). Disubstitution of **203d** was done using **203d** (0.123 g; 0.353 mmol), *n*-BuLi (1.80 ml of 1.6 M solution in hexane; 2.880 mmol), TMEDA (0.54 ml, 0.416 g, 99 %, 3.542 mmol), and chlorotrimethylsilane (0.48 ml, 0.408 g, 98 %, 3.680 mmol) as described in the general procedure above. Product distribution of major components in the crude product: **207d** (39 %) and **208d** (61 %). Attempts to isolate each isomer by column chromatography were unsuccessful. The mixture of **207d** and **208d** was isolated as a blue oil. **Yield:** 0.110 g, 0.223 mmol, 63 %. **207d:** See **Table 2.3.1.1** for NMR data. **208d:** ^1H NMR (499.9 MHz, C_6D_6), $^{13}\text{C}\{^1\text{H}\}$ NMR (125.7 MHz, C_6D_6), ^{29}Si DEPT NMR (99.3 MHz, C_6D_6): See **Table 3.2.2.2**. $m/e = 492$ (M^+).

Disubstitution of $\{\eta^7\text{-(Trimethylsilyl)cycloheptatrienyl}\}\{\eta^5\text{-(trimethylsilyl)cyclopentadienyl}\}\text{titanium(II)}$ (**203d**) to produce $\{\eta^7\text{-(1-Trimethylsilyl-4-dimethylsilyl)cycloheptatrienyl}\}\{\eta^5\text{-(1-trimethylsilyl-3-dimethylsilyl)cyclopentadienyl}\}\text{titanium(II)}$ (**207da**), $\{\eta^7\text{-(1-Trimethylsilyl-3-dimethylsilyl)cycloheptatrienyl}\}\{\eta^5\text{-(1-trimethylsilyl-3-dimethylsilyl)cyclopentadienyl}\}\text{titanium(II)}$ (**208da**). Disubstitution of **203d** was done using **203d** (0.130 g, 0.373 mmol), *n*-BuLi (1.90 ml of 1.6 M solution in hexane; 3.040 mmol), TMEDA (0.56 ml, 0.431 g, 99 %, 3.673 mmol), and chlorodimethylsilane (0.44 ml, 0.374 g, 96 %, 3.795 mmol) as described in the general procedure above. Product distribution of major components in the crude product: **207da** (40 %) and **208da** (60 %). Attempts to isolate each isomer by column chromatography were unsuccessful. The mixture of **207da** and **208da** was isolated as a blue oil. **Yield:** 0.119 g, 0.256 mmol, 69 %. **207da:** ^1H NMR (499.9 MHz, C_6D_6), $^{13}\text{C}\{^1\text{H}\}$ NMR (125.7 MHz, C_6D_6), ^{29}Si DEPT NMR (99.3 MHz, C_6D_6): See **Table 3.2.2.3**. $m/e = 464$ (M^+). **208da:** ^1H NMR (499.9 MHz, C_6D_6), $^{13}\text{C}\{^1\text{H}\}$ NMR (125.7 MHz, C_6D_6), ^{29}Si DEPT NMR (99.3 MHz, C_6D_6): See **Table 3.2.2.3**. $m/e = 464$ (M^+).

Hydrosilylation Reactions

Pretreatment of Karstedt's catalyst. Karstedt's catalyst (platinum-divinyltetramethyldisiloxane complex; 3-3.5% Pt concentration in vinyl terminated polydimethylsiloxane) was treated in the following manner before use in hydrosilylation reactions. Five drops were dissolved in 0.30 g of d_6 -benzene in a sealed 25 ml Schlenk flask in air and stirred overnight at room temperature. All volatile components were then

removed under vacuum and the residue dissolved in 0.30 g of d₆-benzene under nitrogen. Three drops of the pretreated catalyst solution was used for each hydrosilylation reaction. Each batch is sufficient for up to 8 reactions.

General Procedure for Hydrosilylation Reactions. Pt-catalyzed hydrosilylation reactions were carried out at room temperature under a nitrogen atmosphere in NMR tubes with d₆-benzene (0.80 g) as solvent. Karstedt's catalyst (3 drops of pretreated catalyst solution) was added to a solution of the appropriate silane and alkyne and shaken occasionally. Progress of the reaction was monitored by ¹H NMR spectroscopy. After the reaction was complete, all volatile components were removed under vacuum and the residue extracted with hexane and purified by filtration through a small amount of deactivated alumina (2.20 g) in a pipet. Products requiring further purification were subjected to column chromatography, with silica as support and hexane as eluent. The purified products were characterized using GC/MS, ¹H, ¹³C, and ²⁹Si DEPT NMR spectroscopy following evaporation of solvents. Product distribution was determined from integration of the ¹H NMR spectra. Polymeric/oligomeric products were further characterized using MALDI-TOF/TOF and GPC prior to purification by precipitation into cold hexanes due to insolubility of the precipitated products. For hydrosilylation products derived from {η⁷-(dimethylsilyl)cycloheptatrienyl}{η⁵-(dimethylsilyl)cyclopentadienyl}titanium(II), regioisomers referred to as β(E)-β(E), α-α, β(E)-α, and α-β(E) indicate the regiochemistry of the vinyl protons on the cycloheptatrienyl and cyclopentadienyl ligands, respectively (e.g., the β(E)-α regioisomer has β(E)- vinyl protons on the Cht ligand and α- vinyl protons on the Cp ligand).

Preparation of Type 1 Model Compounds via Alkyne Hydrosilylation

Preparation of Type 1 Model Compound 211a. Model compound **211a** was prepared from **201a** (0.080 g, 0.305 mmol) and ethynylbenzene (0.032 g, 0.313 mmol) as described in the general procedure above and was isolated as a blue oil. **Yield:** 0.077 g, 0.211 mmol, 69 %. **Product distribution (β (E)- / α - ratio):** 78 / 22. **^1H NMR** (399.8 MHz, C_6D_6), **^{13}C { ^1H } NMR** (100.5 MHz, C_6D_6), **^{29}Si DEPT NMR** (79.4 MHz, C_6D_6): See **Table 4.1.1**. **GC/MS:** 2 peaks, $m/e = 364$ (M^+).

Preparation of Type 1 Model Compound 211b. Model compound **211b** was prepared from **201a** (0.037 g, 0.141 mmol) and 2-ethynylthiophene (0.016 g, 0.148 mmol) as described in the general procedure above and was isolated as a blue oil. **Yield:** 0.049 g, 0.132 mmol, 94 %. **Product distribution (β (E)- / α - ratio):** 46 / 54. **^1H NMR** (499.9 MHz, C_6D_6), **^{13}C { ^1H } NMR** (125.7 MHz, C_6D_6), **^{29}Si DEPT NMR** (99.3 MHz, C_6D_6): See **Table 4.1.2**. **GC/MS:** 2 peaks, $m/e = 370$ (M^+).

Preparation of Type 1 Model Compound 212a. Model compound **212a** was prepared from **202a** (0.050 g, 0.191 mmol) and ethynylbenzene (0.020 g, 0.196 mmol) as described in the general procedure above and was isolated as a blue oil. **Yield:** 0.050 g, 0.137 mmol, 72 %. **Product distribution (β (E)- / α - ratio):** 76 / 24. **^1H NMR** (399.8 MHz, C_6D_6), **^{13}C { ^1H } NMR** (100.5 MHz, C_6D_6), **^{29}Si DEPT NMR** (79.4 MHz, C_6D_6): See **Table 4.1.3**. **GC/MS:** 2 peaks, $m/e = 364$ (M^+).

Preparation of Type 1 Model Compound 212b. Model compound **212b** was prepared from **202a** (0.022 g, 0.084 mmol) and 2-ethynylthiophene (0.010 g, 0.092 mmol) as described in the general procedure above and was isolated as a blue oil. **Yield:** 0.029 g, 0.078 mmol, 93 %. **Product distribution (β (E)- / α - ratio):** 56 / 44. **^1H NMR**

(499.9 MHz, C₆D₆), ¹³C {¹H} NMR (125.7 MHz, C₆D₆), ²⁹Si DEPT NMR (99.3 MHz, C₆D₆): See **Table 4.1.4**. GC/MS: 2 peaks, $m/e = 370$ (M⁺).

Preparation of Type 1 Model Compound 213a. Model compound **213a** was prepared from **41** (0.030 g, 0.123 mmol) and ethynylbenzene (0.013 g, 0.127 mmol) as described in the general procedure above and was isolated as an orange oil. . **Yield:** 0.026 g, 0.075 mmol, 61 %. **Product distribution (β(E)- / α- ratio):** 77 / 23. ¹H NMR (499.9 MHz, C₆D₆): See **Table 4.1.5**. GC/MS: 2 peaks, $m/e = 346$ (M⁺).

Preparation of Type 1 Model Compound 213b. Model compound **213b** was prepared from **41** (0.020 g, 0.082 mmol) and 2-ethynylthiophene (0.009 g, 0.083 mmol) as described in the general procedure above and was isolated as an orange oil. **Yield:** 0.016 g, 0.045 mmol, 55 %. **Product distribution (β(E)- / α- ratio):** 61 / 39. ¹H NMR (499.9 MHz, C₆D₆), ¹³C {¹H} NMR (125.7 MHz, C₆D₆), ²⁹Si DEPT NMR (99.3 MHz, C₆D₆): See **Table 4.1.6**. GC/MS: 2 peaks, $m/e = 352$ (M⁺).

Preparation of Type 2 Model Compounds via Alkyne Hydrosilylation

Preparation of Type 2 Model Compound 214a. Model compound **214a** was prepared from **203a** (0.025 g, 0.078 mmol) and ethynylbenzene (0.016 g, 0.157 mmol) as described in the general procedure above and was isolated as a blue oil. **Yield:** 0.030 g, 0.057 mmol, 73 %. **Regiochemical distribution (β(E)- / α- ratio):** 49 / 51. **Product distribution (β(E)-β(E) / α-α / β(E)-α / α-β(E) ratio):** 29 / 31 / 21 / 19. ¹H NMR (499.9 MHz, C₆D₆), ¹³C {¹H} NMR (125.7 MHz, C₆D₆), ²⁹Si DEPT NMR (99.3 MHz, C₆D₆): See **Table 4.2.1**.

Preparation of Type 2 Model Compound 214b. Model compound **214b** was prepared from **203a** (0.046 g, 0.144 mmol) and 2-ethynylthiophene (0.032 g, 0.296 mmol) as described in the general procedure above and was isolated as a blue oil. **Yield:** 0.073 g, 0.136 mmol, 95 %. **Regiochemical distribution (β (E)- / α - ratio):** 16 / 84. **Product distribution (β (E)- β (E) / α - α / β (E)- α / α - β (E) ratio):** 6 / 73 / 11 / 10. ^1H NMR (499.9 MHz, C_6D_6), ^{13}C { ^1H } NMR (125.7 MHz, C_6D_6), ^{29}Si DEPT NMR (99.3 MHz, C_6D_6): See Table 4.2.2.

Preparation of Type 2 Model Compound 215. Model compound **215** was prepared from **28** (0.030 g, 0.099 mmol) and 2-ethynylthiophene (0.022 g, 0.203 mmol) as described in the general procedure above and was isolated as an orange oil. **Yield:** 0.037 g, 0.071 mmol, 72 %. **Regiochemical distribution (β (E)- / α - ratio):** 23 / 77. **Product distribution (β (E)- β (E) / α - α / β (E)- α ratio):** 14 / 69 / 17. ^1H NMR (499.9 MHz, C_6D_6), ^{13}C { ^1H } NMR (125.7 MHz, C_6D_6), ^{29}Si DEPT NMR (99.3 MHz, C_6D_6): See Table 4.2.3. GC/MS: 3 peaks, $m/e = 518$ (M^+).

Preparation of Type 3 Model Compounds via Alkyne Hydrosilylation

Preparation of Type 3 Model Compound 216a. Model compound **216a** was prepared from **201a** (0.034 g, 0.130 mmol) and 1,4-diethynylbenzene (0.008 g, 0.063 mmol) as described in the general procedure above and was isolated as a blue oil. **Yield:** 0.025 g, 0.038 mmol, 61 %. **Regiochemical distribution (β (E)- / α - ratio):** 74 / 26. **Product distribution (β (E)- β (E) / α - α / β (E)- α ratio):** 56 / 7 / 37. ^1H NMR (499.9 MHz, C_6D_6), ^{13}C { ^1H } NMR (125.7 MHz, C_6D_6), ^{29}Si DEPT NMR (79.4 MHz, C_6D_6): See Table 4.3.1.

Preparation of Type 3 Model Compound 216b. Model compound **216b** was prepared from **201a** (0.067 g, 0.255 mmol) and 1,3-diethynylbenzene (0.016 g, 0.127 mmol) as described in the general procedure above and was isolated as a blue oil. **Yield:** 0.061 g, 0.094 mmol, 74 %. **Regiochemical distribution (β (E)- / α - ratio):** 72 / 28. **Product distribution (β (E)- β (E) / α - α / β (E)- α ratio):** 53 / 8 / 39. ^1H NMR (499.9 MHz, C_6D_6), ^{13}C $\{^1\text{H}\}$ NMR (125.7 MHz, C_6D_6), ^{29}Si DEPT NMR (99.3 MHz, C_6D_6): See Table 4.3.2.

Preparation of Type 3 Model Compound 216c. Model compound **216c** was prepared from **201a** (0.044 g, 0.168 mmol) and 2,5-diethynylthiophene (0.011 g, 0.083 mmol) as described in the general procedure above and was isolated as a blue oil. **Yield:** 0.040 g, 0.061 mmol, 73 %. **Regiochemical distribution (β (E)- / α - ratio):** 55 / 45. **Product distribution (β (E)- β (E) / α - α / β (E)- α ratio):** 30 / 19 / 51. ^1H NMR (499.9 MHz, C_6D_6), ^{13}C $\{^1\text{H}\}$ NMR (125.7 MHz, C_6D_6), ^{29}Si DEPT NMR (99.3 MHz, C_6D_6): See Table 4.3.3.

Preparation of Type 3 Model Compound 217a. Model compound **217a** was prepared from **202a** (0.034 g, 0.130 mmol) and 1,4-diethynylbenzene (0.008 g, 0.063 mmol) as described in the general procedure above and was isolated as a blue oil. **Yield:** 0.028 g, 0.043 mmol, 68 %. **Regiochemical distribution (β (E)- / α - ratio):** 76 / 24. **Product distribution (β (E)- β (E) / α - α / β (E)- α ratio):** 58 / 6 / 36. ^1H NMR (499.9 MHz, C_6D_6), ^{13}C $\{^1\text{H}\}$ NMR (125.7 MHz, C_6D_6), ^{29}Si DEPT NMR (79.4 MHz, C_6D_6): See Table 4.3.4.

Preparation of Type 3 Model Compound 217b. Model compound **217b** was prepared from **202a** (0.026 g, 0.099 mmol) and 1,3-diethynylbenzene (0.006 g, 0.048

mmol) as described in the general procedure above and was isolated as a blue oil. **Yield:** 0.021 g, 0.032 mmol, 68 %. **Regiochemical distribution ($\beta(\text{E})$ - / α - ratio):** 76 / 24. **Product distribution ($\beta(\text{E})$ - $\beta(\text{E})$ / α - α / $\beta(\text{E})$ - α ratio):** 59 / 7 / 34. ^1H NMR (499.9 MHz, C_6D_6), ^{13}C $\{^1\text{H}\}$ NMR (125.7 MHz, C_6D_6), ^{29}Si DEPT NMR (99.3 MHz, C_6D_6): See Table 4.3.5.

Preparation of Type 3 Model Compound 217c. Model compound **217c** was prepared from **202a** (0.032 g, 0.122 mmol) and 2,5-diethynylthiophene (0.008 g, 0.061 mmol) as described in the general procedure above and was isolated as a blue oil. **Yield:** 0.029 g, 0.044 mmol, 73 %. **Regiochemical distribution ($\beta(\text{E})$ - / α - ratio):** 62 / 38. **Product distribution ($\beta(\text{E})$ - $\beta(\text{E})$ / α - α / $\beta(\text{E})$ - α ratio):** 39 / 15 / 46. ^1H NMR (499.9 MHz, C_6D_6), ^{13}C $\{^1\text{H}\}$ NMR (125.7 MHz, C_6D_6), ^{29}Si DEPT NMR (99.3 MHz, C_6D_6): See Table 4.3.6.

Preparation of Type 3 Model Compound 218. Model compound **218** was prepared from **41** (0.042 g, 0.172 mmol) and 2,5-diethynylthiophene (0.011 g, 0.083 mmol) as described in the general procedure above and was isolated as an orange oil. **Yield:** 0.049 g, 0.080 mmol, 95 %. **Regiochemical distribution ($\beta(\text{E})$ - / α - ratio):** 61 / 39. **Product distribution ($\beta(\text{E})$ - $\beta(\text{E})$ / α - α / $\beta(\text{E})$ - α ratio):** 34 / 11 / 55. ^1H NMR (499.9 MHz, C_6D_6), ^{13}C $\{^1\text{H}\}$ NMR (125.7 MHz, C_6D_6), ^{29}Si DEPT NMR (99.3 MHz, C_6D_6): See Table 4.3.7.

Preparation of Polymers/Oligomers via Alkyne Hydrosilylation

Preparation of Polymer/Oligomer 219a. Polymer **219a** was prepared from **203a** (0.120 g, 0.374 mmol) and 1,4-diethynylbenzene (0.047 g, 0.373 mmol) as described in

the general procedure above. After the reaction was complete, the crude reaction mixture was dissolved in THF (2 ml), concentrated to about 0.5 ml and precipitated into hexane. Washing with hexane and drying under vacuum gave a blue solid. **Yield:** 0.141 g, 84 %. **Regiochemical distribution (β (E)- / α - ratio):** 54 / 46 (a ratio of 49 / 51 was observed for a trial done at 50°C). **^1H NMR** (499.9 MHz, C_6D_6), **^{13}C { ^1H } NMR** (125.7 MHz, C_6D_6), **^{29}Si DEPT NMR** (99.3 MHz, C_6D_6): See Table 4.4.1.

Preparation of Polymer/Oligomer 219b. Polymer **219b** was prepared from **203a** (0.067 g, 0.209 mmol) and 1,3-diethynylbenzene (0.026 g, 0.206 mmol) as described in the general procedure above. After the reaction was complete, the crude reaction mixture was dissolved in THF (2 ml), concentrated to about 0.5 ml and precipitated into hexane. Washing with hexane and drying under vacuum gave a blue solid. **Yield:** 0.077 g, 83 %. **Regiochemical distribution (β (E)- / α - ratio):** 51 / 49. **^1H NMR** (499.9 MHz, C_6D_6), **^{13}C { ^1H } NMR** (125.7 MHz, C_6D_6), **^{29}Si DEPT NMR** (99.3 MHz, C_6D_6): See Table 4.4.2.

Preparation of Polymer/Oligomer 219c. Polymer **219c** was prepared from **203a** (0.042 g, 0.131 mmol) and 2,5-diethynylthiophene (0.017 g, 0.129 mmol) as described in the general procedure above. After the reaction was complete, the crude reaction mixture was dissolved in THF (2 ml), concentrated to about 0.5 ml and precipitated into hexane. Washing with hexane and drying under vacuum gave a blue-green solid. **Yield:** 0.020 g, 34 %. **Regiochemical distribution (β (E)- / α - ratio):** 34 / 66. **^1H NMR** (499.9 MHz, C_6D_6), **^{13}C { ^1H } NMR** (125.7 MHz, C_6D_6), **^{29}Si DEPT NMR** (99.3 MHz, C_6D_6): See Table 4.4.3.

Preparation of Polymer/Oligomer 220. Polymer **220** was prepared from 1,1'-bis(dimethylsilyl)ferrocene (**28**) (0.040 g, 0.132 mmol) and 2,5-diethynylthiophene (0.017 g, 0.129 mmol) as described in the general procedure above. After the reaction was complete, the crude reaction mixture was dissolved in THF (2 ml), concentrated to about 0.5 ml and precipitated into hexane. Washing with hexane and drying under vacuum gave an orange solid. **Yield:** 0.018 g, 32 %. **Regiochemical distribution (β (E)- / α - ratio):** 36 / 64. ^1H NMR (499.9 MHz, C_6D_6), ^{13}C { ^1H } NMR (125.7 MHz, C_6D_6), ^{29}Si DEPT NMR (99.3 MHz, C_6D_6): See Table 4.4.4.

Hydrosilylation of Phenylacetylene with Various Silanes

Hydrosilylation of Phenylacetylene with Dimethylsilylbenzene (221).³⁰⁵⁻³⁰⁷ **221** was prepared from dimethylsilylbenzene (0.020 g, 0.147 mmol) and phenylacetylene (0.090 g, 0.881 mmol) as described in the general procedure above and was isolated as a colorless oil. **Yield:** 0.025 g, 0.105 mmol, 71 %. **Product distribution (β (E)- / α - ratio):** 77 / 23. ^1H NMR (499.9 MHz, C_6D_6): See Table 5.1.4. GC/MS: 2 peaks, $m/e = 238$ (M^+).

Hydrosilylation of Phenylacetylene with Dimethylsilylferrocene (222). **222** was prepared from dimethylsilylferrocene (0.020 g, 0.082 mmol) and phenylacetylene (0.034 g, 0.333 mmol) as described in the general procedure above and was isolated as an orange oil. **Yield:** 0.018 g, 0.052 mmol, 63 %. **Product distribution (β (E)- / α - ratio):** 75 / 25. ^1H NMR (499.9 MHz, C_6D_6): See Table 4.1.5. GC/MS: 2 peaks, $m/e = 346$ (M^+).

Hydrosilylation of Phenylacetylene with 1,4-Dimethylsilylbenzene (223).^{282,308}

223 was prepared from 1,4-dimethylsilylbenzene (0.030 g, 0.154 mmol) and phenylacetylene (0.095 g, 0.930 mmol) as described in the general procedure above and was isolated as a colorless oil. **Yield:** 0.039 g, 0.098 mmol, 63 %. **Regiochemical distribution (β (E)- / α - ratio):** 75 / 25. **Product distribution (β (E)- β (E) / α - α / β (E)- α ratio):** 56 / 7 / 37. **¹H NMR** (499.9 MHz, C₆D₆): See Table 5.1.4. **GC/MS:** 3 peaks, m/e = 398 (M⁺).

Hydrosilylation of Phenylacetylene with 1,1'-Bis(dimethylsilyl)ferrocene (224).⁵ **224** was prepared from 1,1'-bis(dimethylsilyl)ferrocene (0.030 g, 0.099 mmol) and phenylacetylene (0.061 g, 0.597 mmol) as described in the general procedure above and was isolated as an orange oil. **Yield:** 0.033 g, 0.065 mmol, 66 %. **Regiochemical distribution (β (E)- / α - ratio):** 53 / 47. **Product distribution (β (E)- β (E) / α - α / β (E)- α ratio):** 35 / 30 / 35. **¹H NMR** (499.9 MHz, C₆D₆): See Table 5.1.4. **GC/MS:** 3 peaks, m/e = 506 (M⁺).

Hydrosilylation of *p*-Ethynyltoluene with Various Silanes

Hydrosilylation of *p*-Ethynyltoluene with Dimethylsilylbenzene (225).^{309,310}

225 was prepared from dimethylsilylbenzene (0.020 g, 0.147 mmol) and *p*-ethynyltoluene (0.102 g, 0.878 mmol) as described in the general procedure above and was isolated as a colorless oil. **Yield:** 0.019 g, 0.075 mmol, 51 %. **Product distribution (β (E)- / α - ratio):** 81 / 19. **¹H NMR** (499.9 MHz, C₆D₆): See Table 5.1.5. **GC/MS:** 2 peaks, m/e = 252 (M⁺).

Hydrosilylation of *p*-Ethynyltoluene with Dimethylsilylferrocene (226). 226

was prepared from dimethylsilylferrocene (0.020 g, 0.082 mmol) and *p*-ethynyltoluene (0.057 g, 0.491 mmol) as described in the general procedure above and was isolated as an orange oil. **Yield:** 0.016 g, 0.044 mmol, 54 %. **Product distribution (β (E)- / α - ratio):** 79 / 21. **^1H NMR** (499.9 MHz, C_6D_6): See Table 5.1.5. **GC/MS:** 2 peaks, $m/e = 360$ (M^+).

Hydrosilylation of *p*-Ethynyltoluene with 1,4-Dimethylsilylbenzene (227).

227 was prepared from 1,4-dimethylsilylbenzene (0.020 g, 0.103 mmol) and *p*-ethynyltoluene (0.072 g, 0.620 mmol) as described in the general procedure above and was isolated as a colorless oil. **Yield:** 0.026 g, 0.061 mmol, 59 %. **Regiochemical distribution (β (E)- / α - ratio):** 80 / 20. **Product distribution (β (E)- β (E) / α - α / β (E)- α ratio):** 65 / 5 / 30. **^1H NMR** (499.9 MHz, C_6D_6): See Table 5.1.5.

Hydrosilylation of *p*-Ethynyltoluene with 1,1'-Bis(dimethylsilyl)ferrocene

(228). 228 was prepared from 1,1'-bis(dimethylsilyl)ferrocene (0.030 g, 0.099 mmol) and *p*-ethynyltoluene (0.069 g, 0.594 mmol) as described in the general procedure above and was isolated as an orange oil. **Yield:** 0.030 g, 0.056 mmol, 57 %. **Regiochemical distribution (β (E)- / α - ratio):** 58 / 42. **Product distribution (β (E)- β (E) / α - α / β (E)- α ratio):** 42 / 27 / 31. **^1H NMR** (499.9 MHz, C_6D_6): See Table 5.1.5.

Hydrosilylation of 2-Ethynylthiophene with Various Silanes

Hydrosilylation of 2-Ethynylthiophene with Dimethylsilylbenzene (229).²⁷⁷

229 was prepared from dimethylsilylbenzene (0.020 g, 0.147 mmol) and 2-ethynylthiophene (0.095 g, 0.878 mmol) as described in the general procedure above and

was isolated as a colorless oil. **Yield:** 0.017 g, 0.070 mmol, 47 %. **Product distribution ($\beta(\text{E})$ - / α - ratio):** 61 / 39. **^1H NMR** (499.9 MHz, C_6D_6): See **Table 5.1.6**. **GC/MS:** 2 peaks, $m/e = 244$ (M^+).

Hydrosilylation of 2-Ethynylthiophene with Dimethylsilylferrocene (230). **230** was prepared from dimethylsilylferrocene (0.020 g, 0.082 mmol) and 2-ethynylthiophene (0.053 g, 0.490 mmol) as described in the general procedure above and was isolated as an orange oil. **Yield:** 0.016 g, 0.045 mmol, 55 %. **Product distribution ($\beta(\text{E})$ - / α - ratio):** 63 / 37. **^1H NMR** (499.9 MHz, C_6D_6): See **Table 4.1.6**. **GC/MS:** 2 peaks, $m/e = 352$ (M^+).

Hydrosilylation of 2-Ethynylthiophene with 1,4-Dimethylsilylbenzene (231). **231** was prepared from 1,4-dimethylsilylbenzene (0.030 g, 0.154 mmol) and 2-ethynylthiophene (0.100 g, 0.925 mmol) as described in the general procedure above and was isolated as a colorless oil. **Yield:** 0.030 g, 0.073 mmol, 47 %. **Regiochemical distribution ($\beta(\text{E})$ - / α - ratio):** 60 / 40. **Product distribution ($\beta(\text{E})$ - $\beta(\text{E})$ / α - α / $\beta(\text{E})$ - α ratio):** 36 / 16 / 48. **^1H NMR** (499.9 MHz, C_6D_6): See **Table 5.1.6**. **GC/MS:** 3 peaks, $m/e = 410$ (M^+).

Hydrosilylation of 2-Ethynylthiophene with 1,1'-Bis(dimethylsilyl)ferrocene (232). **232** was prepared from 1,1'-bis(dimethylsilyl)ferrocene (0.030 g, 0.099 mmol) and 2-ethynylthiophene (0.064 g, 0.592 mmol) as described in the general procedure above and was isolated as an orange oil. **Yield:** 0.024 g, 0.046 mmol, 47 %. **Regiochemical distribution ($\beta(\text{E})$ - / α - ratio):** 32 / 68. **Product distribution ($\beta(\text{E})$ - $\beta(\text{E})$ / α - α / $\beta(\text{E})$ - α ratio):** 23 / 59 / 18. **^1H NMR** (499.9 MHz, C_6D_6): See **Table 4.2.3**. **GC/MS:** 3 peaks, $m/e = 518$ (M^+).

Synthesis of Hydrosilylation Mono-Adducts

The hydrosilylation mono-adducts **233B** and **234B** were prepared from either 1,4-*bis*(dimethylsilyl)benzene or 1,1'-*bis*(dimethylsilyl)ferrocene and phenylacetylene. Several hydrosilylation protocols were explored with test reactions using pre-treated Karstedt's catalyst for the hydrosilylation of a six-fold mole excess of 1,1'-*bis*(dimethylsilyl)ferrocene (**28**) with phenylacetylene in d_6 -benzene. All reactions were allowed to proceed overnight after addition of the phenylacetylene to consume any unreacted phenylacetylene. (Table E.1):

- A:** The *bis*-silane **28** and phenylacetylene were mixed in d_6 -benzene, and then the mixture was treated with 3 drops catalyst.
- B:** The *bis*-silane **28** in d_6 -benzene was treated with 3 drops catalyst, aged for 5 minutes, and then phenylacetylene in d_6 -benzene was added all at once to the *bis*-silane **28** solution.
- C:** The *bis*-silane **28** in d_6 -benzene was treated with 3 drops catalyst, aged for 5 minutes, and then phenylacetylene in d_6 -benzene was added dropwise over 6 hours to the *bis*-silane **28** solution.
- D:** Separate d_6 -benzene solutions of the *bis*-silane **28** and phenylacetylene were treated with 3 drops catalyst, aged for 5 minutes, and then the phenylacetylene solution was added dropwise over 6 hours to the *bis*-silane **28** solution.

E: The phenylacetylene in d_6 -benzene was treated with 3 drops catalyst, aged for 5 minutes, and then added dropwise over 6 hours to the *bis*-silane **28** solution in d_6 -benzene.

F: The same as **D**, except that the *bis*-silane used is 1,4-*bis*(dimethylsilyl)benzene.

Table E.1. Test Reactions* for the Monohydrosilylation of the *Bis*-silane **28**.

| Test Reactions | Regiochemical Distribution $\beta(E)$ - / α - Ratio | Mono- $\beta(E)$ - [*] (%) |
|----------------|---|--|
| A | 75 / 25 | 45 |
| B | 85 / 15 | 49 |
| C | 90 / 10 | 58 |
| D | 96 / 4 | 66 |
| E | 85 / 15 | 58 |
| F | 95 / 5 | 75 |

Based on the results summarized in **Table E.1**, the protocol which proved to be the most useful was protocol **D** and **F**. Using these protocols, the mono- $\beta(E)$ - adducts **233B** and **234B** were successfully prepared and isolated. No mono- α - adducts (**233A** and **234A**) were isolated. The crude products were characterized by GC/MS and 1H NMR and purified by column chromatography.

Preparation of 1-{dimethyl(phenylvinylene)silyl}-4-dimethylsilyl-benzene (233B**).** Complex **233B** was prepared from 1,4-*bis*(dimethylsilyl)benzene (0.340 g, 1.749 mmol) and phenylacetylene (0.030 g, 0.294 mmol) as described in the general procedure above. Column chromatography on silica gave no visible bands. Multiple fractions (10 ml each) were collected and checked by GC/MS for presence of the major product 1-

{dimethyl(phenylvinylene)silyl}-4-dimethylsilyl-benzene (**233B**), which was isolated as a colorless/very pale yellow oil. **Yield:** 0.037 g, 0.125 mmol, 42 %. **¹H NMR** (499.9 MHz, C₆D₆), **¹³C {¹H} NMR** (125.7 MHz, C₆D₆), **²⁹Si DEPT NMR** (99.3 MHz, C₆D₆): See **Table 5.2.1.1**. **GC/MS:** 1 peak, $m/e = 296$ (M⁺).

Preparation of 1-{dimethyl(phenylvinylene)silyl}-1'-dimethylsilyl-ferrocene (234B**).** Complex **234B** was prepared from 1,1'-bis(dimethylsilyl)ferrocene (0.360 g, 1.191 mmol) and phenylacetylene (0.020 g, 0.196 mmol) as described in the general procedure above. Column chromatography on silica gave three separate orange bands. The first band is unreacted 1,1'-bis(dimethylsilyl)ferrocene, and the second band is the major product 1-{dimethyl(phenylvinylene)silyl}-1'-dimethylsilyl-ferrocene (**234B**) which was isolated as an orange oil. **Yield:** 0.031 g, 0.077 mmol, 39 %. **GC/MS:** $m/e = 404$ (1 peak). **¹H NMR** (499.9 MHz, C₆D₆), **¹³C {¹H} NMR** (125.7 MHz, C₆D₆), **²⁹Si DEPT NMR** (99.3 MHz, C₆D₆): See **Table 5.2.1.2**. **GC/MS:** 1 peak, $m/e = 404$ (M⁺).

Hydrosilylation of Phenylacetylene using the Mono-β(E)- adducts

Hydrosilylation of Phenylacetylene with 1-{dimethyl(phenylvinylene)silyl}-4-dimethylsilyl-benzene (233**) to produce 1,4-bis{dimethyl(phenylvinylene)silyl}benzene (Scheme 5.2.2.1).** Phenylacetylene (0.013 g, 0.127 mmol) was hydrosilylated with 1-{dimethyl(phenylvinylene)silyl}-4-dimethylsilyl-benzene (**233**) (0.037 g, 0.125 mmol) as described in the general procedure above, and the product was isolated as colorless/very pale yellow oil. **Yield:** 0.042 g, 0.105 mmol, 84 %. **Regiochemical distribution (β(E)- / α- ratio):** 89 / 11. **Product distribution (β(E)-β(E)**

/ $\beta(\text{E})$ - α ratio): 78 / 22. ^1H NMR (499.9 MHz, C_6D_6): See Table 5.1.4; No α - α was produced. GC/MS: 2 peaks, $m/e = 398$ (M^+).

Hydrosilylation of Phenylacetylene with 1-{dimethyl(phenylvinylene)silyl}-1'-dimethylsilyl-ferrocene (234) to produce 1,1'-bis{dimethyl(phenylvinylene)silyl}ferrocene (Scheme 5.2.2.2). Phenylacetylene (0.007 g, 0.069 mmol) was hydrosilylated with 1-{dimethyl(phenylvinylene)silyl}-1'-dimethylsilyl-ferrocene (**234**) (0.026 g, 0.064 mmol) as described in the general procedure above, and the product was isolated as an orange oil. **Yield:** 0.027 g, 0.053 mmol, 83 %. **Regiochemical distribution ($\beta(\text{E})$ - / α -ratio):** 87 / 13. **Product distribution ($\beta(\text{E})$ - $\beta(\text{E})$ / $\beta(\text{E})$ - α ratio):** 74 / 26. ^1H NMR (499.9 MHz, C_6D_6): See Table 5.1.4; No α - α was produced. GC/MS: 2 peaks, $m/e = 506$ (M^+).

^1H NMR Monitored Hydrosilylation of Phenylacetylene.

^1H NMR Monitored Hydrosilylation of Phenylacetylene with 1,4-Bis(dimethylsilyl)benzene. The hydrosilylation of phenylacetylene (0.064 g, 0.627 mmol) with 1,4-bis(dimethylsilyl)benzene (0.020 g, 0.103 mmol) was done as described in the general procedure above. The progress of the reaction was monitored using ^1H NMR at 3, 5, and 20 hours into the reaction, and finally at 48 hours at which the reaction is complete. The crude product mixture was not purified. See Table 5.2.3.1. **Final Regiochemical Distribution ($\beta(\text{E})$ - / α):** 73 / 27. **Final Product distribution ($\beta(\text{E})$ - $\beta(\text{E})$ / α - α / $\beta(\text{E})$ - α ratio):** 53 / 7 / 40.

^1H NMR Monitored Hydrosilylation of Phenylacetylene with 1,1'-Bis(dimethylsilyl)ferrocene. The hydrosilylation of phenylacetylene (0.041 g, 0.401

mmol) with 1,1'-*Bis*(dimethylsilyl)ferrocene (0.020 g, 0.066 mmol) was done as described in the general procedure above. The progress of the reaction was monitored using ^1H NMR at 0.5, 1, 1.5, 2, 5, 8, 12, and 16 hours into the reaction, and finally at 48 hours at which the reaction is complete. The crude product mixture was not purified. See **Table 5.2.3.2. Final Regiochemical Distribution ($\beta(\text{E})$ - / α): 52 / 48. Final Product distribution ($\beta(\text{E})$ - $\beta(\text{E})$ / α - α / $\beta(\text{E})$ - α ratio): 36 / 31 / 33.**

References

1. Groenenboom, C. J.; De Liefde Meijer, H. J.; Jellinek, F. *Journal of Organometallic Chemistry* **1974**, *69*, 235-340.
2. Groenenboom, C. J.; De Liefde Meijer, H. J.; Jellinek, F. *Recueil Des Travaux Chimiques Des Pays-Bas* **1974**, *93*, 6-7.
3. Kool, L. B.; Ogasa, M.; Rausch, M. D.; Rogers, R. D. *Organometallics* **1989**, *8*, 1785-1790.
4. Jain, R.; Lalancette, R. A.; Sheridan, J. B. *Organometallics* **2005**, *24*, 1458-1467.
5. Jain, R.; Choi, H.; Lalancette, R. A.; Sheridan, J. B. *Organometallics* **2005**, *24*, 1468-1476.
6. Van Oven, H. O.; De Liefde Meijer, H. J. *Journal of Organometallic Chemistry* **1970**, *23*, 159-163.
7. Tamm, M.; Kunst, A.; Bannenberg, T.; Herdtweck, E.; Sirsch, P.; Elsevier, C. J.; Ernsting, J. M. *Angewandte Chemie, International Edition* **2004**, *43*, 5530-5534.
8. Gschwend, H. W.; Rodriguez, H. R. In *Organic Reactions*; John Wiley & Sons, Inc.: New York, 1979; Vol. 26, p 1.
9. Gilman, H.; Young, R. V. *Journal of the American Chemical Society* **1934**, *56*, 1415-1416.
10. Gilman, H.; Morton Jr., J. W. In *Organic Reactions*; John Wiley & Sons, Inc.: New York, 1954; Vol. 8, pp 258-304.
11. Seyferth, D. *Organometallics* **2006**, *25*, 2-24.
12. Wittig, G.; Pockels, U.; Dröge, H. *Berichte der Deutschen Chemischen Gesellschaft* **1938**, *71*, 1903-1912.
13. Hsieh, H.; Glaze, W. *Rubber Chemistry and Technology* **1970**, *43*, 22-73.
14. *Polyamine-Chelated Alkali Metal Compounds*; American Chemical Society: Washington, D. C., 1974; Vol. 130.
15. Quirk, R. P.; Yin, J.; Guo, S. H.; Hu, X. W.; Summers, G.; Kim, J.; Zhu, L. F.; Ma, J. J.; Takizawa, T.; Lynch, T. *Rubber Chemistry and Technology* **1991**, *64*, 648-660.

16. Eisch, J. J. *Organometallics* **2002**, *21*, 5439-5463.
17. Halasa, A. F.; Schulz, D. N.; Tate, D. P.; Mochel, V. D. In *Advances in Organometallic Chemistry*; Stone, F. G. A., West, R., Eds.; Academic Press, Inc.: New York, New York, 1980; Vol. 18, pp 55-97.
18. Young, R. N.; Quirk, R. P.; Fetters, L. J. In *Advances in Polymer Science*; Springer: Berlin, 1984; Vol. 56, pp 1-90.
19. Mallan, J. M.; Bebb, R. L. *Chemical Reviews* **1969**, *69*, 693-755.
20. Wakefield, B. J. *The Chemistry of Organolithium Compounds*; Pergamon Press: Oxford, 1974.
21. Leroux, F.; Schlosser, M.; Zohar, E.; Marek, I. In *The Chemistry of Organolithium Compounds*; Rappoport, Z., Marek, I., Eds.; John Wiley & Sons, Ltd.: West Sussex, England, 2004; Vol. 1, pp 435-493.
22. Schlenk, W.; Bergmann, E. *Justus Liebigs Annalen der Chemie* **1928**, *463*, 98.
23. Rausch, M. D.; Ciappenelli, D. J. *Journal of Organometallic Chemistry* **1967**, *10*, 127-136.
24. Slocum, D. W.; Engelmann, T. R.; Ernst, C.; Jennings, C. A.; Jones, W.; Koonsvitsky, B.; Lewis, J.; Shenkin, P. *Journal of Chemical Education* **1969**, *46*, 144-150.
25. Rausch, M. D.; Moser, G. A.; Meade, C. F. *Journal of Organometallic Chemistry* **1973**, *51*, 1-11.
26. Winter, C. H.; Seneviratne, K. N.; Bretschneider-Hurley, A. *Comments on Inorganic Chemistry* **1996**, *19*, 1-23.
27. Conant, J. B.; Wheland, G. W. *Journal of the American Chemical Society* **1932**, *54*, 1212-1221.
28. Benkeser, R. A.; Foster, D. J.; Sauve, D. M.; Nobis, J. F. *Chemical Reviews* **1957**, *57*, 867-894.
29. Truce, W. E.; Norman, O. L. *Journal of the American Chemical Society* **1953**, *75*, 6023-6025.
30. Gronowitz, S. *Arkiv För Kemi* **1954**, *7*, 361-369.

31. Shirley, D. A.; Letho, E. A. *Journal of the American Chemical Society* **1957**, 79, 3481-3485.
32. Gilman, H.; Cheney, L. C.; Willis, H. B. *Journal of the American Chemical Society* **1939**, 61, 951-954.
33. Gilman, H.; Langham, W.; Willis, H. B. *Journal of the American Chemical Society* **1940**, 62, 346-348.
34. Tomooka, K. In *The Chemistry of Organolithium Compounds*; Rappoport, Z., Marek, I., Eds.; John Wiley & Sons, Ltd.: West Sussex, England, 2004; Vol. 2, pp 749-828.
35. Lewis, H. L.; Brown, T. L. *Journal of the American Chemical Society* **1970**, 92, 4664-4670.
36. Katsoulos, G.; Takagishi, S.; Schlosser, M. *Synlett* **1991**, 731-732.
37. Screttas, C. G.; Eastham, J. F. *Journal of the American Chemical Society* **1965**, 87, 3276-3277.
38. Clayden, J. In *The Chemistry of Organolithium Compounds*; Rappoport, Z., Marek, I., Eds.; John Wiley & Sons, Ltd.: West Sussex, England, 2004; Vol. 1, pp 495-646.
39. Eberhardt, G. G.; Butte, W. A. *Journal of Organic Chemistry* **1964**, 29, 2928-2932.
40. Langer Jr., A. W. *Transactions New York Academy of Sciences* **1965**, 27, 741-747.
41. Rausch, M. D.; Sarnelli, A. J. In *Polyamine-Chelated Alkali Metal Compounds*; Langer, A. W., Ed.; American Chemical Society: Washington, D. C., 1974; Vol. 130, pp 248-269.
42. Hay, J. N.; McCabe, J. F.; Robb, J. C. *Journal of the Chemical Society, Faraday Transactions 1: Physical Chemistry in Condensed Phases* **1972**, 68, 1-9.
43. Eastham, J. F.; Gibson, G. W. *Journal of the American Chemical Society* **1963**, 85, 2171.
44. Brown, T. L. In *Advances in Organometallic Chemistry*; Stone, F. G. A., West, R., Eds.; Academic Press, Inc.: New York, New York, 1965; Vol. 3, pp 365-395.
45. Brown, T. L.; Ladd, J. A.; Newman, G. N. *Journal of Organometallic Chemistry* **1965**, 3, 1-6.

46. Cheema, Z. K.; Gibson, G. W.; Eastham, J. F. *Journal of the American Chemical Society* **1963**, 85, 3517-3518.
47. Oliver, J. P.; Smart, J. B.; Emerson, M. T. *Journal of the American Chemical Society* **1966**, 88, 4101.
48. Screttas, C. G.; Eastham, J. F. *Journal of the American Chemical Society* **1966**, 88, 5668-5670.
49. Chalk, A. J.; Hoozeboom, T. J. *Journal of Organometallic Chemistry* **1968**, 11, 615-618.
50. Margerison, D.; Newport, J. P. *Transactions of the Faraday Society* **1963**, 59, 2058-2063.
51. Brown, T. L. *Accounts of Chemical Research* **1968**, 1, 23-32.
52. Elschenbroich, C.; Salzer, A. *Organometallics: A Concise Introduction*; 2nd ed.; VCH Publishers Inc.: New York, New York, 1992.
53. Waack, R.; West, P. *Journal of Organometallic Chemistry* **1966**, 5, 188-191.
54. West, P.; Waack, R. *Journal of the American Chemical Society* **1967**, 89, 4395-4399.
55. Langer Jr., A. W. *Polymer Preprints, American Chemical Society, Division of Polymer Chemistry* **1966**, 7, 132.
56. Brown, T. L.; Gerteis, R. L.; Bafus, D. A.; Ladd, J. A. *Journal of the American Chemical Society* **1964**, 86, 2135-2141.
57. Young, R. V. *Iowa State College Journal of Science* **1937**, 12, 177.
58. Bryce-Smith, D.; Turner, E. E. *Journal of the Chemical Society* **1953**, 861-867.
59. Gilman, H.; Gaj, B. J. *Journal of Organic Chemistry* **1963**, 28, 1725.
60. Eastham, J. F.; Screttas, C. G.; U. S. Patent No. 3,534,113, 1970.
61. Smith, W. N. In *Polyamine-Chelated Alkali Metal Compounds*; Langer, A. W., Ed.; American Chemical Society: Washington, D. C., 1974; Vol. 130, pp 23-55.
62. Schlosser, M. *Journal of Organometallic Chemistry* **1967**, 8, 9-16.
63. Bryce-Smith, D. *Journal of the Chemical Society* **1963**, 5983.

64. Langer Jr., A. W. In *Polyamine-Chelated Alkali Metal Compounds*; Langer, A. W., Ed.; American Chemical Society: Washington, D. C., 1974; Vol. 130, pp 1-22.
65. Clauss, V. K.; Bestian, H. *Justus Liebigs Annalen der Chemie* **1962**, 654, 8-19.
66. Gilman, H.; Gorsich, R. D. *Journal of Organic Chemistry* **1957**, 22, 687-689.
67. Gilman, H.; Gray, S. *Journal of Organic Chemistry* **1958**, 23, 1476-1479.
68. Gilman, H.; Trepka, W. J. *Journal of Organic Chemistry* **1961**, 26, 5202.
69. Gilman, H.; Trepka, W. J. *Journal of Organic Chemistry* **1962**, 27, 1418.
70. Mayo, D. W.; Shaw, P. D.; Rausch, M. *Chemistry and Industry* **1957**, 1388-1389.
71. Gilman, H.; Schwebke, G. L. *Journal of Organometallic Chemistry* **1965**, 4, 483.
72. Peterson, D. J.; Hays, H. R. *Journal of Organic Chemistry* **1965**, 30, 1939-1942.
73. Coates, G. E. *Organometallic Compounds*; 2nd ed.; Wiley: New York, New York, 1960.
74. Applequist, D. E.; O'Brien, D. F. *Journal of the American Chemical Society* **1963**, 85, 743.
75. Tobolsky, A. V.; Rogers, C. E. *Journal of Polymer Science* **1959**, 40, 73.
76. Bywater, S.; Worsfold, D. J. *Canadian Journal of Chemistry* **1962**, 40, 1564.
77. O'Driscoll, K. F.; Tobolsky, A. V. *Journal of Polymer Science* **1959**, 35, 259.
78. Kovrizhnukh, E. A.; Shatenshtein, A. I. *Uspekhi Khimii* **1969**, 38, 1836.
79. Okhlobystin, O. Y. *Uspekhi Khimii* **1967**, 36, 34.
80. Ziegler, K.; Colonius, H. *Justus Liebigs Annalen der Chemie* **1930**, 479, 135-149.
81. Haubein, A. H. *Iowa State College Journal of Science* **1943**, 18, 48-50.
82. Gilman, H.; Clark, R. N. *Journal of the American Chemical Society* **1947**, 69, 1499.
83. Ziegler, K.; Gellert, H. G. *Justus Liebigs Annalen der Chemie* **1950**, 567, 179.

84. Letsinger, R. L.; Schnizer, A. W.; Bobko, E. *Journal of the American Chemical Society* **1951**, *73*, 5708.
85. Bartlett, P. D.; Friedman, S.; Stiles, M. *Journal of the American Chemical Society* **1953**, *75*, 1771-1772.
86. Gilman, H.; Haubein, A. H.; Hartzfeld, H. *Journal of Organic Chemistry* **1954**, *19*, 1034-1040.
87. Honeycutt, S. C. *Journal of Organometallic Chemistry* **1971**, *29*, 1-5.
88. Burwell Jr., R. L. *Chemical Reviews* **1954**, *54*, 615.
89. Bates, R. B.; Kroposki, L. M.; Potter, D. E. *Journal of Organic Chemistry* **1972**, *37*, 560-562.
90. Maercker, A.; Theysohn, W. *Justus Liebigs Annalen der Chemie* **1971**, *747*, 70.
91. Gilman, H.; Moore, F. W.; Baine, O. *Journal of the American Chemical Society* **1941**, *63*, 2479.
92. *Organometallics in Organic Synthesis*; Wiley: New York, New York, 1994.
93. Stanetty, P.; Koller, H.; Mihovilovic *Journal of Organic Chemistry* **1992**, *57*, 6833-6837.
94. Gilman, H.; Gaj, B. J. *Journal of Organic Chemistry* **1957**, *22*, 1165-1168.
95. Esmay, D. L.; Kamienski, C. W. *Chemical Abstracts* **1964**, *60*, 14537.
96. Gilman, H.; Cartledge, F. K.; Sim, S. Y. *Journal of Organometallic Chemistry* **1965**, *4*, 332.
97. Gilman, H.; Trepka, W. J. *Journal of Organometallic Chemistry* **1965**, *3*, 174.
98. Kobrich, G.; Flory, K.; Merkle, H. R.; Trapp, H. *Angewandte Chemie, International Edition* **1965**, *4*, 706.
99. Rausch, M. D.; Tibbetts, F. E.; Gordon, H. B. *Journal of Organometallic Chemistry* **1966**, *5*, 493-500.
100. Schoellkopf, U.; Rizk, M. *Angewandte Chemie, International Edition* **1965**, *4*, 957.
101. Seyferth, D.; Cohen, H. M. *Journal of Organometallic Chemistry* **1963**, *1*, 15.

102. Fitt, J. J.; Gschwend, H. W. *Journal of Organic Chemistry* **1984**, *49*, 209-210.
103. Slocum, D. W.; Jennings, C. A. *Journal of Organic Chemistry* **1976**, *41*, 3653-3664.
104. Klein, K. P.; Hauser, C. R. *Journal of Organic Chemistry* **1967**, *32*, 1479.
105. Schlosser, M. *European Journal of Organic Chemistry* **2001**, 3975-3984.
106. Shirley, D. A.; Cheng, C. F. *Journal of Organometallic Chemistry* **1969**, *20*, 251-252.
107. Baston, E.; Wang, Q.; Schlosser, M. *Tetrahedron Letters* **2000**, *41*, 667-670.
108. Furlano, D. C.; Calderon, S. N.; Chen, G.; Kirk, K. L. *Journal of Organic Chemistry* **1988**, *53*, 3145-3147.
109. Huisgen, R.; Rist, H. *Justus Liebigs Annalen der Chemie* **1955**, *594*, 137-158.
110. Ladd, D. L.; Weinstock, J. *Journal of Organic Chemistry* **1981**, *46*, 203-206.
111. Adejare, A.; Miller, D. D. *Tetrahedron Letters* **1984**, *25*, 5597-5598.
112. Gilman, H.; Soddy, T. S. *Journal of Organic Chemistry* **1957**, *22*, 1715-1716.
113. Wittig, G.; Pohmer, L. *Angewandte Chemie* **1955**, *67*, 348.
114. Wittig, G.; Pohmer, L. *Chemische Berichte* **1956**, *89*, 1334-1351.
115. Gilman, H.; Gorsich, R. D. *Journal of the American Chemical Society* **1956**, *78*, 2217-2222.
116. Gilman, H.; Gorsich, R. D. *Journal of the American Chemical Society* **1957**, *79*, 2625-2629.
117. Ma, S.; He, Q. *Angewandte Chemie, International Edition* **2004**, *43*, 988-990.
118. Ma, S.; He, Q.; Jin, X. *Synlett* **2005**, 514-516.
119. Verkruijsse, H. D.; Verboom, W.; Van Rijn, P. E.; Brandsma, L. *Journal of Organometallic Chemistry* **1982**, *232*, C1-C4.
120. Huynh, C.; Linstrumelle, G. *Journal of the Chemical Society, Chemical Communications* **1983**, 1133-1134.
121. Maercker, A.; Fischenich, J. *Tetrahedron* **1995**, *51*, 10209-10218.

122. Thomson, T.; Stevens, T. S. *Journal of the Chemical Society* **1933**, 556.
123. Glaze, W. H.; Lin, J.; Felton, E. G. *Journal of Organic Chemistry* **1966**, *31*, 2643-2645.
124. Finnegan, R. A.; Kutta, H. W. *Journal of Organic Chemistry* **1965**, *30*, 4138-4144.
125. Eppley, R. L.; Dixon, J. A. *Journal of Organometallic Chemistry* **1968**, *11*, 174.
126. Glaze, W. H.; Adams, G. M. *Journal of the American Chemical Society* **1966**, *88*, 4653-4656.
127. Bryce-Smith, D. *Journal of the Chemical Society* **1955**, 1712-1714.
128. Ziegler, K. *Erdoel und Kohle, Erdgas, Petrochemie Vereinigt mit Brennstoff-Chemie* **1952**, *33*, 193.
129. Gilman, H.; Bradley, C. W. *Journal of the American Chemical Society* **1938**, *60*, 2333-2336.
130. Haiduc, I.; Gilman, H. *Journal of Organometallic Chemistry* **1968**, *13*, P4-P6.
131. Haiduc, I.; Gilman, H. *Revue Roumaine de Chimie* **1971**, *16*, 907-918.
132. Betz, J.; Bauer, W. *Journal of the American Chemical Society* **2002**, *124*, 8699-8706.
133. Kiefel, C.; Mannschreck, A. *Synthesis* **1995**, *8*, 1033-1037.
134. Meyers, A. I.; Avila, W. B. *Tetrahedron Letters* **1980**, *21*, 3335-3338.
135. Shirley, D. A.; Johnson Jr., J. R.; Hendrix, J. P. *Journal of Organometallic Chemistry* **1968**, *11*, 209-216.
136. Gilman, H.; Pacevitz, H. A.; Baine, O. *Journal of the American Chemical Society* **1940**, *62*, 1514-1520.
137. Slocum, D. W.; Engelmann, T. R.; Jennings, C. A. *Australian Journal of Chemistry* **1968**, *21*, 2319-2321.
138. Roberts, J. D.; Curtin, D. Y. *Journal of the American Chemical Society* **1946**, *68*, 1658-1660.

139. Harper Jr., R. J.; Soloski, E. J.; Tamborski, C. *Journal of Organic Chemistry* **1964**, 29, 2385-2389.
140. Tamborski, C.; Soloski, E. J.; Dills, C. E. *Chemistry and Industry* **1965**, 2067-2068.
141. Gilman, H.; Bebb, R. L. *Journal of the American Chemical Society* **1939**, 61, 109-112.
142. Wittig, G.; Fuhrman, G. *Chemische Berichte* **1940**, 73, 1197.
143. Shirley, D. A.; Hendrix, J. P. *Journal of Organometallic Chemistry* **1968**, 11, 217-226.
144. Snieckus, V. *Chemical Reviews* **1990**, 90, 879-933.
145. Dietz, S. D.; Bell, W. L.; Cook, R. L. *Journal of Organometallic Chemistry* **1997**, 545-546, 67-70.
146. Perseghini, M.; Togni, A. In *Science of Synthesis (Houben-Weyl Methods of Molecular Transformations)*; Georg Thieme Verlag: New York, 2001; Vol. 1, pp 889-929.
147. Benkeser, R. A.; Goggin, D.; Schroll, G. *Journal of the American Chemical Society* **1954**, 76, 4025-4026.
148. Nesmeyanov, A. N.; Perevalova, E. G.; Golovnya, R. V.; Nesmeyanova, O. A. *Doklady Akademii Nauk S.S.S.R.* **1954**, 97, 459-461.
149. Rausch, M.; Vogel, M.; Rosenberg, H. *Journal of Organic Chemistry* **1957**, 22, 900-903.
150. Rausch, M. D.; Fischer, E. O.; Grubert, H. *Journal of the American Chemical Society* **1960**, 82, 76-82.
151. Goldberg, S. I.; Keith, L. H.; Prokopov, T. S. *Journal of Organic Chemistry* **1963**, 28, 850-851.
152. Benkeser, R. A.; Bach, J. L. *Journal of the American Chemical Society* **1964**, 86, 890-895.
153. Hedberg, F. L.; Rosenberg, H. *Tetrahedron Letters* **1969**, 10, 4011-4012.
154. Dong, T. Y.; Lai, L. L. *Journal of Organometallic Chemistry* **1996**, 509, 131-134.

155. Nesmeyanov, A. N.; Perevalova, E. G.; Nesmeyanova, O. A. *Doklady Akademii Nauk S.S.S.R.* **1955**, *100*, 1099-1101.
156. Shechter, H.; Helling, J. F. *Journal of Organic Chemistry* **1961**, *26*, 1034.
157. Fish, R. W.; Rosenblum, M. *Journal of Organic Chemistry* **1965**, *30*, 1253.
158. Huffman, J. W.; Keith, L. H.; Asbury, R. L. *Journal of Organic Chemistry* **1965**, *30*, 1600-1604.
159. Nesmeyanov, A. N.; Sazonova, V. A.; Drozd, V. N. *Doklady Akademii Nauk S.S.S.R.* **1959**, *126*, 1004.
160. Seyferth, D.; Hofmann, H. P.; Burton, R.; Helling, J. F. *Inorganic Chemistry* **1962**, *1*, 227-231.
161. Seyferth, D.; Helling, J. F. *Chemistry and Industry* **1961**, 1568.
162. Rausch, M. D. *Inorganic Chemistry* **1962**, *1*, 414-417.
163. Reeve, W.; Group Jr., E. F. *Journal of Organic Chemistry* **1967**, *32*, 122-125.
164. Guillaneux, D.; Kagan, H. B. *Journal of Organic Chemistry* **1995**, *60*, 2502-2505.
165. Rebiere, F.; Samuel, O.; Kagan, H. B. *Tetrahedron Letters* **1990**, *31*, 3121-3124.
166. Mueller-Westerhoff, U. T.; Yang, Z.; Ingram, G. *Journal of Organometallic Chemistry* **1993**, *463*, 163-167.
167. Sanders, R.; Mueller-Westerhoff, U. T. *Journal of Organometallic Chemistry* **1996**, *512*, 219-224.
168. Bildstein, B.; Malaun, M.; Kopacka, H.; Wurst, K.; Mitterböck, M.; Ongania, K. H.; Opromolla, G.; Zanello, P. *Organometallics* **1999**, *18*, 4325-4336.
169. Rautz, H.; Stüger, H.; Kickelbick, G.; Pietzsch, C. *Journal of Organometallic Chemistry* **2001**, *627*, 167-178.
170. Goldberg, S. I.; Mayo, D. W.; Vogel, M.; Rosenberg, H.; Rausch, M. *Journal of Organic Chemistry* **1959**, *24*, 824-826.
171. Nesmeyanov, A. N.; Perevalova, E. G.; Beinoravitschute, S. A. *Doklady Akademii Nauk S.S.S.R.* **1957**, *112*, 439-440.
172. Nesmeyanov, A. N.; Perevalova, E. G.; Beinoravichute, Z. A.; Malygina, I. L. *Doklady Akademii Nauk S.S.S.R.* **1958**, *120*, 1263.

173. Post, E. W.; Crimmins, T. F. *Journal of Organometallic Chemistry* **1978**, *161*, C17-C19.
174. Bishop, J. J.; Davison, A.; Katcher, M. L.; Lichtenberg, D. W.; Merrill, R. E.; Smart, J. C. *Journal of Organometallic Chemistry* **1971**, *27*, 241-249.
175. Walczak, M.; Walczak, K.; Mink, R.; Rausch, M. D.; Stucky, G. *Journal of the American Chemical Society* **1978**, *100*, 6382-6388.
176. Foubelo, F.; Yus, M. *Trends in Organic Chemistry* **1998**, *7*, 1-26.
177. Andrikopoulos, P. C.; Armstrong, D. R.; Clegg, W.; Gilfillan, C. J.; Hevia, E.; Kennedy, A. R.; Mulvey, R. E.; O'Hara, C. T.; Parkinson, J. A.; Tooke, D. M. *Journal of the American Chemical Society* **2004**, *126*, 11612-11620.
178. Benkeser, R. A.; Nagai, Y.; Hooz, J. *Journal of the American Chemical Society* **1964**, *86*, 3742.
179. Osborne, A. G.; Whiteley, R. H. *Journal of Organometallic Chemistry* **1978**, *162*, 79-81.
180. Halasa, A. F.; Tate, D. P. *Journal of Organometallic Chemistry* **1970**, *24*, 769-773.
181. Clegg, W.; Henderson, K. W.; Kennedy, A. R.; Mulvey, R. E.; O'Hara, C. T.; Rowlings, R. B.; Tooke, D. M. *Angewandte Chemie, International Edition* **2001**, *40*, 3902-3905.
182. Boev, V. I.; Dombrovskii, A. V. *Zhurnal Obshchei Khimii* **1977**, *47*, 727.
183. Boev, V. I.; Dombrovskii, A. V. *Izvestiia Vysshikh Uchebnykh Zavedenii, Khimiya i Khimicheskaya Tekhnologiya* **1977**, *20*, 1789.
184. Han, Y. H.; Heeg, M. J.; Winter, C. H. *Organometallics* **1994**, *13*, 3009-3019.
185. Kur, S. A.; Winter, C. H. *Journal of Organometallic Chemistry* **1996**, *512*, 39-44.
186. Jutzi, P.; Lenze, N.; Neumann, B.; Stammeler, H. G. *Angewandte Chemie, International Edition* **2001**, *40*, 1423-1427.
187. Nesmeyanov, A. N.; Perevalova, E. G.; Beynoravichute, Z. A.; Malygina, I. L. *Proceedings of the Academy of Sciences of the U.S.S.R., Chemistry Section* **1958**, *120*, 499-502.

188. Morton, A. A.; Hechenbleickner, I. *Journal of the American Chemical Society* **1936**, 58, 2599.
189. Gilman, H.; Jacoby, A. L. *Journal of Organic Chemistry* **1938**, 3, 108-119.
190. Gilman, H.; Langham, W.; Jacoby, A. L. *Journal of the American Chemical Society* **1939**, 61, 106-109.
191. Maggi, R.; Schlosser, M. *Journal of Organic Chemistry* **1996**, 61, 5430-5434.
192. Schlosser, M.; Faigl, F.; Franzini, L.; Geneste, H.; Katsoulos, G.; Zhong, G. F. *Pure and Applied Chemistry* **1994**, 66, 1439-1446.
193. Slocum, D. W.; Rockett, B. W.; Hauser, C. R. *Chemistry and Industry* **1964**, 1831-1832.
194. Slocum, D. W.; Rockett, B. W.; Hauser, C. R. *Journal of the American Chemical Society* **1965**, 87, 1241-1246.
195. Nesmeyanov, A. N.; Baukova, T.; Grandberg, K. *Izvestiia Akademii Nauk S.S.S.R., Serii Khimicheskaiia* **1967**, 1867.
196. Slocum, D. W.; Koonsvitsky, B. P. *Journal of the Chemical Society, Chemical Communications* **1969**, 846.
197. Slocum, D. W.; Koonsvitsky, B. P.; Ernst, C. R. *Journal of Organometallic Chemistry* **1972**, 38, 125-132.
198. Narasimhan, N. S.; Mali, R. S. *Synthesis* **1983**, 957-986.
199. Beak, P.; Meyers, A. I. *Accounts of Chemical Research* **1986**, 19, 356-363.
200. Queguiner, G.; Marsais, F.; Snieckus, V.; Epszajn, J. In *Advances in Heterocyclic Chemistry*; Katritzky, A. R., Ed.; Academic Press, Inc.: San Diego, California, 1991; Vol. 52, pp 187-304.
201. Shimano, M.; Meyers, A. I. *Journal of the American Chemical Society* **1994**, 116, 10815-10816.
202. Schlosser, M. In *Organometallics in Synthesis: A Manual*; Schlosser, M., Ed.; John Wiley & Sons: Chichester, West Sussex, England, 1994, pp 81-104.
203. Aratani, T.; Gonda, T.; Nozaki, H. *Tetrahedron Letters* **1969**, 10, 2265-2268.
204. Aratani, T.; Gonda, T.; Nozaki, H. *Tetrahedron* **1970**, 26, 5453-5464.

205. Jäkle, F.; Lough, A. J.; Manners, I. *Chemical Communications* **1999**, 453-454.
206. Gamboa, J. A.; Sundararaman, A.; Kakalis, L.; Lough, A. J.; Jäkle, F. *Organometallics* **2002**, *21*, 4169-4181.
207. Mikami, K.; Matsumoto, Y.; Shiono, T. In *Science of Synthesis (Houben-Weyl Methods of Molecular Transformations)*; Georg Thieme Verlag: New York, 2003; Vol. 2, pp 457-679.
208. Demerseman, B.; Dixneuf, P. H. *Journal of Organometallic Chemistry* **1981**, *210*, C20-C22.
209. Demerseman, B.; Dixneuf, P. H.; Douglade, J.; Mercier, R. *Inorganic Chemistry* **1982**, *21*, 3942-3947.
210. Rausch, M. D.; Ogasa, M.; Rogers, R. D.; Rollins, A. N. *Organometallics* **1991**, *10*, 2084-2086.
211. Groenenboom, C. J.; Sawatzky, G.; De Liefde Meijer, H. J.; Jellinek, F. *Journal of Organometallic Chemistry* **1974**, *76*, C4-C6.
212. Groenenboom, C. J.; Jellinek, F. *Journal of Organometallic Chemistry* **1974**, *80*, 229-234.
213. Rausch, M. D.; Ogasa, M.; Ayers, M. A.; Rogers, R. D.; Rollins, A. N. *Organometallics* **1991**, *10*, 2481-2484.
214. Ogasa, M.; Rausch, M. D.; Rogers, R. D. *Journal of Organometallic Chemistry* **1991**, *403*, 279-291.
215. Tamm, M.; Kunst, A.; Herdtweck, E. *Chemical Communications* **2005**, 1729-1731.
216. Tamm, M.; Kunst, A.; Bannenberg, T.; Randoll, S.; Jones, P. G. *Organometallics* **2007**, *26*, 417-424.
217. Tamm, M. *Chemical Communications* **2008**, 2008, 3089-3100.
218. Elschenbroich, C.; Plackmeyer, J.; Harms, K.; Burghaus, O.; Pebler, J. *Organometallics* **2003**, *22*, 3367-3373.
219. Elschenbroich, C.; Plackmeyer, J.; Nowotny, M.; Harms, K.; Pebler, J.; Burghaus, O. *Inorganic Chemistry* **2005**, *44*, 955-963.
220. Elschenbroich, C.; Paganelli, F.; Nowotny, M.; Neumueller, B.; Burghaus, O. *Zeitschrift fuer Anorganische und Allgemeine Chemie* **2004**, *630*, 1599-1606.

221. Tamm, M.; Kunst, A.; Bannenberg, T.; Herdtweck, E.; Schmid, R. *Organometallics* **2005**, *24*, 3163-3171.
222. Braunschweig, H.; Lutz, M.; Radacki, K.; Schaumlöffel, A.; Seeler, F.; Unkelbach, C. *Organometallics* **2006**, *25*, 4433-4435.
223. Fischer, O. E.; Breitschaft, S. *Chemische Berichte* **1966**, *99*, 2905-2917.
224. Braunschweig, H.; Lutz, M.; Radacki, K. *Angewandte Chemie, International Edition* **2005**, *44*, 5647-5651.
225. Braunschweig, H.; Kupfer, T.; Lutz, M.; Radacki, K. *Journal of the American Chemical Society* **2007**, *129*, 8893-8906.
226. Bartole-Scott, A.; Braunschweig, H.; Kupfer, T.; Lutz, M.; Manners, I.; Nguyen, T.; Radacki, K.; Seeler, F. *Chemistry: A European Journal* **2006**, *12*, 1266-1273.
227. Hiyami, T.; Kusumoto, T. In *Comprehensive Organic Synthesis*; Trost, B. M., Flemings, I., Eds.; Pergamon: Oxford, England, 1991; Vol. 8, pp 763-792 and references cited therein.
228. Schumann, H.; Keitsch, M. R.; Winterfeld, J.; Mühle, S.; Molander, G. A. *Journal of Organometallic Chemistry* **1998**, *559*, 181.
229. Wagner, G. H.; Strother, C. O.; U. S. Patent. No. 2,632,013, 1953.
230. Speier, J. L.; Webster, J.; Barnes, G. H. *Journal of the American Chemical Society* **1957**, *79*, 974 and references cited therein.
231. Curry, J. W. *Journal of the American Chemical Society* **1956**, *78*, 1686.
232. Harrod, J. F.; Chalk, A. J. *Journal of the American Chemical Society* **1964**, *86*, 1776.
233. Chalk, A. J.; Harrod, J. F. *Journal of the American Chemical Society* **1965**, *87*, 16.
234. Harrod, J. F.; Chalk, A. J. *Journal of the American Chemical Society* **1965**, *87*, 1133.
235. Harrod, J. F.; Chalk, A. J. *Journal of the American Chemical Society* **1966**, *88*, 3491.
236. Marciniak, B. *Applied Organometallic Chemistry* **2000**, *14*, 527 and references cited therein.

- 237. Brown-Wensley, K. A. *Organometallics* **1987**, 6, 1590.
- 238. Braunstein, P.; Knorr, M. *Journal of Organometallic Chemistry* **1995**, 500, 21.
- 239. Tanke, R. S.; Crabtree, R. H. *Journal of the American Chemical Society* **1990**, 112, 7984.
- 240. Jun, C.-H.; Crabtree, R. H. *Journal of Organometallic Chemistry* **1993**, 447, 177.
- 241. Lewis, L. N.; Lewis, N. *Journal of the American Chemical Society* **1986**, 108, 7228.
- 242. Lewis, L. N. *Journal of the American Chemical Society* **1990**, 112, 5998.
- 243. Stein, J.; Lewis, L. N.; Gao, Y.; Scott, R. A. *Journal of the American Chemical Society* **1999**, 121, 3693.
- 244. Esteruelas, M. A.; Herrero, J.; Oro, L. A. *Organometallics* **1993**, 12, 2377.
- 245. Dash, A. K.; Wang, J. Q.; Eisen, M. S. *Organometallics* **1999**, 18, 4724.
- 246. Lappert, M. F.; Nile, T. A.; Takahashi, S. *Journal of Organometallic Chemistry* **1974**, 72, 425.
- 247. Tsipis, C. A. *Journal of Organometallic Chemistry* **1980**, 188, 53.
- 248. Tsipis, C. A. *Journal of Organometallic Chemistry* **1980**, 187, 427.
- 249. Herzig, C. J. In *Organosilicon Chemistry-From Molecules to Materials*; Auner, N., Weis, J., Eds.; VCH: Germany and USA, 1994, pp 253-260.
- 250. Pang, Y.; Ijadi-Maghsoodi, S.; Barton, T. J. *Macromolecules* **1993**, 26, 5671.
- 251. Ijadi-Maghsoodi, S.; Pang, Y.; Barton, T. J. *Journal of Polymer Science, Part A* **1990**, 28, 955.
- 252. Son, D. Y.; Bucca, D.; Keller, T. M. *Tetrahedron Letters* **1996**, 37, 1579.
- 253. Kim, D. S.; Shim, S. C. *Journal of Polymer Science, Part A* **1999**, 37, 2933.
- 254. Kim, D. S.; Shim, S. C. *Journal of Polymer Science, Part A* **1999**, 37, 2263.
- 255. Barlow, S.; O'Hare, D. *Chemical Reviews* **1999**, 97, 637 and references cited therein.

256. Nguyen, P.; Gómez-Elipé, P.; Manners, I. *Chemical Reviews* **1999**, 99, 1515 and references cited therein.
257. Gonsalves, K. E.; Chen, X. *Ferrocenes*; VCH: Germany, 1995.
258. Greber, G.; Hallensleben, M. L. *Angewandte Chemie, International Edition* **1965**, 4, 701.
259. Asatiani, L. P.; El-Agamey, A. A.; Diab, M. A. *Journal of Polymer Science, Part A* **1983**, 21, 2529.
260. Cuadrado, I.; Carmen, M. C.; Alonso, B.; Moràn, M.; Losada, J.; Belsky, V. *Journal of the American Chemical Society* **1997**, 119, 7613.
261. Manners, I. *Advances in Organometallic Chemistry* **1995**, 37, 131 and references cited therein.
262. Manners, I. *Angewandte Chemie, International Edition* **1996**, 35, 1602 and references cited therein.
263. Sheats, J. E.; Carraher, C. E.; Pittman, C. U. *Metal Containing Polymer Systems*; Plenum: New York, 1985.
264. Inagaki, T.; Lee, H. S.; Skotheim, T. A.; Okamoto, Y. *Journal of the Chemical Society, Chemical Communications* **1989**, 1181.
265. Liu, X.-H.; Bruce, D.; Manners, I. *Journal of Organometallic Chemistry* **1997**, 548, 49.
266. Liu, X.-H.; Bruce, D.; Manners, I. *Journal of the Chemical Society, Chemical Communications* **1997**, 289.
267. Verkouw, H. T.; Van Oven, H. O. *Journal of Organometallic Chemistry* **1973**, 59, 259-266.
268. Zeinstra, J. D.; De Boer, J. L. *Journal of Organometallic Chemistry* **1973**, 54, 207-211.
269. Kaltsoyannis, N. *Journal of the Chemical Society, Dalton Transactions: Inorganic Chemistry* **1995**, 3727-3730.
270. McKenzie, T. C.; Sanner, R. D.; Bercaw, J. E. *Journal of Organometallic Chemistry* **1975**, 102, 457-466.
271. Elian, M.; Chen, M. M. L.; Mingoes, D. M. P.; Hoffmann, R. *Inorganic Chemistry* **1976**, 15, 1148-1155.

272. Haaland, A. *Accounts of Chemical Research* **1979**, *12*, 415-422.
273. Kool, L. B.; Rausch, M. D.; Rogers, R. D. *Journal of Organometallic Chemistry* **1985**, *297*, 289-299.
274. Green, M. L. H.; Ng, D. K. P. *Chemical Reviews* **1995**, *95*, 439-473.
275. Lyssenko, K. A.; Antipin, M. Y.; Ketkov, S. Y. *Russian Chemical Bulletin, International Edition* **2001**, *50*, 130-141.
276. Yamashita, H.; Uchimaru, Y. *Journal of the Chemical Society, Chemical Communications* **1999**, 1763.
277. Lukevics, E.; Sturkovich, R. Y.; Pudova, O. A. *Journal of Organometallic Chemistry* **1985**, *292*, 151-158.
278. Itsuno, S.; Chao, D.; Ito, K. *Journal of Polymer Science, Part A* **1993**, *31*, 287.
279. Xiao, Y.; Wong, R. A.; Son, D. Y. *Macromolecules* **2000**, *33*, 7232.
280. Tsumura, M.; Iwahara, T.; Hirose, T. *Polymer Journal* **1995**, *27*, 1048.
281. Tsumura, M.; Iwahara, T.; Hirose, T. *Journal of Polymer Science, Part A* **1996**, *34*, 3155.
282. Mori, A.; Takahisa, E.; Kajiro, H.; Nishihara, Y.; Hiyama, T. *Macromolecules* **2000**, *33*, 1115-1116.
283. Mori, A.; Takahisa, E.; Kajiro, H.; Nishihara, Y.; Hiyama, T. *Polyhedron* **2000**, *19*, 567.
284. Chen, R.-M.; Chien, K.-M.; Wong, K.-T.; Jin, B.-Y.; Luh, T.-Y.; Hsu, J.-H.; Fann, W. *Journal of the American Chemical Society* **1997**, *119*, 11321.
285. Morán, M.; Casado, C. M.; Cuadrado, I. *Organometallics* **1993**, *12*, 4327.
286. Li, Y.; Kawakami, Y. *Macromolecules* **1998**, *31*, 5592.
287. Zhang, R.; Mark, J. E.; Pinhas, A. R. *Macromolecules* **2000**, *33*, 3508.
288. Rutherford, D. R.; Stille, J. K.; Elliott, C. M.; Reichert, V. R. *Macromolecules* **1992**, *25*, 2294.
289. Li, J.; Pang, Y. *Macromolecules* **1997**, *30*, 7487.

290. Long, N. J.; Martin, A. J.; Vilar, R.; White, A. J. P.; Williams, D. J.; M., Y. *Organometallics* **1999**, *18*, 4261.
291. Zhu, Y.; Wolf, M. O. *Journal of the American Chemical Society* **2000**, *122*, 10121.
292. Hradsky, A.; Bildstein, B.; Schuler, N.; Schottenberger, H.; Jaitner, P.; Ongania, K.-H.; Wurst, K.; Launay, J.-P. *Organometallics* **1997**, *16*, 392.
293. Sheldrick, G. M.; Bruker AXS Inc.: Madison, Wisconsin, USA, 2004.
294. The Cambridge Crystallographic Data Centre: Cambridge, CB2 1EZ, UK, 2005.
295. Bruker; Bruker AXS Inc.: Madison, Wisconsin, USA, 2006.
296. Bruker; Bruker AXS Inc.: Madison, Wisconsin, USA, 2005.
297. Sheldrick, G. M.; University of Göttingen, Germany, 2001.
298. Otwinowski, Z.; Minor, W. In *Methods in Enzymology*; Carter, C. W., Sweet, R. M., Eds.; Academic Press: London, 1997; Vol. 276, pp 307-326.
299. Blessing, R. H. *Acta Crystallographica* **1995**, *A51*, 33-38.
300. Sheldrick, G. M.; Bruker AXS Inc.: Madison, Wisconsin, USA, 2001.
301. Demerseman, B. In *Organometallic Syntheses*; Eisch, J. J., King, R. B., Eds.; Academic Press: New York, 1986; Vol. 3, pp 27-28.
302. Corriu, R. J. P.; Devylder, N.; Guérin, C.; Henner, B.; Jean, A. *Organometallics* **1994**, *13*, 3194.
303. Takahashi, S.; Kuroyama, Y.; Sonogashira, K.; Hagihara, N. *Synthesis* **1980**, 627-630.
304. Neenan, T. X.; Whitesides, G. M. *Journal of Organic Chemistry* **1988**, *53*, 2489-2496.
305. Iovel, I. G.; Goldberg, Y. S.; Shymanska, M. V.; Lukevics, E. *Organometallics* **1987**, *6*, 1410-1413.
306. Caseri, W.; Pregosin, P. S. *Organometallics* **1988**, *7*, 1373-1380.
307. Jimenez, R.; Lopez, J. M.; Cervantes, J. *Canadian Journal of Chemistry* **2000**, *78*, 1491-1495.

- 308. Mori, A.; Takahisa, E.; Yamamura, Y.; Kato, T.; Mudalige, A. P.; Kajiro, H.; Hirabayashi, K.; Nishihara, Y.; Hiyama, T. *Organometallics* **2004**, *23*, 1755-1765.
- 309. Katayama, H.; Taniguchi, K.; Kobayashi, M.; Sagawa, T.; Minami, T.; Ozawa, F. *Journal of Organometallic Chemistry* **2002**, *645*, 192-200.
- 310. Nagao, M.; Asano, K.; Umeda, K.; Katayama, H.; Ozawa, F. *Journal of Organic Chemistry* **2005**, *70*, 10511-10514.

Appendix

The following tables are supplementary material for the X-ray crystal structures of complexes **202c**, **206d**, **204d**, **207d**, and **210c**. The data of fractional atomic coordinates and equivalent isotropic displacement parameters, anisotropic displacement parameters, bond lengths and bond angles are listed.

I. X-Ray Data for **202c**.

Table A.1.1. Crystal Data and Structure Refinement for **202c**.

| | | |
|-----------------------------------|---|---------------------|
| Empirical formula | C ₂₄ H ₂₁ P Ti | |
| Formula weight | 388.28 | |
| Temperature | 293(2) K | |
| Wavelength | 0.71073 Å | |
| Crystal system | Orthorhombic | |
| Space group | P2(1)2(1)2(1) | |
| Unit cell dimensions | a = 11.757(2) Å | $\alpha = 90^\circ$ |
| | b = 17.251(2) Å | $\beta = 90^\circ$ |
| | c = 9.6687(13) Å | $\gamma = 90^\circ$ |
| Volume | 1961.0(5) Å ³ | |
| Z | 4 | |
| Density (calculated) | 1.315 Mg/m ³ | |
| Absorption coefficient | 0.522 mm ⁻¹ | |
| F(000) | 808 | |
| Crystal size / Shape | 0.60 x 0.32 x 0.28 mm ³ | Parallelepiped |
| Theta range for data collection | 2.10 to 25.05° | |
| Index ranges | -14 ≤ h ≤ 14, -20 ≤ k ≤ 20, -11 ≤ l ≤ 11 | |
| Reflections collected | 3984 | |
| Independent reflections | 1992 [R(int) = 0.0404] | |
| Completeness to theta = 25.05° | 100.00% | |
| Absorption correction | None | |
| Refinement method | Full-matrix least-squares on F ² | |
| Data / restraints / parameters | 1992 / 0 / 237 | |
| Goodness-of-fit on F ² | 1.048 | |
| Final R indices [I > 2σ(I)] | R1 = 0.0414, wR2 = 0.0957 | |
| R indices (all data) | R1 = 0.0582, wR2 = 0.1030 | |
| Absolute structure parameter | 0.42(6) | |
| Extinction coefficient | 0.0016(8) | |
| Largest diff. peak and hole | 0.278 and -0.209 e.Å ⁻³ | |

Table A.1.2. Atomic coordinates ($\times 10^4$) and equivalent isotropic displacement parameters ($\text{\AA}^2 \times 10^3$) for **202c**. $U(\text{eq})$ is defined as one third of the trace of the orthogonalized U^{ij} tensor.

| | x | y | z | U(eq) |
|-------|---------|---------|----------|-------|
| Ti(1) | 2861(1) | 1599(1) | 382(1) | 50(1) |
| P(1) | 3647(1) | 1104(1) | 3961(1) | 43(1) |
| C(1) | 3939(3) | 1026(2) | 2115(5) | 42(1) |
| C(2) | 4697(4) | 1440(3) | 1260(5) | 49(1) |
| C(3) | 4675(4) | 1108(3) | -65(5) | 60(1) |
| C(4) | 3910(5) | 475(3) | -49(5) | 61(2) |
| C(5) | 3449(4) | 426(3) | 1294(5) | 51(1) |
| C(6) | 2810(7) | 2452(4) | -1309(7) | 84(2) |
| C(7) | 2870(7) | 2842(3) | -67(8) | 82(2) |
| C(8) | 2260(7) | 2718(4) | 1166(8) | 85(2) |
| C(9) | 1395(6) | 2122(5) | 1424(8) | 94(2) |
| C(10) | 988(5) | 1544(4) | 440(10) | 92(2) |
| C(11) | 1347(6) | 1441(4) | -917(8) | 82(2) |
| C(12) | 2121(7) | 1837(4) | -1668(7) | 86(2) |
| C(14) | 4925(4) | 2508(3) | 4216(6) | 58(1) |
| C(15) | 5016(5) | 3303(3) | 4511(6) | 67(2) |
| C(16) | 4081(5) | 3705(3) | 4929(6) | 68(2) |
| C(17) | 3064(5) | 3337(3) | 5079(6) | 76(2) |
| C(18) | 2969(4) | 2558(3) | 4789(6) | 62(1) |
| C(13) | 3902(3) | 2132(2) | 4341(5) | 41(1) |
| C(19) | 4928(4) | 646(2) | 4668(5) | 43(1) |
| C(20) | 5071(5) | 662(3) | 6104(5) | 60(1) |
| C(21) | 5961(5) | 261(4) | 6715(6) | 73(2) |
| C(22) | 6717(4) | -153(3) | 5939(6) | 62(1) |
| C(23) | 6585(4) | -176(3) | 4530(6) | 53(1) |
| C(24) | 5701(4) | 222(2) | 3909(5) | 47(1) |

Table A.1.3. Bond Lengths [\AA] and Angles [$^\circ$] for **202c**.

| | | | |
|-------------------|-----------|------------------|-----------|
| Ti(1)-C(7) | 2.188(5) | C(8)-H(8A) | 0.98 |
| Ti(1)-C(9) | 2.191(7) | C(9)-C(10) | 1.458(11) |
| Ti(1)-C(8) | 2.192(6) | C(9)-H(9A) | 0.98 |
| Ti(1)-C(11) | 2.195(6) | C(10)-C(11) | 1.391(10) |
| Ti(1)-C(6) | 2.201(6) | C(10)-H(10A) | 0.98 |
| Ti(1)-C(12) | 2.203(6) | C(11)-C(12) | 1.350(9) |
| Ti(1)-C(10) | 2.204(6) | C(11)-H(11A) | 0.98 |
| Ti(1)-C(5) | 2.313(4) | C(12)-H(12A) | 0.98 |
| Ti(1)-C(1) | 2.322(4) | C(14)-C(13) | 1.373(6) |
| Ti(1)-C(4) | 2.335(5) | C(14)-C(15) | 1.405(6) |
| Ti(1)-C(3) | 2.335(5) | C(14)-H(14A) | 0.93 |
| Ti(1)-C(2) | 2.336(5) | C(15)-C(16) | 1.361(7) |
| P(1)-C(1) | 1.823(5) | C(15)-H(15A) | 0.93 |
| P(1)-C(19) | 1.833(5) | C(16)-C(17) | 1.361(8) |
| P(1)-C(13) | 1.836(4) | C(16)-H(16A) | 0.93 |
| C(1)-C(2) | 1.410(6) | C(17)-C(18) | 1.377(7) |
| C(1)-C(5) | 1.425(6) | C(17)-H(17A) | 0.93 |
| C(2)-C(3) | 1.403(7) | C(18)-C(13) | 1.389(6) |
| C(2)-H(2A) | 0.98 | C(18)-H(18A) | 0.93 |
| C(3)-C(4) | 1.416(7) | C(19)-C(24) | 1.378(6) |
| C(3)-H(3A) | 0.98 | C(19)-C(20) | 1.399(7) |
| C(4)-C(5) | 1.409(7) | C(20)-C(21) | 1.386(7) |
| C(4)-H(4A) | 0.98 | C(20)-H(20A) | 0.93 |
| C(5)-H(5A) | 0.98 | C(21)-C(22) | 1.365(8) |
| C(6)-C(7) | 1.378(9) | C(21)-H(21A) | 0.93 |
| C(6)-C(12) | 1.379(9) | C(22)-C(23) | 1.372(8) |
| C(6)-H(6A) | 0.98 | C(22)-H(22A) | 0.93 |
| C(7)-C(8) | 1.408(10) | C(23)-C(24) | 1.383(6) |
| C(7)-H(7A) | 0.98 | C(23)-H(23A) | 0.93 |
| C(8)-C(9) | 1.468(10) | C(24)-H(24A) | 0.93 |
| | | | |
| C(7)-Ti(1)-C(9) | 72.0(3) | C(3)-C(4)-Ti(1) | 72.4(3) |
| C(7)-Ti(1)-C(8) | 37.5(3) | C(5)-C(4)-H(4A) | 126.1 |
| C(9)-Ti(1)-C(8) | 39.1(3) | C(3)-C(4)-H(4A) | 126.1 |
| C(7)-Ti(1)-C(11) | 90.7(3) | Ti(1)-C(4)-H(4A) | 126.1 |
| C(9)-Ti(1)-C(11) | 71.1(3) | C(4)-C(5)-C(1) | 108.3(4) |
| C(8)-Ti(1)-C(11) | 92.6(3) | C(4)-C(5)-Ti(1) | 73.2(3) |
| C(7)-Ti(1)-C(6) | 36.6(2) | C(1)-C(5)-Ti(1) | 72.4(2) |
| C(9)-Ti(1)-C(6) | 92.6(3) | C(4)-C(5)-H(5A) | 125.6 |
| C(8)-Ti(1)-C(6) | 70.1(3) | C(1)-C(5)-H(5A) | 125.6 |
| C(11)-Ti(1)-C(6) | 68.7(3) | Ti(1)-C(5)-H(5A) | 125.6 |
| C(7)-Ti(1)-C(12) | 68.9(3) | C(7)-C(6)-C(12) | 128.6(7) |
| C(9)-Ti(1)-C(12) | 91.5(3) | C(7)-C(6)-Ti(1) | 71.2(3) |
| C(8)-Ti(1)-C(12) | 91.1(3) | C(12)-C(6)-Ti(1) | 71.8(3) |
| C(11)-Ti(1)-C(12) | 35.8(2) | C(7)-C(6)-H(6A) | 113.4 |
| C(6)-Ti(1)-C(12) | 36.5(2) | C(12)-C(6)-H(6A) | 113.4 |

| | | | |
|-------------------|-----------|--------------------|----------|
| C(7)-Ti(1)-C(10) | 92.9(3) | Ti(1)-C(6)-H(6A) | 113.4 |
| C(9)-Ti(1)-C(10) | 38.7(3) | C(6)-C(7)-C(8) | 129.7(6) |
| C(8)-Ti(1)-C(10) | 72.9(3) | C(6)-C(7)-Ti(1) | 72.2(3) |
| C(11)-Ti(1)-C(10) | 36.9(3) | C(8)-C(7)-Ti(1) | 71.4(3) |
| C(6)-Ti(1)-C(10) | 91.2(3) | C(6)-C(7)-H(7A) | 112.7 |
| C(12)-Ti(1)-C(10) | 68.7(3) | C(8)-C(7)-H(7A) | 112.7 |
| C(7)-Ti(1)-C(5) | 158.7(2) | Ti(1)-C(7)-H(7A) | 112.7 |
| C(9)-Ti(1)-C(5) | 114.9(2) | C(7)-C(8)-C(9) | 127.1(6) |
| C(8)-Ti(1)-C(5) | 137.3(2) | C(7)-C(8)-Ti(1) | 71.1(4) |
| C(11)-Ti(1)-C(5) | 110.6(2) | C(9)-C(8)-Ti(1) | 70.4(4) |
| C(6)-Ti(1)-C(5) | 151.2(2) | C(7)-C(8)-H(8A) | 114.1 |
| C(12)-Ti(1)-C(5) | 128.7(2) | C(9)-C(8)-H(8A) | 114.1 |
| C(10)-Ti(1)-C(5) | 104.6(2) | Ti(1)-C(8)-H(8A) | 114.1 |
| C(7)-Ti(1)-C(1) | 123.9(2) | C(10)-C(9)-C(8) | 126.6(7) |
| C(9)-Ti(1)-C(1) | 105.8(2) | C(10)-C(9)-Ti(1) | 71.1(4) |
| C(8)-Ti(1)-C(1) | 107.5(2) | C(8)-C(9)-Ti(1) | 70.5(4) |
| C(11)-Ti(1)-C(1) | 143.4(2) | C(10)-C(9)-H(9A) | 114.6 |
| C(6)-Ti(1)-C(1) | 146.6(2) | C(8)-C(9)-H(9A) | 114.6 |
| C(12)-Ti(1)-C(1) | 160.8(2) | Ti(1)-C(9)-H(9A) | 114.6 |
| C(10)-Ti(1)-C(1) | 120.6(2) | C(11)-C(10)-C(9) | 127.2(7) |
| C(5)-Ti(1)-C(1) | 35.82(15) | C(11)-C(10)-Ti(1) | 71.2(4) |
| C(7)-Ti(1)-C(4) | 140.9(3) | C(9)-C(10)-Ti(1) | 70.1(4) |
| C(9)-Ti(1)-C(4) | 147.1(3) | C(11)-C(10)-H(10A) | 113.9 |
| C(8)-Ti(1)-C(4) | 164.5(2) | C(9)-C(10)-H(10A) | 113.9 |
| C(11)-Ti(1)-C(4) | 102.9(2) | Ti(1)-C(10)-H(10A) | 113.9 |
| C(6)-Ti(1)-C(4) | 115.9(2) | C(12)-C(11)-C(10) | 130.3(7) |
| C(12)-Ti(1)-C(4) | 101.7(2) | C(12)-C(11)-Ti(1) | 72.4(4) |
| C(10)-Ti(1)-C(4) | 119.8(3) | C(10)-C(11)-Ti(1) | 72.0(4) |
| C(5)-Ti(1)-C(4) | 35.29(18) | C(12)-C(11)-H(11A) | 112.5 |
| C(1)-Ti(1)-C(4) | 59.13(16) | C(10)-C(11)-H(11A) | 112.5 |
| C(7)-Ti(1)-C(3) | 108.3(3) | Ti(1)-C(11)-H(11A) | 112.5 |
| C(9)-Ti(1)-C(3) | 162.3(3) | C(11)-C(12)-C(6) | 130.6(7) |
| C(8)-Ti(1)-C(3) | 132.7(3) | C(11)-C(12)-Ti(1) | 71.8(4) |
| C(11)-Ti(1)-C(3) | 126.1(2) | C(6)-C(12)-Ti(1) | 71.7(3) |
| C(6)-Ti(1)-C(3) | 97.4(3) | C(11)-C(12)-H(12A) | 111.9 |
| C(12)-Ti(1)-C(3) | 105.2(2) | C(6)-C(12)-H(12A) | 111.9 |
| C(10)-Ti(1)-C(3) | 154.4(3) | Ti(1)-C(12)-H(12A) | 111.9 |
| C(5)-Ti(1)-C(3) | 58.68(18) | C(13)-C(14)-C(15) | 120.7(4) |
| C(1)-Ti(1)-C(3) | 58.70(17) | C(13)-C(14)-H(14A) | 119.7 |
| C(4)-Ti(1)-C(3) | 35.30(18) | C(15)-C(14)-H(14A) | 119.7 |
| C(7)-Ti(1)-C(2) | 100.5(2) | C(16)-C(15)-C(14) | 119.8(5) |
| C(9)-Ti(1)-C(2) | 127.4(3) | C(16)-C(15)-H(15A) | 120.1 |
| C(8)-Ti(1)-C(2) | 106.0(2) | C(14)-C(15)-H(15A) | 120.1 |
| C(11)-Ti(1)-C(2) | 160.5(2) | C(15)-C(16)-C(17) | 120.2(5) |
| C(6)-Ti(1)-C(2) | 111.9(2) | C(15)-C(16)-H(16A) | 119.9 |
| C(12)-Ti(1)-C(2) | 135.5(2) | C(17)-C(16)-H(16A) | 119.9 |
| C(10)-Ti(1)-C(2) | 155.3(3) | C(16)-C(17)-C(18) | 120.3(5) |
| C(5)-Ti(1)-C(2) | 58.82(17) | C(16)-C(17)-H(17A) | 119.8 |

| | | | |
|------------------|-----------|--------------------|----------|
| C(1)-Ti(1)-C(2) | 35.23(15) | C(18)-C(17)-H(17A) | 119.8 |
| C(4)-Ti(1)-C(2) | 58.63(17) | C(17)-C(18)-C(13) | 121.0(5) |
| C(3)-Ti(1)-C(2) | 34.96(17) | C(17)-C(18)-H(18A) | 119.5 |
| C(1)-P(1)-C(19) | 100.3(2) | C(13)-C(18)-H(18A) | 119.5 |
| C(1)-P(1)-C(13) | 103.7(2) | C(14)-C(13)-C(18) | 118.0(4) |
| C(19)-P(1)-C(13) | 102.0(2) | C(14)-C(13)-P(1) | 125.6(3) |
| C(2)-C(1)-C(5) | 107.3(4) | C(18)-C(13)-P(1) | 116.4(4) |
| C(2)-C(1)-P(1) | 131.0(3) | C(24)-C(19)-C(20) | 117.4(5) |
| C(5)-C(1)-P(1) | 121.5(3) | C(24)-C(19)-P(1) | 124.9(4) |
| C(2)-C(1)-Ti(1) | 72.9(3) | C(20)-C(19)-P(1) | 117.4(4) |
| C(5)-C(1)-Ti(1) | 71.7(2) | C(21)-C(20)-C(19) | 120.3(5) |
| P(1)-C(1)-Ti(1) | 124.9(2) | C(21)-C(20)-H(20A) | 119.9 |
| C(3)-C(2)-C(1) | 108.5(4) | C(19)-C(20)-H(20A) | 119.9 |
| C(3)-C(2)-Ti(1) | 72.5(3) | C(22)-C(21)-C(20) | 121.2(5) |
| C(1)-C(2)-Ti(1) | 71.8(2) | C(22)-C(21)-H(21A) | 119.4 |
| C(3)-C(2)-H(2A) | 125.7 | C(20)-C(21)-H(21A) | 119.4 |
| C(1)-C(2)-H(2A) | 125.7 | C(21)-C(22)-C(23) | 119.2(5) |
| Ti(1)-C(2)-H(2A) | 125.7 | C(21)-C(22)-H(22A) | 120.4 |
| C(2)-C(3)-C(4) | 108.4(5) | C(23)-C(22)-H(22A) | 120.4 |
| C(2)-C(3)-Ti(1) | 72.5(3) | C(22)-C(23)-C(24) | 120.2(5) |
| C(4)-C(3)-Ti(1) | 72.3(3) | C(22)-C(23)-H(23A) | 119.9 |
| C(2)-C(3)-H(3A) | 125.7 | C(24)-C(23)-H(23A) | 119.9 |
| C(4)-C(3)-H(3A) | 125.7 | C(19)-C(24)-C(23) | 121.8(5) |
| Ti(1)-C(3)-H(3A) | 125.7 | C(19)-C(24)-H(24A) | 119.1 |
| C(5)-C(4)-C(3) | 107.5(4) | C(23)-C(24)-H(24A) | 119.1 |
| C(5)-C(4)-Ti(1) | 71.5(3) | | |

Table A.1.4. Anisotropic displacement parameters ($\text{\AA}^2 \times 10^3$) for **202c**. The anisotropic displacement factor exponent takes the form: $-2\pi^2 [h^2 a^{*2} U^{11} + \dots + 2 h k a^* b^* U^{12}]$.

| | U^{11} | U^{22} | U^{33} | U^{23} | U^{13} | U^{12} |
|-------|----------|----------|----------|----------|----------|----------|
| Ti(1) | 52(1) | 38(1) | 61(1) | 8(1) | -18(1) | -3(1) |
| P(1) | 37(1) | 43(1) | 49(1) | 4(1) | 0(1) | 2(1) |
| C(1) | 40(2) | 37(2) | 50(3) | 2(2) | -11(2) | -1(2) |
| C(2) | 42(2) | 54(3) | 49(3) | 1(2) | -5(2) | -5(2) |
| C(3) | 59(3) | 69(3) | 51(3) | 6(3) | -2(2) | 9(3) |
| C(4) | 79(4) | 52(3) | 51(3) | -7(2) | -16(3) | 8(3) |
| C(5) | 58(3) | 34(2) | 62(3) | 5(2) | -15(3) | 0(2) |
| C(6) | 102(5) | 70(4) | 80(5) | 28(4) | -8(4) | -1(4) |
| C(7) | 86(4) | 44(3) | 115(6) | 13(3) | -22(5) | 2(3) |
| C(8) | 100(5) | 64(4) | 91(5) | -7(4) | -32(5) | 28(4) |
| C(9) | 87(5) | 122(6) | 74(4) | 32(4) | 7(4) | 59(5) |
| C(10) | 51(3) | 87(5) | 137(7) | 38(6) | -6(4) | 5(3) |
| C(11) | 71(4) | 76(4) | 99(5) | 4(4) | -38(4) | -7(4) |
| C(12) | 93(5) | 87(4) | 77(4) | 17(4) | -29(4) | 8(4) |
| C(14) | 34(2) | 56(3) | 84(4) | -16(3) | 0(3) | 6(2) |
| C(15) | 55(3) | 55(3) | 91(4) | -18(3) | -2(3) | -1(3) |
| C(16) | 80(4) | 44(3) | 82(4) | -8(3) | 7(3) | 4(3) |
| C(17) | 67(4) | 54(3) | 106(5) | -5(3) | 31(3) | 22(3) |
| C(18) | 46(3) | 60(3) | 80(4) | 0(3) | 21(3) | 9(3) |
| C(13) | 39(2) | 41(2) | 43(3) | 1(2) | -3(2) | 9(2) |
| C(19) | 46(2) | 35(2) | 50(3) | 7(2) | -1(2) | 0(2) |
| C(20) | 66(3) | 68(3) | 46(3) | -1(3) | -5(3) | 19(3) |
| C(21) | 86(4) | 83(4) | 51(3) | 5(3) | -22(3) | 14(4) |
| C(22) | 59(3) | 49(3) | 78(4) | 9(3) | -18(3) | 7(3) |
| C(23) | 44(2) | 39(2) | 75(4) | -2(3) | 4(3) | 6(2) |
| C(24) | 50(3) | 38(2) | 52(3) | 1(2) | -1(2) | 1(2) |

II. X-Ray Data for **206d**.

Table A.2.1. Crystal Data and Structure Refinement for **206d**.

| | | |
|-----------------------------------|--|---------------------|
| Empirical formula | C ₂₁ H ₃₆ Si ₃ Ti | |
| Formula weight | 420.67 | |
| Temperature | 100(2) K | |
| Wavelength | 1.54178 Å | |
| Crystal system | Orthorhombic | |
| Space group | P nma | |
| Unit cell dimensions | a = 12.48130(10) Å | $\alpha = 90^\circ$ |
| | b = 17.4190(2) Å | $\beta = 90^\circ$ |
| | c = 11.1136(2) Å | $\gamma = 90^\circ$ |
| Volume | 2416.23(6) Å ³ | |
| Z | 4 | |
| Density (calculated) | 1.156 Mg/m ³ | |
| Absorption coefficient | 4.424 mm ⁻¹ | |
| F(000) | 904 | |
| Crystal size / Shape | 0.27 x 0.18 x 0.15 mm ³ | Block-shaped |
| Theta range for data collection | 5.33 to 64.89° | |
| Index ranges | -13 ≤ h ≤ 14, -20 ≤ k ≤ 19, -11 ≤ l ≤ 12 | |
| Reflections collected | 6573 | |
| Independent reflections | 2003 [R(int) = 0.019] | |
| Completeness to theta = 64.89° | 94% | |
| Absorption correction | None | |
| Max. and min. transmission | 0.5567 and 0.3813 | |
| Refinement method | Full-matrix least-squares on F ² | |
| Data / restraints / parameters | 2003 / 0 / 133 | |
| Goodness-of-fit on F ² | 1.03 | |
| Final R indices [I > 2σ(I)] | R1 = 0.038, wR2 = 0.094 | |
| R indices (all data) | R1 = 0.038, wR2 = 0.096 | |
| Extinction coefficient | 0.00000(13) | |
| Largest diff. peak and hole | 0.92 and -0.36 e.Å ⁻³ | |

Table A.2.2. Atomic coordinates ($\times 10^4$) and equivalent isotropic displacement parameters ($\text{\AA}^2 \times 10^3$) for **206d**. $U(\text{eq})$ is defined as one third of the trace of the orthogonalized U^{ij} tensor.

| | x | y | z | $U(\text{eq})$ |
|-------|---------|---------|---------|----------------|
| Ti(1) | 7611(1) | 7500 | 4271(1) | 15(1) |
| Si(1) | 8203(1) | 5809(1) | 2313(1) | 24(1) |
| Si(2) | 8834(1) | 7500 | 7412(1) | 28(1) |
| C(1) | 8033(3) | 7500 | 2241(3) | 21(1) |
| C(6) | 6553(2) | 6589(1) | 4993(2) | 23(1) |
| C(5) | 7354(2) | 6766(1) | 5854(2) | 21(1) |
| C(2) | 8498(2) | 6824(1) | 2752(2) | 20(1) |
| C(4) | 5920(2) | 7094(1) | 4303(2) | 22(1) |
| C(7) | 7738(2) | 7500 | 6256(3) | 20(1) |
| C(3) | 9276(2) | 7091(1) | 3589(2) | 22(1) |
| C(8) | 6795(2) | 5736(2) | 1771(3) | 37(1) |
| C(9) | 9105(2) | 5512(1) | 1058(2) | 37(1) |
| C(10) | 8460(2) | 5150(1) | 3608(3) | 43(1) |
| C(12) | 8188(4) | 7500 | 8915(4) | 59(1) |
| C(11) | 9677(3) | 6627(3) | 7268(3) | 85(2) |

Table A.2.3. Bond Lengths [\AA] and Angles [$^\circ$] for **206d**.

| | | | |
|--|------------|--|------------|
| Ti(1)-C(5) ⁱ | 2.199(2) | Si(1)-C(2) | 1.871(2) |
| Ti(1)-C(5) | 2.199(2) | Si(2)-C(12) | 1.854(5) |
| Ti(1)-C(7) | 2.212(3) | Si(2)-C(11) | 1.856(3) |
| Ti(1)-C(6) | 2.216(2) | Si(2)-C(11) ⁱ | 1.856(3) |
| Ti(1)-C(6) ⁱ | 2.216(2) | Si(2)-C(7) | 1.877(3) |
| Ti(1)-C(4) | 2.227(2) | C(1)-C(2) | 1.431(3) |
| Ti(1)-C(4) ⁱ | 2.227(2) | C(1)-C(2) ⁱ | 1.431(3) |
| Ti(1)-C(1) | 2.317(3) | C(6)-C(4) | 1.410(3) |
| Ti(1)-C(3) | 2.324(2) | C(6)-C(5) | 1.419(3) |
| Ti(1)-C(3) ⁱ | 2.324(2) | C(5)-C(7) | 1.437(3) |
| Ti(1)-C(2) | 2.337(2) | C(2)-C(3) | 1.423(3) |
| Ti(1)-C(2) ⁱ | 2.337(2) | C(4)-C(4) ⁱ | 1.414(4) |
| Si(1)-C(8) | 1.862(3) | C(7)-C(5) ⁱ | 1.437(3) |
| Si(1)-C(9) | 1.865(2) | C(3)-C(3) ⁱ | 1.424(4) |
| Si(1)-C(10) | 1.869(3) | | |
| | | | |
| C(5) ⁱ -Ti(1)-C(5) | 71.10(12) | C(3)-Ti(1)-C(2) | 35.56(8) |
| C(5) ⁱ -Ti(1)-C(7) | 38.01(6) | C(3) ⁱ -Ti(1)-C(2) | 59.69(8) |
| C(5)-Ti(1)-C(7) | 38.01(7) | C(5) ⁱ -Ti(1)-C(2) ⁱ | 110.74(8) |
| C(5) ⁱ -Ti(1)-C(6) | 92.28(8) | C(5)-Ti(1)-C(2) ⁱ | 160.11(8) |
| C(5)-Ti(1)-C(6) | 37.48(8) | C(7)-Ti(1)-C(2) ⁱ | 133.36(8) |
| C(7)-Ti(1)-C(6) | 71.43(8) | C(6)-Ti(1)-C(2) ⁱ | 154.83(8) |
| C(5) ⁱ -Ti(1)-C(6) ⁱ | 37.48(8) | C(6) ⁱ -Ti(1)-C(2) ⁱ | 100.52(8) |
| C(5)-Ti(1)-C(6) ⁱ | 92.28(8) | C(4)-Ti(1)-C(2) ⁱ | 128.37(8) |
| C(7)-Ti(1)-C(6) ⁱ | 71.43(8) | C(4) ⁱ -Ti(1)-C(2) ⁱ | 107.50(8) |
| C(6)-Ti(1)-C(6) ⁱ | 91.55(11) | C(1)-Ti(1)-C(2) ⁱ | 35.81(7) |
| C(5) ⁱ -Ti(1)-C(4) | 91.90(8) | C(3)-Ti(1)-C(2) ⁱ | 59.69(8) |
| C(5)-Ti(1)-C(4) | 70.36(8) | C(3) ⁱ -Ti(1)-C(2) ⁱ | 35.56(8) |
| C(7)-Ti(1)-C(4) | 92.96(9) | C(2)-Ti(1)-C(2) ⁱ | 60.54(10) |
| C(6)-Ti(1)-C(4) | 37.00(8) | C(8)-Si(1)-C(9) | 108.01(12) |
| C(6) ⁱ -Ti(1)-C(4) | 69.91(8) | C(8)-Si(1)-C(10) | 111.71(13) |
| C(5) ⁱ -Ti(1)-C(4) ⁱ | 70.36(8) | C(9)-Si(1)-C(10) | 107.59(13) |
| C(5)-Ti(1)-C(4) ⁱ | 91.90(8) | C(8)-Si(1)-C(2) | 109.50(11) |
| C(7)-Ti(1)-C(4) ⁱ | 92.96(9) | C(9)-Si(1)-C(2) | 109.77(10) |
| C(6)-Ti(1)-C(4) ⁱ | 69.91(8) | C(10)-Si(1)-C(2) | 110.20(12) |
| C(6) ⁱ -Ti(1)-C(4) ⁱ | 37.00(8) | C(12)-Si(2)-C(11) | 108.91(17) |
| C(4)-Ti(1)-C(4) ⁱ | 37.03(11) | C(12)-Si(2)-C(11) ⁱ | 108.91(17) |
| C(5) ⁱ -Ti(1)-C(1) | 144.35(6) | C(11)-Si(2)-C(11) ⁱ | 110.0(3) |
| C(5)-Ti(1)-C(1) | 144.35(6) | C(12)-Si(2)-C(7) | 107.47(18) |
| C(7)-Ti(1)-C(1) | 162.76(11) | C(11)-Si(2)-C(7) | 110.73(11) |
| C(6)-Ti(1)-C(1) | 119.22(8) | C(11) ⁱ -Si(2)-C(7) | 110.73(11) |
| C(6) ⁱ -Ti(1)-C(1) | 119.22(8) | C(2)-C(1)-C(2) ⁱ | 110.8(3) |
| C(4)-Ti(1)-C(1) | 103.38(10) | C(2)-C(1)-Ti(1) | 72.87(15) |
| C(4) ⁱ -Ti(1)-C(1) | 103.38(10) | C(2) ⁱ -C(1)-Ti(1) | 72.87(15) |
| C(5) ⁱ -Ti(1)-C(3) | 124.74(8) | C(4)-C(6)-C(5) | 128.7(2) |
| C(5)-Ti(1)-C(3) | 102.33(8) | C(4)-C(6)-Ti(1) | 71.92(12) |

| | | | |
|--|-----------|-------------------------------|------------|
| C(7)-Ti(1)-C(3) | 105.15(9) | C(5)-C(6)-Ti(1) | 70.61(12) |
| C(6)-Ti(1)-C(3) | 115.57(8) | C(6)-C(5)-C(7) | 129.7(2) |
| C(6) ⁱ -Ti(1)-C(3) | 150.55(8) | C(6)-C(5)-Ti(1) | 71.91(12) |
| C(4)-Ti(1)-C(3) | 139.10(8) | C(7)-C(5)-Ti(1) | 71.49(15) |
| C(4) ⁱ -Ti(1)-C(3) | 161.89(8) | C(3)-C(2)-C(1) | 105.46(19) |
| C(1)-Ti(1)-C(3) | 58.60(9) | C(3)-C(2)-Si(1) | 127.90(16) |
| C(5) ⁱ -Ti(1)-C(3) ⁱ | 102.33(8) | C(1)-C(2)-Si(1) | 126.50(18) |
| C(5)-Ti(1)-C(3) ⁱ | 124.74(8) | C(3)-C(2)-Ti(1) | 71.71(12) |
| C(7)-Ti(1)-C(3) ⁱ | 105.15(9) | C(1)-C(2)-Ti(1) | 71.32(14) |
| C(6)-Ti(1)-C(3) ⁱ | 150.55(8) | Si(1)-C(2)-Ti(1) | 124.87(10) |
| C(6) ⁱ -Ti(1)-C(3) ⁱ | 115.57(8) | C(6)-C(4)-C(4) ⁱ | 128.67(13) |
| C(4)-Ti(1)-C(3) ⁱ | 161.89(8) | C(6)-C(4)-Ti(1) | 71.08(12) |
| C(4) ⁱ -Ti(1)-C(3) ⁱ | 139.10(8) | C(4) ⁱ -C(4)-Ti(1) | 71.49(6) |
| C(1)-Ti(1)-C(3) ⁱ | 58.60(10) | C(5) ⁱ -C(7)-C(5) | 125.7(3) |
| C(3)-Ti(1)-C(3) ⁱ | 35.68(10) | C(5) ⁱ -C(7)-Si(2) | 117.13(14) |
| C(5) ⁱ -Ti(1)-C(2) | 160.11(8) | C(5)-C(7)-Si(2) | 117.13(14) |
| C(5)-Ti(1)-C(2) | 110.74(8) | C(5) ⁱ -C(7)-Ti(1) | 70.50(15) |
| C(7)-Ti(1)-C(2) | 133.36(8) | C(5)-C(7)-Ti(1) | 70.50(15) |
| C(6)-Ti(1)-C(2) | 100.52(8) | Si(2)-C(7)-Ti(1) | 137.33(15) |
| C(6) ⁱ -Ti(1)-C(2) | 154.83(8) | C(3) ⁱ -C(3)-C(2) | 109.12(12) |
| C(4)-Ti(1)-C(2) | 107.50(8) | C(3) ⁱ -C(3)-Ti(1) | 72.16(5) |
| C(4) ⁱ -Ti(1)-C(2) | 128.37(8) | C(2)-C(3)-Ti(1) | 72.74(12) |
| C(1)-Ti(1)-C(2) | 35.80(7) | | |

Symmetry transformations used to generate equivalent atoms: ⁱ x,-y+3/2,z

Table A.2.4. Anisotropic displacement parameters ($\text{\AA}^2 \times 10^3$) for **206d**. The anisotropic displacement factor exponent takes the form: $-2\pi^2 [h^2 a^{*2} U^{11} + \dots + 2 h k a^* b^* U^{12}]$.

| | U^{11} | U^{22} | U^{33} | U^{23} | U^{13} | U^{12} |
|-------|----------|----------|----------|----------|----------|----------|
| Ti(1) | 16(1) | 18(1) | 13(1) | 0 | 1(1) | 0 |
| Si(1) | 25(1) | 20(1) | 27(1) | -5(1) | 8(1) | -2(1) |
| Si(2) | 25(1) | 42(1) | 18(1) | 0 | -7(1) | 0 |
| C(1) | 25(2) | 24(2) | 13(2) | 0 | 5(1) | 0 |
| C(6) | 23(1) | 25(1) | 21(1) | 1(1) | 5(1) | -4(1) |
| C(5) | 20(1) | 26(1) | 17(1) | 4(1) | 4(1) | 0(1) |
| C(2) | 20(1) | 23(1) | 16(1) | -2(1) | 8(1) | 0(1) |
| C(4) | 17(1) | 31(1) | 18(1) | 0(1) | 2(1) | -5(1) |
| C(7) | 17(1) | 32(2) | 12(2) | 0 | 3(1) | 0 |
| C(3) | 18(1) | 26(1) | 23(1) | 2(1) | 6(1) | 2(1) |
| C(8) | 31(1) | 37(1) | 44(2) | -16(1) | 5(1) | -7(1) |
| C(9) | 36(1) | 30(1) | 43(2) | -19(1) | 16(1) | -9(1) |
| C(10) | 52(2) | 26(1) | 50(2) | 6(1) | 12(1) | 6(1) |
| C(12) | 47(3) | 110(5) | 19(2) | 0 | -6(2) | 0 |
| C(11) | 73(2) | 115(3) | 67(3) | -40(2) | -49(2) | 59(2) |

III. X-Ray Data for **204d**.

Table A.3.1. Crystal Data and Structure Refinement for **204d**.

| | | |
|-----------------------------------|--|---------------------------|
| Empirical formula | C ₂₁ H ₃₆ Si ₃ Ti | |
| Formula weight | 420.67 | |
| Temperature | 150(2) K | |
| Wavelength | 0.71073 Å | |
| Crystal system | Monoclinic | |
| Space group | C c | |
| Unit cell dimensions | a = 10.8928(3) Å | $\alpha = 90^\circ$ |
| | b = 19.3203(8) Å | $\beta = 96.633(2)^\circ$ |
| | c = 34.9944(12) Å | $\gamma = 90^\circ$ |
| Volume | 7315.4(4) Å ³ | |
| Z | 12 | |
| Density (calculated) | 1.146 Mg/m ³ | |
| Absorption coefficient | 0.501 mm ⁻¹ | |
| F(000) | 2712 | |
| Crystal size / Shape | 0.14 x 0.08 x 0.06 mm ³ | Needle-shaped |
| Theta range for data collection | 2.56 to 25.04° | |
| Index ranges | -11 ≤ h ≤ 12, -21 ≤ k ≤ 22, -41 ≤ l ≤ 39 | |
| Reflections collected | 22714 | |
| Independent reflections | 9788 [R(int) = 0.0852] | |
| Completeness to theta = 25.04° | 99.70% | |
| Absorption correction | Semi-empirical from equivalents | |
| Max. and min. transmission | 0.984 and 0.683 | |
| Refinement method | Full-matrix least-squares on F ² | |
| Data / restraints / parameters | 9788 / 2 / 703 | |
| Goodness-of-fit on F ² | 1.045 | |
| Final R indices [I > 2σ(I)] | R1 = 0.0678, wR2 = 0.1556 | |
| R indices (all data) | R1 = 0.1069, wR2 = 0.1767 | |
| Absolute structure parameter | 0.06(4) | |
| Largest diff. peak and hole | 0.454 and -0.344 e.Å ⁻³ | |

Table A.3.2. Atomic coordinates ($\times 10^4$) and equivalent isotropic displacement parameters ($\text{\AA}^2 \times 10^3$) for **204d**. $U(\text{eq})$ is defined as one third of the trace of the orthogonalized U^{ij} tensor.

| | x | y | z | U(eq) |
|--------|-----------|----------|---------|-------|
| Ti(1A) | 8316(1) | -202(1) | 5656(1) | 28(1) |
| Si(1A) | 11747(2) | -150(2) | 5769(1) | 39(1) |
| Si(2A) | 6969(2) | -1797(1) | 6102(1) | 37(1) |
| Si(3A) | 6848(2) | 1580(1) | 5484(1) | 39(1) |
| C(1A) | 10270(7) | -324(5) | 5460(2) | 33(2) |
| C(2A) | 9642(8) | -967(5) | 5404(2) | 42(2) |
| C(3A) | 8613(8) | -893(6) | 5123(2) | 45(2) |
| C(4A) | 8578(7) | -209(6) | 5004(2) | 42(2) |
| C(5A) | 9584(7) | 143(5) | 5204(2) | 36(2) |
| C(6A) | 7273(7) | -864(4) | 6031(2) | 31(2) |
| C(7AA) | 6418(7) | -515(5) | 5751(2) | 34(2) |
| C(8A) | 6404(7) | 179(4) | 5620(2) | 30(2) |
| C(9A) | 7220(7) | 743(5) | 5732(2) | 33(2) |
| C(10A) | 8255(7) | 717(4) | 6028(2) | 34(2) |
| C(11A) | 8706(7) | 148(5) | 6263(2) | 32(2) |
| C(12A) | 8287(7) | -542(5) | 6262(2) | 33(2) |
| C(13A) | 11930(9) | -776(5) | 6176(3) | 55(3) |
| C(14A) | 13020(8) | -287(7) | 5468(3) | 77(4) |
| C(15A) | 11788(10) | 750(6) | 5944(3) | 71(3) |
| C(16A) | 5556(8) | -1876(5) | 6352(3) | 50(3) |
| C(17A) | 8301(9) | -2200(6) | 6403(3) | 62(3) |
| C(18A) | 6718(10) | -2255(5) | 5626(3) | 58(3) |
| C(19A) | 6605(10) | 1446(5) | 4955(2) | 58(3) |
| C(20A) | 5375(10) | 1918(5) | 5643(3) | 64(3) |
| C(21A) | 8096(9) | 2223(5) | 5601(3) | 58(3) |
| Ti(1B) | 9915(1) | 6087(1) | 9008(1) | 28(1) |
| Si(1B) | 6596(2) | 6020(2) | 9167(1) | 45(1) |
| Si(2B) | 11492(2) | 7714(1) | 9413(1) | 39(1) |
| Si(3B) | 11230(2) | 4334(1) | 8791(1) | 39(1) |
| C(1B) | 7786(7) | 6197(5) | 8843(2) | 33(2) |
| C(2B) | 8361(7) | 6840(5) | 8777(2) | 37(2) |
| C(3B) | 9126(8) | 6767(5) | 8489(2) | 44(2) |
| C(4B) | 9072(8) | 6081(6) | 8365(2) | 45(2) |
| C(5B) | 8258(7) | 5724(5) | 8576(2) | 39(2) |
| C(6B) | 11245(7) | 6763(4) | 9365(2) | 30(2) |
| C(7B) | 11850(7) | 6422(4) | 9074(2) | 33(2) |
| C(8B) | 11821(7) | 5721(4) | 8951(2) | 30(2) |
| C(9B) | 11107(7) | 5149(5) | 9068(2) | 32(2) |
| C(10B) | 10344(7) | 5171(5) | 9379(2) | 33(2) |
| C(11B) | 10079(7) | 5724(5) | 9618(2) | 35(2) |
| C(12B) | 10454(7) | 6424(5) | 9610(2) | 33(2) |

| | | | | |
|--------|-----------|----------|---------|--------|
| C(13B) | 6811(10) | 6611(6) | 9586(3) | 72(3) |
| C(14B) | 5072(9) | 6191(9) | 8891(4) | 118(6) |
| C(15B) | 6654(11) | 5108(6) | 9323(3) | 69(3) |
| C(16B) | 11391(10) | 8128(5) | 8930(3) | 60(3) |
| C(17B) | 10312(9) | 8121(5) | 9686(3) | 56(3) |
| C(18B) | 13074(9) | 7876(5) | 9664(3) | 59(3) |
| C(19B) | 11032(10) | 4504(5) | 8257(2) | 56(3) |
| C(20B) | 12790(9) | 3966(5) | 8924(3) | 54(3) |
| C(21B) | 10033(10) | 3696(5) | 8901(2) | 61(3) |
| Ti(1C) | 7119(1) | 1998(1) | 7349(1) | 29(1) |
| Si(1C) | 10555(2) | 1882(2) | 7583(1) | 49(1) |
| Si(2C) | 5606(2) | 274(1) | 7090(1) | 37(1) |
| Si(3C) | 5853(2) | 3649(1) | 7721(1) | 38(1) |
| C(1C) | 9183(7) | 2078(4) | 7232(2) | 26(2) |
| C(2C) | 8569(7) | 1621(5) | 6956(2) | 35(2) |
| C(3C) | 7641(8) | 1981(5) | 6724(2) | 42(2) |
| C(4C) | 7677(8) | 2675(5) | 6843(2) | 44(2) |
| C(5C) | 8624(7) | 2732(5) | 7158(2) | 34(2) |
| C(6C) | 5913(7) | 1078(5) | 7374(2) | 34(2) |
| C(7A) | 5151(7) | 1669(5) | 7253(2) | 34(2) |
| C(8C) | 5208(7) | 2363(5) | 7385(2) | 32(2) |
| C(9C) | 6009(7) | 2697(5) | 7683(2) | 34(2) |
| C(10C) | 6932(7) | 2338(4) | 7941(2) | 30(2) |
| C(11C) | 7277(8) | 1639(5) | 7953(2) | 36(2) |
| C(12C) | 6839(7) | 1072(4) | 7705(2) | 33(2) |
| C(13C) | 10531(10) | 978(6) | 7732(3) | 74(3) |
| C(14C) | 11938(9) | 2044(10) | 7338(4) | 153(9) |
| C(15C) | 10577(10) | 2465(6) | 8005(3) | 72(3) |
| C(16C) | 4165(9) | -128(6) | 7216(3) | 56(3) |
| C(17C) | 6909(9) | -343(5) | 7192(2) | 59(3) |
| C(18C) | 5384(8) | 462(5) | 6564(2) | 46(2) |
| C(19C) | 5642(9) | 4062(5) | 7237(2) | 49(3) |
| C(20C) | 4457(9) | 3841(6) | 7966(3) | 59(3) |
| C(21C) | 7251(9) | 4032(5) | 8000(2) | 51(3) |

Table A.3.3. Bond Lengths [\AA] and Angles [$^\circ$] for **204d**.

| | | | | | |
|----------------------|-----------|----------------------|-----------|----------------------|-----------|
| Ti(1A)-C(8A) | 2.199(8) | Ti(1B)-C(7B) | 2.192(8) | Ti(1C)-C(10C) | 2.207(7) |
| Ti(1A)-C(10A) | 2.207(8) | Ti(1B)-C(10B) | 2.212(8) | Ti(1C)-C(11C) | 2.214(7) |
| Ti(1A)-C(9A) | 2.215(9) | Ti(1B)-C(12B) | 2.218(7) | Ti(1C)-C(8C) | 2.215(7) |
| Ti(1A)-C(7AA) | 2.216(8) | Ti(1B)-C(9B) | 2.224(8) | Ti(1C)-C(6C) | 2.218(9) |
| Ti(1A)-C(11A) | 2.221(7) | Ti(1B)-C(8B) | 2.225(8) | Ti(1C)-C(12C) | 2.221(8) |
| Ti(1A)-C(12A) | 2.223(7) | Ti(1B)-C(6B) | 2.225(8) | Ti(1C)-C(7A) | 2.224(8) |
| Ti(1A)-C(6A) | 2.234(8) | Ti(1B)-C(11B) | 2.233(7) | Ti(1C)-C(9C) | 2.232(8) |
| Ti(1A)-C(2A) | 2.311(9) | Ti(1B)-C(2B) | 2.307(7) | Ti(1C)-C(3C) | 2.323(8) |
| Ti(1A)-C(5A) | 2.315(8) | Ti(1B)-C(5B) | 2.325(7) | Ti(1C)-C(5C) | 2.323(8) |
| Ti(1A)-C(1A) | 2.323(7) | Ti(1B)-C(3B) | 2.325(8) | Ti(1C)-C(2C) | 2.328(8) |
| Ti(1A)-C(4A) | 2.333(8) | Ti(1B)-C(4B) | 2.330(8) | Ti(1C)-C(1C) | 2.336(7) |
| Ti(1A)-C(3A) | 2.347(8) | Ti(1B)-C(1B) | 2.334(7) | Ti(1C)-C(4C) | 2.336(8) |
| Si(1A)-C(15A) | 1.843(11) | Si(1B)-C(15B) | 1.845(11) | Si(1C)-C(13C) | 1.823(11) |
| Si(1A)-C(14A) | 1.853(10) | Si(1B)-C(13B) | 1.850(11) | Si(1C)-C(14C) | 1.844(12) |
| Si(1A)-C(13A) | 1.863(9) | Si(1B)-C(1B) | 1.851(9) | Si(1C)-C(15C) | 1.855(10) |
| Si(1A)-C(1A) | 1.863(8) | Si(1B)-C(14B) | 1.852(10) | Si(1C)-C(1C) | 1.860(8) |
| Si(2A)-C(6A) | 1.854(9) | Si(2B)-C(6B) | 1.860(8) | Si(2C)-C(16C) | 1.849(10) |
| Si(2A)-C(17A) | 1.862(9) | Si(2B)-C(16B) | 1.862(10) | Si(2C)-C(6C) | 1.855(9) |
| Si(2A)-C(16A) | 1.862(9) | Si(2B)-C(17B) | 1.862(10) | Si(2C)-C(17C) | 1.855(9) |
| Si(2A)-C(18A) | 1.878(9) | Si(2B)-C(18B) | 1.869(9) | Si(2C)-C(18C) | 1.863(8) |
| Si(3A)-C(21A) | 1.854(9) | Si(3B)-C(20B) | 1.852(9) | Si(3C)-C(9C) | 1.853(9) |
| Si(3A)-C(9A) | 1.857(9) | Si(3B)-C(9B) | 1.863(9) | Si(3C)-C(19C) | 1.861(8) |
| Si(3A)-C(19A) | 1.860(8) | Si(3B)-C(21B) | 1.867(10) | Si(3C)-C(21C) | 1.865(9) |
| Si(3A)-C(20A) | 1.874(10) | Si(3B)-C(19B) | 1.885(8) | Si(3C)-C(20C) | 1.867(9) |
| C(1A)-C(5A) | 1.420(11) | C(1B)-C(2B) | 1.422(11) | C(1C)-C(5C) | 1.413(11) |
| C(1A)-C(2A) | 1.421(12) | C(1B)-C(5B) | 1.443(11) | C(1C)-C(2C) | 1.419(11) |
| C(2A)-C(3A) | 1.410(12) | C(2B)-C(3B) | 1.388(12) | C(2C)-C(3C) | 1.405(11) |
| C(3A)-C(4A) | 1.386(13) | C(3B)-C(4B) | 1.393(13) | C(3C)-C(4C) | 1.405(13) |
| C(4A)-C(5A) | 1.407(12) | C(4B)-C(5B) | 1.400(12) | C(4C)-C(5C) | 1.425(11) |
| C(6A)-C(12A) | 1.433(11) | C(6B)-C(7B) | 1.437(11) | C(6C)-C(12C) | 1.445(10) |
| C(6A)-C(7AA) | 1.439(10) | C(6B)-C(12B) | 1.441(11) | C(6C)-C(7A) | 1.447(11) |
| C(7AA)-C(8A) | 1.419(11) | C(7B)-C(8B) | 1.420(11) | C(7A)-C(8C) | 1.416(12) |
| C(8A)-C(9A) | 1.433(11) | C(8B)-C(9B) | 1.437(11) | C(8C)-C(9C) | 1.435(11) |
| C(9A)-C(10A) | 1.440(10) | C(9B)-C(10B) | 1.443(11) | C(9C)-C(10C) | 1.448(11) |
| C(10A)-C(11A) | 1.425(11) | C(10B)-C(11B) | 1.409(11) | C(10C)-C(11C) | 1.402(11) |
| C(11A)-C(12A) | 1.409(11) | C(11B)-C(12B) | 1.413(11) | C(11C)-C(12C) | 1.444(11) |
| | | | | | |
| C(8A)-Ti(1A)-C(10A) | 70.8(3) | C(7B)-Ti(1B)-C(10B) | 92.3(3) | C(10C)-Ti(1C)-C(11C) | 37.0(3) |
| C(8A)-Ti(1A)-C(9A) | 37.9(3) | C(7B)-Ti(1B)-C(12B) | 70.6(3) | C(10C)-Ti(1C)-C(8C) | 70.3(3) |
| C(10A)-Ti(1A)-C(9A) | 38.0(3) | C(10B)-Ti(1B)-C(12B) | 70.3(3) | C(11C)-Ti(1C)-C(8C) | 90.9(3) |
| C(8A)-Ti(1A)-C(7AA) | 37.5(3) | C(7B)-Ti(1B)-C(9B) | 71.7(3) | C(10C)-Ti(1C)-C(6C) | 94.7(3) |
| C(10A)-Ti(1A)-C(7AA) | 92.2(3) | C(10B)-Ti(1B)-C(9B) | 38.0(3) | C(11C)-Ti(1C)-C(6C) | 72.0(3) |
| C(9A)-Ti(1A)-C(7AA) | 71.5(3) | C(12B)-Ti(1B)-C(9B) | 93.6(3) | C(8C)-Ti(1C)-C(6C) | 71.8(3) |
| C(8A)-Ti(1A)-C(11A) | 91.6(3) | C(7B)-Ti(1B)-C(8B) | 37.5(3) | C(10C)-Ti(1C)-C(12C) | 71.3(3) |

| | | | | | |
|----------------------|----------|----------------------|----------|----------------------|----------|
| C(10A)-Ti(1A)-C(11A) | 37.5(3) | C(10B)-Ti(1B)-C(8B) | 70.3(3) | C(11C)-Ti(1C)-C(12C) | 38.0(3) |
| C(9A)-Ti(1A)-C(11A) | 71.3(3) | C(12B)-Ti(1B)-C(8B) | 91.8(3) | C(8C)-Ti(1C)-C(12C) | 91.9(3) |
| C(7AA)-Ti(1A)-C(11A) | 91.1(3) | C(9B)-Ti(1B)-C(8B) | 37.7(3) | C(6C)-Ti(1C)-C(12C) | 38.0(3) |
| C(8A)-Ti(1A)-C(12A) | 92.1(3) | C(7B)-Ti(1B)-C(6B) | 38.0(3) | C(10C)-Ti(1C)-C(7A) | 92.0(3) |
| C(10A)-Ti(1A)-C(12A) | 70.8(3) | C(10B)-Ti(1B)-C(6B) | 93.5(3) | C(11C)-Ti(1C)-C(7A) | 91.2(3) |
| C(9A)-Ti(1A)-C(12A) | 93.5(3) | C(12B)-Ti(1B)-C(6B) | 37.9(3) | C(8C)-Ti(1C)-C(7A) | 37.2(3) |
| C(7AA)-Ti(1A)-C(12A) | 70.1(3) | C(9B)-Ti(1B)-C(6B) | 95.2(3) | C(6C)-Ti(1C)-C(7A) | 38.0(3) |
| C(11A)-Ti(1A)-C(12A) | 37.0(3) | C(8B)-Ti(1B)-C(6B) | 71.5(3) | C(12C)-Ti(1C)-C(7A) | 70.2(3) |
| C(8A)-Ti(1A)-C(6A) | 71.6(3) | C(7B)-Ti(1B)-C(11B) | 91.3(3) | C(10C)-Ti(1C)-C(9C) | 38.1(3) |
| C(10A)-Ti(1A)-C(6A) | 93.6(3) | C(10B)-Ti(1B)-C(11B) | 37.0(3) | C(11C)-Ti(1C)-C(9C) | 71.1(3) |
| C(9A)-Ti(1A)-C(6A) | 94.8(3) | C(12B)-Ti(1B)-C(11B) | 37.0(3) | C(8C)-Ti(1C)-C(9C) | 37.7(3) |
| C(7AA)-Ti(1A)-C(6A) | 37.7(3) | C(9B)-Ti(1B)-C(11B) | 71.0(3) | C(6C)-Ti(1C)-C(9C) | 96.0(3) |
| C(11A)-Ti(1A)-C(6A) | 70.6(3) | C(8B)-Ti(1B)-C(11B) | 90.8(3) | C(12C)-Ti(1C)-C(9C) | 94.3(3) |
| C(12A)-Ti(1A)-C(6A) | 37.5(3) | C(6B)-Ti(1B)-C(11B) | 70.9(3) | C(7A)-Ti(1C)-C(9C) | 71.4(3) |
| C(8A)-Ti(1A)-C(2A) | 145.3(3) | C(7B)-Ti(1B)-C(2B) | 120.5(3) | C(10C)-Ti(1C)-C(3C) | 161.5(3) |
| C(10A)-Ti(1A)-C(2A) | 143.3(3) | C(10B)-Ti(1B)-C(2B) | 143.8(3) | C(11C)-Ti(1C)-C(3C) | 153.4(3) |
| C(9A)-Ti(1A)-C(2A) | 160.4(3) | C(12B)-Ti(1B)-C(2B) | 104.5(3) | C(8C)-Ti(1C)-C(3C) | 113.1(3) |
| C(7AA)-Ti(1A)-C(2A) | 121.2(3) | C(9B)-Ti(1B)-C(2B) | 160.7(3) | C(6C)-Ti(1C)-C(3C) | 103.7(3) |
| C(11A)-Ti(1A)-C(2A) | 120.0(3) | C(8B)-Ti(1B)-C(2B) | 145.5(3) | C(12C)-Ti(1C)-C(3C) | 125.5(3) |
| C(12A)-Ti(1A)-C(2A) | 104.7(3) | C(6B)-Ti(1B)-C(2B) | 103.3(3) | C(7A)-Ti(1C)-C(3C) | 101.0(3) |
| C(6A)-Ti(1A)-C(2A) | 104.0(3) | C(11B)-Ti(1B)-C(2B) | 120.5(3) | C(9C)-Ti(1C)-C(3C) | 135.2(3) |
| C(8A)-Ti(1A)-C(5A) | 120.0(3) | C(7B)-Ti(1B)-C(5B) | 145.3(3) | C(10C)-Ti(1C)-C(5C) | 103.5(3) |
| C(10A)-Ti(1A)-C(5A) | 103.4(3) | C(10B)-Ti(1B)-C(5B) | 103.6(3) | C(11C)-Ti(1C)-C(5C) | 119.1(3) |
| C(9A)-Ti(1A)-C(5A) | 102.5(3) | C(12B)-Ti(1B)-C(5B) | 143.8(3) | C(8C)-Ti(1C)-C(5C) | 121.4(3) |
| C(7AA)-Ti(1A)-C(5A) | 145.3(3) | C(9B)-Ti(1B)-C(5B) | 102.5(3) | C(6C)-Ti(1C)-C(5C) | 160.3(3) |
| C(11A)-Ti(1A)-C(5A) | 120.1(3) | C(8B)-Ti(1B)-C(5B) | 120.6(3) | C(12C)-Ti(1C)-C(5C) | 143.1(3) |
| C(12A)-Ti(1A)-C(5A) | 144.3(3) | C(6B)-Ti(1B)-C(5B) | 161.6(3) | C(7A)-Ti(1C)-C(5C) | 146.2(3) |
| C(6A)-Ti(1A)-C(5A) | 161.9(3) | C(11B)-Ti(1B)-C(5B) | 119.8(3) | C(9C)-Ti(1C)-C(5C) | 102.9(3) |
| C(2A)-Ti(1A)-C(5A) | 58.3(3) | C(2B)-Ti(1B)-C(5B) | 58.6(3) | C(3C)-Ti(1C)-C(5C) | 58.7(3) |
| C(8A)-Ti(1A)-C(1A) | 155.6(3) | C(7B)-Ti(1B)-C(3B) | 100.3(3) | C(10C)-Ti(1C)-C(2C) | 142.2(3) |
| C(10A)-Ti(1A)-C(1A) | 110.3(3) | C(10B)-Ti(1B)-C(3B) | 160.8(3) | C(11C)-Ti(1C)-C(2C) | 118.9(3) |
| C(9A)-Ti(1A)-C(1A) | 130.0(3) | C(12B)-Ti(1B)-C(3B) | 127.6(4) | C(8C)-Ti(1C)-C(2C) | 147.1(3) |
| C(7AA)-Ti(1A)-C(1A) | 156.9(3) | C(9B)-Ti(1B)-C(3B) | 133.8(3) | C(6C)-Ti(1C)-C(2C) | 102.6(3) |
| C(11A)-Ti(1A)-C(1A) | 103.5(3) | C(8B)-Ti(1B)-C(3B) | 111.9(3) | C(12C)-Ti(1C)-C(2C) | 103.0(3) |
| C(12A)-Ti(1A)-C(1A) | 111.5(3) | C(6B)-Ti(1B)-C(3B) | 105.3(3) | C(7A)-Ti(1C)-C(2C) | 122.0(3) |
| C(6A)-Ti(1A)-C(1A) | 131.4(3) | C(11B)-Ti(1B)-C(3B) | 154.9(3) | C(9C)-Ti(1C)-C(2C) | 160.9(3) |
| C(2A)-Ti(1A)-C(1A) | 35.7(3) | C(2B)-Ti(1B)-C(3B) | 34.9(3) | C(3C)-Ti(1C)-C(2C) | 35.2(3) |
| C(5A)-Ti(1A)-C(1A) | 35.7(3) | C(5B)-Ti(1B)-C(3B) | 58.2(3) | C(5C)-Ti(1C)-C(2C) | 58.1(3) |
| C(8A)-Ti(1A)-C(4A) | 99.6(3) | C(7B)-Ti(1B)-C(4B) | 111.7(3) | C(10C)-Ti(1C)-C(1C) | 109.8(3) |
| C(10A)-Ti(1A)-C(4A) | 126.6(3) | C(10B)-Ti(1B)-C(4B) | 126.6(3) | C(11C)-Ti(1C)-C(1C) | 102.5(3) |
| C(9A)-Ti(1A)-C(4A) | 104.5(3) | C(12B)-Ti(1B)-C(4B) | 161.8(3) | C(8C)-Ti(1C)-C(1C) | 156.7(3) |
| C(7AA)-Ti(1A)-C(4A) | 111.5(3) | C(9B)-Ti(1B)-C(4B) | 104.3(3) | C(6C)-Ti(1C)-C(1C) | 130.2(3) |
| C(11A)-Ti(1A)-C(4A) | 154.8(3) | C(8B)-Ti(1B)-C(4B) | 100.3(3) | C(12C)-Ti(1C)-C(1C) | 110.4(3) |
| C(12A)-Ti(1A)-C(4A) | 161.5(4) | C(6B)-Ti(1B)-C(4B) | 134.7(3) | C(7A)-Ti(1C)-C(1C) | 157.4(3) |
| C(6A)-Ti(1A)-C(4A) | 134.4(3) | C(11B)-Ti(1B)-C(4B) | 154.2(3) | C(9C)-Ti(1C)-C(1C) | 129.9(3) |
| C(2A)-Ti(1A)-C(4A) | 58.0(3) | C(2B)-Ti(1B)-C(4B) | 58.2(3) | C(3C)-Ti(1C)-C(1C) | 59.4(3) |

| | | | | | |
|----------------------|----------|----------------------|----------|----------------------|----------|
| C(5A)-Ti(1A)-C(4A) | 35.2(3) | C(5B)-Ti(1B)-C(4B) | 35.0(3) | C(5C)-Ti(1C)-C(1C) | 35.3(3) |
| C(1A)-Ti(1A)-C(4A) | 59.3(3) | C(3B)-Ti(1B)-C(4B) | 34.8(3) | C(2C)-Ti(1C)-C(1C) | 35.4(3) |
| C(8A)-Ti(1A)-C(3A) | 111.2(3) | C(7B)-Ti(1B)-C(1B) | 156.2(3) | C(10C)-Ti(1C)-C(4C) | 127.2(4) |
| C(10A)-Ti(1A)-C(3A) | 160.5(3) | C(10B)-Ti(1B)-C(1B) | 110.8(3) | C(11C)-Ti(1C)-C(4C) | 154.3(3) |
| C(9A)-Ti(1A)-C(3A) | 133.7(3) | C(12B)-Ti(1B)-C(1B) | 110.8(3) | C(8C)-Ti(1C)-C(4C) | 101.1(3) |
| C(7AA)-Ti(1A)-C(3A) | 100.4(3) | C(9B)-Ti(1B)-C(1B) | 130.6(3) | C(6C)-Ti(1C)-C(4C) | 133.3(3) |
| C(11A)-Ti(1A)-C(3A) | 154.7(3) | C(8B)-Ti(1B)-C(1B) | 156.6(3) | C(12C)-Ti(1C)-C(4C) | 160.1(3) |
| C(12A)-Ti(1A)-C(3A) | 127.5(4) | C(6B)-Ti(1B)-C(1B) | 130.5(3) | C(7A)-Ti(1C)-C(4C) | 112.1(3) |
| C(6A)-Ti(1A)-C(3A) | 105.5(3) | C(11B)-Ti(1B)-C(1B) | 103.5(3) | C(9C)-Ti(1C)-C(4C) | 105.2(3) |
| C(2A)-Ti(1A)-C(3A) | 35.2(3) | C(2B)-Ti(1B)-C(1B) | 35.7(3) | C(3C)-Ti(1C)-C(4C) | 35.1(3) |
| C(5A)-Ti(1A)-C(3A) | 58.2(3) | C(5B)-Ti(1B)-C(1B) | 36.1(3) | C(5C)-Ti(1C)-C(4C) | 35.6(3) |
| C(1A)-Ti(1A)-C(3A) | 59.5(3) | C(3B)-Ti(1B)-C(1B) | 59.2(3) | C(2C)-Ti(1C)-C(4C) | 58.3(3) |
| C(4A)-Ti(1A)-C(3A) | 34.5(3) | C(4B)-Ti(1B)-C(1B) | 59.4(3) | C(1C)-Ti(1C)-C(4C) | 59.4(3) |
| C(15A)-Si(1A)-C(14A) | 109.4(6) | C(15B)-Si(1B)-C(13B) | 110.9(5) | C(13C)-Si(1C)-C(14C) | 109.6(7) |
| C(15A)-Si(1A)-C(13A) | 111.2(5) | C(15B)-Si(1B)-C(1B) | 110.8(5) | C(13C)-Si(1C)-C(15C) | 110.7(5) |
| C(14A)-Si(1A)-C(13A) | 108.7(5) | C(13B)-Si(1B)-C(1B) | 109.8(4) | C(14C)-Si(1C)-C(15C) | 109.3(8) |
| C(15A)-Si(1A)-C(1A) | 110.4(4) | C(15B)-Si(1B)-C(14B) | 108.9(6) | C(13C)-Si(1C)-C(1C) | 110.3(4) |
| C(14A)-Si(1A)-C(1A) | 107.3(4) | C(13B)-Si(1B)-C(14B) | 109.2(6) | C(14C)-Si(1C)-C(1C) | 107.3(5) |
| C(13A)-Si(1A)-C(1A) | 109.7(4) | C(1B)-Si(1B)-C(14B) | 107.2(5) | C(15C)-Si(1C)-C(1C) | 109.6(4) |
| C(6A)-Si(2A)-C(17A) | 110.1(4) | C(6B)-Si(2B)-C(16B) | 110.5(4) | C(16C)-Si(2C)-C(6C) | 109.2(4) |
| C(6A)-Si(2A)-C(16A) | 108.2(4) | C(6B)-Si(2B)-C(17B) | 111.2(4) | C(16C)-Si(2C)-C(17C) | 109.7(5) |
| C(17A)-Si(2A)-C(16A) | 109.4(5) | C(16B)-Si(2B)-C(17B) | 108.2(5) | C(6C)-Si(2C)-C(17C) | 110.3(4) |
| C(6A)-Si(2A)-C(18A) | 110.5(4) | C(6B)-Si(2B)-C(18B) | 108.9(4) | C(16C)-Si(2C)-C(18C) | 107.5(4) |
| C(17A)-Si(2A)-C(18A) | 109.1(5) | C(16B)-Si(2B)-C(18B) | 108.1(5) | C(6C)-Si(2C)-C(18C) | 111.2(4) |
| C(16A)-Si(2A)-C(18A) | 109.5(5) | C(17B)-Si(2B)-C(18B) | 109.9(5) | C(17C)-Si(2C)-C(18C) | 109.0(4) |
| C(21A)-Si(3A)-C(9A) | 111.4(4) | C(20B)-Si(3B)-C(9B) | 108.2(4) | C(9C)-Si(3C)-C(19C) | 111.3(4) |
| C(21A)-Si(3A)-C(19A) | 109.3(5) | C(20B)-Si(3B)-C(21B) | 109.7(5) | C(9C)-Si(3C)-C(21C) | 110.8(4) |
| C(9A)-Si(3A)-C(19A) | 110.1(4) | C(9B)-Si(3B)-C(21B) | 110.9(4) | C(19C)-Si(3C)-C(21C) | 108.3(4) |
| C(21A)-Si(3A)-C(20A) | 109.4(5) | C(20B)-Si(3B)-C(19B) | 108.2(5) | C(9C)-Si(3C)-C(20C) | 108.4(4) |
| C(9A)-Si(3A)-C(20A) | 108.3(4) | C(9B)-Si(3B)-C(19B) | 111.2(4) | C(19C)-Si(3C)-C(20C) | 108.1(5) |
| C(19A)-Si(3A)-C(20A) | 108.4(5) | C(21B)-Si(3B)-C(19B) | 108.5(4) | C(21C)-Si(3C)-C(20C) | 109.9(5) |
| C(5A)-C(1A)-C(2A) | 105.0(7) | C(2B)-C(1B)-C(5B) | 104.7(7) | C(5C)-C(1C)-C(2C) | 105.8(7) |
| C(5A)-C(1A)-Si(1A) | 127.4(7) | C(2B)-C(1B)-Si(1B) | 127.8(7) | C(5C)-C(1C)-Si(1C) | 126.8(6) |
| C(2A)-C(1A)-Si(1A) | 127.3(7) | C(5B)-C(1B)-Si(1B) | 127.3(7) | C(2C)-C(1C)-Si(1C) | 127.0(6) |
| C(5A)-C(1A)-Ti(1A) | 71.8(4) | C(2B)-C(1B)-Ti(1B) | 71.1(4) | C(5C)-C(1C)-Ti(1C) | 71.8(4) |
| C(2A)-C(1A)-Ti(1A) | 71.7(4) | C(5B)-C(1B)-Ti(1B) | 71.6(4) | C(2C)-C(1C)-Ti(1C) | 72.0(4) |
| Si(1A)-C(1A)-Ti(1A) | 124.7(4) | Si(1B)-C(1B)-Ti(1B) | 125.3(4) | Si(1C)-C(1C)-Ti(1C) | 126.0(4) |
| C(3A)-C(2A)-C(1A) | 109.8(8) | C(3B)-C(2B)-C(1B) | 109.9(9) | C(3C)-C(2C)-C(1C) | 109.7(8) |
| C(3A)-C(2A)-Ti(1A) | 73.8(5) | C(3B)-C(2B)-Ti(1B) | 73.3(5) | C(3C)-C(2C)-Ti(1C) | 72.2(5) |
| C(1A)-C(2A)-Ti(1A) | 72.6(5) | C(1B)-C(2B)-Ti(1B) | 73.2(4) | C(1C)-C(2C)-Ti(1C) | 72.6(4) |
| C(4A)-C(3A)-C(2A) | 107.4(8) | C(2B)-C(3B)-C(4B) | 108.4(8) | C(4C)-C(3C)-C(2C) | 107.9(8) |
| C(4A)-C(3A)-Ti(1A) | 72.2(5) | C(2B)-C(3B)-Ti(1B) | 71.9(4) | C(4C)-C(3C)-Ti(1C) | 73.0(5) |
| C(2A)-C(3A)-Ti(1A) | 71.0(5) | C(4B)-C(3B)-Ti(1B) | 72.8(5) | C(2C)-C(3C)-Ti(1C) | 72.6(4) |
| C(3A)-C(4A)-C(5A) | 108.5(8) | C(3B)-C(4B)-C(5B) | 108.2(8) | C(3C)-C(4C)-C(5C) | 107.2(8) |
| C(3A)-C(4A)-Ti(1A) | 73.3(5) | C(3B)-C(4B)-Ti(1B) | 72.4(5) | C(3C)-C(4C)-Ti(1C) | 71.9(5) |
| C(5A)-C(4A)-Ti(1A) | 71.7(4) | C(5B)-C(4B)-Ti(1B) | 72.3(4) | C(5C)-C(4C)-Ti(1C) | 71.7(4) |

| | | | | | |
|----------------------|----------|----------------------|----------|----------------------|----------|
| C(4A)-C(5A)-C(1A) | 109.3(8) | C(4B)-C(5B)-C(1B) | 108.8(8) | C(1C)-C(5C)-C(4C) | 109.3(8) |
| C(4A)-C(5A)-Ti(1A) | 73.1(5) | C(4B)-C(5B)-Ti(1B) | 72.7(4) | C(1C)-C(5C)-Ti(1C) | 72.8(4) |
| C(1A)-C(5A)-Ti(1A) | 72.5(4) | C(1B)-C(5B)-Ti(1B) | 72.3(4) | C(4C)-C(5C)-Ti(1C) | 72.7(5) |
| C(12A)-C(6A)-C(7AA) | 125.2(8) | C(7B)-C(6B)-C(12B) | 124.6(8) | C(12C)-C(6C)-C(7A) | 124.3(8) |
| C(12A)-C(6A)-Si(2A) | 119.0(6) | C(7B)-C(6B)-Si(2B) | 116.3(6) | C(12C)-C(6C)-Si(2C) | 119.3(6) |
| C(7AA)-C(6A)-Si(2A) | 115.7(6) | C(12B)-C(6B)-Si(2B) | 119.1(6) | C(7A)-C(6C)-Si(2C) | 116.3(6) |
| C(12A)-C(6A)-Ti(1A) | 70.8(5) | C(7B)-C(6B)-Ti(1B) | 69.8(4) | C(12C)-C(6C)-Ti(1C) | 71.1(5) |
| C(7AA)-C(6A)-Ti(1A) | 70.4(5) | C(12B)-C(6B)-Ti(1B) | 70.8(4) | C(7A)-C(6C)-Ti(1C) | 71.2(5) |
| Si(2A)-C(6A)-Ti(1A) | 138.2(4) | Si(2B)-C(6B)-Ti(1B) | 135.1(4) | Si(2C)-C(6C)-Ti(1C) | 136.2(4) |
| C(8A)-C(7AA)-C(6A) | 130.2(8) | C(8B)-C(7B)-C(6B) | 131.0(8) | C(8C)-C(7A)-C(6C) | 130.6(7) |
| C(8A)-C(7AA)-Ti(1A) | 70.6(5) | C(8B)-C(7B)-Ti(1B) | 72.5(4) | C(8C)-C(7A)-Ti(1C) | 71.0(4) |
| C(6A)-C(7AA)-Ti(1A) | 71.8(4) | C(6B)-C(7B)-Ti(1B) | 72.3(4) | C(6C)-C(7A)-Ti(1C) | 70.8(4) |
| C(7AA)-C(8A)-C(9A) | 130.3(7) | C(7B)-C(8B)-C(9B) | 129.8(7) | C(7A)-C(8C)-C(9C) | 131.5(7) |
| C(7AA)-C(8A)-Ti(1A) | 71.9(5) | C(7B)-C(8B)-Ti(1B) | 70.0(4) | C(7A)-C(8C)-Ti(1C) | 71.7(4) |
| C(9A)-C(8A)-Ti(1A) | 71.7(5) | C(9B)-C(8B)-Ti(1B) | 71.1(4) | C(9C)-C(8C)-Ti(1C) | 71.8(4) |
| C(8A)-C(9A)-C(10A) | 125.5(8) | C(8B)-C(9B)-C(10B) | 124.8(8) | C(8C)-C(9C)-C(10C) | 124.0(8) |
| C(8A)-C(9A)-Si(3A) | 116.0(6) | C(8B)-C(9B)-Si(3B) | 115.3(6) | C(8C)-C(9C)-Si(3C) | 116.4(6) |
| C(10A)-C(9A)-Si(3A) | 118.5(6) | C(10B)-C(9B)-Si(3B) | 119.9(7) | C(10C)-C(9C)-Si(3C) | 119.6(6) |
| C(8A)-C(9A)-Ti(1A) | 70.4(5) | C(8B)-C(9B)-Ti(1B) | 71.2(5) | C(8C)-C(9C)-Ti(1C) | 70.5(4) |
| C(10A)-C(9A)-Ti(1A) | 70.7(5) | C(10B)-C(9B)-Ti(1B) | 70.6(5) | C(10C)-C(9C)-Ti(1C) | 70.0(4) |
| Si(3A)-C(9A)-Ti(1A) | 138.9(4) | Si(3B)-C(9B)-Ti(1B) | 135.7(4) | Si(3C)-C(9C)-Ti(1C) | 134.2(4) |
| C(11A)-C(10A)-C(9A) | 129.1(8) | C(11B)-C(10B)-C(9B) | 130.1(8) | C(11C)-C(10C)-C(9C) | 130.1(7) |
| C(11A)-C(10A)-Ti(1A) | 71.8(5) | C(11B)-C(10B)-Ti(1B) | 72.4(5) | C(11C)-C(10C)-Ti(1C) | 71.8(4) |
| C(9A)-C(10A)-Ti(1A) | 71.3(5) | C(9B)-C(10B)-Ti(1B) | 71.5(5) | C(9C)-C(10C)-Ti(1C) | 71.9(4) |
| C(12A)-C(11A)-C(10A) | 129.7(7) | C(10B)-C(11B)-C(12B) | 129.4(8) | C(10C)-C(11C)-C(12C) | 130.1(7) |
| C(12A)-C(11A)-Ti(1A) | 71.6(4) | C(10B)-C(11B)-Ti(1B) | 70.7(4) | C(10C)-C(11C)-Ti(1C) | 71.2(4) |
| C(10A)-C(11A)-Ti(1A) | 70.7(4) | C(12B)-C(11B)-Ti(1B) | 70.9(4) | C(12C)-C(11C)-Ti(1C) | 71.2(4) |
| C(11A)-C(12A)-C(6A) | 129.8(7) | C(11B)-C(12B)-C(6B) | 129.9(8) | C(11C)-C(12C)-C(6C) | 129.0(8) |
| C(11A)-C(12A)-Ti(1A) | 71.4(4) | C(11B)-C(12B)-Ti(1B) | 72.1(4) | C(11C)-C(12C)-Ti(1C) | 70.8(5) |
| C(6A)-C(12A)-Ti(1A) | 71.7(4) | C(6B)-C(12B)-Ti(1B) | 71.3(4) | C(6C)-C(12C)-Ti(1C) | 70.9(5) |

Table A.3.4. Anisotropic displacement parameters ($\text{\AA}^2 \times 10^3$) for **204d**. The anisotropic displacement factor exponent takes the form: $-2\pi^2 [h^2 a^{*2} U^{11} + \dots + 2 h k a^* b^* U^{12}]$.

| | U^{11} | U^{22} | U^{33} | U^{23} | U^{13} | U^{12} |
|--------|----------|----------|----------|----------|----------|----------|
| Ti(1A) | 27(1) | 33(1) | 25(1) | -2(1) | 7(1) | 0(1) |
| Si(1A) | 30(1) | 49(2) | 38(1) | 4(1) | 6(1) | 2(1) |
| Si(2A) | 47(1) | 35(2) | 31(1) | 3(1) | 4(1) | 3(1) |
| Si(3A) | 50(1) | 26(2) | 39(1) | 0(1) | 4(1) | -3(1) |
| C(1A) | 29(4) | 41(6) | 34(5) | 0(4) | 22(4) | 4(4) |
| C(2A) | 43(5) | 36(6) | 50(6) | -7(5) | 14(4) | 3(4) |
| C(3A) | 36(5) | 62(8) | 37(5) | -21(5) | 7(4) | -8(5) |
| C(4A) | 29(4) | 74(8) | 26(4) | -3(5) | 11(4) | 4(5) |
| C(5A) | 33(4) | 47(6) | 30(4) | 8(4) | 12(4) | 5(4) |
| C(6A) | 35(4) | 34(5) | 26(4) | -3(4) | 8(4) | 7(4) |
| C(7AA) | 31(4) | 45(6) | 26(4) | -7(4) | 3(3) | 8(4) |
| C(8A) | 38(4) | 28(5) | 26(4) | -4(4) | 6(3) | -3(4) |
| C(9A) | 35(4) | 36(6) | 31(4) | 0(4) | 6(4) | -5(4) |
| C(10A) | 33(4) | 37(6) | 32(4) | 0(4) | 8(4) | -3(4) |
| C(11A) | 34(4) | 41(6) | 22(4) | -8(4) | 10(3) | -1(4) |
| C(12A) | 43(5) | 35(6) | 20(4) | -1(4) | 6(4) | 5(4) |
| C(13A) | 62(6) | 51(7) | 50(6) | 5(5) | -2(5) | 5(5) |
| C(14A) | 31(5) | 137(12) | 66(7) | -7(7) | 12(5) | -7(6) |
| C(15A) | 60(6) | 56(8) | 94(8) | -11(7) | -9(6) | -9(6) |
| C(16A) | 58(6) | 48(7) | 46(5) | 4(5) | 13(5) | -16(5) |
| C(17A) | 63(6) | 51(7) | 70(7) | 8(6) | -7(5) | 7(5) |
| C(18A) | 76(7) | 47(7) | 50(6) | -5(5) | 6(5) | -2(6) |
| C(19A) | 97(8) | 34(6) | 39(5) | 9(5) | -7(5) | -4(6) |
| C(20A) | 77(7) | 39(7) | 71(7) | -3(6) | -5(6) | 25(6) |
| C(21A) | 79(7) | 33(6) | 59(6) | 15(5) | 1(5) | -20(5) |
| Ti(1B) | 28(1) | 33(1) | 25(1) | 2(1) | 4(1) | 1(1) |
| Si(1B) | 31(1) | 52(2) | 53(2) | 5(1) | 10(1) | 0(1) |
| Si(2B) | 58(2) | 31(2) | 31(1) | 0(1) | 9(1) | 1(1) |
| Si(3B) | 56(2) | 29(2) | 34(1) | 0(1) | 11(1) | -1(1) |
| C(1B) | 25(4) | 42(6) | 31(4) | 0(4) | -5(3) | 2(4) |
| C(2B) | 32(4) | 27(5) | 50(5) | 13(4) | -7(4) | 10(4) |
| C(3B) | 40(5) | 53(7) | 39(5) | 21(5) | 2(4) | -1(5) |
| C(4B) | 39(5) | 69(8) | 26(5) | -3(5) | -2(4) | 6(5) |
| C(5B) | 36(5) | 45(6) | 33(5) | -7(4) | -4(4) | -1(4) |
| C(6B) | 26(4) | 31(5) | 32(4) | -3(4) | 4(3) | 5(4) |
| C(7B) | 36(4) | 24(5) | 38(4) | 6(4) | 0(4) | 6(4) |
| C(8B) | 31(4) | 24(5) | 35(5) | 1(4) | 3(4) | 2(4) |
| C(9B) | 30(4) | 36(6) | 29(4) | 0(4) | 3(3) | 3(4) |
| C(10B) | 28(4) | 45(6) | 26(4) | 0(4) | 1(3) | -6(4) |
| C(11B) | 37(4) | 51(7) | 18(4) | 2(4) | 7(3) | -2(4) |
| C(12B) | 31(4) | 38(6) | 32(4) | -1(4) | 7(3) | 7(4) |
| C(13B) | 74(7) | 71(9) | 83(8) | 4(7) | 52(6) | 10(6) |

| | | | | | | |
|--------|--------|---------|---------|--------|--------|--------|
| C(14B) | 32(6) | 204(19) | 118(11) | 73(11) | 3(6) | -7(8) |
| C(15B) | 89(8) | 52(8) | 74(8) | -11(6) | 36(6) | -28(6) |
| C(16B) | 95(8) | 38(7) | 47(6) | 4(5) | 0(5) | -3(6) |
| C(17B) | 83(7) | 39(6) | 46(6) | 6(5) | 13(5) | 17(5) |
| C(18B) | 73(7) | 53(7) | 48(6) | -6(5) | 1(5) | -25(6) |
| C(19B) | 104(8) | 40(6) | 25(5) | -5(4) | 17(5) | -7(6) |
| C(20B) | 71(6) | 43(7) | 53(6) | 8(5) | 26(5) | 19(5) |
| C(21B) | 98(8) | 48(7) | 38(5) | -5(5) | 12(5) | -26(6) |
| Ti(1C) | 27(1) | 34(1) | 26(1) | 1(1) | 7(1) | -2(1) |
| Si(1C) | 31(1) | 65(2) | 52(2) | 6(1) | 4(1) | 0(1) |
| Si(2C) | 46(1) | 34(2) | 33(1) | -2(1) | 6(1) | -3(1) |
| Si(3C) | 47(1) | 34(2) | 31(1) | -2(1) | 6(1) | 1(1) |
| C(1C) | 27(4) | 25(5) | 29(4) | -1(4) | 16(3) | -5(4) |
| C(2C) | 40(5) | 37(6) | 32(4) | -3(4) | 18(4) | 0(4) |
| C(3C) | 48(5) | 61(7) | 17(4) | 8(4) | 7(4) | -7(5) |
| C(4C) | 38(5) | 53(7) | 45(5) | 27(5) | 15(4) | 1(5) |
| C(5C) | 36(4) | 27(5) | 42(5) | -2(4) | 20(4) | -7(4) |
| C(6C) | 32(4) | 45(6) | 26(4) | 1(4) | 9(3) | -1(4) |
| C(7A) | 30(4) | 38(6) | 34(4) | -2(4) | 2(4) | 1(4) |
| C(8C) | 32(4) | 33(6) | 31(4) | 4(4) | 10(3) | 7(4) |
| C(9C) | 36(4) | 42(6) | 25(4) | 2(4) | 10(3) | 2(4) |
| C(10C) | 33(4) | 30(5) | 27(4) | -4(4) | 6(3) | -6(4) |
| C(11C) | 40(4) | 44(6) | 26(4) | 10(4) | 3(4) | 3(4) |
| C(12C) | 40(5) | 29(5) | 29(4) | -3(4) | 6(4) | 5(4) |
| C(13C) | 86(8) | 53(8) | 78(8) | 0(6) | -10(6) | 28(6) |
| C(14C) | 29(6) | 310(30) | 128(12) | 84(14) | 23(7) | 26(10) |
| C(15C) | 78(7) | 55(8) | 74(7) | -11(6) | -29(6) | 0(6) |
| C(16C) | 70(6) | 52(7) | 45(6) | -5(5) | -1(5) | -19(5) |
| C(17C) | 87(8) | 47(7) | 41(5) | -16(5) | 1(5) | 23(6) |
| C(18C) | 54(5) | 46(6) | 38(5) | -1(4) | 6(4) | -5(5) |
| C(19C) | 73(6) | 44(7) | 30(5) | 5(4) | 9(4) | 6(5) |
| C(20C) | 64(6) | 59(8) | 55(6) | -10(5) | 10(5) | 28(5) |
| C(21C) | 67(6) | 47(7) | 37(5) | 6(5) | 2(4) | -1(5) |

Table A.3.5. Hydrogen coordinates ($\times 10^4$) and isotropic displacement parameters ($\text{\AA}^2 \times 10^3$) for **204d**.

| | x | y | z | U(eq) |
|--------|-------|-------|------|-------|
| H(2AA) | 9936 | -1414 | 5526 | 51 |
| H(3AA) | 8058 | -1274 | 5013 | 54 |
| H(4AA) | 7987 | -11 | 4792 | 51 |
| H(5AA) | 9825 | 632 | 5156 | 43 |
| H(7AA) | 6046 | -839 | 5547 | 41 |
| H(8AA) | 6016 | 224 | 5347 | 36 |
| H(10A) | 8910 | 1064 | 5990 | 41 |
| H(11A) | 9612 | 185 | 6347 | 38 |
| H(12A) | 8966 | -876 | 6347 | 39 |
| H(13A) | 11314 | -678 | 6352 | 82 |
| H(13B) | 12761 | -732 | 6315 | 82 |
| H(13C) | 11813 | -1249 | 6076 | 82 |
| H(14A) | 12919 | 31 | 5249 | 116 |
| H(14B) | 12999 | -765 | 5375 | 116 |
| H(14C) | 13814 | -198 | 5622 | 116 |
| H(15A) | 11264 | 793 | 6152 | 107 |
| H(15B) | 11481 | 1060 | 5733 | 107 |
| H(15C) | 12639 | 876 | 6040 | 107 |
| H(16A) | 5700 | -1653 | 6605 | 75 |
| H(16B) | 5365 | -2367 | 6385 | 75 |
| H(16C) | 4861 | -1650 | 6198 | 75 |
| H(17A) | 8386 | -1993 | 6660 | 93 |
| H(17B) | 9059 | -2121 | 6283 | 93 |
| H(17C) | 8158 | -2699 | 6423 | 93 |
| H(18A) | 6117 | -1997 | 5451 | 86 |
| H(18B) | 6404 | -2723 | 5664 | 86 |
| H(18C) | 7503 | -2285 | 5516 | 86 |
| H(19A) | 7398 | 1344 | 4861 | 87 |
| H(19B) | 6251 | 1866 | 4829 | 87 |
| H(19C) | 6037 | 1057 | 4895 | 87 |
| H(20A) | 4719 | 1573 | 5587 | 95 |
| H(20B) | 5139 | 2347 | 5504 | 95 |
| H(20C) | 5497 | 2010 | 5920 | 95 |
| H(21A) | 8852 | 2062 | 5503 | 86 |
| H(21B) | 8250 | 2281 | 5881 | 86 |
| H(21C) | 7846 | 2668 | 5482 | 86 |
| H(2BA) | 8175 | 7289 | 8901 | 45 |
| H(3BA) | 9575 | 7151 | 8372 | 53 |
| H(4BA) | 9476 | 5889 | 8145 | 54 |
| H(5BA) | 7986 | 5233 | 8532 | 46 |
| H(7BA) | 12030 | 6746 | 8865 | 39 |
| H(8BA) | 11968 | 5680 | 8675 | 36 |

| | | | | |
|--------|-------|------|------|-----|
| H(10B) | 9669 | 4817 | 9349 | 40 |
| H(11B) | 9254 | 5672 | 9714 | 42 |
| H(12B) | 9838 | 6746 | 9705 | 40 |
| H(13D) | 7616 | 6521 | 9734 | 109 |
| H(13E) | 6154 | 6532 | 9750 | 109 |
| H(13F) | 6778 | 7091 | 9496 | 109 |
| H(14D) | 4796 | 5778 | 8742 | 177 |
| H(14E) | 5143 | 6580 | 8715 | 177 |
| H(14F) | 4470 | 6305 | 9069 | 177 |
| H(15D) | 7514 | 4976 | 9404 | 104 |
| H(15E) | 6315 | 4812 | 9109 | 104 |
| H(15F) | 6165 | 5050 | 9539 | 104 |
| H(16D) | 11882 | 7862 | 8764 | 91 |
| H(16E) | 11713 | 8602 | 8956 | 91 |
| H(16F) | 10527 | 8140 | 8815 | 91 |
| H(17D) | 10462 | 7982 | 9957 | 83 |
| H(17E) | 9486 | 7969 | 9578 | 83 |
| H(17F) | 10369 | 8626 | 9667 | 83 |
| H(18D) | 13692 | 7688 | 9510 | 88 |
| H(18E) | 13156 | 7649 | 9917 | 88 |
| H(18F) | 13203 | 8375 | 9698 | 88 |
| H(19D) | 11587 | 4878 | 8198 | 84 |
| H(19E) | 10174 | 4638 | 8174 | 84 |
| H(19F) | 11232 | 4083 | 8120 | 84 |
| H(20D) | 13416 | 4308 | 8872 | 81 |
| H(20E) | 12888 | 3548 | 8772 | 81 |
| H(20F) | 12893 | 3848 | 9198 | 81 |
| H(21D) | 10130 | 3598 | 9178 | 91 |
| H(21E) | 10134 | 3266 | 8759 | 91 |
| H(21F) | 9209 | 3887 | 8824 | 91 |
| H(2CA) | 8803 | 1127 | 6919 | 42 |
| H(3CA) | 7121 | 1790 | 6494 | 50 |
| H(4CA) | 7187 | 3066 | 6714 | 53 |
| H(5CA) | 8904 | 3174 | 7290 | 41 |
| H(7AB) | 4851 | 1645 | 6972 | 41 |
| H(8CA) | 4934 | 2692 | 7171 | 38 |
| H(10C) | 7622 | 2650 | 8048 | 36 |
| H(11C) | 8158 | 1574 | 8064 | 44 |
| H(12C) | 7485 | 710 | 7686 | 39 |
| H(13G) | 10439 | 680 | 7504 | 111 |
| H(13H) | 9835 | 902 | 7881 | 111 |
| H(13I) | 11306 | 866 | 7891 | 111 |
| H(14G) | 11891 | 1769 | 7102 | 230 |
| H(14H) | 12680 | 1913 | 7508 | 230 |
| H(14I) | 11980 | 2537 | 7274 | 230 |
| H(15G) | 11388 | 2440 | 8158 | 108 |

| | | | | |
|--------|-------|------|------|-----|
| H(15H) | 9935 | 2322 | 8163 | 108 |
| H(15I) | 10420 | 2942 | 7916 | 108 |
| H(16G) | 4223 | -193 | 7495 | 84 |
| H(16H) | 4046 | -577 | 7087 | 84 |
| H(16I) | 3463 | 175 | 7132 | 84 |
| H(17G) | 6985 | -476 | 7464 | 89 |
| H(17H) | 7677 | -122 | 7135 | 89 |
| H(17I) | 6753 | -755 | 7031 | 89 |
| H(18G) | 4706 | 793 | 6508 | 69 |
| H(18H) | 5183 | 32 | 6421 | 69 |
| H(18I) | 6146 | 658 | 6486 | 69 |
| H(19G) | 6428 | 4056 | 7126 | 73 |
| H(19H) | 5368 | 4541 | 7261 | 73 |
| H(19I) | 5019 | 3805 | 7069 | 73 |
| H(20G) | 4550 | 3630 | 8222 | 88 |
| H(20H) | 3722 | 3651 | 7813 | 88 |
| H(20I) | 4365 | 4343 | 7990 | 88 |
| H(21G) | 7994 | 3815 | 7921 | 76 |
| H(21H) | 7220 | 3952 | 8275 | 76 |
| H(21I) | 7273 | 4531 | 7951 | 76 |

IV. X-Ray Data for **207d**.**Table A.4.1.** Crystal Data and Structure Refinement for **207d**.

| | | |
|-----------------------------------|--|-----------------------------|
| Empirical formula | C ₂₄ H ₄₄ Si ₄ Ti | |
| Formula weight | 492.85 | |
| Temperature | 150(2) K | |
| Wavelength | 0.71073 Å | |
| Crystal system | Monoclinic | |
| Space group | P 2 ₁ /n | |
| Unit cell dimensions | a = 12.6310(5) Å | $\alpha = 90^\circ$ |
| | b = 10.5146(2) Å | $\beta = 91.3990(14)^\circ$ |
| | c = 21.5304(8) Å | $\gamma = 90^\circ$ |
| Volume | 2858.60(16) Å ³ | |
| Z | 4 | |
| Density (calculated) | 1.145 Mg/m ³ | |
| Absorption coefficient | 0.476 mm ⁻¹ | |
| F(000) | 1064 | |
| Crystal size / Shape | 0.30 x 0.20 x 0.10 mm ³ | Needle-shaped |
| Theta range for data collection | 2.68 to 27.49° | |
| Index ranges | -16 ≤ h ≤ 16, -13 ≤ k ≤ 13, -23 ≤ l ≤ 27 | |
| Reflections collected | 23215 | |
| Independent reflections | 6541 [R(int) = 0.0593] | |
| Completeness to theta = 27.49° | 99.60% | |
| Absorption correction | Semi-empirical from equivalents | |
| Max. and min. transmission | 0.966 and 0.700 | |
| Refinement method | Full-matrix least-squares on F ² | |
| Data / restraints / parameters | 6541 / 0 / 307 | |
| Goodness-of-fit on F ² | 1.043 | |
| Final R indices [I > 2σ(I)] | R1 = 0.0403, wR2 = 0.0932 | |
| R indices (all data) | R1 = 0.0639, wR2 = 0.1041 | |
| Extinction coefficient | none | |
| Largest diff. peak and hole | 0.566 and -0.490 e.Å ⁻³ | |

Table A.4.2. Atomic coordinates ($\times 10^4$) and equivalent isotropic displacement parameters ($\text{\AA}^2 \times 10^3$) for **207d**. $U(\text{eq})$ is defined as one third of the trace of the orthogonalized U^{ij} tensor.

| | x | y | z | U(eq) |
|-------|---------|---------|---------|-------|
| Ti(1) | 4634(1) | 5931(1) | 2858(1) | 23(1) |
| Si(1) | 4748(1) | 2454(1) | 3387(1) | 27(1) |
| Si(2) | 6894(1) | 7354(1) | 3817(1) | 27(1) |
| Si(3) | 5198(1) | 7230(1) | 1240(1) | 34(1) |
| Si(4) | 2723(1) | 7236(1) | 4078(1) | 28(1) |
| C(1) | 5388(2) | 4029(2) | 3240(1) | 26(1) |
| C(2) | 5603(2) | 5013(2) | 3677(1) | 25(1) |
| C(3) | 6254(2) | 5971(2) | 3411(1) | 26(1) |
| C(4) | 6448(2) | 5550(2) | 2794(1) | 27(1) |
| C(5) | 5926(2) | 4379(2) | 2692(1) | 27(1) |
| C(6) | 4401(2) | 6869(2) | 1942(1) | 27(1) |
| C(7) | 4409(2) | 7814(2) | 2421(1) | 27(1) |
| C(8) | 3914(2) | 7829(2) | 3005(1) | 26(1) |
| C(9) | 3243(2) | 6904(2) | 3285(1) | 25(1) |
| C(10) | 2909(2) | 5733(2) | 3003(1) | 27(1) |
| C(11) | 3147(2) | 5204(2) | 2414(1) | 29(1) |
| C(12) | 3815(2) | 5704(2) | 1954(1) | 30(1) |
| C(13) | 4810(2) | 1487(2) | 2665(1) | 42(1) |
| C(14) | 5537(2) | 1692(2) | 4030(1) | 37(1) |
| C(15) | 3349(2) | 2600(2) | 3632(1) | 39(1) |
| C(16) | 8312(2) | 6933(2) | 3966(1) | 46(1) |
| C(17) | 6228(2) | 7632(2) | 4565(1) | 43(1) |
| C(18) | 6820(2) | 8810(2) | 3322(1) | 37(1) |
| C(19) | 6436(2) | 8125(3) | 1444(1) | 62(1) |
| C(20) | 4380(3) | 8239(3) | 708(1) | 68(1) |
| C(21) | 5561(2) | 5735(3) | 834(1) | 58(1) |
| C(22) | 3155(2) | 6006(2) | 4659(1) | 40(1) |
| C(23) | 3125(2) | 8859(2) | 4350(1) | 38(1) |
| C(24) | 1243(2) | 7209(2) | 4030(1) | 43(1) |

Table A.4.3. Bond Lengths [\AA] and Angles [$^\circ$] for **207d**.

| | | | |
|-------------------|------------|-------------------|------------|
| Ti(1)-C(12) | 2.196(2) | Si(3)-C(20) | 1.858(3) |
| Ti(1)-C(7) | 2.207(2) | Si(3)-C(21) | 1.861(3) |
| Ti(1)-C(6) | 2.2180(19) | Si(3)-C(19) | 1.868(3) |
| Ti(1)-C(10) | 2.219(2) | Si(3)-C(6) | 1.875(2) |
| Ti(1)-C(8) | 2.219(2) | Si(4)-C(23) | 1.871(2) |
| Ti(1)-C(11) | 2.223(2) | Si(4)-C(24) | 1.871(2) |
| Ti(1)-C(9) | 2.2493(19) | Si(4)-C(22) | 1.871(2) |
| Ti(1)-C(2) | 2.3310(19) | Si(4)-C(9) | 1.877(2) |
| Ti(1)-C(4) | 2.332(2) | C(1)-C(2) | 1.421(3) |
| Ti(1)-C(5) | 2.3412(19) | C(1)-C(5) | 1.424(3) |
| Ti(1)-C(3) | 2.3423(19) | C(2)-C(3) | 1.429(3) |
| Ti(1)-C(1) | 2.3549(18) | C(3)-C(4) | 1.427(3) |
| Si(1)-C(13) | 1.859(2) | C(4)-C(5) | 1.411(3) |
| Si(1)-C(15) | 1.862(2) | C(6)-C(7) | 1.432(3) |
| Si(1)-C(14) | 1.867(2) | C(6)-C(12) | 1.432(3) |
| Si(1)-C(1) | 1.873(2) | C(7)-C(8) | 1.418(3) |
| Si(2)-C(17) | 1.859(2) | C(8)-C(9) | 1.432(3) |
| Si(2)-C(16) | 1.865(2) | C(9)-C(10) | 1.433(3) |
| Si(2)-C(18) | 1.866(2) | C(10)-C(11) | 1.424(3) |
| Si(2)-C(3) | 1.870(2) | C(11)-C(12) | 1.417(3) |
| | | | |
| C(12)-Ti(1)-C(7) | 70.51(8) | C(13)-Si(1)-C(1) | 108.34(10) |
| C(12)-Ti(1)-C(6) | 37.86(7) | C(15)-Si(1)-C(1) | 113.05(9) |
| C(7)-Ti(1)-C(6) | 37.75(7) | C(14)-Si(1)-C(1) | 106.22(10) |
| C(12)-Ti(1)-C(10) | 70.77(8) | C(17)-Si(2)-C(16) | 109.96(12) |
| C(7)-Ti(1)-C(10) | 91.55(8) | C(17)-Si(2)-C(18) | 110.41(11) |
| C(6)-Ti(1)-C(10) | 93.26(7) | C(16)-Si(2)-C(18) | 109.11(11) |
| C(12)-Ti(1)-C(8) | 92.18(8) | C(17)-Si(2)-C(3) | 109.10(10) |
| C(7)-Ti(1)-C(8) | 37.38(7) | C(16)-Si(2)-C(3) | 107.32(10) |
| C(6)-Ti(1)-C(8) | 71.40(7) | C(18)-Si(2)-C(3) | 110.89(9) |
| C(10)-Ti(1)-C(8) | 69.92(7) | C(20)-Si(3)-C(21) | 109.37(15) |
| C(12)-Ti(1)-C(11) | 37.41(8) | C(20)-Si(3)-C(19) | 107.85(15) |
| C(7)-Ti(1)-C(11) | 91.50(8) | C(21)-Si(3)-C(19) | 108.76(15) |
| C(6)-Ti(1)-C(11) | 71.21(8) | C(20)-Si(3)-C(6) | 108.15(11) |
| C(10)-Ti(1)-C(11) | 37.39(7) | C(21)-Si(3)-C(6) | 110.57(11) |
| C(8)-Ti(1)-C(11) | 91.47(8) | C(19)-Si(3)-C(6) | 112.08(11) |
| C(12)-Ti(1)-C(9) | 93.22(8) | C(23)-Si(4)-C(24) | 107.10(11) |
| C(7)-Ti(1)-C(9) | 70.89(7) | C(23)-Si(4)-C(22) | 110.46(10) |
| C(6)-Ti(1)-C(9) | 94.21(7) | C(24)-Si(4)-C(22) | 107.54(11) |
| C(10)-Ti(1)-C(9) | 37.41(7) | C(23)-Si(4)-C(9) | 110.84(9) |
| C(8)-Ti(1)-C(9) | 37.38(7) | C(24)-Si(4)-C(9) | 108.55(10) |
| C(11)-Ti(1)-C(9) | 70.87(7) | C(22)-Si(4)-C(9) | 112.14(9) |
| C(12)-Ti(1)-C(2) | 148.56(7) | C(2)-C(1)-C(5) | 105.82(17) |
| C(7)-Ti(1)-C(2) | 138.93(7) | C(2)-C(1)-Si(1) | 127.48(15) |

| | | | |
|-------------------|------------|-------------------|------------|
| C(6)-Ti(1)-C(2) | 155.87(7) | C(5)-C(1)-Si(1) | 125.84(15) |
| C(10)-Ti(1)-C(2) | 110.74(7) | C(2)-C(1)-Ti(1) | 71.43(10) |
| C(8)-Ti(1)-C(2) | 118.30(7) | C(5)-C(1)-Ti(1) | 71.83(11) |
| C(11)-Ti(1)-C(2) | 127.26(7) | Si(1)-C(1)-Ti(1) | 129.61(10) |
| C(9)-Ti(1)-C(2) | 106.24(7) | C(1)-C(2)-C(3) | 110.53(18) |
| C(12)-Ti(1)-C(4) | 111.81(8) | C(1)-C(2)-Ti(1) | 73.27(11) |
| C(7)-Ti(1)-C(4) | 104.23(8) | C(3)-C(2)-Ti(1) | 72.63(11) |
| C(6)-Ti(1)-C(4) | 97.66(7) | C(4)-C(3)-C(2) | 105.52(17) |
| C(10)-Ti(1)-C(4) | 164.01(7) | C(4)-C(3)-Si(2) | 126.43(15) |
| C(8)-Ti(1)-C(4) | 124.74(7) | C(2)-C(3)-Si(2) | 127.43(15) |
| C(11)-Ti(1)-C(4) | 137.40(7) | C(4)-C(3)-Ti(1) | 71.85(11) |
| C(9)-Ti(1)-C(4) | 151.67(7) | C(2)-C(3)-Ti(1) | 71.77(11) |
| C(2)-Ti(1)-C(4) | 58.36(7) | Si(2)-C(3)-Ti(1) | 127.84(9) |
| C(12)-Ti(1)-C(5) | 95.98(7) | C(5)-C(4)-C(3) | 108.99(18) |
| C(7)-Ti(1)-C(5) | 130.05(7) | C(5)-C(4)-Ti(1) | 72.76(11) |
| C(6)-Ti(1)-C(5) | 104.61(7) | C(3)-C(4)-Ti(1) | 72.60(11) |
| C(10)-Ti(1)-C(5) | 130.25(7) | C(4)-C(5)-C(1) | 109.12(18) |
| C(8)-Ti(1)-C(5) | 159.80(7) | C(4)-C(5)-Ti(1) | 72.08(11) |
| C(11)-Ti(1)-C(5) | 106.20(7) | C(1)-C(5)-Ti(1) | 72.88(11) |
| C(9)-Ti(1)-C(5) | 159.00(7) | C(7)-C(6)-C(12) | 125.12(19) |
| C(2)-Ti(1)-C(5) | 58.12(7) | C(7)-C(6)-Si(3) | 116.48(15) |
| C(4)-Ti(1)-C(5) | 35.15(7) | C(12)-C(6)-Si(3) | 118.38(15) |
| C(12)-Ti(1)-C(3) | 147.13(8) | C(7)-C(6)-Ti(1) | 70.71(11) |
| C(7)-Ti(1)-C(3) | 107.63(7) | C(12)-C(6)-Ti(1) | 70.23(11) |
| C(6)-Ti(1)-C(3) | 122.66(7) | Si(3)-C(6)-Ti(1) | 138.09(10) |
| C(10)-Ti(1)-C(3) | 141.17(7) | C(8)-C(7)-C(6) | 130.62(19) |
| C(8)-Ti(1)-C(3) | 105.53(7) | C(8)-C(7)-Ti(1) | 71.76(11) |
| C(11)-Ti(1)-C(3) | 160.62(7) | C(6)-C(7)-Ti(1) | 71.54(11) |
| C(9)-Ti(1)-C(3) | 117.72(7) | C(7)-C(8)-C(9) | 130.11(19) |
| C(2)-Ti(1)-C(3) | 35.60(7) | C(7)-C(8)-Ti(1) | 70.86(11) |
| C(4)-Ti(1)-C(3) | 35.55(7) | C(9)-C(8)-Ti(1) | 72.47(11) |
| C(5)-Ti(1)-C(3) | 59.13(7) | C(8)-C(9)-C(10) | 125.12(18) |
| C(12)-Ti(1)-C(1) | 113.25(7) | C(8)-C(9)-Si(4) | 118.75(14) |
| C(7)-Ti(1)-C(1) | 163.25(7) | C(10)-C(9)-Si(4) | 116.11(14) |
| C(6)-Ti(1)-C(1) | 137.03(7) | C(8)-C(9)-Ti(1) | 70.15(11) |
| C(10)-Ti(1)-C(1) | 105.13(7) | C(10)-C(9)-Ti(1) | 70.14(11) |
| C(8)-Ti(1)-C(1) | 151.38(7) | Si(4)-C(9)-Ti(1) | 138.66(10) |
| C(11)-Ti(1)-C(1) | 100.82(7) | C(11)-C(10)-C(9) | 130.38(19) |
| C(9)-Ti(1)-C(1) | 123.82(7) | C(11)-C(10)-Ti(1) | 71.46(12) |
| C(2)-Ti(1)-C(1) | 35.31(7) | C(9)-C(10)-Ti(1) | 72.46(11) |
| C(4)-Ti(1)-C(1) | 59.04(7) | C(12)-C(11)-C(10) | 128.28(19) |
| C(5)-Ti(1)-C(1) | 35.29(7) | C(12)-C(11)-Ti(1) | 70.27(12) |
| C(3)-Ti(1)-C(1) | 59.82(7) | C(10)-C(11)-Ti(1) | 71.15(11) |
| C(13)-Si(1)-C(15) | 110.02(12) | C(11)-C(12)-C(6) | 130.28(19) |
| C(13)-Si(1)-C(14) | 110.61(11) | C(11)-C(12)-Ti(1) | 72.32(12) |
| C(15)-Si(1)-C(14) | 108.55(11) | C(6)-C(12)-Ti(1) | 71.91(11) |

Table A.4.4. Anisotropic displacement parameters ($\text{\AA}^2 \times 10^3$) for **207d**. The anisotropic displacement factor exponent takes the form: $-2\pi^2 [h^2 a^{*2} U^{11} + \dots + 2 h k a^* b^* U^{12}]$.

| | U^{11} | U^{22} | U^{33} | U^{23} | U^{13} | U^{12} |
|-------|----------|----------|----------|----------|----------|----------|
| Ti(1) | 21(1) | 21(1) | 25(1) | 1(1) | -2(1) | 1(1) |
| Si(1) | 33(1) | 21(1) | 29(1) | 0(1) | -3(1) | -1(1) |
| Si(2) | 24(1) | 27(1) | 30(1) | -2(1) | -2(1) | -3(1) |
| Si(3) | 37(1) | 39(1) | 26(1) | 3(1) | 5(1) | 6(1) |
| Si(4) | 28(1) | 29(1) | 26(1) | 1(1) | 2(1) | 0(1) |
| C(1) | 24(1) | 23(1) | 31(1) | 1(1) | -3(1) | 4(1) |
| C(2) | 22(1) | 26(1) | 27(1) | 2(1) | -4(1) | 1(1) |
| C(3) | 20(1) | 27(1) | 31(1) | 1(1) | -3(1) | 2(1) |
| C(4) | 21(1) | 29(1) | 32(1) | 1(1) | 4(1) | 2(1) |
| C(5) | 26(1) | 26(1) | 29(1) | -3(1) | 0(1) | 4(1) |
| C(6) | 27(1) | 29(1) | 24(1) | 2(1) | -2(1) | 4(1) |
| C(7) | 28(1) | 25(1) | 29(1) | 4(1) | 0(1) | 1(1) |
| C(8) | 26(1) | 23(1) | 28(1) | -1(1) | 0(1) | 1(1) |
| C(9) | 22(1) | 24(1) | 28(1) | 2(1) | 0(1) | 3(1) |
| C(10) | 22(1) | 29(1) | 31(1) | 4(1) | -2(1) | -2(1) |
| C(11) | 27(1) | 25(1) | 35(1) | -2(1) | -6(1) | -1(1) |
| C(12) | 28(1) | 35(1) | 26(1) | -3(1) | -5(1) | 3(1) |
| C(13) | 60(2) | 30(1) | 37(1) | -2(1) | -4(1) | -4(1) |
| C(14) | 43(1) | 34(1) | 35(1) | 4(1) | -3(1) | -1(1) |
| C(15) | 35(1) | 31(1) | 52(1) | 7(1) | -1(1) | -6(1) |
| C(16) | 31(1) | 47(1) | 59(2) | -5(1) | -12(1) | -2(1) |
| C(17) | 50(2) | 45(1) | 34(1) | -7(1) | 4(1) | -6(1) |
| C(18) | 38(1) | 32(1) | 42(1) | 2(1) | -2(1) | -8(1) |
| C(19) | 58(2) | 83(2) | 46(2) | 8(1) | 17(1) | -22(2) |
| C(20) | 71(2) | 89(2) | 45(2) | 31(2) | 18(1) | 31(2) |
| C(21) | 70(2) | 60(2) | 46(2) | -5(1) | 21(1) | 9(1) |
| C(22) | 51(2) | 37(1) | 31(1) | 2(1) | 5(1) | 1(1) |
| C(23) | 44(1) | 35(1) | 36(1) | -2(1) | 4(1) | 2(1) |
| C(24) | 32(1) | 59(2) | 38(1) | -3(1) | 8(1) | -1(1) |

Table A.4.5. Hydrogen coordinates ($\times 10^4$) and isotropic displacement parameters ($\text{\AA}^2 \times 10^3$) for **207d**.

| | x | y | z | U(eq) |
|--------|----------|----------|----------|-------|
| H(13A) | 4453 | 1943 | 2323 | 64 |
| H(13B) | 4458 | 669 | 2729 | 64 |
| H(13C) | 5552 | 1341 | 2563 | 64 |
| H(14A) | 5518 | 2230 | 4401 | 56 |
| H(14B) | 6272 | 1590 | 3903 | 56 |
| H(14C) | 5237 | 856 | 4122 | 56 |
| H(15A) | 2900 | 2846 | 3275 | 59 |
| H(15B) | 3303 | 3249 | 3957 | 59 |
| H(15C) | 3109 | 1781 | 3795 | 59 |
| H(16A) | 8651 | 6761 | 3570 | 69 |
| H(16B) | 8355 | 6173 | 4229 | 69 |
| H(16C) | 8673 | 7642 | 4176 | 69 |
| H(17A) | 5479 | 7830 | 4483 | 65 |
| H(17B) | 6568 | 8347 | 4783 | 65 |
| H(17C) | 6285 | 6867 | 4823 | 65 |
| H(18A) | 6084 | 9102 | 3288 | 56 |
| H(18B) | 7078 | 8612 | 2907 | 56 |
| H(18C) | 7261 | 9480 | 3510 | 56 |
| H(19A) | 6800 | 8352 | 1063 | 93 |
| H(19B) | 6901 | 7593 | 1705 | 93 |
| H(19C) | 6256 | 8902 | 1670 | 93 |
| H(20A) | 3766 | 7752 | 554 | 102 |
| H(20B) | 4805 | 8505 | 356 | 102 |
| H(20C) | 4137 | 8991 | 932 | 102 |
| H(21A) | 4920 | 5334 | 659 | 88 |
| H(21B) | 5908 | 5152 | 1130 | 88 |
| H(21C) | 6046 | 5932 | 499 | 88 |
| H(22A) | 3927 | 6036 | 4716 | 60 |
| H(22B) | 2943 | 5161 | 4509 | 60 |
| H(22C) | 2821 | 6176 | 5057 | 60 |
| H(23A) | 3897 | 8900 | 4397 | 57 |
| H(23B) | 2804 | 9036 | 4751 | 57 |
| H(23C) | 2883 | 9493 | 4045 | 57 |
| H(24A) | 991 | 7863 | 3738 | 64 |
| H(24B) | 959 | 7377 | 4442 | 64 |
| H(24C) | 1002 | 6371 | 3885 | 64 |
| H(2) | 5328(16) | 5022(18) | 4105(10) | 25(5) |
| H(4) | 6824(17) | 6000(20) | 2504(10) | 32(6) |
| H(5) | 5902(16) | 3878(19) | 2306(10) | 24(5) |
| H(7) | 4909(18) | 8470(20) | 2366(10) | 34(6) |
| H(8) | 4107(16) | 8440(20) | 3242(10) | 25(5) |
| H(10) | 2542(17) | 5180(20) | 3265(10) | 33(6) |

| | | | | |
|-------|----------|----------|----------|-------|
| H(11) | 2927(18) | 4350(20) | 2350(10) | 37(6) |
| H(12) | 3968(18) | 5110(20) | 1621(11) | 38(6) |

V. X-Ray Data for **210c**.

Table A.5.1. Crystal Data and Structure Refinement for **210c**.

| | | |
|-----------------------------------|---|---------------------|
| Empirical formula | C ₃₆ H ₃₀ P ₂ Ti | |
| Formula weight | 572.44 | |
| Temperature | 273(2) K | |
| Wavelength | 1.54178 Å | |
| Crystal system | Orthorhombic | |
| Space group | Pnma | |
| Unit cell dimensions | a = 12.8573(5) Å | $\alpha = 90^\circ$ |
| | b = 26.8838(9) Å | $\beta = 90^\circ$ |
| | c = 8.3110(3) Å | $\gamma = 90^\circ$ |
| Volume | 2872.72(18) Å ³ | |
| Z | 4 | |
| Density (calculated) | 1.324 Mg/m ³ | |
| Absorption coefficient | 3.748 mm ⁻¹ | |
| F(000) | 1192 | |
| Crystal size / Shape | 0.30 x 0.26 x 0.24 mm ³ | Block-shaped |
| Theta range for data collection | 3.29 to 64.75° | |
| Index ranges | -14 ≤ h ≤ 14, -31 ≤ k ≤ 28, -9 ≤ l ≤ 9 | |
| Reflections collected | 13638 | |
| Independent reflections | 2448 [R(int) = 0.0249] | |
| Completeness to theta = 64.75° | 98.70% | |
| Absorption correction | None | |
| Max. and min. transmission | 0.4653 and 0.4013 | |
| Refinement method | Full-matrix least-squares on F ² | |
| Data / restraints / parameters | 2448 / 0 / 183 | |
| Goodness-of-fit on F ² | 1.058 | |
| Final R indices [I > 2σ(I)] | R1 = 0.0341, wR2 = 0.0880 | |
| R indices (all data) | R1 = 0.0357, wR2 = 0.0892 | |
| Extinction coefficient | 0.00012(7) | |
| Largest diff. peak and hole | 0.381 and -0.338 e.Å ⁻³ | |

Table A.5.2. Atomic coordinates ($\times 10^4$) and equivalent isotropic displacement parameters ($\text{\AA}^2 \times 10^3$) for **210c**. $U(\text{eq})$ is defined as one third of the trace of the orthogonalized U^{ij} tensor.

| | x | y | z | $U(\text{eq})$ |
|-------|---------|---------|----------|----------------|
| Ti(1) | 1396(1) | 2500 | 1415(1) | 18(1) |
| P(2) | 1899(1) | 3468(1) | 4600(1) | 20(1) |
| C(2) | 1171(1) | 2983(1) | 3538(2) | 19(1) |
| C(7) | 1721(2) | 2500 | -1332(3) | 30(1) |
| C(9) | 23(2) | 3401(1) | 6404(2) | 23(1) |
| C(4) | -236(1) | 2765(1) | 1456(2) | 20(1) |
| C(3) | 388(1) | 3097(1) | 2368(2) | 20(1) |
| C(8) | 961(1) | 3647(1) | 6165(2) | 21(1) |
| C(14) | 1874(2) | 4018(1) | 3280(3) | 30(1) |
| C(11) | -341(2) | 3897(1) | 8742(2) | 31(1) |
| C(10) | -625(2) | 3526(1) | 7684(2) | 27(1) |
| C(1) | 1506(2) | 2500 | 4049(3) | 19(1) |
| C(6) | 2196(2) | 2923(1) | -666(3) | 37(1) |
| C(12) | 596(2) | 4144(1) | 8520(3) | 36(1) |
| C(13) | 1242(2) | 4019(1) | 7251(3) | 30(1) |
| C(5) | 2967(2) | 2760(1) | 416(3) | 47(1) |
| C(15) | 1114(2) | 4384(1) | 3329(3) | 44(1) |
| C(19) | 2718(2) | 4084(1) | 2259(3) | 50(1) |
| C(16) | 1203(3) | 4808(1) | 2375(4) | 68(1) |
| C(17) | 2035(3) | 4867(1) | 1356(4) | 79(1) |
| C(18) | 2787(3) | 4507(2) | 1295(4) | 78(1) |

Table A.5.3. Bond Lengths [\AA] and Angles [$^\circ$] for **210c**.

| | | | |
|--|------------|-------------------------------|------------|
| Ti(1)-C(1) | 2.193(3) | C(7)-C(6) | 1.403(3) |
| Ti(1)-C(2) ⁱ | 2.2094(18) | C(9)-C(8) | 1.389(3) |
| Ti(1)-C(2) | 2.2094(18) | C(9)-C(10) | 1.393(3) |
| Ti(1)-C(3) ⁱ | 2.2101(18) | C(4)-C(3) | 1.419(3) |
| Ti(1)-C(3) | 2.2102(18) | C(4)-C(4) ⁱ | 1.425(4) |
| Ti(1)-C(4) ⁱ | 2.2163(18) | C(8)-C(13) | 1.395(3) |
| Ti(1)-C(4) | 2.2163(18) | C(14)-C(15) | 1.388(3) |
| Ti(1)-C(5) ⁱ | 2.293(2) | C(14)-C(19) | 1.390(3) |
| Ti(1)-C(5) | 2.293(2) | C(11)-C(10) | 1.379(3) |
| Ti(1)-C(6) | 2.311(2) | C(11)-C(12) | 1.388(3) |
| Ti(1)-C(6) ⁱ | 2.311(2) | C(1)-C(2) ⁱ | 1.432(2) |
| Ti(1)-C(7) | 2.321(3) | C(6)-C(5) | 1.409(3) |
| P(2)-C(2) | 1.8313(18) | C(12)-C(13) | 1.383(3) |
| P(2)-C(8) | 1.8385(19) | C(5)-C(5) ⁱ | 1.396(6) |
| P(2)-C(14) | 1.840(2) | C(15)-C(16) | 1.392(4) |
| C(2)-C(1) | 1.432(2) | C(19)-C(18) | 1.393(4) |
| C(2)-C(3) | 1.433(3) | C(16)-C(17) | 1.374(5) |
| C(7)-C(6) ⁱ | 1.403(3) | C(17)-C(18) | 1.369(5) |
| | | | |
| C(1)-Ti(1)-C(2) ⁱ | 37.97(5) | C(1)-Ti(1)-C(7) | 165.94(10) |
| C(1)-Ti(1)-C(2) | 37.97(5) | C(2) ⁱ -Ti(1)-C(7) | 143.99(5) |
| C(2) ⁱ -Ti(1)-C(2) | 71.99(9) | C(2)-Ti(1)-C(7) | 143.99(5) |
| C(1)-Ti(1)-C(3) ⁱ | 71.36(6) | C(3) ⁱ -Ti(1)-C(7) | 117.25(6) |
| C(2) ⁱ -Ti(1)-C(3) ⁱ | 37.85(7) | C(3)-Ti(1)-C(7) | 117.25(6) |
| C(2)-Ti(1)-C(3) ⁱ | 93.68(7) | C(4) ⁱ -Ti(1)-C(7) | 100.69(8) |
| C(1)-Ti(1)-C(3) | 71.36(6) | C(4)-Ti(1)-C(7) | 100.69(8) |
| C(2) ⁱ -Ti(1)-C(3) | 93.68(7) | C(5) ⁱ -Ti(1)-C(7) | 59.02(9) |
| C(2)-Ti(1)-C(3) | 37.85(7) | C(5)-Ti(1)-C(7) | 59.02(9) |
| C(3) ⁱ -Ti(1)-C(3) | 93.16(9) | C(6)-Ti(1)-C(7) | 35.27(7) |
| C(1)-Ti(1)-C(4) ⁱ | 92.62(8) | C(6) ⁱ -Ti(1)-C(7) | 35.27(7) |
| C(2) ⁱ -Ti(1)-C(4) ⁱ | 71.03(7) | C(2)-P(2)-C(8) | 101.09(8) |
| C(2)-Ti(1)-C(4) ⁱ | 93.03(7) | C(2)-P(2)-C(14) | 105.99(9) |
| C(3) ⁱ -Ti(1)-C(4) ⁱ | 37.40(7) | C(8)-P(2)-C(14) | 101.53(9) |
| C(3)-Ti(1)-C(4) ⁱ | 70.88(7) | C(1)-C(2)-C(3) | 127.33(18) |
| C(1)-Ti(1)-C(4) | 92.62(8) | C(1)-C(2)-P(2) | 110.42(14) |
| C(2) ⁱ -Ti(1)-C(4) | 93.03(7) | C(3)-C(2)-P(2) | 122.25(14) |
| C(2)-Ti(1)-C(4) | 71.03(7) | C(1)-C(2)-Ti(1) | 70.41(12) |
| C(3) ⁱ -Ti(1)-C(4) | 70.88(7) | C(3)-C(2)-Ti(1) | 71.10(10) |
| C(3)-Ti(1)-C(4) | 37.40(7) | P(2)-C(2)-Ti(1) | 137.42(9) |
| C(4) ⁱ -Ti(1)-C(4) | 37.50(10) | C(6) ⁱ -C(7)-C(6) | 108.1(3) |
| C(1)-Ti(1)-C(5) ⁱ | 107.74(8) | C(6) ⁱ -C(7)-Ti(1) | 71.96(14) |
| C(2) ⁱ -Ti(1)-C(5) ⁱ | 103.04(8) | C(6)-C(7)-Ti(1) | 71.96(14) |
| C(2)-Ti(1)-C(5) ⁱ | 125.68(8) | C(8)-C(9)-C(10) | 120.88(18) |
| C(3) ⁱ -Ti(1)-C(5) ⁱ | 115.19(9) | C(3)-C(4)-C(4) ⁱ | 128.99(10) |
| C(3)-Ti(1)-C(5) ⁱ | 150.18(9) | C(3)-C(4)-Ti(1) | 71.06(10) |
| C(4) ⁱ -Ti(1)-C(5) ⁱ | 137.90(9) | C(4) ⁱ -C(4)-Ti(1) | 71.25(5) |

| | | | |
|--|-----------|-------------------------------|------------|
| C(4)-Ti(1)-C(5) ⁱ | 159.64(8) | C(4)-C(3)-C(2) | 128.65(17) |
| C(1)-Ti(1)-C(5) | 107.74(8) | C(4)-C(3)-Ti(1) | 71.53(10) |
| C(2) ⁱ -Ti(1)-C(5) | 125.68(8) | C(2)-C(3)-Ti(1) | 71.05(10) |
| C(2)-Ti(1)-C(5) | 103.04(8) | C(9)-C(8)-C(13) | 118.29(18) |
| C(3) ⁱ -Ti(1)-C(5) | 150.18(9) | C(9)-C(8)-P(2) | 123.05(14) |
| C(3)-Ti(1)-C(5) | 115.18(9) | C(13)-C(8)-P(2) | 118.43(15) |
| C(4) ⁱ -Ti(1)-C(5) | 159.64(8) | C(15)-C(14)-C(19) | 118.4(2) |
| C(4)-Ti(1)-C(5) | 137.89(9) | C(15)-C(14)-P(2) | 124.43(18) |
| C(5) ⁱ -Ti(1)-C(5) | 35.43(15) | C(19)-C(14)-P(2) | 116.94(19) |
| C(1)-Ti(1)-C(6) | 135.91(7) | C(10)-C(11)-C(12) | 119.42(19) |
| C(2) ⁱ -Ti(1)-C(6) | 160.87(8) | C(11)-C(10)-C(9) | 120.19(18) |
| C(2)-Ti(1)-C(6) | 111.53(8) | C(2) ⁱ -C(1)-C(2) | 130.0(2) |
| C(3) ⁱ -Ti(1)-C(6) | 152.40(8) | C(2) ⁱ -C(1)-Ti(1) | 71.62(12) |
| C(3)-Ti(1)-C(6) | 99.91(8) | C(2)-C(1)-Ti(1) | 71.62(12) |
| C(4) ⁱ -Ti(1)-C(6) | 126.22(8) | C(7)-C(6)-C(5) | 107.9(2) |
| C(4)-Ti(1)-C(6) | 105.95(8) | C(7)-C(6)-Ti(1) | 72.77(14) |
| C(5) ⁱ -Ti(1)-C(6) | 59.09(9) | C(5)-C(6)-Ti(1) | 71.49(12) |
| C(5)-Ti(1)-C(6) | 35.63(9) | C(13)-C(12)-C(11) | 120.41(19) |
| C(1)-Ti(1)-C(6) ⁱ | 135.91(7) | C(12)-C(13)-C(8) | 120.80(19) |
| C(2) ⁱ -Ti(1)-C(6) ⁱ | 111.53(8) | C(5) ⁱ -C(5)-C(6) | 108.12(15) |
| C(2)-Ti(1)-C(6) ⁱ | 160.87(8) | C(5) ⁱ -C(5)-Ti(1) | 72.28(7) |
| C(3) ⁱ -Ti(1)-C(6) ⁱ | 99.91(8) | C(6)-C(5)-Ti(1) | 72.88(11) |
| C(3)-Ti(1)-C(6) ⁱ | 152.40(8) | C(14)-C(15)-C(16) | 120.5(3) |
| C(4) ⁱ -Ti(1)-C(6) ⁱ | 105.95(8) | C(14)-C(19)-C(18) | 120.4(3) |
| C(4)-Ti(1)-C(6) ⁱ | 126.22(8) | C(17)-C(16)-C(15) | 120.6(3) |
| C(5) ⁱ -Ti(1)-C(6) ⁱ | 35.63(9) | C(18)-C(17)-C(16) | 119.4(3) |
| C(5)-Ti(1)-C(6) ⁱ | 59.10(9) | C(17)-C(18)-C(19) | 120.7(3) |
| C(6)-Ti(1)-C(6) ⁱ | 58.88(12) | | |

Symmetry transformations used to generate equivalent atoms: ⁱ x,-y+1/2,z

Table A.5.4. Anisotropic displacement parameters ($\text{\AA}^2 \times 10^3$) for **210c**. The anisotropic displacement factor exponent takes the form: $-2\pi^2 [h^2 a^{*2} U^{11} + \dots + 2 h k a^* b^* U^{12}]$.

| | U^{11} | U^{22} | U^{33} | U^{23} | U^{13} | U^{12} |
|-------|----------|----------|----------|----------|----------|----------|
| Ti(1) | 14(1) | 25(1) | 15(1) | 0 | 1(1) | 0 |
| P(2) | 18(1) | 21(1) | 21(1) | 0(1) | -2(1) | -3(1) |
| C(2) | 18(1) | 21(1) | 18(1) | 0(1) | 2(1) | -2(1) |
| C(7) | 22(1) | 54(2) | 16(1) | 0 | 2(1) | 0 |
| C(9) | 22(1) | 26(1) | 21(1) | -3(1) | -4(1) | -2(1) |
| C(4) | 14(1) | 26(1) | 19(1) | 3(1) | 1(1) | 2(1) |
| C(3) | 18(1) | 20(1) | 22(1) | 2(1) | 2(1) | 1(1) |
| C(8) | 21(1) | 21(1) | 21(1) | 1(1) | -4(1) | 2(1) |
| C(14) | 38(1) | 26(1) | 27(1) | 3(1) | -10(1) | -15(1) |
| C(11) | 29(1) | 38(1) | 24(1) | -5(1) | 1(1) | 6(1) |
| C(10) | 23(1) | 32(1) | 27(1) | 0(1) | 0(1) | 0(1) |
| C(1) | 15(1) | 26(1) | 16(1) | 0 | 1(1) | 0 |
| C(6) | 37(1) | 47(1) | 26(1) | 6(1) | 12(1) | -10(1) |
| C(12) | 41(1) | 34(1) | 33(1) | -16(1) | -5(1) | 0(1) |
| C(13) | 27(1) | 29(1) | 34(1) | -5(1) | -3(1) | -6(1) |
| C(5) | 21(1) | 96(2) | 24(1) | -6(1) | 7(1) | -22(1) |
| C(15) | 78(2) | 23(1) | 31(1) | -1(1) | -13(1) | 3(1) |
| C(19) | 37(1) | 72(2) | 42(2) | 23(1) | -11(1) | -27(1) |
| C(16) | 140(3) | 21(1) | 42(2) | 0(1) | -39(2) | -5(2) |
| C(17) | 131(3) | 52(2) | 53(2) | 32(2) | -57(2) | -60(2) |
| C(18) | 70(2) | 111(3) | 53(2) | 48(2) | -30(2) | -67(2) |

Curriculum Vitae

Rhyan Joseph Soriano Terrado

- | | |
|-----------|--|
| 1978 | Born March 9 in Dagupan City, Philippines. |
| 1993 | Attended University of the Philippines at Los Baños, Laguna, Philippines. |
| 1997 | B.S. in Chemistry, University of the Philippines, Philippines. |
| 1997-1998 | Teaching Assistantship at Department of Chemistry, University of the Philippines, Philippines. |
| 1999 | Employed by Alpha Metals Jersey City, NJ, via On Assignment Lab Support, Elmwood Park, NJ. |
| 1999-2009 | Graduate work in Chemistry, Rutgers University, Newark, NJ. |
| 1999-2006 | Teaching Assistantship at Department of Chemistry, Rutgers University, Newark, NJ. |
| 2005 | M.S. in Chemistry, Rutgers University, Newark, NJ. |
| 2007 | Employed by AZ Electronic Materials, Branchburg, NJ, via Atrium Staffing, Iselin, NJ. |
| 2007 | Employed by US Customs and Border Protection, Department of Homeland Security, Newark, NJ. |
| 2009 | Ph.D. in Chemistry, Rutgers University, Newark, NJ. |